

**Iridium(I) Complexes of Phenanthroline-Derived  
Benzimidazolylienes: Synthetic, Structural and Catalytic Studies**

By

Xiangdong Du, B. Sc., Dalian University of Technology

A Thesis

submitted to the Department of Chemistry

in partial fulfillment of the requirements for the degree of

Master of Science

Supervised by

Professor Costa Metallinos

January, 2009

Brock University

St. Catharines, Ontario

© Xiangdong Du 2009

JAMES A GIBSON LIBRARY  
BROCK UNIVERSITY  
ST. CATHARINES ON

## Abstract

*N*-heterocyclic carbenes (NHCs) have undergone rapid development in recent years. Due to their strong  $\sigma$ -electron donation and structural variability properties, NHCs are becoming a major class of ligands in organometallic chemistry.

Compared with the other two types of NHCs (imidazolyidenes and imidazolinyliidenes), benzimidazolyliidenes have not been well represented. Limited synthetic approaches may impede the development of benzimidazolyliidenes.

This thesis is focused on the synthesis of phenanthroline-derived benzimidazolyliidene ligands and their metal complexes. A series of benzimidazolyliidene-iridium complexes were synthesized and characterized spectroscopically and crystallographically. All of the new complexes showed varying degrees of catalytic activity and enantioselectivity toward transfer hydrogenation and asymmetric hydrogenation. The best results were achieved in hydrogenation of methyl-2-acetamidoacrylate, which afforded (–)-(*R*)-methyl-2-acetamidopropanoate in 97% yield and 81% ee.

## Acknowledgments

First and foremost, I want to thank my supervisor, Dr. Costa Metallinos for his guidance, many valuable discussions and great helping during the past two years.

Second, I would like to express my appreciation to my committee members, Dr. Yan and Dr. Gordon. Their valuable advice and suggestions help me a lot to improve my research work. Thanks also go to Mr. Tim Jones for helping me with Mass Spectroscopy, Mr. Razvan Simonescu for his big help with NMR.

Third, great gratitude is expressed to my research group members, Josh Zaifman, Shufen Xu, Laura Dodge, Lori Van Belle and Fred Barrett for their invaluable help and suggestions.

Finally, I thank my wife and my daughter for supporting me throughout the two years.

## Table of Contents

	Page Number
<b>Abstract</b>	ii
<b>Acknowledgments</b>	iii
<b>Table of contents</b>	iv
<b>List of Tables</b>	vi
<b>List of Figures</b>	vi
<b>List of Schemes</b>	ix
<b>Abbreviations</b>	xiii
<b>1. Introduction</b>	1
1.1 Types of NHCs	1
1.2 The properties of NHCs	6
1.2.1 Electronic properties	6
1.2.2 Steric properties	9
1.3 History of <i>N</i> -heterocyclic carbenes	11
1.4 Synthesis of chiral NHCs and their metal complex	12
1.5 Applications of NHC-metal complexes in asymmetric catalysis	18
1.6 Benzimidazolyliidenes	23
1.7 Benzimidazolyliidenes derived from substituted 1,10-phenanthrolines	24
1.8 Aims and objectives	28

<b>2. Results and Discussion</b>	30
2.1 Synthesis of chiral and achiral benzimidazolium salts derived from 1,10-phenanthroline	30
2.1.1 Preparation of 2,9-disubstituted 1,10-phenanthrolines	30
2.1.2 Reduction of 2,9-disubstituted 1,10-phenanthrolines	32
2.1.3 Resolution of 2,9-disubstituted 1,10-octahydrophenanthrolines	34
2.1.4 Synthesis of chiral benzimidazolium salts	36
2.1.5 Hydrolysis of ureas to octahydrophenanthrolines	37
2.2 Synthesis and applications of benzimidazolylidene-metal complexes	39
2.2.1 Attempts to make NHC-Ru alkylidene complexes	39
2.2.2 Synthesis of benzimidazolylidene-Ir complexes	42
2.2.3 Transfer hydrogenation of acetophenone and its derivatives using NHC-Ir catalysts	52
2.2.4 Hydrogenation of methyl-2-acetamidoacrylate and <i>trans</i> -methyl- $\alpha$ -acetamidocinnamate	54
2.2.5 Hydrogenation of ( <i>E</i> )- <i>N</i> -(1-phenylethylidene)benzenamine	56
<b>3. Conclusions and future work</b>	58
<b>4. Experimental</b>	60
<b>5. References</b>	91
<b>6. Appendix</b>	99
<b>VITA</b>	198

## List of Tables

Table Number	Table Title	Page Number
Table 1	Average pK <sub>a</sub> for carbenes in DMSO and CH <sub>3</sub> CN	4
Table 2	Average $\nu(\text{CO})$ of (L)Ir(CO) <sub>2</sub> Cl measured in CH <sub>2</sub> Cl <sub>2</sub>	5

## List of Figures

Figure Number	Figure Title	Page Number
Figure 1	Examples of NHCs with imidazoline framework	1
Figure 2	Early examples of stable NHCs	9
Figure 3	Grubbs' first and second generation olefin metathesis catalysts	11
Figure 4	Examples of NHC-Ru alkylidene catalysts for olefin metathesis	40
Figure 5	Examples of NHC-Ir complexes	44
Figure 6	<sup>1</sup> H- <sup>13</sup> C HSQC experiment of complex <b>91</b>	46
Figure 7	<sup>1</sup> H- <sup>13</sup> C HSQC experiment of complex <b>92</b>	47
Figure 8	ORTEP plot of ( <i>R,R</i> )- <b>93a</b> at 50% probability	50
Figure 9	ORTEP plot of ( <i>S,S</i> )- <b>93f</b> at 50% probability	50
Figure 10	<sup>1</sup> H- <sup>13</sup> C HSQC experiment of complex ( <i>S,S</i> )- <b>93f</b>	51

Figure 11	$^1\text{H}$ - $^{13}\text{C}$ HSQC Experiment of complex ( <i>S,S</i> )- <b>94a</b>	51
Figure 12	$^1\text{H}$ NMR spectrum of <b>74d</b>	99
Figure 13	$^{13}\text{C}$ NMR spectrum of <b>74d</b>	100
Figure 14	$^1\text{H}$ NMR spectrum of <b>54d</b>	101
Figure 15	$^{13}\text{C}$ NMR spectrum of <b>54d</b>	102
Figure 16	$^1\text{H}$ NMR spectrum of <b>54e</b>	103
Figure 17	$^{13}\text{C}$ NMR spectrum of <b>54e</b>	104
Figure 18	$^1\text{H}$ NMR spectrum of <b>54f</b>	105
Figure 19	$^{13}\text{C}$ NMR spectrum of <b>54f</b>	106
Figure 20	$^1\text{H}$ NMR spectrum of <b>56d</b>	107
Figure 21	$^{13}\text{C}$ NMR spectrum of <b>56d</b>	108
Figure 22	$^1\text{H}$ NMR spectrum of <b>75e</b>	109
Figure 23	$^{13}\text{C}$ NMR spectrum of <b>75e</b>	110
Figure 24	$^1\text{H}$ NMR spectrum of <b>56e</b>	111
Figure 25	$^{13}\text{C}$ NMR spectrum of <b>56e</b>	112
Figure 26	$^1\text{H}$ NMR spectrum of ( <i>R,R</i> )- <b>57a</b>	113
Figure 27	$^{13}\text{C}$ NMR spectrum of ( <i>R,R</i> )- <b>57a</b>	114
Figure 28	$^1\text{H}$ NMR spectrum of ( <i>S,S</i> )- <b>57f</b>	115
Figure 29	$^{13}\text{C}$ NMR spectrum of ( <i>S,S</i> )- <b>57f</b>	116
Figure 30	$^1\text{H}$ NMR Spectrum of ( <i>R,R</i> )- <b>57a</b>	117
Figure 31	$^{13}\text{C}$ NMR Spectrum of ( <i>R,R</i> )- <b>57a</b>	118

Figure 32	$^1\text{H}$ NMR Spectrum of ( <i>R,R</i> )-57f	119
Figure 33	$^{13}\text{C}$ NMR Spectrum of ( <i>R,R</i> )-57f	120
Figure 34	$^1\text{H}$ NMR spectrum of <i>meso</i> -57f	121
Figure 35	$^{13}\text{C}$ NMR spectrum of <i>meso</i> -57f	122
Figure 36	$^1\text{H}$ NMR spectrum of ( <i>R,R</i> )-56a	123
Figure 37	$^1\text{H}$ NMR spectrum of ( <i>S,S</i> )-56f	124
Figure 38	$^{13}\text{C}$ NMR spectrum of ( <i>S,S</i> )-56f	125
Figure 39	$^1\text{H}$ NMR Spectrum of ( <i>R,R</i> )-56f	126
Figure 40	$^{13}\text{C}$ NMR spectrum of ( <i>R,R</i> )-56f	127
Figure 41	$^{13}\text{C}$ NMR spectrum of <i>meso</i> -99c	128
Figure 42	$^1\text{H}$ NMR spectrum of ( <i>R,R</i> )-58a	129
Figure 43	$^{13}\text{C}$ NMR spectrum of ( <i>R,R</i> )-58a	130
Figure 44	$^1\text{H}$ NMR spectrum of ( <i>S,S</i> )-58f	131
Figure 45	$^{13}\text{C}$ NMR spectrum of ( <i>S,S</i> )-58f	132
Figure 46	$^1\text{H}$ NMR spectrum of 90	133
Figure 47	$^{13}\text{C}$ NMR spectrum of 90	134
Figure 48	$^1\text{H}$ NMR spectrum of ( <i>S,S</i> )-82a	135
Figure 49	$^{13}\text{C}$ NMR spectrum of ( <i>R,R</i> )-82a	136
Figure 50	$^1\text{H}$ NMR spectrum of 89	137
Figure 51	$^1\text{H}$ NMR spectrum of 91	138
Figure 52	$^{13}\text{C}$ NMR spectrum of 91	139



Figure 53	$^1\text{H}$ NMR spectrum of <b>92</b>	140
Figure 54	$^{13}\text{C}$ NMR spectrum of <b>92</b>	141
Figure 55	$^1\text{H}$ NMR spectrum of ( <i>S,S</i> )- <b>93a</b>	142
Figure 56	$^{13}\text{C}$ NMR spectrum of ( <i>S,S</i> )- <b>93a</b>	143
Figure 57	$^1\text{H}$ NMR spectrum of ( <i>S,S</i> )- <b>94a</b>	144
Figure 58	$^{13}\text{C}$ NMR spectrum of ( <i>S,S</i> )- <b>94a</b>	145
Figure 59	$^1\text{H}$ NMR spectrum of ( <i>S,S</i> )- <b>93f</b>	146
Figure 60	$^{13}\text{C}$ NMR spectrum of ( <i>S,S</i> )- <b>93f</b>	147

### List of Schemes

Scheme Number	Scheme Title	Page Number
Scheme 1	Screening of ligands for Suzuki-Miyaura cross coupling of substrates	7
Scheme 2	The first NHC-metal complexes	8
Scheme 3	First application of NHC-metal complex as the catalyst in reactions	10
Scheme 4	The first chiral NHC-metal complex	12
Scheme 5	Synthetic routes to chiral NHC	12
Scheme 6	Internal base used in preparation of binaphthyl NHC-metal complexes	14

Scheme 7	Chiral NHC-Pd complex synthesis by silver transmetalation	15
Scheme 8	NHC-Ru complex synthesis using free NHCs	16
Scheme 9	Olefin metathesis catalyzed by Grubbs chiral NHC-Ru complex	17
Scheme 10	Asymmetric ring opening metathesis catalyzed by <b>32</b>	17
Scheme 11	Asymmetric hydrogenation by the mixture of diastereomers <b>35</b>	18
Scheme 12	Burgess' NHC-Ir catalyst and its application in asymmetric hydrogenation	19
Scheme 13	The first example of asymmetric hydrosilylation	20
Scheme 14	Asymmetric hydrosilylation using chiral NHC ligand <b>46</b>	20
Scheme 15	Asymmetric 1, 4-addition catalyzed by NHC-copper complexes	21
Scheme 16	Aryl amination and <i>N</i> -alkylation routes to prepare benzimidazolium salts	22
Scheme 17	Preparation and reduction of 2,9-disubstituted phenanthrolines	23
Scheme 18	Resolution of racemic 2,9-diphenyloctahydrophenanthrolines	24

Scheme 19	Asymmetric synthesis of a phenanthroline-derived benzimidazolium salt	25
Scheme 20	Asymmetric reduction of 2,9-dialkyl-1,10-phenanthrolines	26
Scheme 21	Phenanthroline-derived NHC-Pd complex synthesis and their application	27
Scheme 22	Palladium-catalyzed $\alpha$ -arylation using chiral ligand ( <i>S,S</i> )- <b>58a</b>	27
Scheme 23	Synthesis of benzimidazolylidene-metal complexes	29
Scheme 24	Synthesis of bulky 2,9-disubstituted-1,10-phenanthrolines	31
Scheme 25	Reduction of 2,9-disubstituted phenanthrolines using different methods	33
Scheme 26	Reduction of 2,9-disubstituted phenanthrolines using Na/alcohol	34
Scheme 27	Resolution of <i>rac/meso</i> 2,9-disubstituted octahydrophenanthrolines	36
Scheme 28	Synthesis of rigid chiral benzimidazolium salts	37
Scheme 29	Attempts at converting urea <b>77</b> to octahydrophenanthroline <b>53</b>	38
Scheme 30	Ring-opening of urea <b>77</b> to benzamide <b>78</b>	38

Scheme 31	Attempts to prepare benzimidazolylidene-Ru alkylidene complexes	42
Scheme 32	Synthesis of achiral benzimidazolylidene-Ir complexes	45
Scheme 33	Synthesis of chiral phenanthroline-derived NHC-Ir complexes	48
Scheme 34	Proposed mechanism for NHC-Ir catalyzed transfer hydrogenation	53
Scheme 35	Transfer hydrogenation of <b>44a-d</b>	54
Scheme 36	Hydrogenation of <b>36a-b</b> using NHC-Ir catalyst	56
Scheme 37	Hydrogenation of <b>96</b> using cationic catalysts	57
Scheme 38	Proposed synthetic route for a chiral bidentate benzimidazolium salt	59

## Abbreviations

Ac	acetyl
Ad	adamantyl
AROM	asymmetric ring opening cross-metathesis
b	broad
BDE	bond dissociation energy
Bu	butyl
calcd	calculated
Cp	cyclopentadienyl
d	doublet
DBU	1,8-diazabicyclo[5.4.0]undec-7-ene
DDQ	2,3-dichloro-5,6-dicyanobenzoquinone
DMA	<i>N,N</i> -dimethylacetamide
ee	enantiomeric excess
EIMS	electron impact mass spectrometry
FAB	fast-atom bombardment
HRMS	high resolution mass spectrometry
IR	infrared
IAd	1,3-di(1-adamantyl) imidazol-2-ylidene
IMes	1,3-dimesityl-imidazol-2-ylidene
Icy	1,3-dicyclohexylimidazol-2-ylidene
HDHP	Hantzsch dihydropyridine

m	multiplet
mp	melting point
NaBARF	sodium tetrakis(3,5-trifluoromethylphenyl)borate
NHC	<i>N</i> -heterocyclic carbene
NMR	nuclear magnetic resonance
q	quartet
rac	racemic
rt	room temperature
s	singlet
SIMes	1,3-dimesitylimidazolin-2-ylidene
SI <i>t</i> -Bu	1,3-bis(2,6-di- <i>tert</i> -butylphenyl)imidazolin-2-ylidene
TFA	trifluoroacetic acid
TfO	trifluoromethanesulfonate
THF	tetrahydrofuran
TMS	trimethylsilyl
$t_R$	retention time of the <i>R</i> isomer
$t_S$	retention time of the <i>S</i> isomer

# 1. Introduction

## 1.1 Types of NHCs

Carbenes are defined as neutral carbon species containing a carbon atom with six valence electrons.<sup>1,2</sup> *N*-Heterocyclic carbenes (NHCs), with the carbene being incorporated in a nitrogen-containing heterocyclic ring, are major members of carbene families.<sup>3</sup> According to the ring size, four-,<sup>4</sup> five-, six-<sup>5,6</sup> and seven-<sup>7</sup> membered NHCs have been reported and the majority are based on five-membered ring systems, especially with an imidazoline framework. Depending on the saturation degree of the backbone, NHCs with an imidazoline framework can be classified into three general types (**Figure 1**): (a) saturated imidazolinylienes (**A**), (b) unsaturated imidazolylienes (**B**), and (c) benzimidazolylienes (**C**).<sup>8,9</sup>

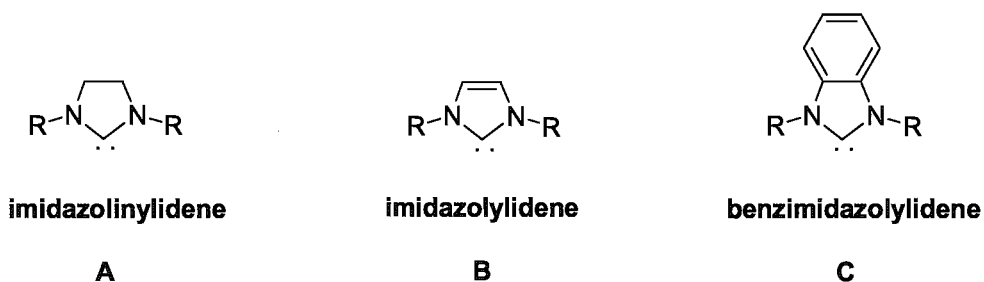


**Figure 1.** Examples of NHCs with imidazoline framework.

Saturated imidazolinylienes and unsaturated imidazolylienes are the most extensively examined NHCs and a large number of them have been employed

successfully in organometallic transformations, notably in C-C and C-N bond forming reactions. However, compared with imidazolinylienes and imidazolylienes, benzimidazolylienes have not been well represented. Limited synthetic approaches may have impeded the development of chiral benzimidazolylienes.<sup>8</sup>

## 1.2 The Properties of NHCs

### 1.2.1 Electronic Properties

NHCs can form strong metal-carbon bonds through  $\sigma$ -electron donation from a filled  $sp^2$  orbital of the carbenoid carbon atom. The adjacent nitrogen donates its  $p$  orbital lone pair electrons into the empty  $p$  orbital of the carbon, helping to reduce the carbene electron deficiency. In addition, the carbene is also stabilized by the inductive effect of the adjacent electronegative nitrogen atoms.<sup>10</sup> As a result, NHCs have good nucleophilic and little electrophilic properties. Compared with the commonly used phosphine ligands, NHCs often have better thermal stability and resist dissociation from the metallic center.<sup>11</sup>

For the NHC-metal complexes used to catalyze the reactions, many reports have shown that changing the electronic properties of NHCs significantly affects the activity of the catalysts. For example, unsaturated imidazolylienes were often used as ligands in ruthenium-catalyzed olefin metathesis reactions, but incorporation of saturated imidazolinylienes into the ruthenium catalysts (for example, complex **29**) can result in

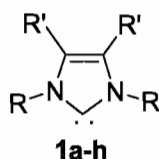


much higher catalytic activities.<sup>12,13</sup> It has been suggested that this is due to the increased basicity of the ligand systems.<sup>13</sup>

Some methods have been applied to measure the electronic properties of NHCs since they have been shown to greatly influence catalysts' activities. One protocol was designed to measure or calculate the pKa values of the corresponding NHCs. Alder reported that the pKa of 1,3-diisopropyl-4,5-dimethylimidazol-2-ylidene in DMSO-*d*<sub>6</sub> was 24.0.<sup>14</sup> Kim measured the pKa of 1,3-di-*tert*-butylimidazol-2-ylidene in DMSO as 22.7.<sup>15</sup> In 2004, Yates calculated the absolute and relative pKa values of different nucleophilic carbenes using computational methods.<sup>16</sup> For the substituted imidazolylidenes, pKa values range from 16.1 to 24.5 in DMSO, while values in CH<sub>3</sub>CN are determined to be between 27.4 to 35.8. **Table 1** shows that carbene **1c** has lower basicity because of the electron withdrawing nature of the chlorines at the 4 and 5 positions of the imidazole ring. The electron-withdrawing inductive effects of aryl rings also dramatically reduce the pKa, as evidenced by carbenes **1g** and **1h**. Compared to **1a** (21.1 in DMSO), the saturated carbene **2** exhibits a slightly higher pKa (22.3 in DMSO).

**Table 1.** Average pKa for Carbenes in DMSO and CH<sub>3</sub>CN.

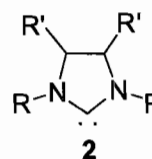
	dimethylsulfoxide	acetonitrile
carbene	pKa	pKa
<b>1a</b>	21.1±0.23	32.4±0.22
<b>1b</b>	23.7±0.21	34.9±0.21
<b>1c</b>	16.2±0.10	27.4±0.10
<b>1d</b>	22.0±0.21	33.3±0.21
<b>1e</b>	22.6±0.09	33.9±0.09
<b>1f</b>	24.5±0.15	35.8±0.14
<b>1g</b>	16.1±0.05	27.4±0.07
<b>1h</b>	16.8±0.09	28.2±0.12
<b>2</b>	22.3±0.25	33.6±0.25



**1a** R=Me, R'=H  
**1d** R=*i*-Pr, R'=H  
**1g** R=Ph, R'=H

**1b** R=Me, R'=Me  
**1e** R=*t*-Bu, R'=H  
**1h** R=2,6-Xyl, R'=H

**1c** R=Me, R'=Cl  
**1f** R=*i*-Pr, R'=Me  
**2** R=Me, R'=H



Though pKa values can provide a rough estimation for an NHC's  $\sigma$ -donor characteristics, the most widely accepted methodology for the estimation of NHC ligands is the IR spectroscopic analysis of the CO stretching frequencies in the corresponding [(NHC)M(CO)<sub>2</sub>Cl] (M=Ir, Rh,) complexes.<sup>17,18</sup>  $\sigma$ -Donor NHCs lead to an increased electron density on the metal center that causes stronger back-bonding from the transition metal to the  $\pi^*$  orbital of the CO ligands and thus a weakening of the C-O bond which can be detected by IR spectroscopy. Therefore, a very basic NHC ligand should result in a relatively low wavenumber value for C-O bond (Table 2).<sup>19-21</sup>

**Table 2.** Average  $\nu_{\text{av}}(\text{CO})$  of (L)-Ir(CO)<sub>2</sub>Cl measured in CH<sub>2</sub>Cl<sub>2</sub>.

entry	ligand	$\nu_{\text{av}}(\text{CO})$ (cm <sup>-1</sup> )
1	PPh <sub>3</sub>	2044.0
2	PCy <sub>3</sub>	2028.0
3	SIPr	2024.9
4	SIMes	2024.6
5	IPr	2023.9
6	IMes	2023.1
7	ICy	2023.0

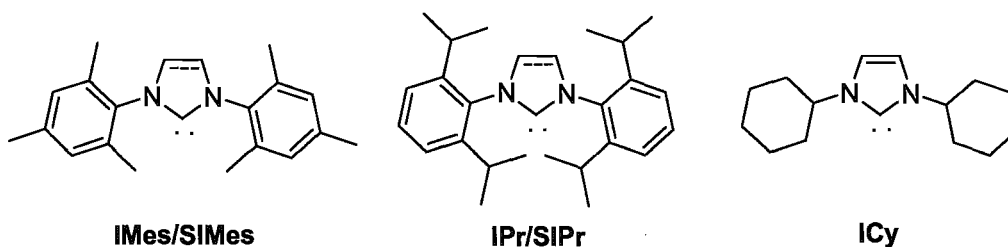


**Table 2** shows that *N*-heterocyclic carbenes are more electron rich ligands than even the very basic phosphine PCy<sub>3</sub>, but the electronic differences for NHC ligands are quite small. The very similar stretching frequency between IMes and SIMes in (L)Ir(CO)<sub>2</sub>Cl clearly demonstrates that saturated NHC ligands have similar electron donating abilities with unsaturated ones in NHC-metal complexes. Electronic properties of NHC ligands are probably not the main reason for explaining that saturated NHC-metal complexes have better catalytic activities in some reactions.

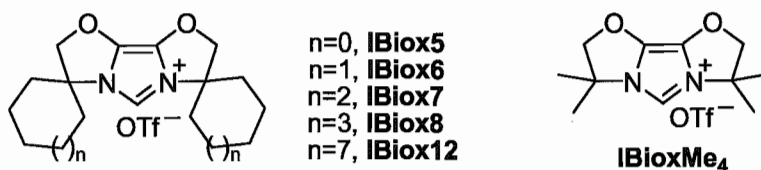
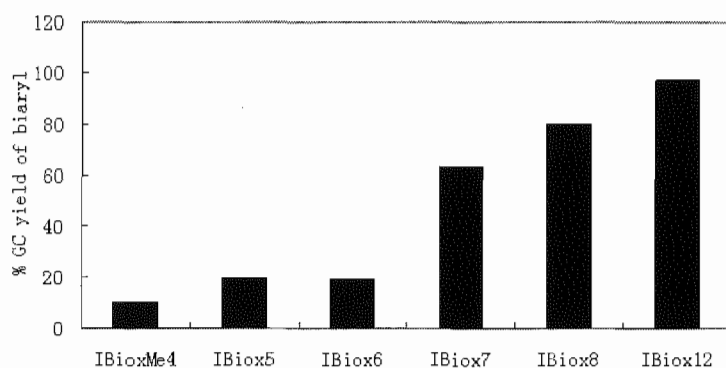
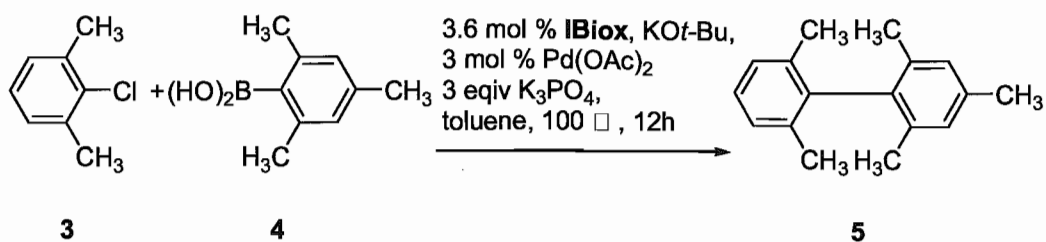
Based on the data in **Table 2**, it can be concluded that after reaching a certain level of electron richness required for the reaction, modification of the ligand's steric demand might become more important than adjustment of the ligand's electronic properties in NHC-metal catalysts.<sup>22</sup>

### 1.2.2 Steric Properties

The shape of NHCs is significantly different than that of phosphine ligands. The phosphine-metal complexes look like a cone and they can be easily assessed by the size of the phosphines using Tolman's cone angle ( $\theta$ ) descriptors.<sup>23</sup> For NHC-complexes, though Sigman described them as fence or fan like,<sup>24</sup> their shapes are strongly affected by the substituents on the nitrogen atoms, so it is difficult to find an appropriate method to measure the steric properties of NHC ligands.

In 2003, Nolan introduced a "buried volume" parameter,  $\%V_{\text{bur}}$ , the volume buried by overlap between a sphere with a radius of 3 Å centered around the metal with the atoms of the ligand within this sphere to measure the percentage of spherical space around the metal that is occupied by a ligand.<sup>19,25</sup> Based on the  $\%V_{\text{bur}}$ , the large NHCs, like 1,3-bis(2,6-di-*tert*-butylphenyl)imidazolin-2-ylidene (SI*t*-Bu,  $\%V_{\text{bur}}$  = 38) and 1,3-di(1-adamantyl) imidazol-2-ylidene (IAd,  $\%V_{\text{bur}}$  = 37), are significantly bigger than even the largest phosphine, *Pt*-Bu<sub>3</sub> ( $\%V_{\text{bur}}$  = 30).

In order to investigate the steric influence of an NHC, a series of related bioxazoline-derived carbene ligands (IBiox) as triflate salts with similar electronic character and different steric demand were synthesized and used in Pd-catalyzed Suzuki-Miyaura coupling reactions.<sup>26</sup> The most hindered NHC ligand, **IBiox12**, gave the highest yield (96%, **Scheme 1**). The results show that steric properties of NHC ligands greatly affect the catalytic activities of NHC-metal catalysts.

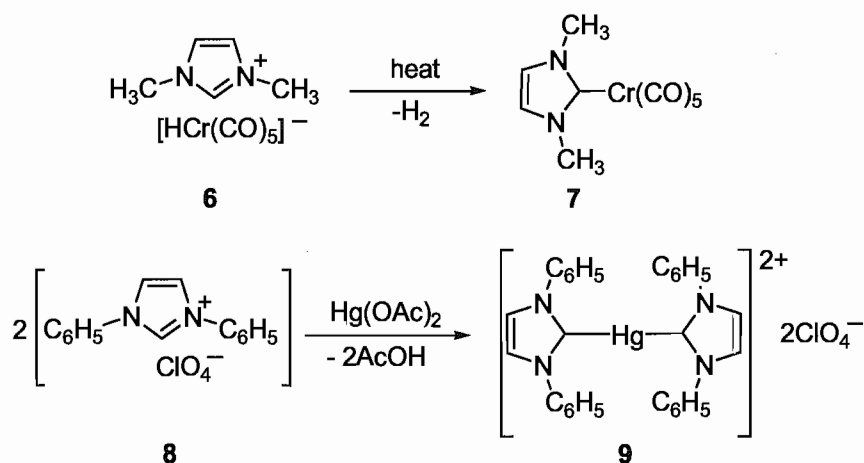


**Scheme 1.** Screening of ligands for Suzuki-Miyaura cross-coupling of substrates.

### 1.3 History of *N*-Heterocyclic Carbenes and Their Metal Complexes

In the early 1960s, Wanzlick first investigated nucleophilic carbene chemistry and discussed the likely existence of stable carbenes,<sup>27</sup> which were previously postulated to be too unable to isolate due to their high reactivity. He pointed out that there would be an increase in stability in carbenes if their adjacent substituents were sufficiently strong electron donors. The preparation of NHC-metal complexes was independently described

by Öfele<sup>28</sup> and Wanzlick<sup>29</sup> in 1968. Öfele prepared an imidazolylidene-chromium complex **7** by heating dimethylimidazolium hydridopentacarbonylchromate **6**, while Wanzlick obtained an imidazolylidene-mercury(II) complex **9** by treating imidazolium salt **8** with mercury acetate (Scheme 2).



**Scheme 2.** The first NHC-metal complexes.

Few developments in *N*-heterocyclic carbene chemistry occurred until Arduengo reported the first isolated crystalline NHC (IAd, **10**) by deprotonation of the imidazolium salt using sodium hydride as the base and DMSO as the catalyst in 1991.<sup>30</sup> Carbene **10** can be stored as colorless crystals in the absence of moisture and oxygen, and the spectroscopic and X-ray analysis proved the structure of the stable carbene.

The first stable carbene sparked considerable research interest in the chemistry of NHCs. In 1992, Arduengo isolated and acquired an X-Ray structure of another stable carbene **11** in which the bulky *N*-adamantyl group was replaced with smaller methyl groups.<sup>1</sup> The lack of bulky groups demonstrated that sterics were not the predominant factor for the stability of the tetramethylimidazol-2-ylidene. Three years later, Arduengo

synthesized the first stable saturated 1,3-dimesitylimidazolin-2-ylidene (SIMes, **12**), which has been one of the most popular NHC ligands in transition metal chemistry.<sup>31</sup> The stable saturated NHC demonstrated that the aromatic five-membered imidazole ring with the 4,5-carbon-carbon double bond was not a necessity to produce a stable NHC.

The first air stable carbene, 1,3-dimesityl-4,5-dichloroimidazol-2-ylidene **13** was synthesized by the Arduengo group by chlorination of 1,3-dimesitylimidazol-2-ylidene using two equivalents of carbon tetrachloride.<sup>32</sup> The introduction of chlorine in the 4 and 5 positions of the imidazole ring improves greatly the stability of the carbene because of an inductive electron withdrawal by the strongly electronegative chlorine atom.<sup>32</sup>

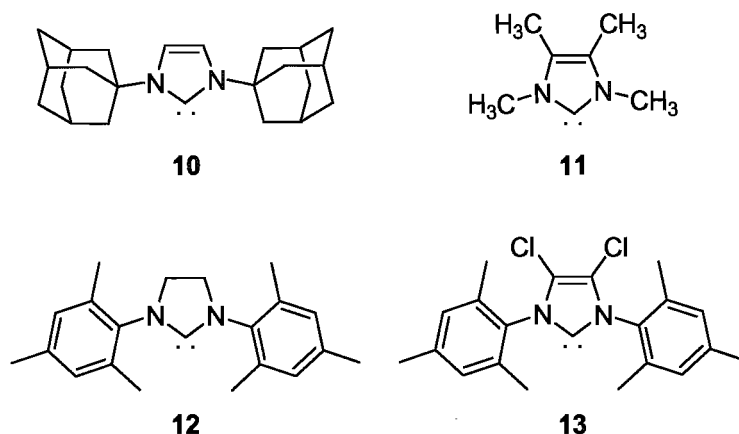
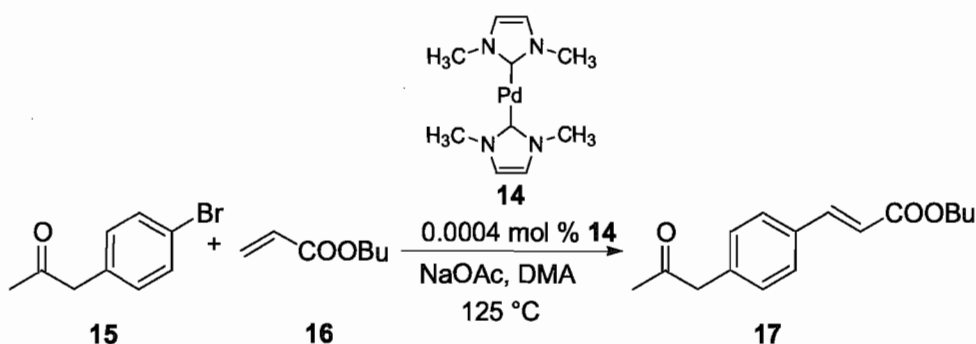


**Figure 2.** Early examples of stable NHCs.

In 1995, Herrmann first demonstrated NHC-palladium complexes as the catalysts in Heck reactions.<sup>33</sup> NHC-Pd complexes **14** showed pronounced thermal stability and excellent catalytic activity. Full conversion of the substrates **15** can be obtained with

catalyst loadings of only 0.0004 mol % (**Scheme 3**). This finding attracted many chemists' attention immediately. Since then, numerous NHCs and NHC-metal complexes were reported and used in all kinds of organometallic catalytic reactions such as olefin metathesis, cross coupling reactions, aryl amination reactions, asymmetric hydrogenation. In 1999, a particularly noteworthy application was reported by Grubbs. A second generation olefin metathesis catalyst **19** was generated by replacing one tricyclohexyl phosphine group of the first generation catalyst **18**<sup>34</sup> with an NHC ligand (**Figure 3**).<sup>35</sup> The NHC-ruthenium alkylidene catalyst was not only air and moisture stable, but also exhibited higher activity and more tolerance towards functional groups.



**Scheme 3.** First application of NHC-metal complex as the catalyst in reactions.

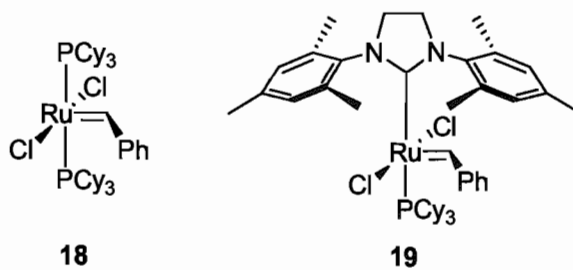
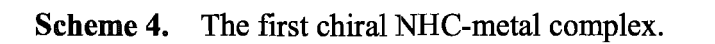
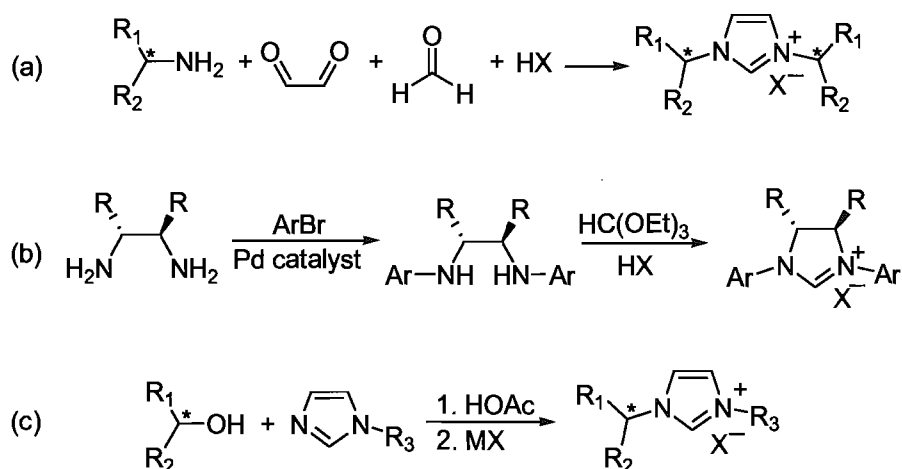


**Figure 3.** Grubbs' first and second generation olefin metathesis catalysts.





straightforward synthetic pathway (**Scheme 5, a**).<sup>37</sup>



**Scheme 5.** Synthetic routes to chiral NHCs.

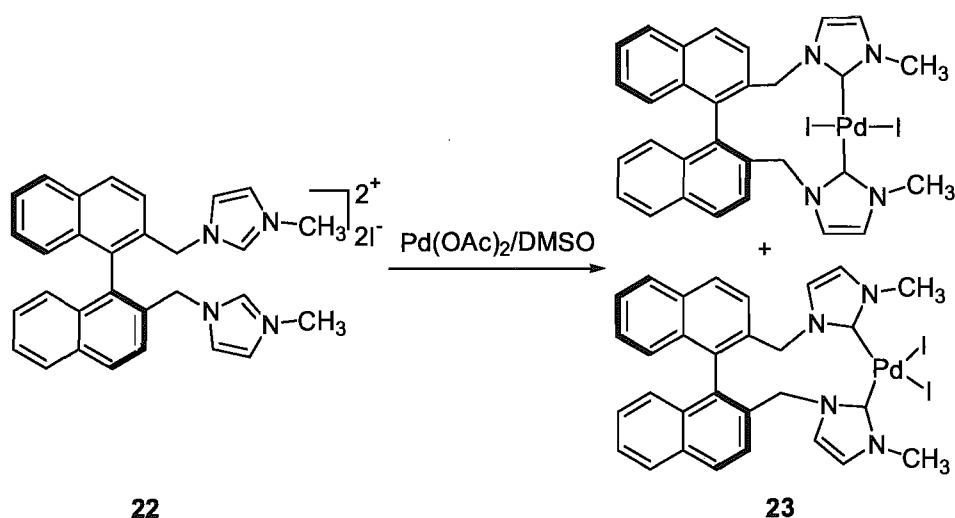
In 2001, Grubbs synthesized an imidazolium salt with chiral centers at the 4,5 positions of imidazoline ring by first making chiral tertiary amines by palladium-catalyzed Buchwald-Hartwig coupling, then cyclization with triethylorthoformate and hydro-halogen acid (**Scheme 5, b**).<sup>38</sup>  $C_1$ -symmetric chiral imidazolium salts could be synthesized using Chung's method.<sup>39</sup> Treatment of a chiral alcohol with monosubstituted imidazole in acetic acid followed by basic workup and anion exchange resulted in an unsymmetrically chiral imidazolium salt (**Scheme 5, c**).

The coordination of NHCs to metal centers is relatively less accessible than phosphine-metal compounds because it usually requires the activation of an NHC precursor.<sup>40</sup> The methods for preparing chiral NHC-metal complexes can be classified as follows:

i. Deprotonation of an NHC precursor with a base:

Using a base, NHC precursors can be deprotonated *in situ* to produce the free NHCs, which react directly with metal to form NHC-metal complexes. The free carbenes, which are usually air and moisture sensitive, do not need to be isolated during the reaction. The ease of control and simplicity of the method makes it the most widely used in the preparation of NHC-metal complexes. Several strong bases such as NaH,<sup>41</sup> KO<sup>t</sup>Bu,<sup>42</sup> NaOEt,<sup>43</sup> KN[Si(CH<sub>3</sub>)<sub>3</sub>]<sub>2</sub>,<sup>44</sup> *t*-BuLi<sup>45</sup> are the most widely used bases for this kind of reaction and sometimes even weak bases like NEt<sub>3</sub>,<sup>46</sup> NaOAc,<sup>47</sup> Cs<sub>2</sub>CO<sub>3</sub><sup>48</sup> are capable of the deprotonation. The choice of base is quite important during the deprotonation process to avoid production byproducts and obtain higher yields.<sup>45</sup>

Besides external bases, basic ligands on the metal complexes can also be used as the internal bases to deprotonate NHC precursors. Metal compounds with hydride, alkoxide, acetate are often treated with NHC ligands directly in dry solvent to generate NHC-metal complexes. For example, direct treatment of a binaphthyl bisimidazolium salt **22** with Pd(OAc)<sub>2</sub> in hot DMSO gives the mixture of bidentate NHC-Pd isomers **23** by elimination of acetic acid in the reaction (**Scheme 6**).<sup>49</sup>

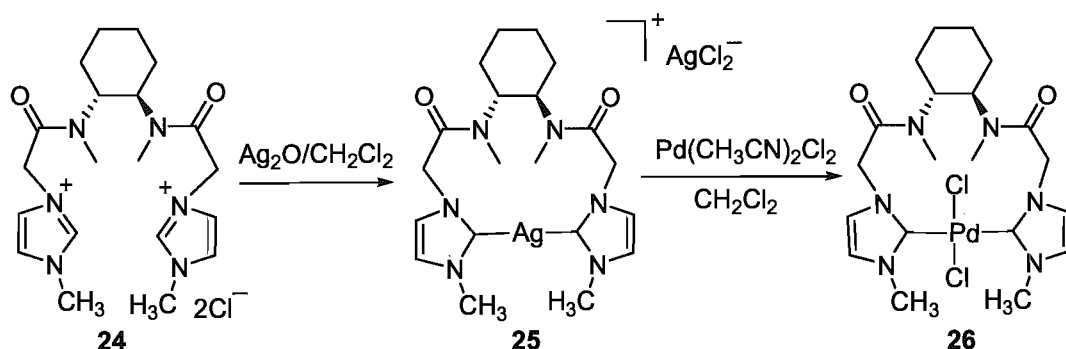


**Scheme 6.** Internal base used in preparation of binaphthyl NHC-metal complexes.

ii. Transmetalation from NHC-silver complexes:

Using NHC-Ag complexes as carbene transfer agents to make NHC-metal complexes was first reported by Wang and Lin in 1998.<sup>50</sup> By reacting Ag<sub>2</sub>O with *N,N*-diethylbenzimidazolium chloride salts in dichloromethane, the bisbenzimidazolyliene-silver complexes were prepared and used as carbene sources to make NHC complexes of Pd and Au by reacting with Pd(CH<sub>3</sub>CN)<sub>2</sub>Cl<sub>2</sub> and Au[S(CH<sub>3</sub>)<sub>2</sub>]Cl respectively. The driving force for the reactions is the formation of insoluble silver chloride salt. This convenient process avoids using strong base, a strictly inert atmosphere, complicated workups and has been successfully demonstrated with a variety of metals such as Pd, Ni, Rh, Ir, Ru, Au, Cr and Cu.<sup>21, 51-55</sup> For example, the reaction of the chiral imidazolium salt **24** with Ag<sub>2</sub>O gives the NHC-Ag complex **25**, which reacts with Pd(CH<sub>3</sub>CN)<sub>2</sub>Cl<sub>2</sub> to afford chiral bidentate NHC-Pd complex **26** (Scheme 7).<sup>56</sup>

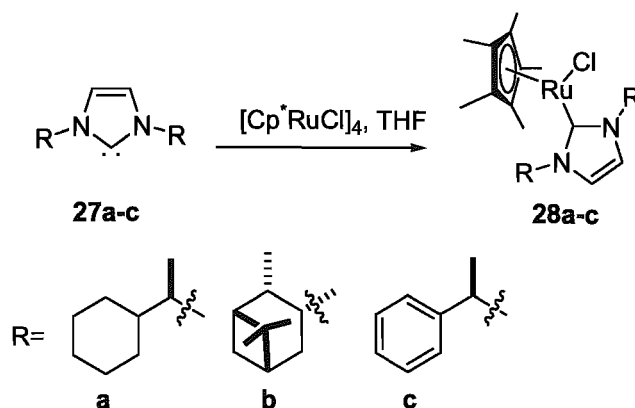
Because of its mild conditions, this method is also useful if NHC precursors have protons of comparable acidity to the imidazolium C-H proton and treatment with base is not productive.<sup>40</sup>



**Scheme 7.** Chiral NHC-Pd complex synthesis by silver transmetalation.

iii. Stable carbene directly reacting with metal precursor:

Free stable carbenes can replace labile ligands on suitable metal complexes.  $\text{Pd}(\text{bipy})(\text{CH}_3)_2$ ,<sup>57</sup>  $[\text{Rh}(\text{COD})\text{Cl}]_2$ ,<sup>58</sup>  $\text{Ni}(\text{CO})_4$ ,<sup>59</sup>  $\text{W}(\text{CO})_6$ ,<sup>59</sup> etc. were reported to be used as metal precursors reacting with isolated stable carbenes to provide NHC-metal complexes. In 2001, the Nolan group prepared a series of chiral NHC-Rh complexes by mixing the free chiral carbenes with  $[\text{Cp}^*\text{RuCl}]_4$  in THF with good yields (**Scheme 8**).<sup>60</sup>



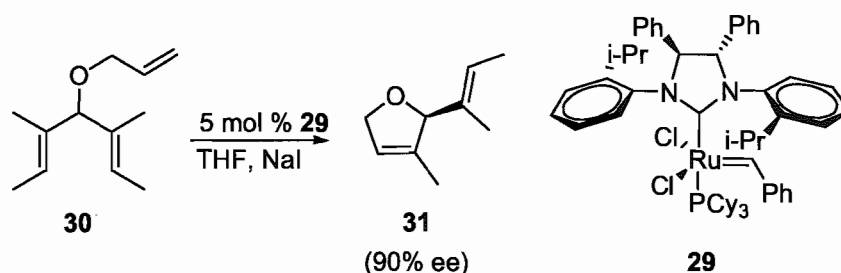
**Scheme 8.** NHC-Ru complex synthesis using free NHCs.

### 1.5 Applications of Chiral NHC-metal Complexes in Asymmetric Catalysis

Increasing experimental data shows that the NHC systems have surpassed their phosphine-containing analogues in both activity and scope in the area of organometallic chemistry.<sup>61</sup> Transformations catalyzed by chiral NHC-metal complexes have been exhibited in all kinds of reactions such as in asymmetric olefin metathesis, asymmetric hydrogenation, hydrosilylation and in asymmetric 1,4-addition.

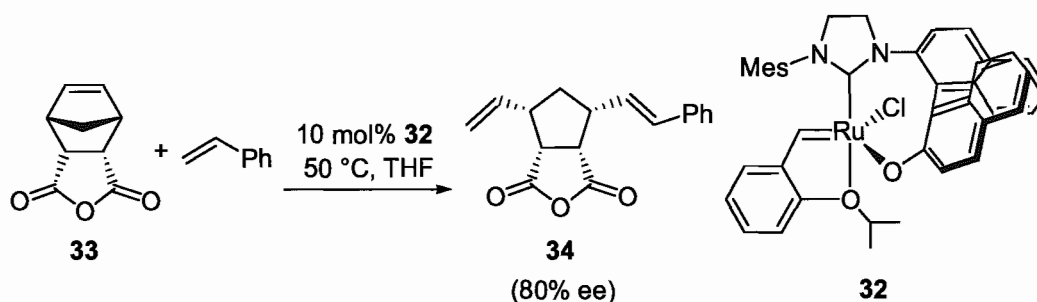
Metal-catalyzed olefin metathesis is always regarded as a powerful tool for the construction of carbon carbon double bonds in organic chemistry.<sup>62</sup> In 2001, Grubbs reported a chiral NHC-ruthenium alkylidene complex **29** which was shown to promote desymmetrization of trienes in up to 82% conversion to give a ring closing metathesis product **31** with 90% ee (**Scheme 9**).<sup>63</sup> The strategy for the chiral induction is based on a transfer of stereochemistry from the stereogenic centres of the backbone to the

*N*-substituents of the NHC through the *N*-aryl rings.



**Scheme 9.** Olefin metathesis catalyzed by Grubbs chiral NHC-Ru complex.

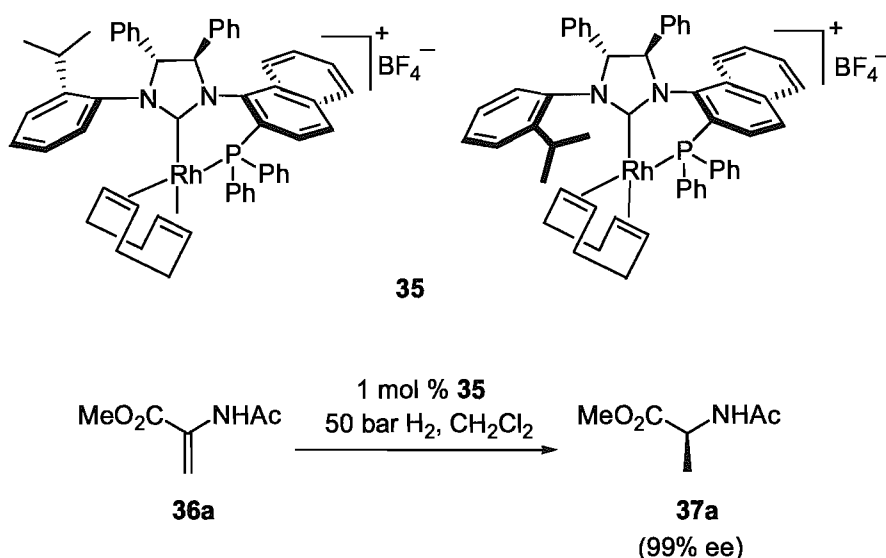
Prepared from an unsymmetrical NHC bearing a naphtholato donor by transmetalation with silver *in situ*, Hoveyda's metathesis catalyst **32** was tested in asymmetric ring opening cross-metathesis reaction (AROM) and provided almost exclusively *trans*-configuration (>98/2) and good enantioselectivity (80% ee, **Scheme 10**).<sup>64</sup>



**Scheme 10.** Asymmetric ring opening metathesis catalyzed by **32**.

Asymmetric hydrogenation has been well established and is becoming an effective method to make chiral compounds with high degree of enantiocontrol. In 2004, Helmchen's group synthesized a chiral bidentate ligand by replacement of one of the two

*N*-aryl groups of Grubb's imidazolinylienes with a 2-diphenylphosphinonaphth-1-yl unit, which was coupled with Grubbs' NHC to provide two isomers. The isomers reacted with Ag<sub>2</sub>O and [Rh(COD)Cl]<sub>2</sub> to yield two diastereomers **35**. The mixture of **35** was tested in the enantioselective hydrogenation of methyl 2-acetamidoacrylate to give 100% conversion and 99% ee of product **37a**.<sup>65</sup>

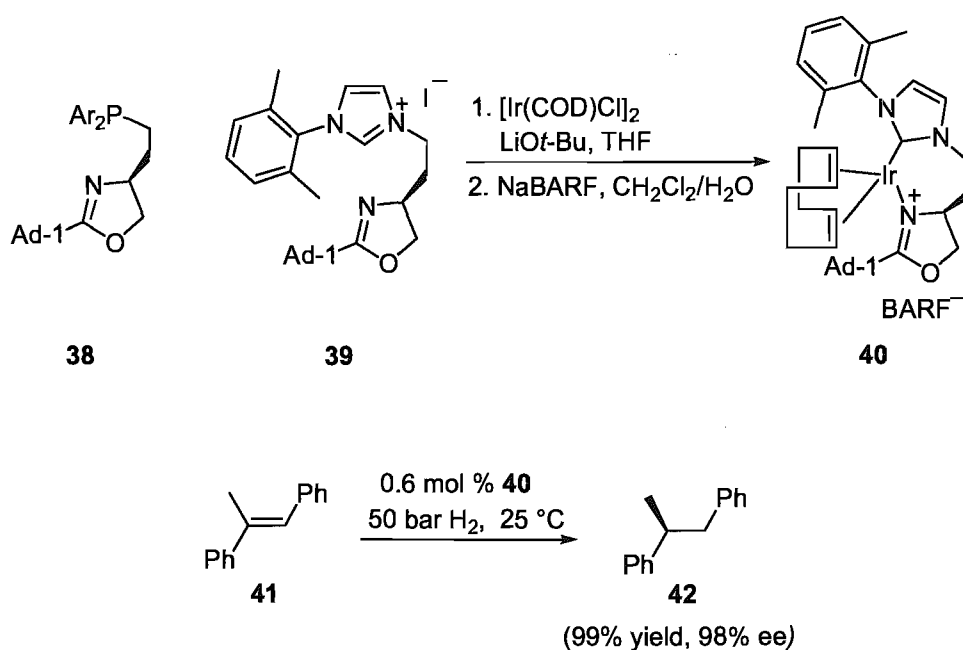


**Scheme 11.** Asymmetric hydrogenation by the mixture of diastereomers **35**.

Recently, Burgess designed a chiral NHC ligand as an analogue of his JM-PHOS ligand **38**<sup>66</sup> by replacement of the phosphine group with an imidazolium salt to provide **39**. The carbene, generated *in situ*, reacted with [Ir(COD)Cl]<sub>2</sub> followed by anion exchange with sodium tetrakis(3,5-bistrifluoromethylphenyl)borate (NaBARF) to give iridium complex **40**. The iridium complex **40** was investigated in asymmetric hydrogenation of (*E*)-1,2-diphenylpropene, reaching 99% yield and 98% ee at room

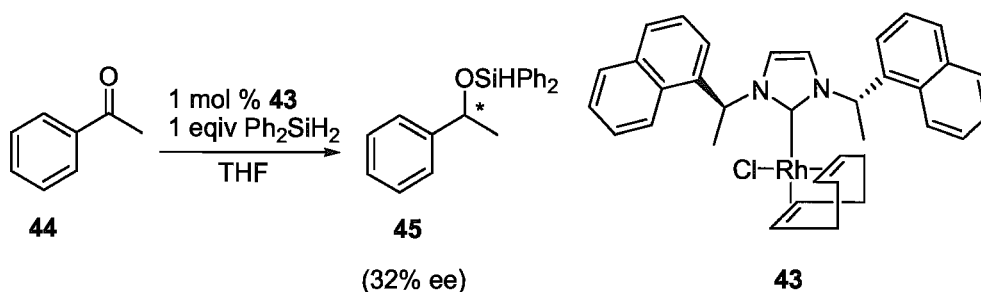


temperature and 50 bar H<sub>2</sub> (**Scheme 12**).<sup>67</sup>



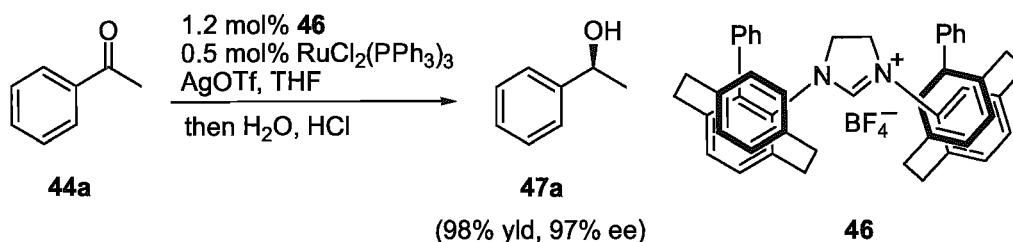
**Scheme 12.** Burgess' NHC-Ir catalyst and its application in asymmetric hydrogenation.

As an alternative to asymmetric hydrogenation, asymmetric hydrosilylation is also receiving much attention because the silylated product can be hydrolyzed easily under acidic or basic conditions to give the reduced product. Ruthenium, rhodium and iridium are usually used as the catalysts. Herrmann first investigated the stereoselective hydrosilylation of acetophenone with the chiral NHC-Ru complex **43**, which displayed moderate enantioselectivity (32% ee, **Scheme 13**).<sup>36</sup>



**Scheme 13.** The first example of asymmetric hydrosilylation.

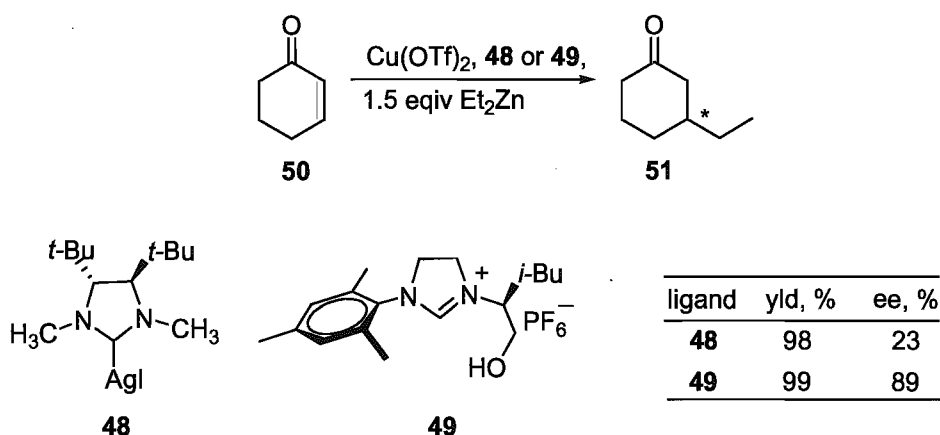
Excellent results were reported by Andrus for the same reaction, where he employed the planar chiral paracyclophane imidazolium salt **46** and  $\text{RuCl}_2(\text{PPh}_3)_3$  as the catalyst. The NHC-Ru complex formed *in situ* and led to 98% yield and 97% ee (**Scheme 14**).<sup>68</sup>



**Scheme 14.** Asymmetric hydrosilylation using chiral NHC ligand **46**.

Enantioselective NHC-copper-catalyzed 1,4-addition of dialkylzinc reagents to enones was first reported by Roland in 2001.<sup>69</sup> Based on the  $C_2$ -symmetric element containing the 1,2-di-*tert*-butyl ethylenediamine skeleton, the silver carbene compound **48** catalyzed the addition of diethylzinc to cyclohexenone in the presence of  $\text{Cu}(\text{OTf})_2$ , but the enantioselectivity only reached 23% ee. Four years later, Mauduit developed a new class of imidazolinyldene ligand **49**. This ligand was formed *in situ* by addition of

1,8-diazabicyclo[5.4.0]undec-7-ene (DBU) to the appropriate imidazolium precursor, and in the presence of  $\text{Cu}(\text{OTf})_2$  catalyzed the addition of diethylzinc to cyclohexenone in up to 89% ee (**Scheme 15**).<sup>70</sup>



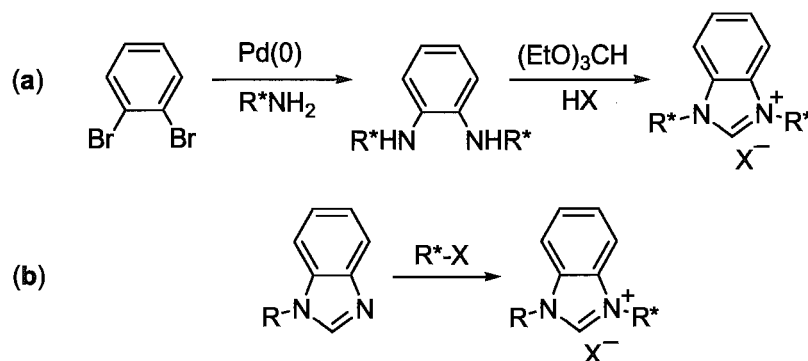
**Scheme 15.** Asymmetric 1, 4-addition catalyzed by NHC-copper complexes.

Surely, chiral NHCs and their metal complexes are still experiencing a rapid progress. With further investigation, more chiral NHC derivatives will certainly be developed and their use will lead to greater success in asymmetric catalysis.

## 1.6 Benzimidazolylienes

Though fundamental thermodynamic studies have shown that benzimidazolylienes behave intermediately between imidazolinylienes and imidazolylienes,<sup>71,72</sup> benzimidazolylienes are not well developed as ligands in transition metal-catalyzed

transformations. This is probably because existing methodology used to make imidazolylienes and their saturated analogues is less applicable for the preparation of chiral benzimidazolylienes.<sup>8</sup> For example, the common way of making chiral imidazolylienes by condensation of glyoxal, a chiral primary amine and paraformaldehyde is not possible for benzimidazolylienes. To date, most reported chiral benzimidazolium salts are prepared by the introduction of a chiral substituent  $\alpha$  to nitrogen by aryl amination (for example, Figure 1, **C**<sup>73</sup>) or direct *N*-alkylation (**Scheme 16**).



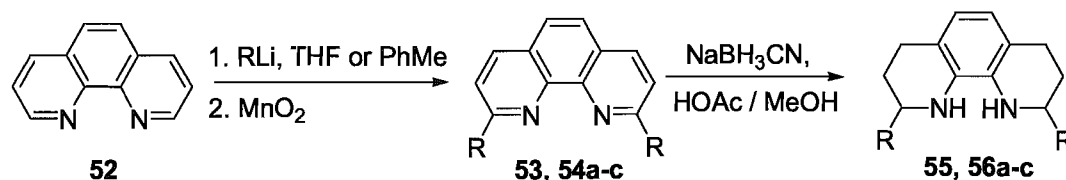
**Scheme 16.** Aryl amination and *N*-alkylation routes to prepare benzimidazolium salts.

Recently, Shi's group synthesized a binaphthyl dibenzimidazolium salt, which complexed with ruthenium and palladium, providing high enantioselectivities (up to 98% ee) in the hydrosilylation of acetophenone<sup>74</sup> and conjugate addition of arylboronic acids to cyclic enones.<sup>75</sup> Except for this ligand, to the best of our knowledge, few reported benzimidazolylienes so far gave good chiral induction in asymmetric catalysis. The reason is probably that the rapid internal rotation of the chiral substituent around the C-N axis leads to the active chiral space at the metal center being relatively poorly

defined.<sup>76</sup> Based on that, new approaches towards the preparation of benzimidazolium salts with rigid chiral architectures may result in useful ligands for asymmetric catalysis.

### 1.7 Benzimidazolylienes Derived from Substituted 1,10-Phenanthrolines

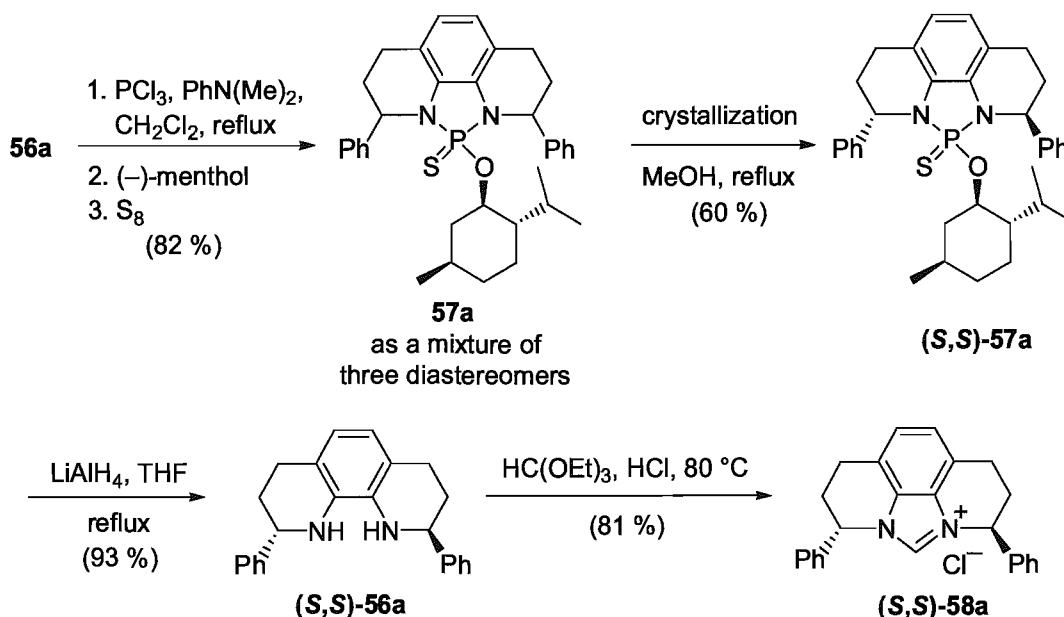
1,10-phenanthroline and its derivatives have a long history as nitrogen donor ligands in transition-metal catalysis,<sup>77</sup> but their reduced pyridyl forms, substituted and unsubstituted octahydrophenanthrolines, received little attention as precursors for new ligands. Previously, several routes to synthesize phenanthroline-derived chiral NHC ligands were developed by our group. Treatment of 1,10-phenanthroline with an excess of an organolithium reagent, followed by oxidation with MnO<sub>2</sub>, provided 2,9-disubstituted phenanthrolines (**54a-c**). These compounds were reduced with NaBH<sub>3</sub>CN in acetic acid/methanol to yield octahydrophenanthrolines as 1:1 mixtures of *meso/rac* stereoisomers (**56a-c**, Scheme 17).<sup>8</sup>



R	53, 54a-c, yld, %	55, 56a-c, yld, %
H	53, NA	55, 42
Ph	54a, 61	56a, 63
<i>n</i> -Bu	54b, 76	56b, 63
Me	54c, 76	56c, 57

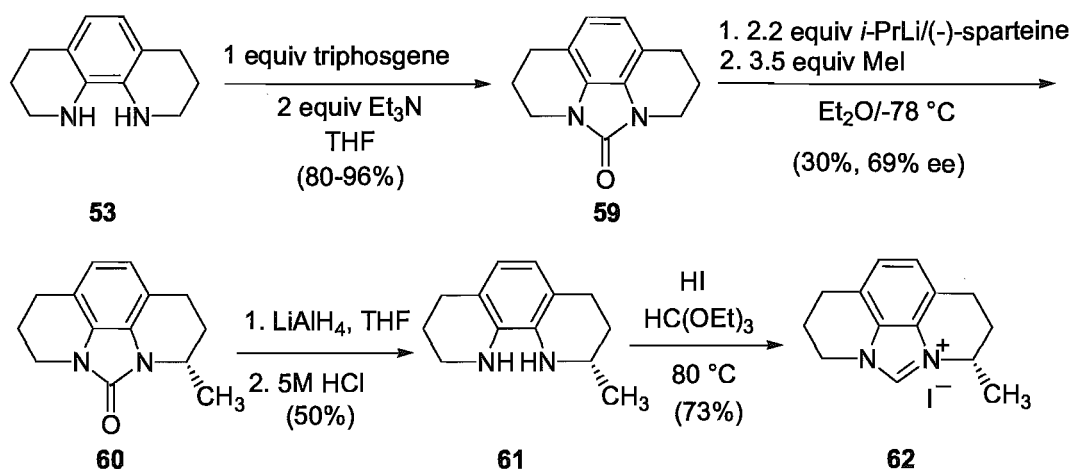
**Scheme 17.** Preparation and reduction of 2,9-disubstituted phenanthrolines.

The racemic  $C_2$ -symmetric reduction mixture **56a** was resolved by converting them to covalent diastereomers **57a** using  $\text{PCl}_3$ , (–)-menthol and sulfur.<sup>78</sup> Crystallization in hot methanol solution afforded pure diastereomer (*S,S*)-**57a**. Removal of the chiral auxiliary gave optically pure diamine (*S,S*)-**56a**, which was converted to chiral benzimidazolium salt (*S,S*)-**58a** by reaction with triethylorthoformate and one equivalent of hydrochloride acid (Scheme 18).



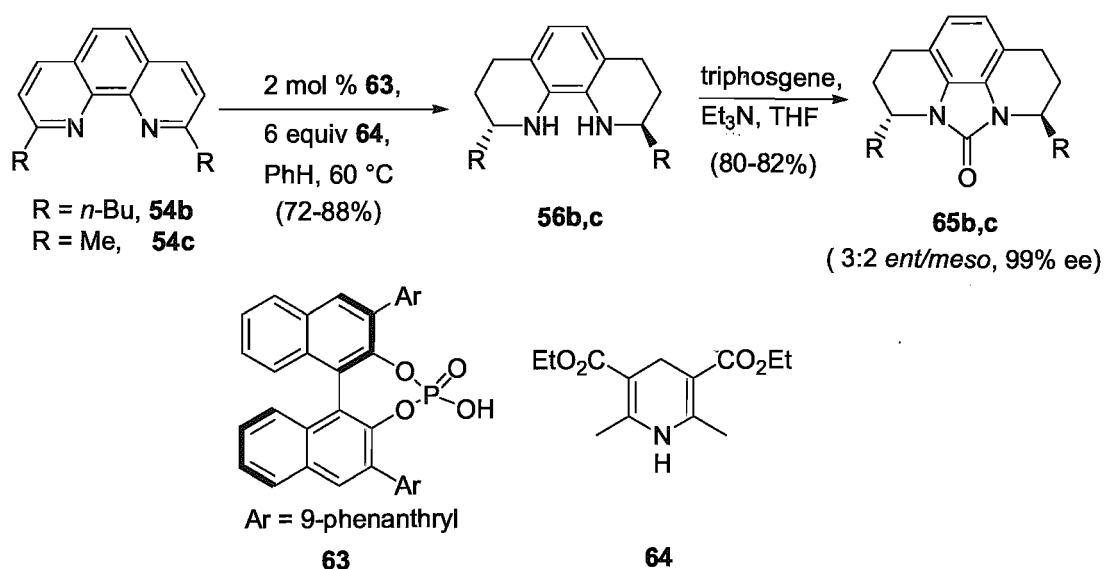
**Scheme 18.** Resolution of racemic 2,9-diphenyloctahydrophenanthrolines.

Another method to introduce chirality at  $\alpha$  to nitrogen position of phenanthroline core involved asymmetric lithiation of urea **59** by *i*-PrLi-(–)-sparteine at  $-78^\circ\text{C}$  followed by electrophilic substitution using MeI.<sup>79</sup> 25-30% yields and 69% ee for **60** was obtained. **60** could be hydrolyzed by  $\text{LiAlH}_4$  to give back to octahydrophenanthroline **61**. Ring closure by  $\text{HC(OEt)}_3/\text{HI}$  afforded the chiral benzimidazolium salt **62** (Scheme 19).



**Scheme 19.** Asymmetric synthesis of a phenanthroline-derived benzimidazolium salt.

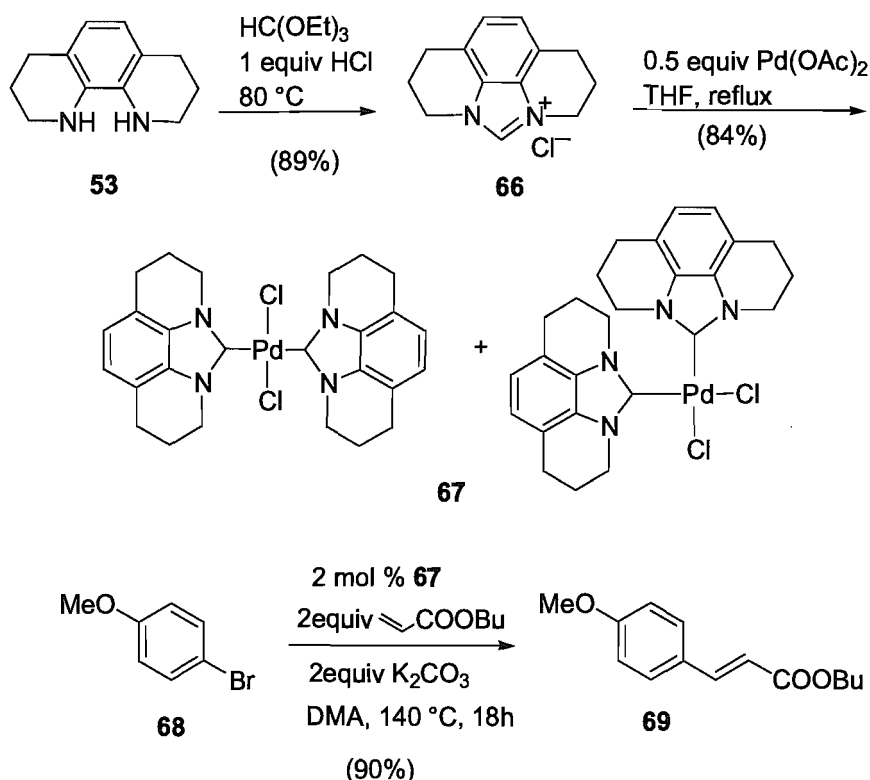
Recently, asymmetric reduction of 2,9-disubstituted phenanthrolines using diethyl-1,4-dihydro-2,6-dimethylpyridine-3,5-dicarboxylate **64** as a Hantzsch dihydropyridine (HDHP) reducing agent in the presence of a BINOL-derived phosphoric acid catalyst **63** was reported by our group.<sup>80</sup> The reduction of 2,9-disubstituted 1,10-phenanthrolines **54b** and **54c** (R = *n*-butyl, Me) gave a 3:2 mixture of *ent* and *meso* isomers, which could be converted to urea adducts for easy separation of the stereoisomers by column chromatography. Chiral HPLC analysis of the urea adducts **65b** and **65c** returned a value of 99% ee for enantiomers **56b** and **56c** (Scheme 20). In contrast, reduction of the 2,9-diphenyl-1,10-phenanthroline **56a** under the same conditions provided only the tetrahydro reduction product with low 25% ee, which implied that this asymmetric reduction method was not applicable for preparation of chiral diaryl substituted octahydrophenanthrolines.



**Scheme 20.** Asymmetric reduction of 2,9-dialkyl-1,10-phenanthrolines.

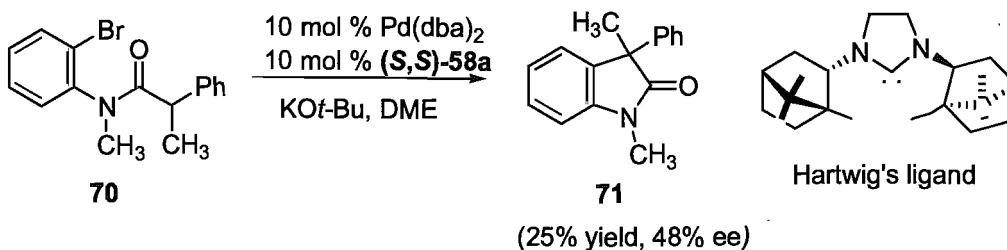
Applications of phenanthroline-derived NHC ligands were first reported in 2004.<sup>81</sup> Achiral octahydrophenanthroline **53**, which is turned into benzimidazolium salt **66** by ring closure in the presence of triethylorthoformate and HCl, was treated with  $\text{Pd}(\text{OAc})_2$  in THF to generate a *cis/trans* NHC-Pd mixture **67**. The *cis/trans* complexes **67** were employed to catalyze Heck reactions in about 90% yield (Scheme 21).<sup>81</sup>





**Scheme 21.** Phenanthroline-derived NHC-Pd complex synthesis and their application.

Palladium-catalyzed oxindole synthesis by amide  $\alpha$ -arylation was investigated using *in situ*-generated chiral carbene ligand in 2007.<sup>82</sup> Substrate **70** was stirred with 10 mol %  $\text{Pd(dba)}_2$ , 10 mol % benzimidazolium salt (*S,S*)-**58a** and 1.5 equivalents of  $\text{KO}t\text{-Bu}$  in DME at  $50^\circ\text{C}$  for 15 h, generating chiral oxindole **71** in 25% yield and 48% ee (**Scheme 22**). Although the yield was low, the selectivity was similar to that observed by Hartwig using a different chiral NHC ligand (57% ee).<sup>83</sup>



**Scheme 22.** Palladium-catalyzed  $\alpha$ -arylation using chiral ligand (*S,S*)-**58a**.

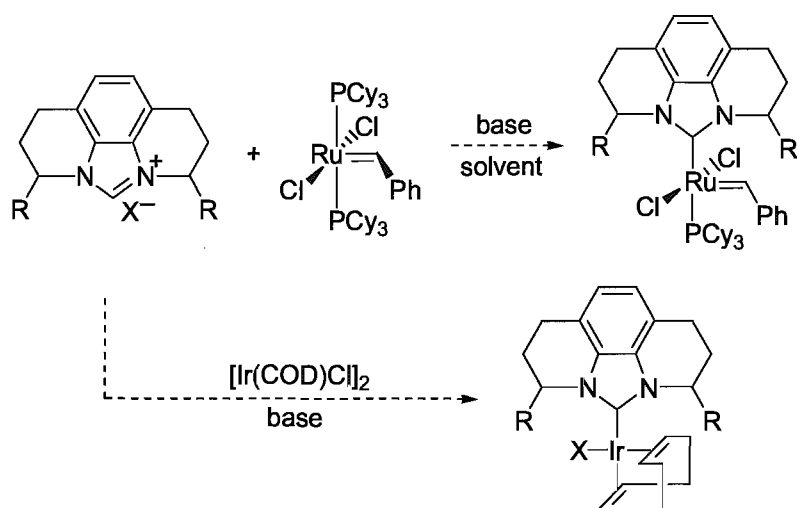
The preceding results encouraged us to do more research in transition metal catalysis. The successful synthetic routes to make chiral benzimidazolylidenes derived from 1,10-phenanthroline provided us a good opportunity to prepare more chiral NHC ligands and to test their applications in metal catalytic transformations. The results in those aspects will be described in this thesis.

## 1.8 Aims and Objectives

A series of sterically bulky groups, including 2-methylphenyl, 2-methoxyphenyl, ferrocenyl, will be introduced to 2,9 positions of 1,10-phenanthroline. The resulting NHC ligands will be used for the preparation of transition metal compounds, and the potential of these complexes in catalysis will be investigated.

Reduction of 2,9-disubstituted 1,10-phenanthrolines to the corresponding octahydrophenanthrolines will be investigated using different methods such as  $\text{NaBH}_3\text{CN}$  in  $\text{HOAc/MeOH}$ , high pressure hydrogenation or sodium metal in alcoholic media, etc.

Synthesis of chiral and achiral NHC-metal complexes and their applications will be the emphasis in this thesis. Attempts to prepare NHC-Ru and NHC-Ir complexes by treatment of phenanthroline-derived benzimidazolium salts with Grubbs' first generation catalyst and  $[\text{Ir}(\text{COD})\text{Cl}]_2$  respectively will be described (**Scheme 23**). These complexes are expected to show catalytic activities and enantioselectivities in asymmetric catalysis.



**Scheme 23.** Synthesis of benzimidazolylidene-metal complexes.

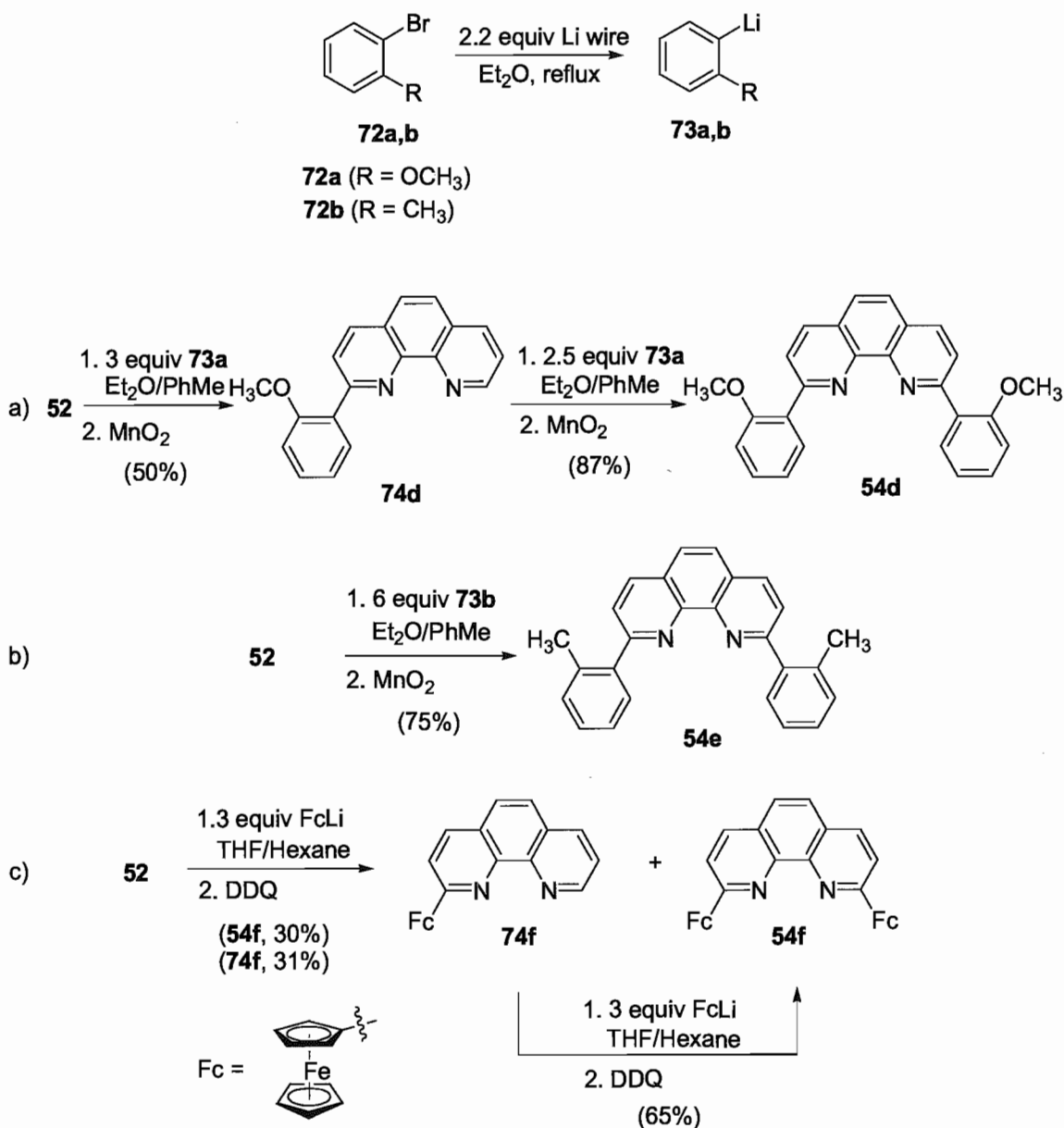
## 2. Results and Discussion

### 2.1 Synthesis of Chiral and Achiral Benzimidazolium Salts Derived from 1,10-Phenanthroline

#### 2.1.1 Preparation of 2,9-Disubstituted 1,10-Phenanthrolines

2,9-Disubstituted 1,10-phenanthrolines can be prepared by nucleophilic aromatic substitution and oxidation.<sup>84</sup> In this manner, treatment of 1,10-phenanthroline **52** with 3 equivalents of 2-lithioanisole **73a** (prepared from 2-bromoanisole and freshly cut lithium)<sup>85</sup> followed by MnO<sub>2</sub> oxidation afforded monosubstituted product **74d**, which was subsequently treated with 2-lithioanisole and MnO<sub>2</sub> yielding 2,9-di(2-methoxyphenyl)phenanthroline **54d** in 44% overall yield. Treatment of 1,10-phenanthroline **52** with 6 equivalents of 2-lithiotoluene **73b** (also prepared from 2-bromotoluene and freshly cut lithium)<sup>86</sup> in toluene followed by MnO<sub>2</sub> oxidation gave directly 2,9-di(2-methylphenyl)phenanthroline **54e** in 75% yield. The preparation of 2,9-diferrocenylphenanthroline required isolated lithioferrocene (FcLi)<sup>87</sup> and 2,3-dichloro-5,6-dicyanobenzoquinone (DDQ) as oxidants. The reaction afforded desired 2,9-diferrocenylphenanthroline **54f** (30%), along with 31% monoferrocenyl phenanthroline **74f** when 3 equivalents of FcLi was used. The isolated 2-substituted product **74f** could be transformed to the desired **54f** in 65% yield in a separate reaction

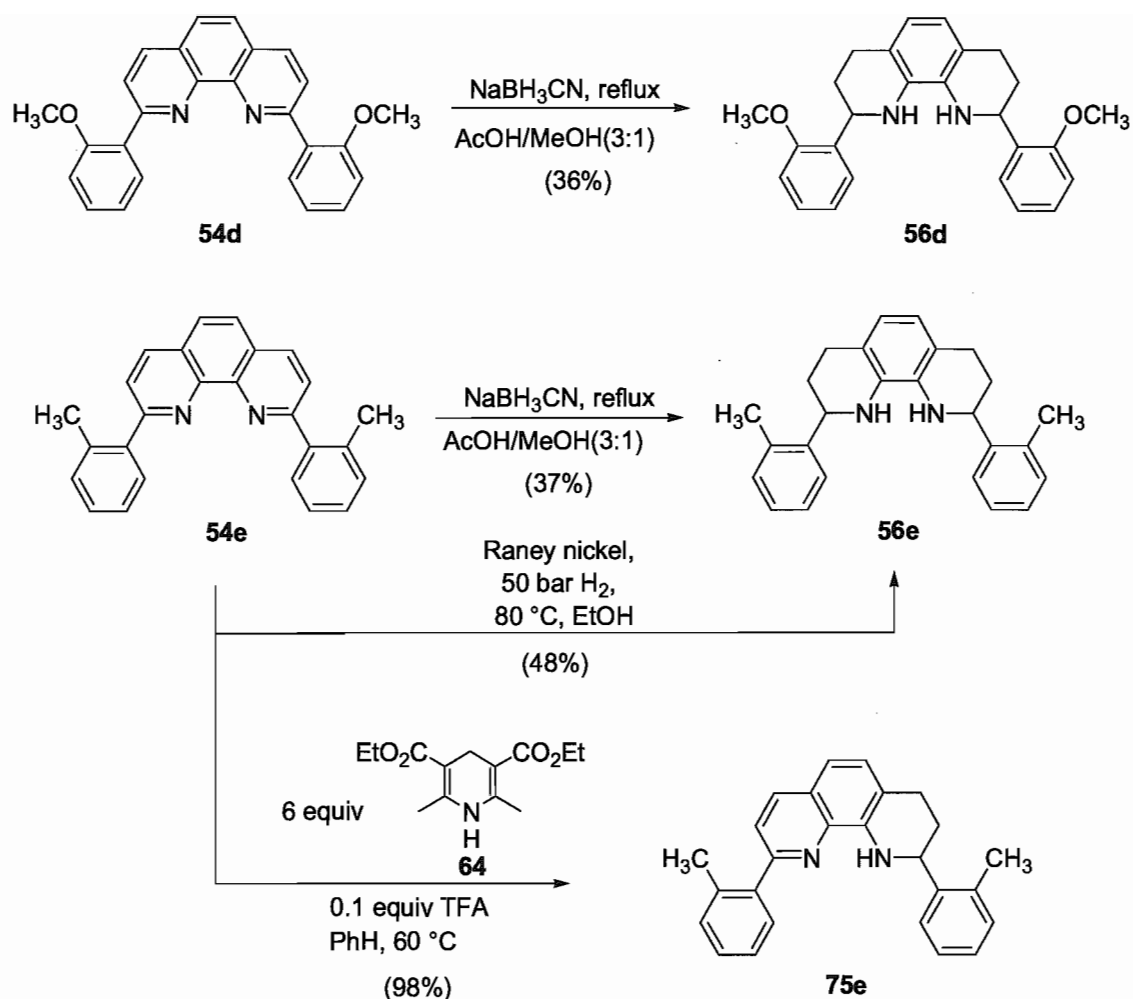
with 2 equivalents of lithioferrocene and 1 equivalent of DDQ at room temperature (Scheme 24).



**Scheme 24.** Synthesis of bulky 2,9-disubstituted-1,10-phenanthrolines.

### 2.1.2 Reduction of 2,9-Disubstituted 1,10-Phenanthrolines

Reduction of 2,9-disubstituted 1,10-phenanthrolines to the corresponding octahydrophenanthrolines by  $\text{NaBH}_3\text{CN}$  in  $\text{AcOH}/\text{MeOH}$  was developed by our group in 2006.<sup>8</sup> For compound **54d** and **54e**, low yields (36% and 37% respectively) of the mixture of *rac/meso* isomers **56d** and **56e** were obtained under these conditions ( $\text{NaBH}_3\text{CN}$ ,  $\text{HOAc}/\text{MeOH}=3:1$ ). Several other approaches were attempted to reduce these sterically demanding substituted phenanthrolines in order to obtain better yields. First, **56e** was obtained in higher yield (48%) using Raney nickel in ethanol as the catalyst under 50 bar hydrogen,<sup>88</sup> but the high pressure required and moderate yield obtained limited the practicality of this method. Second, reduction of **54e** with diethyl-1,4-dihydro-2,6-dimethylpyridine-3,5-dicarboxylate **64** in the presence of catalytic TFA<sup>89</sup> gave only the corresponding tetrahydro reduction product **75e**, though the yield was excellent (98%).

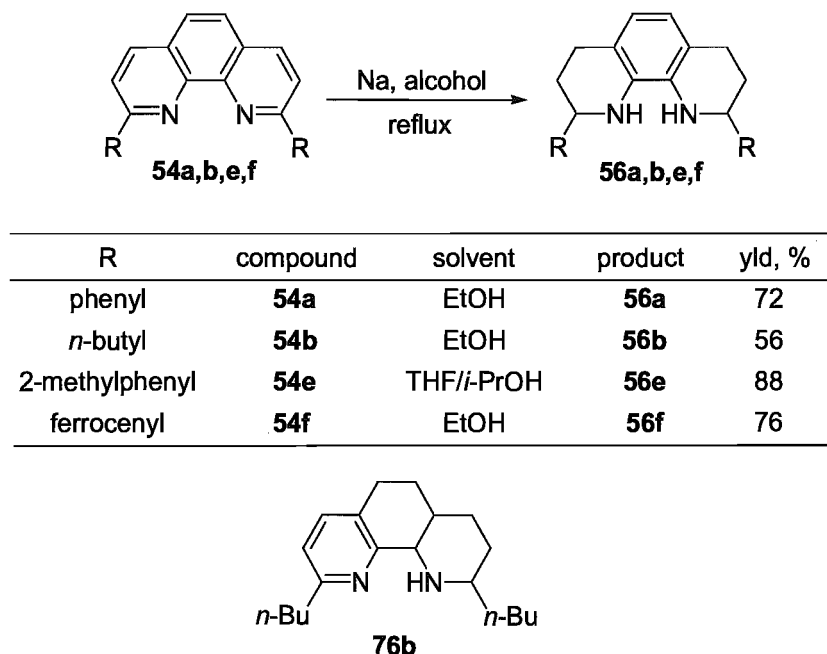


**Scheme 25.** Reduction of 2,9-disubstituted phenanthrolines using different methods.

A significant improvement was observed using sodium in alcohol as the reducing medium.<sup>90</sup> Thus, 2,9-diaryl-1,10-phenanthrolines such as **54a,e,f** (R=Ph, 2-methylphenyl, Fc) were reduced smoothly to give 2,9-diaryloctahydrophenanthrolines **56a,e,f** as 1:1 mixtures of *meso* and *rac* stereoisomers. Specifically, addition of sodium to a solution of **54a** and **54e** in abs. EtOH gave **56a** and **56e** in 72% and 88% yield respectively. In a similar manner, 2,9-diferrocenyl-1,10-phenanthroline **54f** was reduced to the corresponding octahydrophenanthroline **56f** in 76% yield using sodium in THF/*i*-PrOH

(Scheme 26). This reduction route was particularly useful for **54f**, which would be expected to decompose under exposure to hot acetic acid or TFA needed for NaBH<sub>3</sub>CN or HDHP reduction protocols.

A limitation to this procedure was observed in the reduction of 2,9-dibutyl-1,10-phenanthroline **54b**, which appeared to give the mixture of two octahydrophenanthrolines **56b** and **76b** in 4:1 ratio probably as a result of lower radical stability  $\alpha$  to nitrogen as compared to the 2,9-diaryl adducts.



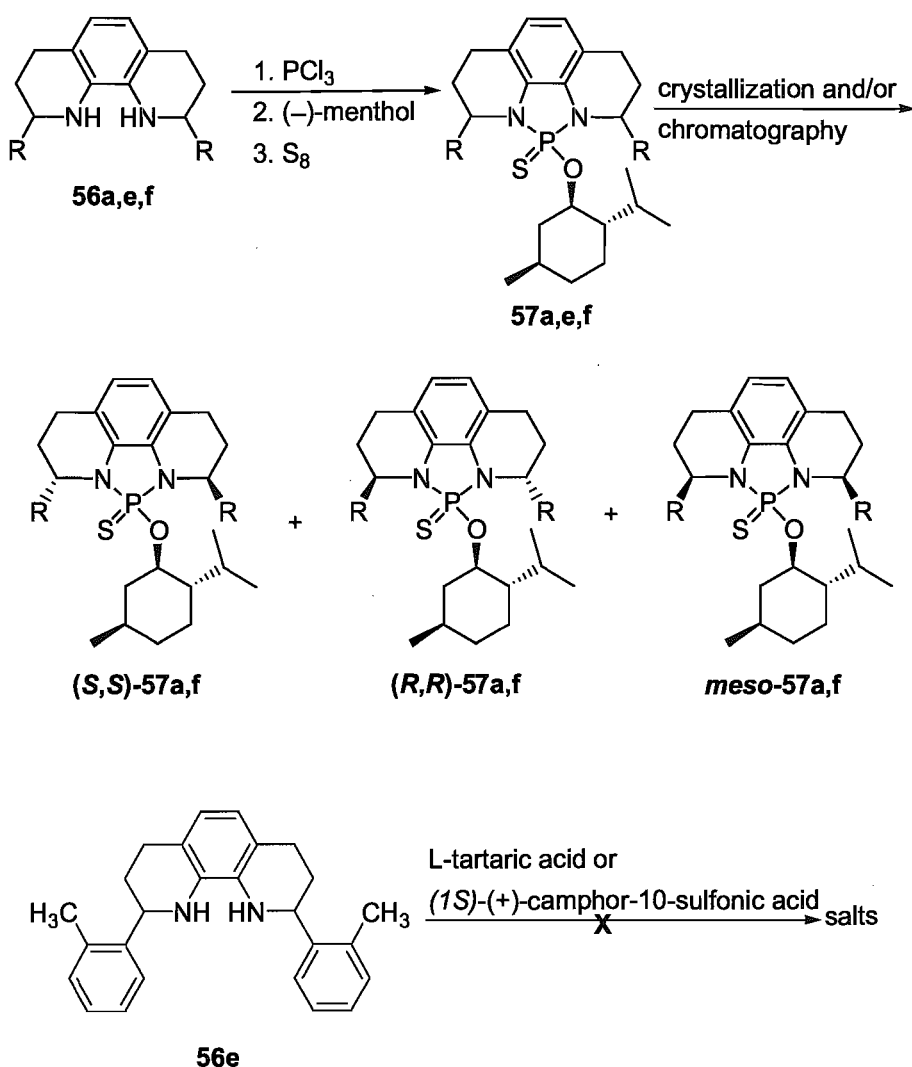
**Scheme 26.** Reduction of 2,9-disubstituted phenanthrolines using Na/alcohol.

### 2.1.3 Resolution of 2,9-Disubstituted 1,10-Octahydrophenanthrolines

Previously, our group demonstrated that the Herrmann procedure<sup>78</sup> could be used to



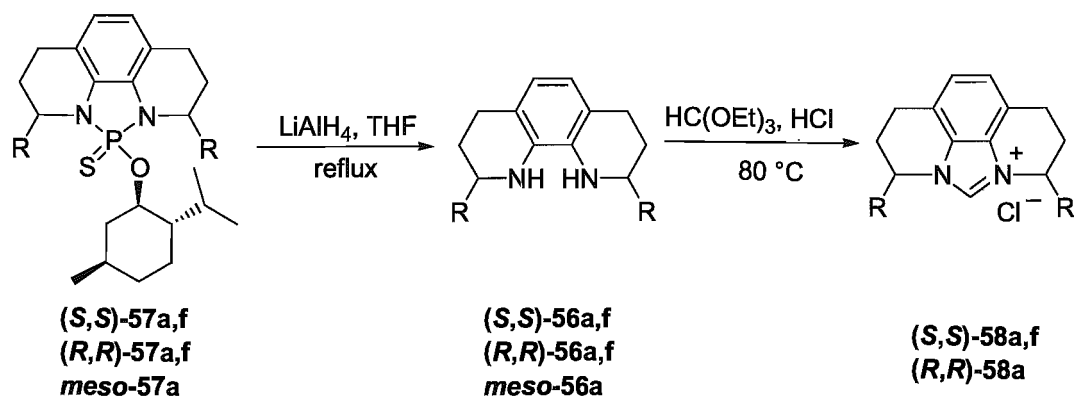
resolve 2,9-diphenyloctahydrophenanthroline **56a**. This procedure was repeated for other diaryl octahydrophenanthrolines **56d,e,f**. The *rac/meso* diamines **56e** or **56f** were sequentially reacted with PCl<sub>3</sub>, (-)-menthol and sulfur in one pot to give the phosphorous adduct mixture **57e** and **57f**. Unfortunately, the phosphorous(V) adduct **57d** failed to form. It was found that the 2,9-diferrocenyloctahydrophenanthroline mixture **57f** could be separated by column chromatography to give three pure diastereoisomers (*S,S*)-**57f**, (*R,R*)-**57f** and *meso*-**57f**. Verification of their stereochemical purity was confirmed by <sup>31</sup>P NMR analysis, which also established their order of elution ( $\delta$  66.1,  $\delta$  65.3 and  $\delta$  74.5). For **57a**, crystallization from hot methanol solution afforded diastereoisomer (*S,S*)-**57a**. Further careful column chromatography of the remaining uncrystallized material resulted in (*R,R*)-**57a** and *meso*-**57a**. Notably, the (*R,R*)-**57a** was not previously isolated.<sup>8</sup> For the mixture **57e**, several methods such as crystallization from different solvents (MeOH, EtOH, EtOAc, hexane/Et<sub>2</sub>O, MeOH/H<sub>2</sub>O, etc) or column chromatography could not give the desired pure diastereomer product. Attempts to prepare ammonium salts for **56e** using L-tartaric acid or (*1S*)-(+)-camphor-10-sulfonic acid were also unsuccessful.



**Scheme 27.** Resolution of *rac/meso* 2,9-disubstituted octahydrophenanthrolines.

#### 2.1.4 Synthesis of Chiral Benzimidazolium Salts

Treatment of pure phosphorous adduct diastereomers **57a,f** with  $\text{LiAlH}_4$  in refluxing THF gave free chiral diamines **56a,f** in good yields (75-87%). Enantiomerically pure diamines **(S,S)-57a,f** and **(R,R)-57a** were reacted with  $\text{HC}(\text{OEt})_3$  and  $\text{HCl}$  to afford the corresponding benzimidazolium salts [**(S,S)-58a,f** and **(R,R)-58a**, Scheme 28)].



R	compound	diamine, yld, %	salts, yld, %
phenyl	<b>(S,S)-57a</b>	<b>(S,S)-56a</b> , 79	<b>(S,S)-58a</b> , 85
phenyl	<b>(R,R)-57a</b>	<b>(R,R)-56a</b> , 78	<b>(R,R)-58a</b> , 84
ferrocenyl	<b>(S,S)-57f</b>	<b>(S,S)-56f</b> , 84	<b>(S,S)-58f</b> , 59
ferrocenyl	<b>(R,R)-57f</b>	<b>(R,R)-56f</b> , 75	<b>(R,R)-58f</b> , -
ferrocenyl	<b>meso-57f</b>	<b>meso-56f</b> , 87	<b>meso-58f</b> , -

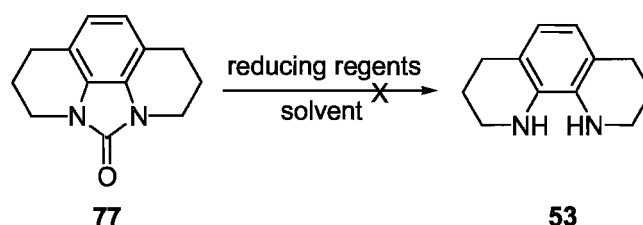
**Scheme 28.** Synthesis of rigid chiral benzimidazolium salts.

### 2.1.5 Hydrolysis of Ureas to Octahydrophenanthrolines

Asymmetric reduction of 2,9-dialkyl phenanthrolines **54b,c** using a Hantzsch dihydropyridine (HDHP) **64** in the presence of catalytic BINOL-derived phosphoric acid afforded optically pure enantiomers **56b,c** (99% ee) when their corresponding urea adducts **65b,c** were measured by chiral HPLC (Scheme 20).<sup>80</sup> The results provided an alternative route to make additional chiral 2,9-dialkyl-1,10-octahydrophenanthrolines if the five-membered ring of the urea adducts **65b,c** can be opened to generate the optically pure amines by appropriate reducing reagents.

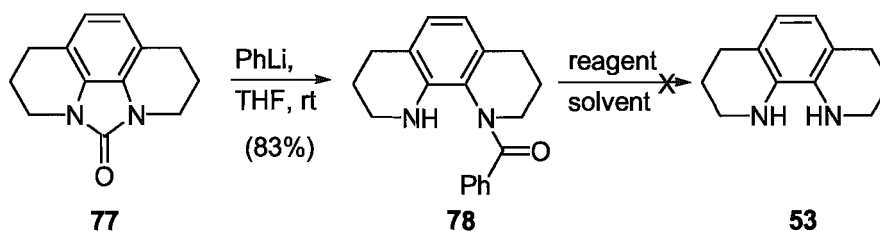
Unsubstituted urea **77** was chosen as a model to try this reaction because of its ready

availability by treatment of **53** with triphosgene. Several reagents such as super hydride ( $\text{LiBHEt}_3$ ), lithium pyrrolidinoborohydride ( $\text{LiBH}_3\text{Pyr}$ ),<sup>90</sup> and  $\text{NaNH}_2$  were employed, but no desired products were observed (**Scheme 29**). However, treatment of **77** with  $\text{PhLi}$  afforded the amide **78**. Further attempt to convert **78** to amine using different reagents were unsuccessful (**Scheme 30**), although the reactivity of Schwartz's reagent ( $(\text{C}_5\text{H}_5)_2\text{ZrHCl}$ ) with other secondary and tertiary amides offers hope that **53** can be derived from **78**. Studies in the lab are ongoing.



reagent	equiv	solvent	T, °C
$\text{LiBHEt}_3$	1	THF	25
$\text{LiH}_3\text{BPyr}$	1	THF	66
$\text{NaNH}_2$	2.5	dimethylaniline	35

**Scheme 29.** Attempts at converting urea **77** to octahydrophenanthroline **53**.



reagent	equiv	solvent	T, °C
$\text{LiBHEt}_3$	1.1	THF	66
$\text{LiH}_3\text{BPyr}$	4	THF	66
50% $\text{H}_2\text{SO}_4$	20	$\text{H}_2\text{O}$	100

**Scheme 30.** Ring-opening of urea **77** to benzamide **78**.

## 2.2 Synthesis and Applications of Benzimidazolylidene-metal Complexes

### 2.2.1 Attempts to Make NHC-Ru Alkylidene Complexes

Previously, our group tested the efficiency of NHC precursor (*S,S*)-**58a** in palladium-catalyzed oxindole synthesis, which provided oxindole **71** in 48% ee.<sup>82</sup> The result also encouraged the development of catalysts with other metals such as ruthenium and iridium.

Ruthenium complexes have established themselves as powerful catalysts in olefin metathesis and have evolved significantly in recent years. In particular, Grubbs' second generation catalyst, containing one NHC ligand, further spurred the development of NHC-Ru complexes. For example, Collins<sup>92</sup> recently designed a new NHC-ruthenium alkylidene complex **79** in which the ligand has *C*<sub>1</sub>-symmetry based on Grubbs' chiral catalysts **29**. The bulkier *tert*-butyl group was chosen for the 4,5 positions of the imidazoline ring in order to increase the effectiveness of the chiral transfer by restricting the conformation of the arene. The difficulties encountered in preparation of a *C*<sub>2</sub>-symmetric analogue of this ligand forced the use of a small *N*-methyl group. This *C*<sub>1</sub>-symmetric catalyst showed good reactivity and up to 95% ee was obtained in asymmetric ring-closing olefin metathesis (ARCM) reactions. In 2001, The Diver group synthesized a chiral benzimidazolylidene-Ru complex **80**, but the catalyst provided little activity in tandem dienyne cross-metathesis/ring-closing metathesis between propargyl

benzoate and 1,5-hexadiene.<sup>73</sup>

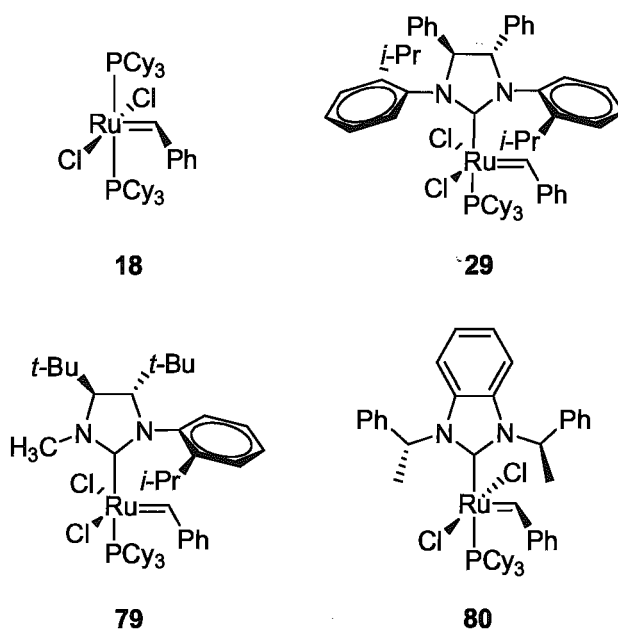


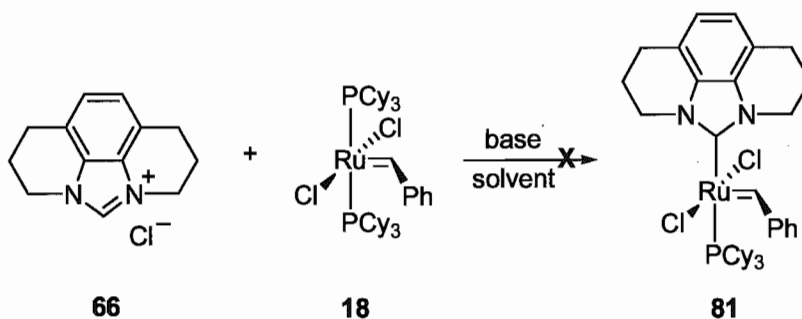
**Figure 4.** Examples of NHC-Ru alkylidene catalysts for olefin metathesis.

Comparison of **80** to Grubbs' chiral catalyst **29** and Collins' catalyst **79** shows that a catalyst **83** with our diphenyl ligand (*S,S*)-**58a** may have similar electronic properties as **29**, **79** and **80**, but with the advantage of increased rigidity. Notably, **29** and **79** can also be considered to be aniline derivatives like **83**, but with the relative position of the chiral centers and the aromatic ring reversed.

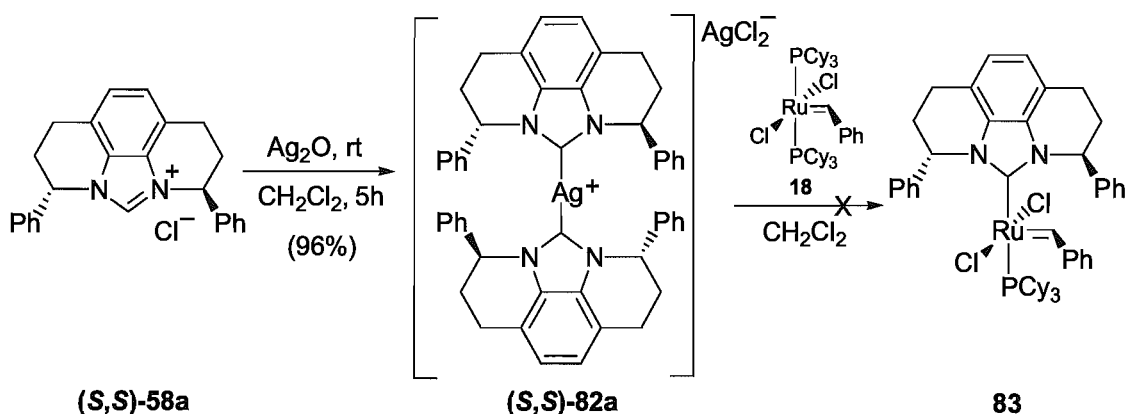
Unfortunately, attempts to complex Grubbs' first generation catalyst **18** using our phenanthroline-derived benzimidazolyliidenes formed *in situ* with a base were unsuccessful. Reactions were carried out using Diver and Smulik's procedure.<sup>93</sup> Different temperatures, various solvents (THF, hexane or toluene) and bases including KN(SiMe<sub>3</sub>)<sub>2</sub>, KO*t*-Bu and potassium 1,1,1,3,3,3-hexafluoro-2-methyl-2-propoxide were

investigated, but no desired product was observed. Transmetalation from NHC-silver complex (*S,S*)-**82a** to ruthenium with **18** in CH<sub>2</sub>Cl<sub>2</sub> also failed (**Scheme 31**). Curiously, the color changes observed during the reaction (from purple to dark brown) matched Smulik's report<sup>93</sup> for **80**. However, the reaction mixture turned black quickly during the isolation and purification process (precipitation or column chromatography on TSI silica gel). This occurred even in an inert atmosphere indicating that the putative NHC-Ru complex was unstable.

A survey of the literature has not revealed the successful synthesis of any Ru-alkylidene complexes with annulated NHC ligands. Thus, there may be an inherent problem with the steric demand of these ligands. For complexes **81** and **83**, the C-N bonds which are locked in the piperidyl rings may lead to a forced steric interaction between the  $\alpha$  to nitrogen position and a chloride or alkylidene group of the ruthenium catalyst. The steric crowding might greatly decrease the stability of the pentacoordinate NHC-Ru complexes.



X	base	T, °C	solvent
Cl	KOt-Bu	-78-25	THF/toluene
Cl	KOt-Bu	-78-25	toluene
Cl	KN[Si(CH <sub>3</sub> ) <sub>3</sub> ] <sub>2</sub>	-78-25	THF/toluene
Cl	KN[Si(CH <sub>3</sub> ) <sub>3</sub> ] <sub>2</sub>	-20-25	THF/toluene
Cl	KOC(CH <sub>3</sub> )(CF <sub>3</sub> ) <sub>2</sub>	-78-25	toluene
BF <sub>4</sub>	KOt-Bu	-30-25	hexane
BF <sub>4</sub>	KOt-Bu	-78-25	THF/toluene
BPh <sub>4</sub>	KOt-Bu	-20-25	toluene



**Scheme 31.** Attempts to prepare benzimidazolyliene-Ru alkylidene complexes.

### 2.2.2 Synthesis of Benzimidazolyliene-Ir Complexes

The area of NHC-iridium catalysis has been gaining much attention in recent years.<sup>94-96</sup> The iridium catalysts prepared by replacement of phosphine ligands with NHCs based on Crabtree's catalyst<sup>97</sup> show generally high activity in olefin hydrogenation.<sup>96</sup> Further improvement can be realized when non-coordinating tetrakis[3,5-bis(trifluoromethyl)phenyl]borate (BARF) anions<sup>98,99</sup> are used in cationic iridium complexes. An example is **84** (Figure 6), which at a catalyst loading of 0.1



mol % catalyzed hydrogenation of a tetrasubstituted alkene (2,3-dimethylbut-2-ene) with 100% yield at 1 atm hydrogen and room temperature.<sup>96</sup>

The development of chiral versions of NHC-Ir complexes for enantioselective catalysis is a logical extension. In 2006, Herrmann's group synthesized a chiral NHC-Ir catalyst **85**, which was tested in transfer hydrogenation of acetophenone with 2-propanol as hydrogen source. The reaction gave products in only 24% ee.<sup>78</sup> One year later, a substituted analogue was designed by the same group and the monodentate iridium complex **86** was used in asymmetric hydrogenation of methyl 2-acetamidoacrylate, yielding up to 67% ee.<sup>76</sup>

Relatively few examples of chiral benzimidazolylidene-Ir complexes have been reported in asymmetric catalysis. Shi and Duan synthesized an axially chiral monodentate NHC-Ir complex **87** derived from BINAM, but no applications were reported for this complex.<sup>100</sup> In 2003, Chung synthesized complex **88**, which displayed moderate stereoselectivity (53% ee) in transfer hydrogenation of 4'-methylacetophenone. Some analogues of **88** gave much lower enantioselectivities.<sup>39</sup>

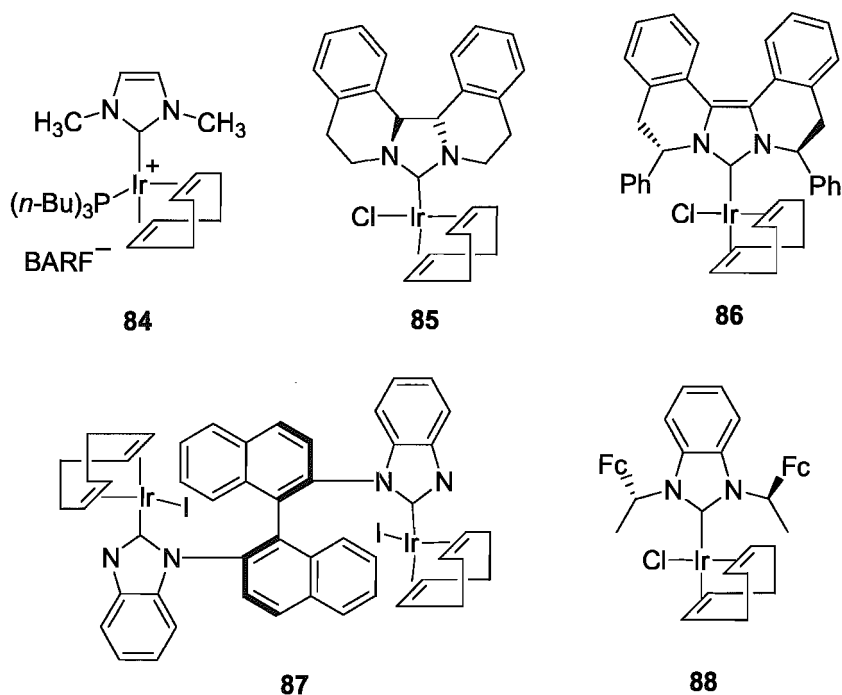
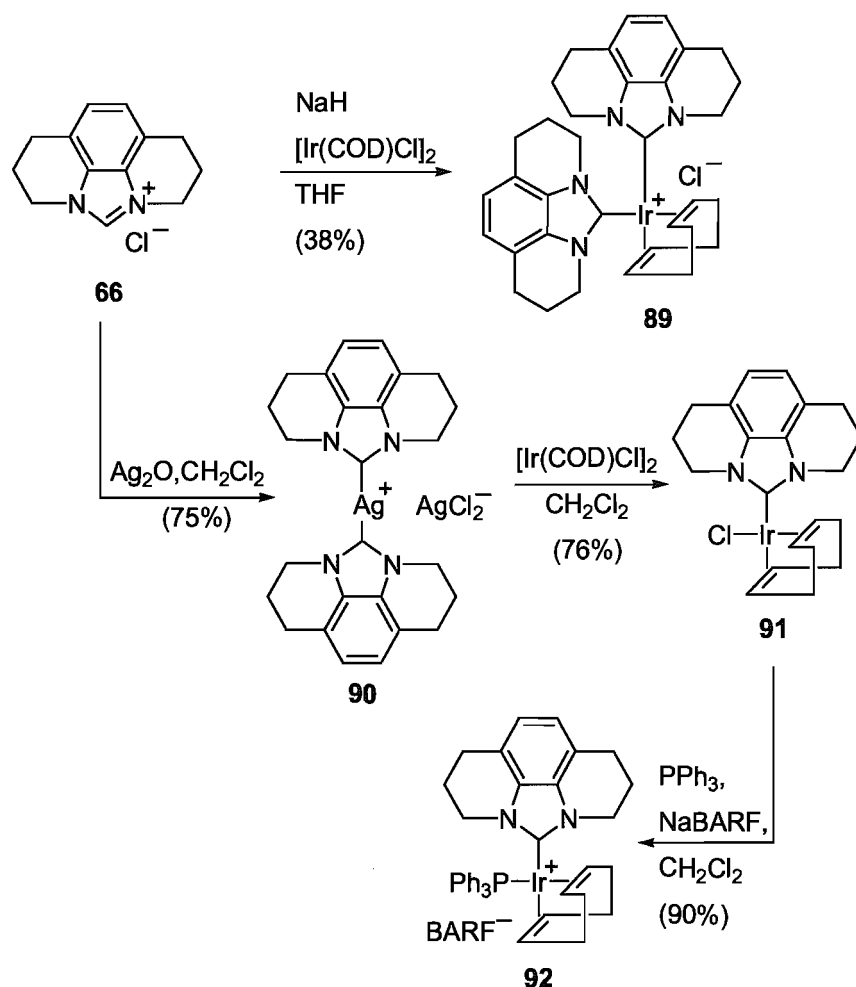


**Figure 5.** Examples of NHC-Ir complexes.

Unlike the preparation of ruthenium complexes, the synthesis of NHC-Ir catalysts using phenanthroline-derived benzimidazolylidenes as the ligands was straightforward. The bis-substituted cationic NHC-iridium chloride **89** was produced by direct deprotonation of **66** with sodium hydride in the presence of  $[\text{Ir}(\text{COD})\text{Cl}]_2$  in 38% yield. In order to introduce only one NHC ligand on the iridium center, a silver complex was prepared to allow for transmetalation to iridium. This was done by treatment of unsubstituted benzimidazolium chloride **66** with  $\text{Ag}_2\text{O}$ , which gave the corresponding bis-substituted silver(I) complex **90** as the  $\text{AgCl}_2^-$  salt. Transmetalation of silver to iridium was carried out by mixing silver salt **90** with metal catalyst precursor  $[\text{Ir}(\text{COD})\text{Cl}]_2$  to give the monodentate complex **91** in 76% yield. Direct displacement of

the chloride counterion in **91** could be accomplished with triphenylphosphine and sodium tetrakis(3,5-trifluoromethylphenyl)borate (NaBARF) in dichloromethane to afford the additional cationic four-coordinate complex **92**, which is expected to have better catalytic activity due to its cationic property and the weak coordination ability of the BARF anion.<sup>101</sup>



**Scheme 32.** Synthesis of achiral benzimidazolylidene-Ir complexes.

According to 2-dimensional HSQC (Heteronuclear Single Quantum Coherence) analysis, each of the monosubstituted complexes **91** and **92** exhibited two distinct

resonances for the  $\alpha$  to nitrogen methylene groups in their  $^1\text{H}$  NMR spectra at room temperature and at  $-50\text{ }^\circ\text{C}$  (**91**:  $\delta$  4.60, 4.38; **92**:  $\delta$  4.14, 3.58) which correlated to only one  $^{13}\text{C}$  NMR signal (**91**:  $\delta$  44.9; **92**:  $\delta$  45.1, **Figure 6** and **Figure 7**). This observation implied that the principal plane of the NHC ligand in each complex, as defined by the imidazole ring, was probably orthogonal to the Ir-Cl or Ir-P bond and that the complex possessed  $C_s$  symmetry.

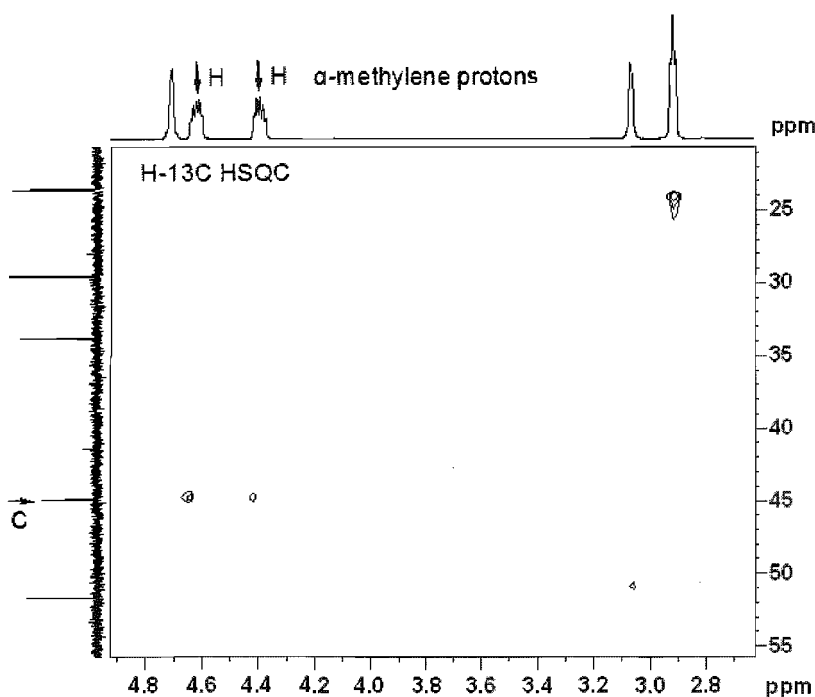


**Figure 6.**  $^1\text{H}$ - $^{13}\text{C}$  HSQC experiment of complex **91**.

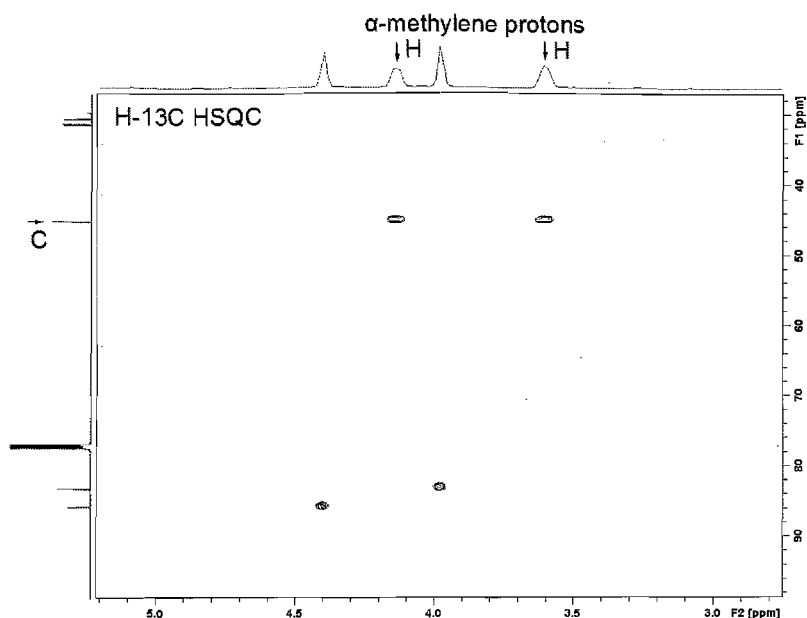
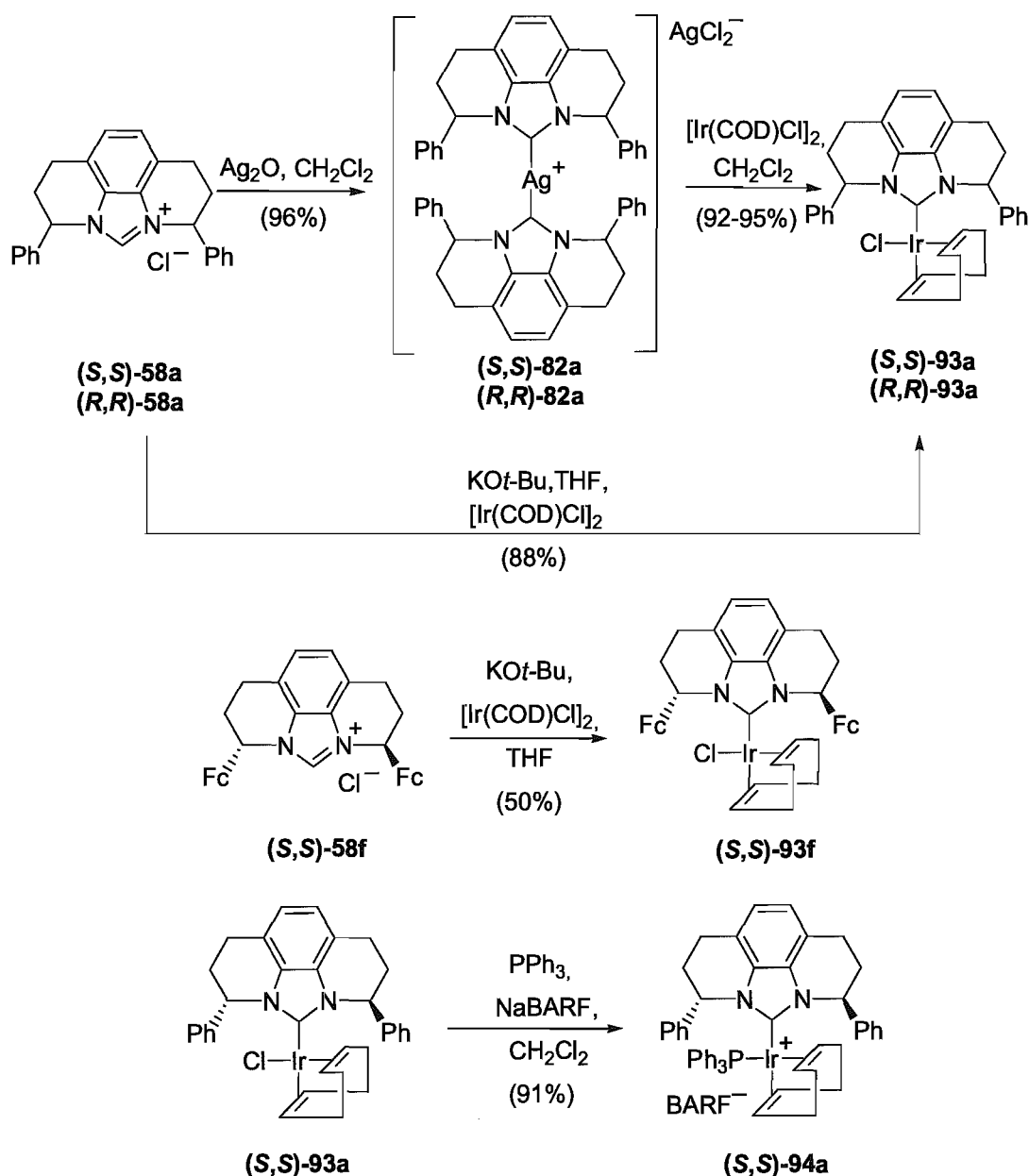


**Figure 7.**  $^1\text{H}$ - $^{13}\text{C}$  HSQC experiment of complex **92**.

Similarly, chiral NHC-Ir complexes were prepared according to the procedure used for complex **91**. Chiral silver salts (*S,S*)-**82a** and (*R,R*)-**82a** were transmetalated with  $[\text{Ir}(\text{COD})\text{Cl}]_2$  to give the monodentate complexes (*S,S*)-**93a**, (*R,R*)-**93a** respectively in excellent yield. In addition, deprotonation of chiral benzimidazolium chloride salt (*S,S*)-**58a** by  $\text{KO}^t\text{-Bu}$  in the presence of  $[\text{Ir}(\text{COD})\text{Cl}]_2$  gave complex (*S,S*)-**93a** directly without formation of a bis-NHC complex. This is most likely due to the increased steric bulk of this ligand. The same sequence of transformations afforded diferrocenyl (*S,S*)-**93f** from (*S,S*)-**58f**. Complex (*S,S*)-**93a** was further reacted with  $\text{PPh}_3$  in the presence of NaBARF to furnish the cationic complex (*S,S*)-**94a**.



**Scheme 33.** Synthesis of chiral phenanthroline-derived NHC-Ir complexes.

To determine the absolute stereochemistry of the chiral iridium complexes, crystals of  $(R,R)\text{-}93a$  and  $(S,S)\text{-}93f$  suitable for X-Ray were obtained by slow diffusion of pentane into toluene, or evaporation from a mixed solvent system of

hexane/dichloromethane, respectively. X-Ray analysis showed that both complexes were four-coordinate with square planar geometry at the iridium, but that the plane of the imidazole ring was twisted out of orthogonality with respect to the Ir-Cl bond in both chiral complexes. This conformation avoids excessive steric interactions between the COD ligand and one of the aryl substituents of the NHC ligand. This effect was more pronounced for the diferrocenyl NHC ligand ( **Figure 8** and **Figure 9**). The differential steric interaction between the COD moiety and a proximal phenyl or ferrocenyl group is reflected in the torsion angles defined by N3a-C4-Ir1-Cl1 for (*R,R*)-**93a** (104.0(2)°) versus N4a-C4-Ir1-Cl1 in (*S,S*)-**93f** (112.89(18)°). In contrast, Chung's diferrocenyl iridium catalyst **88** (**Figure 5**)<sup>39</sup> has a torsion angle of only 96.9(3)°.

X-Ray structures of (*R,R*)-**93a** and (*S,S*)-**93f** clearly demonstrated that the formation Ir-C bond can overcome the steric repulsion in the four-coordinate square planar geometry of NHC-Ir complexes, although the steric hindrance is substantially greater than complexes with non-annulated ligands such as **88**. However, for the five-coordinate pentahedral NHC-Ru alkylidene **81** and **83**, maybe excessive steric demand around the ruthenium metal center precluded their formation or isolation.

The twist of the NHC ligands in the iridium complexes is corroborated by NMR spectroscopy. Complexes (*S,S*)-**93a,f**, (*R,R*)-**93a** and (*S,S*)-**94a** necessarily show two different  $\alpha$ -methine signals in their <sup>1</sup>H NMR spectra (for example, (*S,S*)-**93a**:  $\delta$  6.56, 5.78; (*S,S*)-**94a**:  $\delta$  5.97, 5.22) that correlate to two distinct carbon atoms ((*S,S*)-**93a**:  $\delta$  59.4, 58.2; (*S,S*)-**94a**:  $\delta$  60.1, 59.2, **Figure 10** and **Figure 11**).

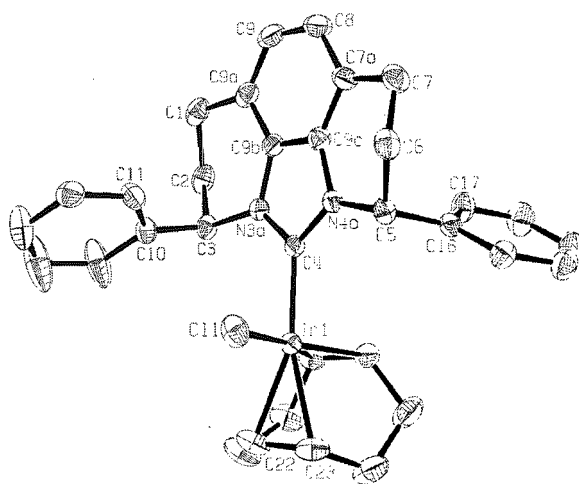


**Figure 8.** ORTEP plot of (*R,R*)-93a at 50% probability.

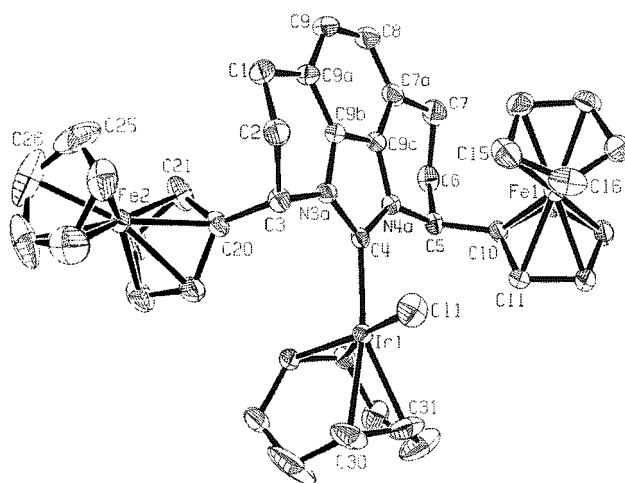


**Figure 9.** ORTEP plot of (*S,S*)-93f at 50% probability.



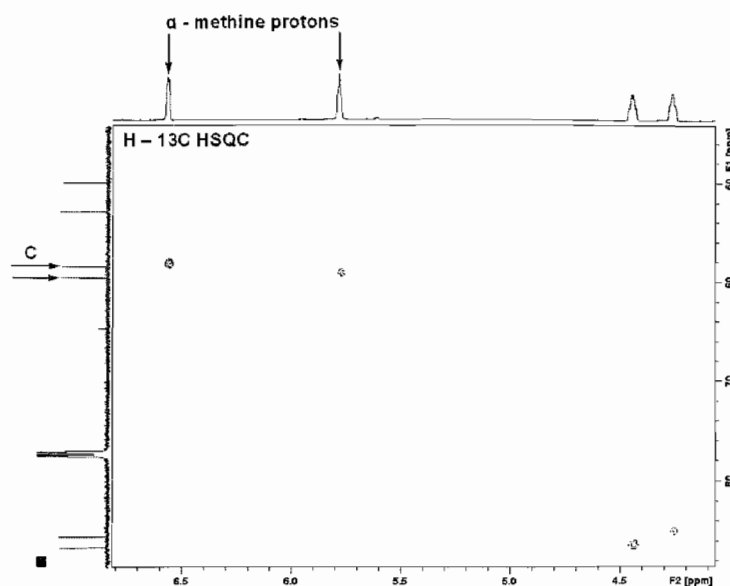


**Figure 10.**  $^1\text{H}$ - $^{13}\text{C}$  HSQC experiment of complex (*S,S*)-93a.

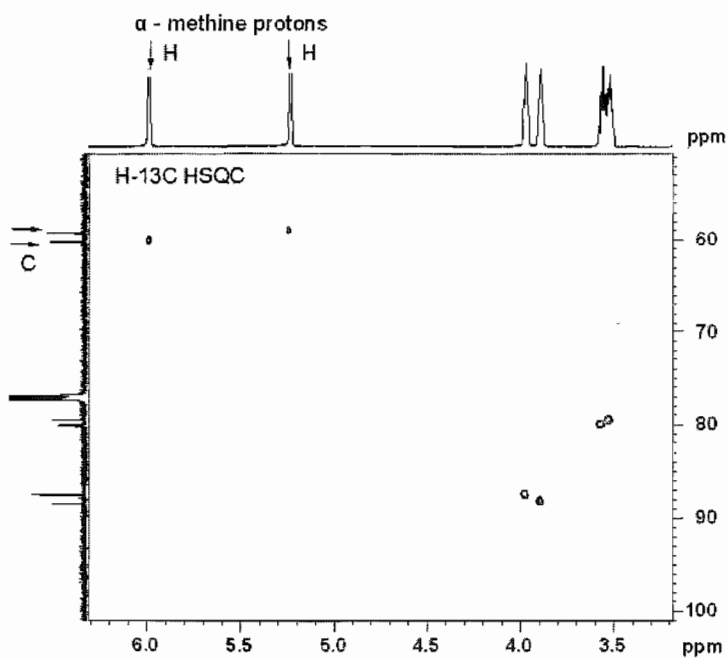
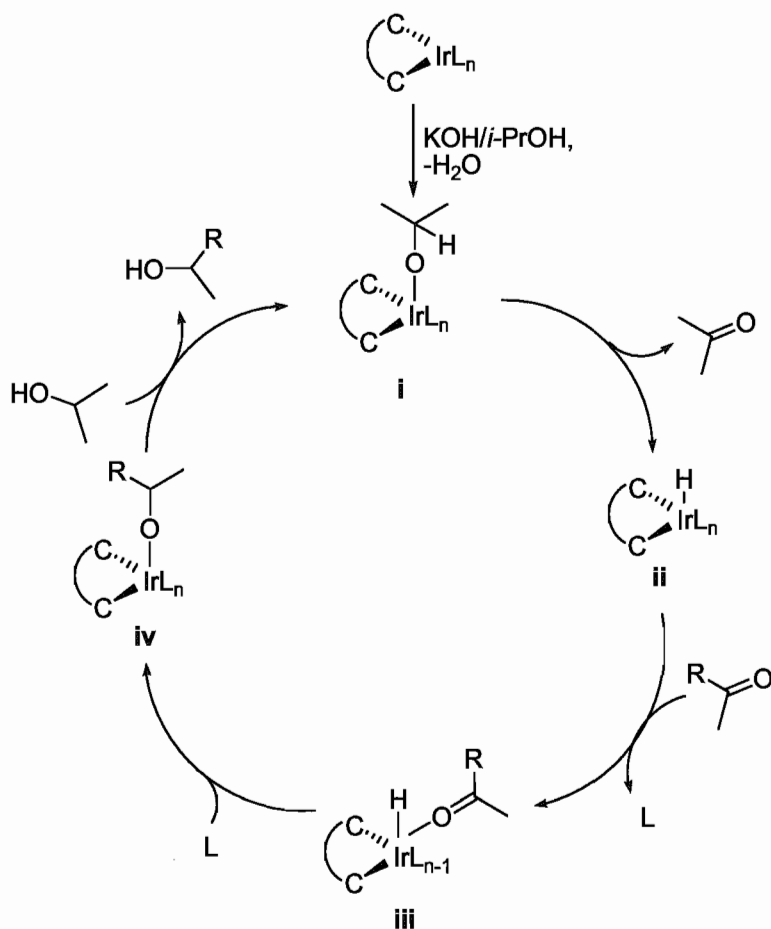


**Figure 11.**  $^1\text{H}$ - $^{13}\text{C}$  HSQC experiment of complex (*S,S*)-94a.

### 2.2.3 Transfer Hydrogenation of Acetophenone and Its Derivatives Using NHC-Ir

#### Catalysts

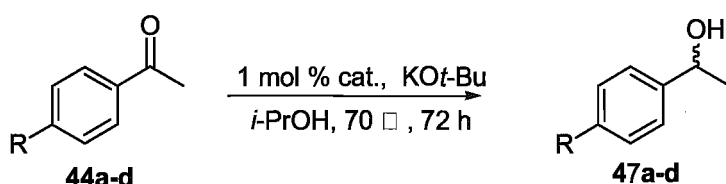
Transfer hydrogenation of ketones is an attractive approach for generating secondary alcohols from a hydrogen source other than hydrogen gas. Metal complex catalytic transfer hydrogenation is widely applied in industry and organic synthesis, in part because of the inconvenience of hydrogen.<sup>102</sup> A proposed mechanism for transfer hydrogenation of a ketone from *i*-PrOH to an alcohol using bidentate NHC-Ir complexes as catalysts and KOH as a co-catalyst was presented by Crabtree in 2004.<sup>103</sup> *i*-PrOH is deprotonated by KOH to give an *i*-PrO-Ir species **i**. Beta-elimination of *i*-PrO-Ir species **i** affords an iridium hydride intermediate **ii** which attacks the substrate ketone to form intermediate **iii**. Proton migration from Ir to the ketone gives intermediate **iv**. Alkoxide exchange with *i*-PrOH forms the product and re-generates the *i*-PrO-Ir species **i** which can go to the next catalytic cycle (**Scheme 34**).



**Scheme 34.** Proposed mechanism for NHC-Ir catalyzed transfer hydrogenation.

To establish the feasibility of this reaction, complexes **89**, **91**, (*S,S*)-**93a** and (*S,S*)-**93f** were tested in transfer hydrogenation of acetophenone and its derivatives. The reactions were carried out using 1 mol % catalyst in the presence of KO*t*-Bu in *i*-PrOH at 70 °C and the overall excellent yields (87-98%) demonstrated the good catalytic activities of the catalysts. However, the chiral catalysts generally showed low enantioselectivities. The highest ee (18%) was obtained when 4'-methylacetophenone was used as a substrate and (*S,S*)-**93f** as the catalyst. As a comparison, Chung's diferrocenyl catalyst **88** gave up to

52% ee for similar transformations. Interestingly, the sense of chiral induction was different for catalyst **(*S,S*)-93a**, which gave an *S*-configured product, while **(*S,S*)-93f** gave an *R*-configured product in the reduction of 4'-methylacetophenone to the corresponding alcohol (**Scheme 35**).



R	Substrate	Catalyst	Product	yld, %	Optical purity <sup>1</sup> or ee <sup>2</sup> , %
H	<b>44a</b>	<b>89</b>	<b>47a</b>	99	NA
H	<b>44a</b>	<b>91</b>	<b>47a</b>	98	NA
H	<b>44a</b>	<b>(<i>S,S</i>)-93a</b>	<b>47a</b>	92	4( <i>S</i> ) <sup>1</sup>
Cl	<b>44b</b>	<b>89</b>	<b>47b</b>	92	NA
Cl	<b>44b</b>	<b>91</b>	<b>47b</b>	90	NA
Cl	<b>44b</b>	<b>(<i>S,S</i>)-93a</b>	<b>47b</b>	91	5( <i>S</i> ) <sup>1</sup>
OMe	<b>44c</b>	<b>(<i>S,S</i>)-93a</b>	<b>47c</b>	87	3( <i>S</i> ) <sup>1</sup>
CH <sub>3</sub>	<b>44d</b>	<b>(<i>S,S</i>)-93a</b>	<b>47d</b>	91	1( <i>S</i> ) <sup>2</sup>
CH <sub>3</sub>	<b>44d</b>	<b>(<i>S,S</i>)-93f</b>	<b>47d</b>	90	18( <i>R</i> ) <sup>2</sup>

**Scheme 35.** Transfer hydrogenation of **44a-d**.

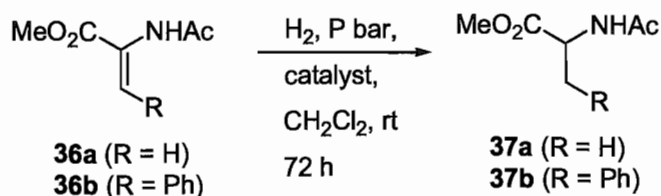
#### 2.2.4 Hydrogenation of Methyl-2-acetamidoacrylate and *trans*-Methyl- $\alpha$ -acetamidocinnamate

The importance in modern chemistry of hydrogenation, especially asymmetric iridium catalyzed hydrogenation, is well-recognized.<sup>104</sup> Despite the numerous studies that

have addressed the possible mechanism of the iridium-catalyzed asymmetric hydrogenation of olefins including those of Burgess<sup>105</sup> or Brandt's<sup>106</sup> proposed Ir<sup>III</sup> - Ir<sup>V</sup> catalytic cycle and Chen's<sup>107</sup> Ir<sup>I</sup> - Ir<sup>III</sup> pathway, the mechanism remains far from understood. "Any selectivity model based on the information collected to date should be considered with caution."<sup>108</sup>

Six monodentate NHC-Ir catalysts **89**, **91**, **92**, (*S,S*)-**93a**, (*S,S*)-**93f** and (*S,S*)-**94a** were employed in the hydrogenation of methyl-2-acetamidoacrylate **36a** and *trans*-methyl- $\alpha$ -acetamidocinnamate **36b** (Scheme 35). The neutral iridium catalysts (*S,S*)-**93a**, cationic catalysts **92** and (*S,S*)-**94a** showed much better catalytic activities than other complexes (yields: 93-99%). Complex (*S,S*)-**93a** proved to be the most selective catalyst for this transformation, providing **36a** and **36b** in moderate to very good enantiomeric purities (**37a**: 81% ee; **37b**: 48% ee, *R* configuration). The result using (*S,S*)-**93a** compares favorably to that reported by Herrmann and co-workers (67% ee for **37a**), which represented the best results obtained with monodentate bis-isoquinoline derived NHC-iridium complex **86**.<sup>76</sup> The yield of the (*S,S*)-**93f** catalyzed hydrogenation was improved by performing the reaction at 50 °C, but at the expense of selectivity (22% ee). In addition, it was found that the sense of chiral induction was reversed using the cationic catalyst (*S,S*)-**94a**, which provided (*S*)-**37a** preferentially in 23% ee. A similar reversal of selectivity was observed upon hydrogenation of *trans*-methyl- $\alpha$ -acetamidocinnamate (**36b**, R = Ph), in which catalyst (*S,S*)-**93a** gave **37a** as an *S* configured product in 41% ee, while (*S,S*)-**94a** provided **37a** as an *R*

configured one in 25% ee. The bulkier 2,9-diferrocenyl catalyst (**(S,S)**-**93f**) required a higher temperature for this transformation (50 °C), resulting in racemic product (**Scheme 36**).



substrate	cat. (mol %)	P, bar	product	yld, %	ee, %
<b>36a</b>	<b>89</b> (3)	69	<b>37a</b>	50	NA
<b>36a</b>	<b>91</b> (3)	69	<b>37a</b>	70	NA
<b>36a</b>	<b>92</b> (2)	50	<b>37a</b>	90	0
<b>36a</b>	<b>(S,S)</b> - <b>93f</b> (3)	69	<b>37a</b>	96 <sup>a</sup>	22( <i>R</i> )
<b>36a</b>	<b>(S,S)</b> - <b>93f</b> (3)	69	<b>37a</b>	45	48( <i>R</i> )
<b>36a</b>	<b>(S,S)</b> - <b>93a</b> (3)	69	<b>37a</b>	97	81( <i>R</i> )
<b>36a</b>	<b>(S,S)</b> - <b>94a</b> (2)	50	<b>37a</b>	90	23( <i>S</i> )
<b>36b</b>	<b>89</b> (3)	69	<b>37b</b>	0	NA
<b>36b</b>	<b>(S,S)</b> - <b>93f</b> (3)	69	<b>37b</b>	88 <sup>a</sup>	0
<b>36b</b>	<b>(S,S)</b> - <b>93a</b> (3)	69	<b>37b</b>	97	41( <i>R</i> )
<b>36b</b>	<b>(S,S)</b> - <b>94a</b> (2)	50	<b>37b</b>	99	25( <i>S</i> )

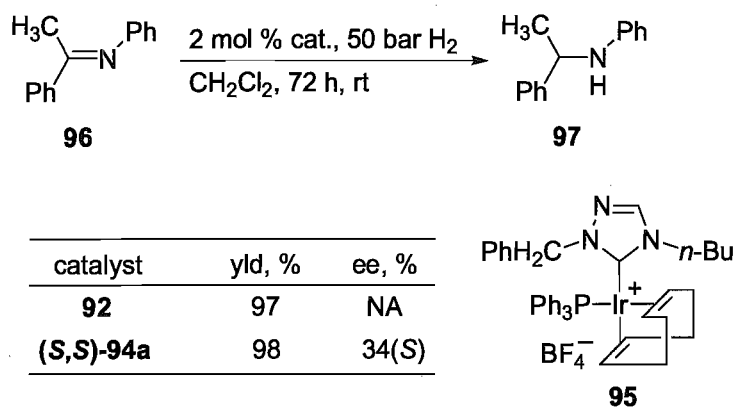
<sup>a</sup> Reaction performed at 50 °C

**Scheme 36.** Hydrogenation of **36a-b** using NHC-Ir catalyst.

### 2.2.5 Hydrogenation of (*E*)-*N*-(1-phenylethylidene)benzenamine

As a trial experiment, (*E*)-*N*-(1-phenylethylidene)benzenamine **96** was reduced with cationic phosphino-NHC complexes **92** and **(S,S)**-**94a**. Notably, achiral complex **95** reported by Crabtree have been effective at catalyzing this transformation.<sup>109</sup>

Encouragingly reduction of imine **96** with **92** and (*S,S*)-**94a** gave the excellent yield in 50 bar hydrogen. 35% ee was obtained for **97** using chiral catalyst (*S,S*)-**94a**.



**Scheme 37.** Hydrogenation of **96** using cationic catalysts.

### 3. Conclusions and Future work

During the synthesis of chiral benzimidazolylidene ligands derived from 1,10-phenanthroline, an effective and simple method for reduction of 2,9-diaryl-1,10-phenanthrolines using sodium metal in absolute alcohol was discovered and gave the mixture of *rac/meso* bulky substituted octahydrophenanthroline products in relatively good yields (>70%).

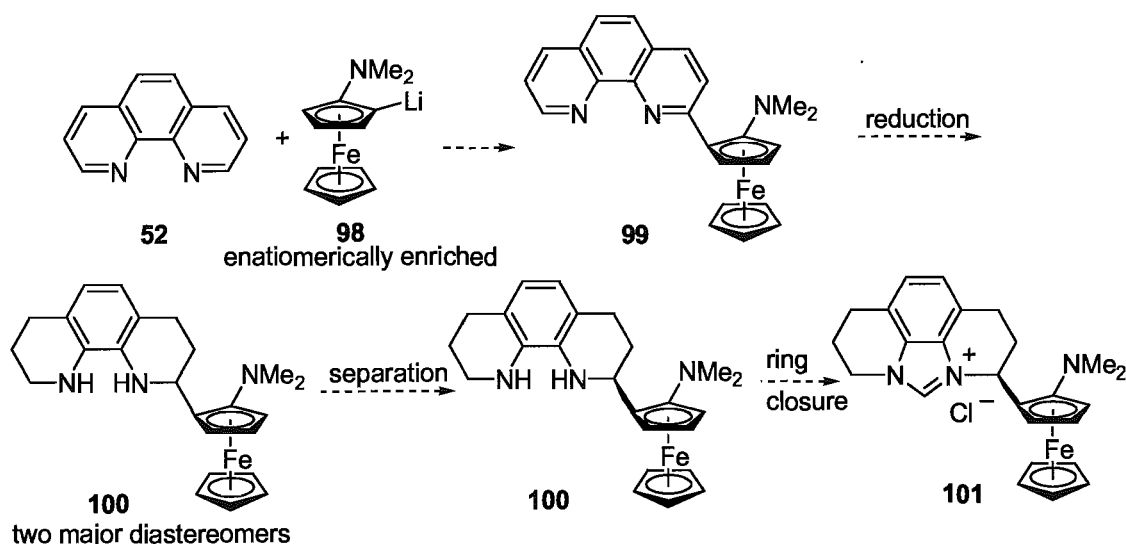
Several air-stable neutral and cationic phenanthroline-derived benzimidazolylidene-iridium complexes were synthesized. Spectroscopic and crystallographic data indicate the likelihood that the principal plane of the NHC ligand in achiral complexes **91** and **92** is positioned orthogonally to the Ir-Cl or Ir-P bond, while the NHC ligands in the corresponding chiral complexes are twisted with respect to the Ir-Cl bond by a torsion angle that appears to depend on the size of the 2,9-substituents. All of the new achiral and chiral complexes showed varying degrees of catalytic activity and enantioselectivity toward transfer hydrogenation of acetophenone and its derivatives and hydrogenation of acetamidoacrylates, with the best results being achieved using (*S,S*)-**93a** (97% yield, 81% ee) for hydrogenation of **36a** (R = H), which to the best of our knowledge is the highest ee observed to date using a chiral monodentate NHC-Ir complex of any type. The results seem to indicate that our catalysts behave more similarly to other annulated NHC-Ir catalysts (for example, **86**) than to acyclic benzimidazolylidene-Ir complexes.

In the future more  $C_2$ -symmetric benzimidazolium salts derived from



2,9-disubstituted phenanthrolines will be synthesized, especially for the appropriate size substituents (for example, parabiphenyl group). Those chiral ligands will be expected to provide an increased enantioselectivity in asymmetric transformations.

Recently, more bidentate chiral NHC/N and NHC/P ligands and their metal complexes (for example, **35** and **40**) were developed and demonstrated excellent enantioselectivities. Based on these results, a chiral bidentate NHC/N ligand derived from 1,10-phenanthroline which can be synthesized in several steps is certainly worthy to be tested in asymmetric transformations. For example, our group is developing a way to make **98** in enantiomerically enriched form. Thus, addition of planar chiral **98** to **52** gives **99**, which upon reduction will give two optically enriched diastereomers. Separation and ring closure will provide bidentate NHC **101** for use in iridium catalysis.



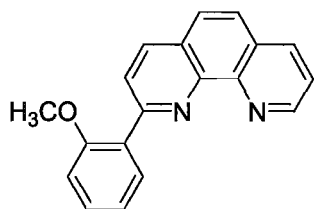
**Scheme 38.** Proposed synthetic route for a chiral bidentate benzimidazolium salt.

In addition, the hydrolysis of ureas **65b,c** (R= *n*-Bu, Me) needs to be followed up using Schwartz's reagent or stepwise treatment with PhLi and then Schwartz's reagent.

## 4. Experimental

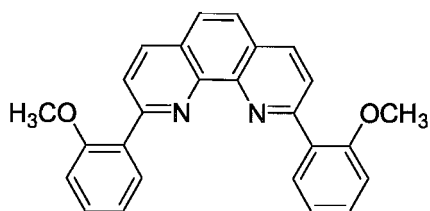
**General.** All reagents were purchased from commercial sources and used as received unless otherwise indicated. Tetrahydrofuran (THF) was freshly dried and distilled over sodium/benzophenone ketyl under an atmosphere of nitrogen. Dichloromethane and hexane were distilled over  $\text{CaH}_2$  under an atmosphere of nitrogen. All reactions were performed under argon in flame- or oven-dried glassware using syringe-septum cap techniques or Schlenk conditions unless otherwise indicated. Column chromatography was performed on silica gel 60 (70-230 mesh) or neutral alumina. NMR spectra were obtained on a Bruker Avance 300 or 600 MHz instrument and are referenced to TMS or to the residual proton signal of the deuterated solvent for  $^1\text{H}$  spectra, and to the carbon multiplet of the deuterated solvent for  $^{13}\text{C}$  spectra according to published values. Pressurized reactions were performed with a Parr 4760 bomb. Enantiomeric ratios were determined on an Agilent 1100 series HPLC at  $\lambda = 254$  nm with a Chiralcel OD-H column, or on a Hewlett-Packard 6890 GC with a Chirasil DEX-CB column, and were compared against racemic material. FT-IR spectra were obtained on an ATI Mattson Research Series spectrometer as KBr pellets for solids or on KBr discs for liquids. Optical rotations were measured on a Rudolph Research Autopol III automatic polarimeter. Mass spectra were obtained on an MSI/Kratos Concept 1S Mass Spectrometer. Combustion analyses were performed by Atlantic Microlab Inc., Norcross, GA. Melting points were determined on a Kofler hot-stage apparatus and are uncorrected.

## 2-(2-Methoxyphenyl)-1,10-phenanthroline (74d)



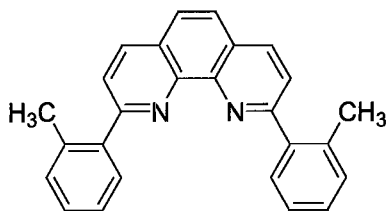
The solution of 1,10-phenanthroline (1.0 g, 5.55 mmol) in dry toluene (20 mL) at 0°C under Argon was treated with the solution of 2-lithioanisole, prepared from 2-bromoanisole (3.17 g, 17 mmol) and freshly cut lithium (260 mg, 34 mmol) in diethyl ether (25 mL). The resulting red-brown solution was allowed to warm to room temperature then stirred for 16 h. Water (25 mL) was added cautiously and the deep yellow organic layer was separated, the remaining aqueous layer was extracted with CH<sub>2</sub>Cl<sub>2</sub> (3x12 mL). The combined organic layer was treated with MnO<sub>2</sub> (4 g, 34.8 mmol) and stirred for 1.5h, after which anhyd MgSO<sub>4</sub> was added, and stirring continue for an additional 30 min. The resulting mixture was filtered and concentrated in vacuo. Column chromatography (Silica gel, 5:95 MeOH/CH<sub>2</sub>Cl<sub>2</sub>, R<sub>f</sub> 0.20) gave **74d** in 50% yield as a yellow solid. Mp: 87-89 °C (MeOH/CH<sub>2</sub>Cl<sub>2</sub>); <sup>1</sup>H NMR (300MHz, CDCl<sub>3</sub>): δ 9.20 (d, 1H, J=1.6Hz), 8.22 (d, 2H, J=1.8Hz), 8.16 (s, 1H), 8.12 (m, 1H), 7.84-7.76 (m, 2H), 7.63-7.59 (m, 1H), 7.43 (m, 1H), 7.15 (m, 1H), 7.02 (d, 1H, J=8.4Hz), 3.87 (s, 3H); <sup>13</sup>C NMR (75.5 MHz, CDCl<sub>3</sub>): δ 157.2, 157.0, 150.3, 146.4, 140.1, 135.9, 135.2, 132.4, 130.2, 129.9, 128.7, 127.3, 126.4, 126.0, 125.2, 122.6, 121.4, 111.3, 55.7; EIMS [*m/z* (%)]: 286 (M<sup>+</sup>, 4), 255(11), 61(100); HRMS (EI) calcd for C<sub>19</sub>H<sub>14</sub>N<sub>2</sub>O: 286.1106; found 286.1110.

## 2, 9-Di(2-methoxyphenyl)-1,10-phenanthroline (54d)



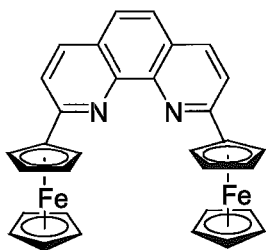
The solution of 2-(2-methoxyphenyl)-1,10-phenanthroline **74d** (1.34 g, 4.68 mmol) in dry toluene (35mL) at 0°C under Argon was treated with the solution of 2-lithioanisole, prepared from 2-bromoanisole (2.41 g, 12.8 mmol) and freshly cut lithium (178 mg, 25.6 mmol) in diethyl ether (15 mL). The resulting dark solution was allowed to warm to room temperature then stirred for 24 h. Water (25 mL) was added cautiously and the brown organic layer was separated, the remaining aqueous layer was extracted with CH<sub>2</sub>Cl<sub>2</sub> (4x10mL). The combined organic layer was treated with MnO<sub>2</sub> (3.5 g, 30.5 mmol) and stirred for 1.5h, after which anhyd MgSO<sub>4</sub> was added, and stirring continue for an additional 30 min. The resulting mixture was filtered and concentrated in vacuo. Column chromatography (Silica gel, 1:1:98 Et<sub>3</sub>N/MeOH/CH<sub>2</sub>Cl<sub>2</sub>, R<sub>f</sub> 0.31) gave **54d** in 87% yield as a yellow solid. Mp: 198-199 °C (CH<sub>2</sub>Cl<sub>2</sub>/MeOH); IR (KBr)  $\nu_{max}$  3095, 3010, 2922, 2852, 1579 cm<sup>-1</sup>; <sup>1</sup>H NMR (300MHz, CDCl<sub>3</sub>):  $\delta$  8.28 (d, 2H, J=6Hz), 8.24-8.20 (dd, 4H, J=11.1, 8.4Hz), 7.79 (s, 2H), 7.45-7.39 (m, 2H), 7.24-7.19 (t, 2H, J=7.5Hz), 7.04 (d, J=8.1Hz), 3.89(s, 6H); <sup>13</sup>C NMR (75.5 MHz, CDCl<sub>3</sub>):  $\delta$  157.6, 156.2, 146.2, 135.2, 132.5, 130.2, 129.8, 127.4, 125.9, 124.8, 121.3, 111.5, 55.8; EIMS [*m/z* (%): 392 (M<sup>+</sup>, 30), 196(9), 84(100); HRMS (EI) calcd for C<sub>26</sub>H<sub>20</sub>N<sub>2</sub>O<sub>2</sub>: 392.1525; found 392.1529.

### 2,9-Di(2-methylphenyl)-1,10-phenanthroline (54e)



A solution of 1,10-phenanthroline (360 mg, 2.0 mmol) in dry PhMe (10 mL) at 0 °C under Argon was treated with the solution of 2-lithiotoluene, prepared from 2-bromotoluene (2.05 g, 12 mmol) and freshly cut lithium (250 mg, 36 mmol) in 12 mL Et<sub>2</sub>O. The resulting dark red solution was warmed up to 35 °C and stirred for 20 h, cooled to 0 °C, work-up by addition of water (9 mL). The organic layer was separated and the remaining aqueous layer was extracted with CH<sub>2</sub>Cl<sub>2</sub> (3x8 mL). The combined organic layer was treated with MnO<sub>2</sub> (1.4 g, 16.1 mmol) and stirred for 1.5 h, after which anhyd MgSO<sub>4</sub> was added, and stirring continued for an additional 30 min. The resulting mixture was filtered and concentrated in vacuo. Column chromatography (silica gel, 1:3 EtOAc/Hexane, R<sub>f</sub> 0.28) afforded **54e** (540 mg, 75%) as a yellow solid; mp: 76-77 °C (EtOAc/Hexane); <sup>1</sup>H NMR (300 MHz, CDCl<sub>3</sub>): δ 8.32 (d, 2H, J=8.1 Hz), 7.85-7.81 (m, 4H), 7.61-7.60 (m, 2H), 7.32-7.24 (m, 6H), 2.60 (s, 6H); <sup>13</sup>C NMR (75.5 MHz, CDCl<sub>3</sub>): δ 160.0, 145.6, 140.6, 136.8, 131.0, 130.3, 128.3, 127.0, 126.0, 125.7, 123.7, 20.7; EIMS [m/z (%): 360 (M<sup>+</sup>, 3), 179(2), 43(100); HRMS (EI) calcd for C<sub>26</sub>H<sub>20</sub>N<sub>2</sub>: 360.1627; found 360.1621.

### 2,9-Diferrocenyl-1,10-phenanthroline (54f).



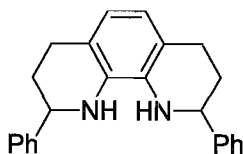
*Method A.* To a dry flask under inert atmosphere (glovebox) was added lithioferrocene (1.60 g, 8.32 mmol) and hexane (15

mL). A solution of 1,10-phenanthroline (515 mg, 2.78 mmol) in THF (5 mL) was then transferred by cannula to the mixture of lithioferrocene and the resulting dark, almost black mixture was heated at 60 °C for 10 h. A solution of DDQ (693 mg, 3.05 mmol) in THF (2 mL) was transferred by cannula to the reaction mixture, and the whole was heated at 50 °C for 20 min before cooling to room temperature. The crude reaction mixture was filtered through a pad of neutral alumina, eluting with CH<sub>2</sub>Cl<sub>2</sub>. To the orange filtrate was added neutral alumina, and the solvent was removed on a rotary evaporator. Column chromatography of the pre-adsorbed material (neutral alumina, 70.2:29:0.5:0.3 hexane/CH<sub>2</sub>Cl<sub>2</sub>/Et<sub>3</sub>N/MeOH) gave, sequentially, 2,9-diferrocenyl-1,10-phenanthroline **54f** (459 mg, 30%, R<sub>f</sub> 0.23) and 2-ferrocenyl-1,10-phenanthroline **74f** (312 mg, 31%, R<sub>f</sub> 0.19) as a red-orange solid.

*Method B.* A solution of 2-ferrocenyl-1,10-phenanthroline **74f** (265 mg, 0.73 mmol) in THF (5 mL) was transferred by cannula to a stirred suspension of lithioferrocene (280 mg, 1.46 mmol) in hexane (15 mL) and stirred at room temperature for 90 min. A solution of DDQ (181 mg, 0.80 mol) in THF (2 mL) was transferred by cannula to the reaction mixture and the almost black mixture was stirred for 20 min. The crude reaction mixture was filtered through a pad of neutral alumina, eluting with CH<sub>2</sub>Cl<sub>2</sub>. To the orange filtrate was added neutral alumina, and the solvent was removed on a rotary evaporator. Column chromatography of the pre-adsorbed material (neutral alumina, 70.2:29:0.5:0.3 hexane/CH<sub>2</sub>Cl<sub>2</sub>/Et<sub>3</sub>N/MeOH) gave 2,9-diferrocenyl-1,10-phenanthroline **54f** (259 mg, 65%, R<sub>f</sub> 0.23) as a red-orange solid. Mp: >250 °C (CH<sub>2</sub>Cl<sub>2</sub>/hexane); IR (KBr)  $\nu_{max}$  3090,

2955, 2923, 2853, 1504  $\text{cm}^{-1}$ ;  $^1\text{H}$  NMR (300 MHz,  $\text{CDCl}_3$ )  $\delta$  8.10 (d, 2H,  $J = 8.4$  Hz), 7.75 (d, 2H,  $J = 8.4$  Hz), 7.68 (s, 2H), 5.26 (t, 4H,  $J = 2.1$  Hz), 4.52 (t, 4H,  $J = 1.8$  Hz), 4.11 (s, 10H);  $^{13}\text{C}$  NMR (75.5 MHz,  $\text{CDCl}_3$ )  $\delta$  159.4, 145.7, 135.6, 127.2, 125.2, 120.6, 84.7, 70.3, 69.7, 68.6, 68.4; EIMS [ $m/z(\%)$ ] 548 ( $\text{M}^+$ , 55), 483 (40), 84 (100); HRMS (EI) calcd for  $\text{C}_{32}\text{H}_{24}\text{N}_2^{56}\text{Fe}_2$ : 548.0638; found 548.0634.

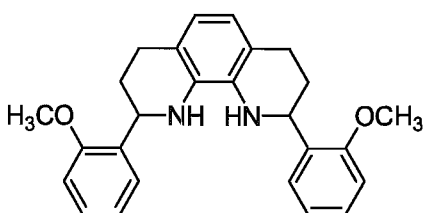
***rac/meso*-2,9-Diphenyl-1,2,3,4,7,8,9,10-octahydro-1,10-phenanthroline (56a).**



A mixture of 2,9-diphenyl-1,10-phenanthroline (3.00 g, 9.03 mmol) in abs. EtOH (150 mL) and THF (15 mL) was warmed gently to dissolve the starting material and then cooled to room temperature. Sodium metal (10.5 g, 0.46 mol) was added in six portions over 1 h. The reaction mixture was left for an additional 3.5 h to allow gas and heat evolution to subside. Any remaining large pieces of sodium were removed, water (60 mL) was added to the ice-cooled solution, and the bulk of the organic solvents were removed on a rotary evaporator. The resulting mixture was extracted with  $\text{CH}_2\text{Cl}_2$  (3 x 30 mL) and the combined organic layer was washed with water and brine, dried over anhyd.  $\text{Na}_2\text{SO}_4$ , filtered and concentrated under reduced pressure. Column chromatography of the pre-adsorbed crude product (silica gel, 95:3:2 hexane/EtOAc/ $\text{Et}_3\text{N}$ ) gave **56a** (2.15 g, 72%), a colorless solid, as a 1:1 mixture of *rac* and *meso* isomers;  $^1\text{H}$  NMR (300 MHz,  $\text{CDCl}_3$ )  $\delta$  7.45-7.28 (m, 10H), 6.56 (s, 2H), 4.42-4.41 (m, 1H), 4.38 (s, 1H), 3.53 (b, 1H), 3.42 (b, 1H), 3.02-2.94 (m, 2H), 2.81-2.72 (m, 2H), 2.16-1.99 (m, 4H);  $^{13}\text{C}$  NMR (75.5 MHz, acetone- $d_6$ )  $\delta$  146.3, 132.8, 129.0,

127.7, 127.4, 119.6, 118.9, 57.0, 31.4, 26.9; EIMS [ $m/z$ (%)] 340( $M^+$ , 54); HRMS (EI) calcd for  $C_{24}H_{24}N_2$ : 340.1939; found 340.1942;

***rac/meso*-2,9-Di(2-methoxyphenyl)-1,2,3,4,7,8,9,10-octahydro-1,10-phenanthroline**



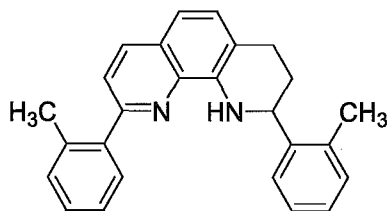
**(56d)** A solution of 2,9-di(2-methoxyphenyl)-1,10-phenanthroline **54d** (655 mg, 1.67 mmol) in HOAc (7 mL) and MeOH (3 mL) was treated with  $NaBH_3CN$  (675 mg, 10.7 mmol) carefully then the red mixture was

heated to reflux. After 2h, an additional 675 mg  $NaBH_3CN$  was added. The process was repeated every 2h for 4 more hours (total 2.7 g, 42 mmol  $NaBH_3CN$  was added). The solution was cooled to room temperature and the majority of the methanol was removed in vacuo. The resulting mixture was treated with 6M aq NaOH (30 mL) and the mixture was extracted with  $CH_2Cl_2$  (3x10 mL). The combined organic extract was washed with water, brine, dried by anhyd  $Na_2SO_4$ , filtered, and concentrated in vacuo. Column chromatography (Silica gel, 1:9:90  $Et_3N/Et_2O/Hexane$ ,  $R_f$  0.22) gave diamine **56d** (240 mg, 36%) as a yellow solid; mp: 170-171°C ( $Et_2O/Hexane$ ); IR (KBr)  $\nu_{max}$  3407, 3012, 2998, 2920, 2833, 1581, 1488, 1238  $cm^{-1}$ ;  $^1H$  NMR (300 MHz,  $CDCl_3$ )  $\delta$  7.57 (d, 2H,  $J=6.6Hz$ ), 7.31 (m, 2H), 7.02-6.92 (m, 4H), 6.58 (s, 2H), 4.86 (d, 2H,  $J=7.8Hz$ ), 3.90 (s, 6H), 3.68 (bd, 2H), 3.10-3.00 (m, 2H), 2.82-2.74 (m, 2H), 2.23-2.20 (m, 2H), 2.06-2.00 (m, 2H);  $^{13}C$  NMR (150.9 MHz,  $CDCl_3$ )  $\delta$  156.6, 133.1, 132.9, 127.9, 126.9, 120.7, 120.0, 118.7, 110.2, 55.3, 49.7, 28.7, 26.9; EIMS [ $m/z$  (%)]: 400 ( $M^+$ , 76), 159(17), 56(100);



HRMS (EI) calcd for C<sub>26</sub>H<sub>28</sub>N<sub>2</sub>O<sub>2</sub>: 400.2151; found 400.2153.

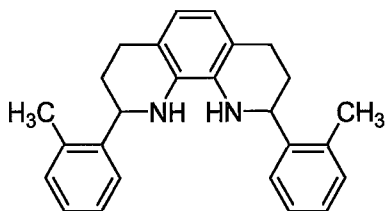
**2,9-Di(2-methylphenyl)-1,2,3,4-tetrahydro-1,10-phenanthroline (75e)**



2,9-di(2-methylphenyl)-1,10-phenanthroline **54e**

(100mg, 0.27mmol), diethyl-1,4-dihydro-2,6-dimethylpyridine-3,5-dicarboxylate (255mg, 1.67mmol) and TFA (3mg, 2.23mmol) were dissolved in dry benzene (6 mL). The orange solution was stirred at 60 °C under Argon for 72h. The reaction mixture was concentrated in vacuo. Column chromatography (Silica gel, 3: 97 EtOAc/Hexane, R<sub>f</sub> 0.19) gave **75e** (100 mg, 98%) as a yellow solid. Mp: 136-138 °C (EtOAc/Hexane); <sup>1</sup>H NMR (300 MHz, CDCl<sub>3</sub>) δ 8.14 (m, 1H), 7.57 (m, 3H), 7.35-7.28 (m, 4H), 7.14 (b, 3H), 7.12 (d, 1H, J=8.1Hz), 6.37 (b, 1H), 4.94 (m, 1H), 3.19-3.09 (m, 1H), 2.99-2.92 (m, 1H), 2.52 (s, 3H), 2.48 (s, 3H), 2.33-2.28 (m, 1H), 2.16-2.08 (m, 1H); <sup>13</sup>C NMR (75.5 MHz, CDCl<sub>3</sub>) δ 156.6, 142.7, 141.1, 136.6, 135.9, 134.5, 130.8, 130.4, 130.0, 128.6, 128.1, 126.9, 126.1, 125.8, 125.7, 121.7, 116.1, 112.9, 51.5, 28.8, 26.2, 20.8, 19.0; EIMS [*m/z*(%)] 364 (M<sup>+</sup>, 100), 273 (53), 182 (12); HRMS (EI) calcd for C<sub>32</sub>H<sub>24</sub>N<sub>2</sub><sup>56</sup>Fe<sub>2</sub>: 360.1627; found 360.1615

***rac/meso*-2,9-Di(2-methylphenyl)-1,2,3,4,7,8,9,10-octahydro-1,10-phenanthroline**

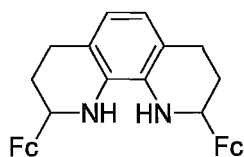


**(56e)**

The solution of 2,9-di(2-methylphenyl)-1,10-

phenanthroline **54e** (30mg, 0.083 mmol) in abs. EtOH (3 mL) was added sodium metal (114mg, 4.9 mol) in 3 portions over 1 h. The reaction mixture was refluxed for 1h till sodium was consumed. The yellow solution was cooled to 0 °C and water (5 mL) was added to the solution. The resulting mixture was extracted with CH<sub>2</sub>Cl<sub>2</sub> (3 x 3 mL) and the combined organic layer was washed with water and brine, dried over anhyd. Na<sub>2</sub>SO<sub>4</sub>, filtered and concentrated under reduced pressure. Column chromatography (silica gel, 98.5:1.5 hexane/Et<sub>2</sub>O, R<sub>f</sub> 0.20) gave diamine **56e** (27mg, 88%), a yellow solid, as a mixture of *rac/meso* isomers; mp: 170-171°C (Hexane/ Et<sub>2</sub>O); <sup>1</sup>H NMR (300 MHz, CDCl<sub>3</sub>) δ 7.62 (d, 2H, J=6.3Hz), 7.28 (m, 6H), 6.39 (s, 2H), 4.69 (d, 2H, J=6.3Hz), 3.57(b, 2H), 3.14-3.03 (b, 2H), 2.87-2.82 (b, 2H), 2.45 (2, 6H), 2.14(b, 2H), 1.97 (b, 2H); <sup>13</sup>C NMR (150.9 MHz, CDCl<sub>3</sub>) δ 142.6, 134.9, 133.0, 130.5, 127.0, 126.4, 126.2, 120.0, 119.0, 52.9, 29.7, 27.3, 19.1; EIMS [*m/z*(%)] 368 (M<sup>+</sup>, 100), 275 (9), 159 (19); HRMS (EI) calcd for C<sub>26</sub>H<sub>28</sub>N<sub>2</sub>: 368.2253; found 368.2248.

***rac/meso*-2,9-Ferrocenyl-1,2,3,4,7,8,9,10-octahydrophenanthroline (56f).**



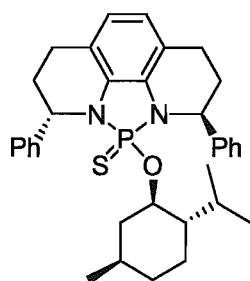
To a solution of 2,9-diferrocenyl-1,10-phenanthroline **54f** (806 mg, 1.47 mmol) in THF (300 mL) and *i*-PrOH (150 mL) was added a chunk of sodium metal (4.06 g, 176 mmol) and the mixture was heated to reflux until the sodium was consumed (5 h). Most of the solvent was removed on a rotary evaporator and water (100 mL) was added. The aqueous mixture was extracted with CH<sub>2</sub>Cl<sub>2</sub> (3 x 20 mL), dried over anhyd. Na<sub>2</sub>SO<sub>4</sub>, filtered and concentrated

under reduced pressure. Column chromatography (silica gel, 91:8:1 hexane/Et<sub>2</sub>O/Et<sub>3</sub>N, R<sub>f</sub> 0.23) gave **56f** (622 mg, 76%), an orange solid, as a 1:1 mixture of *rac* and *meso* isomers. The mixture obtained in this way was of sufficient purity for resolution; mp 143-146 °C; <sup>1</sup>H NMR (300 MHz, CDCl<sub>3</sub>) δ 6.38 (s, 2H, *meso*) 6.37 (s, 2H, *dl*), 4.38-4.37 (m, 2H), 4.34-4.32 (m, 4H), 4.30 (s, 10H, *dl*), 4.29 (s, 10H, *meso*), 4.20-4.08 (m, 10H), 3.94 (b, 2H), 3.89 (b, 2H), 2.91-2.77 (m, 8H), 2.70-2.60 (m, 4H), 2.18-2.06 (m, 4H), 1.79-1.66 (m, 4H); <sup>13</sup>C NMR (75.5 MHz, CDCl<sub>3</sub>) δ 133.6, 120.6, 120.4, 119.5, 119.3, 94.5, 94.0, 69.2, 68.6, 68.5, 68.1, 67.9, 67.3, 67.2, 67.0, 66.8, 52.5, 52.0, 31.9, 31.0, 27.6, 27.3; EIMS [*m/z*(%)] 556 (M<sup>+</sup>, 65), 548 (100), 483 (85); HRMS (EI) calcd for C<sub>32</sub>H<sub>32</sub><sup>56</sup>Fe<sub>2</sub>N<sub>2</sub>: 556.1264; found 556.1270.

#### Resolution of *rac/meso* **57a**.

A solution of *rac/meso* **57a** (1.68 g, 4.93 mmol) and dimethylaniline (3.4 mL, 27 mmol) in CH<sub>2</sub>Cl<sub>2</sub> (17 mL) under argon was treated with PCl<sub>3</sub> (0.43 mL, 4.93 mmol) added dropwise by syringe. The resulting yellow solution darkened and evolved heat for 15 min, at which point a reflux condenser was attached and the mixture heated to reflux under argon. After 1 h, (-)-menthol (770 mg, 4.93 mmol) was added in one portion from the top of the condenser and reflux was continued. After an additional 1 h, **S<sub>8</sub>** (1.58 g, 49.3 mmol) was added in one portion and the mixture was refluxed for an additional 25 min. The solvent was removed *in vacuo* and the residue was suspended in 8M aq. HCl (32 mL). The aqueous phase was extracted with Et<sub>2</sub>O (3 x 40 mL), and the combined

organic extract was dried over anhyd.  $\text{Na}_2\text{SO}_4$ , filtered, and concentrated *in vacuo*. Column chromatography (silica gel, first with hexanes to remove  $\text{S}_8$ , then 96:4 hexanes/EtOAc,  $R_f$  0.30) gave *rac/meso* **57a** (1.76 g, 64%), a pale yellow solid, as an approximately 1:1:1 mixture of three stereoisomers as determined by  $^{31}\text{P}$  NMR [ $\delta$  69.7 ((*S,S*)-**57a**),  $\delta$  66.4 ((*R,R*)-**57b**),  $\delta$  64.4 (*meso*-**57c**)]. The mixture of diastereomers was suspended in abs. MeOH (75 mL) and heated to reflux for 4 h. Hot filtration of the mixture afforded the pure (*S,S*)-**57a** diastereomer (450 mg). The filtrate was evaporated to dryness and 269 mg was taken up in  $\text{Et}_2\text{O}$  and pre-adsorbed on silica gel. Careful column chromatography (silica gel, 99.4:0.6 hexane/ $\text{Et}_2\text{O}$ ) afforded, sequentially and *meso*-**57a** (97 mg) and (*R,R*)-**57a** (68 mg).



(*S,S*)-**57a**. pale yellow solid; mp 235-237 °C (pentane/ $\text{CH}_2\text{Cl}_2$ )

(lit. mp 225-227 °C (pentane/ $\text{CH}_2\text{Cl}_2$ ));  $[\alpha]_D^{20}$  -252 (*c* 1.00,  $\text{CHCl}_3$ );

$^{31}\text{P}$  NMR (121.5 MHz,  $\text{CDCl}_3$ )  $\delta$  69.7;  $^1\text{H}$  NMR (300 MHz,  $\text{CDCl}_3$ )  $\delta$

7.31-7.11 (m, 10H), 6.57 (s, 2H), 5.34-5.28 (m, 1H), 5.18-5.13 (m,

1H), 4.20 (qd, 1H,  $J$  = 10.5, 4.2 Hz), 2.62-2.57 (m, 1H), 2.52-2.39 (m, 2H), 2.34-2.06 (m,

5H), 1.60-1.58 (m, 2H), 1.47-1.35 (m, 2H), 1.18-1.07 (m, 1H), 1.02-0.98 (m, 1H), 0.94 (d,

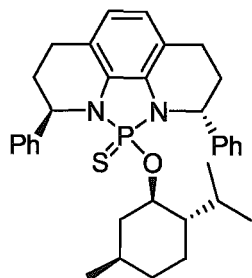
3H,  $J$  = 6.9 Hz), 0.88-0.67 (m, 3H), 0.30 (d, 3H,  $J$  = 6.9 Hz), 0.25 (d, 3H,  $J$  = 6.9 Hz);  $^{13}\text{C}$

NMR (150.9 MHz,  $\text{CDCl}_3$ )  $\delta$  142.9, 141.3, 128.5, 128.4, 128.1, 127.1, 127.0, 126.4,

126.3, 117.85, 117.82, 117.25, 117.21, 116.8, 116.7, 80.9 (d,  $J^{13}\text{C}-^{31}\text{P}$  = 8.8 Hz), 52.69,

52.66, 47.31, 47.25, 44.2, 33.9, 31.5, 30.3, 30.2, 29.9, 29.87, 24.4, 22.3, 22.2, 20.9, 19.52,

19.48, 15.2; EIMS [ $m/z(\%)$ ] 556 ( $M^+$ , 12), 418 (100); HRMS (EI) calcd for  $C_{34}H_{41}N_2OPS$ : 556.2677; found 556.2673.



**(*R,R*)-57a.** pale yellow solid; mp 119-121 °C

(pentane/ $CH_2Cl_2$ );  $[\alpha]_D^{20} +141$  ( $c$  1.00,  $CHCl_3$ ); IR (KBr)  $\nu_{max}$  3052,

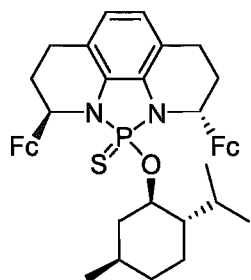
3030, 2950, 2923, 2866, 1473, 1290, 1161. 1110  $cm^{-1}$ ;  $^{31}P$  NMR

(121.5 MHz,  $CDCl_3$ )  $\delta$  66.4;  $^1H$  NMR (600 MHz,  $CDCl_3$ )  $\delta$

7.28-7.25 (m, 4H), 7.22(d, 2H,  $J=7.2Hz$ ), 7.18 (d, 2H,  $J=7.2Hz$ ), 7.10 (d, 2H,  $J=7.8Hz$ ), 6.60 (m, 2H), 5.30 (s, 1H), 5.13 (s, 1H), 4.18-4.12(m, 1H), 2.61-2.54 (m, 3H), 2.47-2.42 (m, 1H), 2.30-2.08 (m, 6H), 1.52 (m, 1H), 1.43 (m, 1H), 1.20 (d, 1H,  $J=12Hz$ ), 1.15-1.06 (m, 2H), 0.91 (d, 3H,  $J = 7.2$  Hz), 0.85 (d, 3H,  $J = 7.2$  Hz), 0.51-0.45 (m, 4H), -0.41- -0.47 (dd, 1H,  $J=23.4, 12Hz$ );  $^{13}C$  NMR (150.9 MHz,  $CDCl_3$ )  $\delta$  143.1, 141.7, 128.54, 128.46, 128.1, 127.01, 126.98, 126.91, 126.2, 117.77, 116.96, 116.92, 116.67, 116.62, 81.7 (d,  $J^{13}C-^{31}P = 9.0$  Hz), 52.79, 52.76, 52.25, 52.21, 47.85, 47.80, 41.5, 33.8, 30.9, 29.9 (d,  $J^{13}C-^{31}P = 4.5$  Hz), 29.7 (d,  $J^{13}C-^{31}P = 7.5$  Hz), 22.6, 21.8, 20.9, 19.6, 19.5, 16.0; EIMS [ $m/z(\%)$ ] 556 ( $M^+$ , 4), 418 (19), 95 (100); HRMS (EI) calcd for  $C_{34}H_{41}N_2OPS$ : 556.2677; found 556.2673; Anal. Calcd for  $C_{34}H_{41}N_2OPS$ : C, 73.35; H, 7.42; found C, 72.82; H, 7.61.

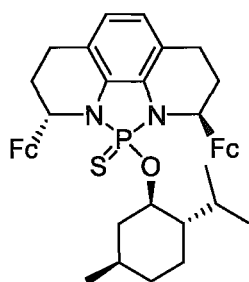
### Resolution of *rac/meso* **57f**.

A flame-dried flask with an attached reflux condenser containing a solution of *rac/meso*-2,9-diferrocenyl-1,2,3,4,7,8,9,10-octahydrophenanthroline **56f** (700 mg, 1.26 mmol) and *N,N*-dimethylaniline (838 mg, 6.92 mmol) in CH<sub>2</sub>Cl<sub>2</sub> (20 mL) was stirred at room temperature for 10 min. To the orange solution was added a solution of freshly distilled PCl<sub>3</sub> in solution CH<sub>2</sub>Cl<sub>2</sub> (2.77 mL, 0.5 M, 1.38 mmol) slowly by syringe and the dark red solution heated to reflux. After 1.5 h, (–)-menthol (197 mg, 1.26 mmol) was added from the top of the condenser to the reaction mixture and stirring was continued at reflux. After an additional 40 min, S<sub>8</sub> (402 mg, 12.6 mmol) was added and the mixture was heated at reflux for 75 min. The solvent was evaporated under reduced pressure and 8 M aq. HCl (10 mL) was poured into the flask. The mixture was extracted with Et<sub>2</sub>O (3 x 20 mL), washed with water (10 mL) and sat. aq. NaHCO<sub>3</sub> (10 mL), dried over anhyd. Na<sub>2</sub>SO<sub>4</sub>, filtered and pre-adsorbed on silica gel on a rotary evaporator. Column chromatography (silica gel, first with 99:1 hexane/Et<sub>2</sub>O to elute excess S<sub>8</sub>, then 97.5:2:0.5 hexane/Et<sub>2</sub>O/Et<sub>3</sub>N) gave, sequentially **(*R,R*)-57f** (142 mg, 13%, R<sub>f</sub> 0.27, <sup>31</sup>P δ 66.1), **(*S,S*)-57f** (120 mg, 11%, R<sub>f</sub> 0.24, <sup>31</sup>P: δ 65.3) and ***meso*-57f** (200 mg, 18%, R<sub>f</sub> 0.17, <sup>31</sup>P: δ 74.5).



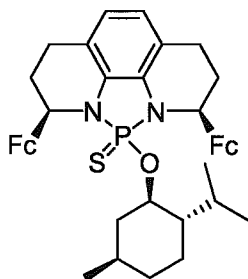
**(*R,R*)-57f**. Orange solid; mp 116-118 °C (Et<sub>2</sub>O/hexanes); [ $\alpha$ ]<sub>D</sub><sup>20</sup> +112.5 (*c* 0.80, CHCl<sub>3</sub>); IR (KBr)  $\nu_{max}$  3092, 2950, 2924, 2865,

1468  $\text{cm}^{-1}$ ;  $^{31}\text{P}$  NMR (121.5 MHz,  $\text{CDCl}_3$ )  $\delta$  66.1;  $^1\text{H}$  NMR (300 MHz,  $\text{CDCl}_3$ )  $\delta$  6.55 (d, 1H,  $J = 7.8$  Hz), 6.50 (d, 1H,  $J = 7.8$  Hz), 5.06-5.03 (m, 1H), 4.90-4.87 (m, 1H), 4.65 (s, 1H), 4.51 (s, 1H), 4.18 (s, 5H), 4.16 (s, 5H), 4.14 (m, 1H), 4.11 (m, 1H), 4.08-4.05 (m, 2H), 4.03 (m, 2H), 3.17-3.12 (m, 1H), 2.80-2.74 (m, 2H), 2.73-2.69 (m, 1H), 2.61-2.58 (m, 1H), 2.42-2.40 (m, 1H), 2.12-2.09 (m, 1H), 2.04-1.99 (m, 1H), 1.96-1.90 (m, 1H), 1.55-1.53 (m, 3H), 1.46-1.43 (m, 1H), 1.23-1.20 (m, 1H), 1.04 (m, 1H), 0.93-0.88 (m, 1H), 0.84 (d, 6H,  $J = 7.2$  Hz), 0.78 (d, 3H,  $J = 6.6$  Hz), 0.69-0.62 (m, 1H), 0.39 (q, 1H,  $J = 12$  Hz);  $^{13}\text{C}$  NMR (150.9 MHz,  $\text{CDCl}_3$ )  $\delta$  128.80 (d,  $J^{13}_{\text{C}-^{31}\text{P}} = 10.6$  Hz), 127.56 (d,  $J^{13}_{\text{C}-^{31}\text{P}} = 10.6$  Hz), 117.88, 117.44, 117.38, 116.45 (d,  $J^{13}_{\text{C}-^{31}\text{P}} = 7.5$  Hz), 92.2, 89.6, 80.45 (d,  $J^{13}_{\text{C}-^{31}\text{P}} = 9.1$  Hz), 72.0, 71.7, 69.0, 68.8, 68.3, 68.0, 67.5, 66.8, 66.5, 65.8, 49.4, 49.2, 48.25 (d,  $J^{13}_{\text{C}-^{31}\text{P}} = 6.0$  Hz), 42.9, 34.0, 31.5, 30.5, 28.3, 25.1, 22.9, 22.7, 21.9, 21.3, 21.0, 16.4; EIMS [ $m/z(\%)$ ] 772 ( $\text{M}^+$ , 6), 634 (4), 57 (100); HRMS (EI) calcd for  $\text{C}_{42}\text{H}_{49}\text{Fe}_2\text{N}_2\text{OPS}$ : 772.2001; found 772.2002; Anal. Calcd for  $\text{C}_{42}\text{H}_{49}\text{Fe}_2\text{N}_2\text{OPS}$ : C, 65.29, H, 6.39; found C, 65.27, H, 6.40.



**(*S,S*)-57f.** Orange solid; mp 95-96 °C (hexane/ $\text{Et}_2\text{O}$ );  $[\alpha]_{\text{D}}^{20}$  -89.7 ( $c$  1.26,  $\text{CHCl}_3$ ); IR (KBr)  $\nu_{\text{max}}$  3092, 2951, 2923, 2865, 1600, 1468  $\text{cm}^{-1}$ ;  $^{31}\text{P}$  NMR (121.5 MHz,  $\text{CDCl}_3$ )  $\delta$  65.3;  $^1\text{H}$  NMR (300 MHz,  $\text{CDCl}_3$ )  $\delta$  6.53 (d, 1H,  $J = 7.8$  Hz), 6.48 (d, 1H,  $J = 7.8$  Hz), 5.11 (m, 1H), 5.03 (m, 1H), 4.83 (s, 1H), 4.60 (s, 1H), 4.20 (s, 5H), 4.18 (s, 5H), 4.21-4.15 (m, 3H), 4.09 (m, 1H), 4.07 (s, 2H), 3.68-3.56 (m, 1H), 3.00-2.60 (m, 5H),

2.50-2.39 (m, 1H), 2.12-1.96 (m, 3H), 1.53-1.36 (m, 3H), 1.10-0.96 (m, 2H), 0.83 (d, 3H,  $J = 6.9$  Hz), 0.72 (d, 3H,  $J = 6.9$  Hz), 0.61 (d, 3H,  $J = 8.4$  Hz), 0.91-0.58 (m, 2H), 0.37 (q, 1H,  $J = 11.4$  Hz);  $^{13}\text{C}$  NMR (75.5 MHz,  $\text{CDCl}_3$ )  $\delta$  128.88 (d,  $J^{13}\text{C}-^{31}\text{P} = 11.3$  Hz), 127.96 (d,  $J^{13}\text{C}-^{31}\text{P} = 11.3$  Hz), 117.8, 117.6, 117.45 (d,  $J^{13}\text{C}-^{31}\text{P} = 6.8$  Hz), 116.56 (d,  $J^{13}\text{C}-^{31}\text{P} = 6.8$  Hz), 90.9, 88.9, 80.0, 79.8, 72.1, 72.0, 69.1, 68.8, 67.8, 67.7, 67.3, 66.8, 66.7, 66.0, 50.1, 49.0, 48.3 (d,  $J^{13}\text{C}-^{31}\text{P} = 9.0$  Hz), 41.7, 33.7, 31.3, 28.8, 27.92 (d,  $J^{13}\text{C}-^{31}\text{P} = 6.8$  Hz), 25.3, 23.2, 23.0, 22.0, 21.3, 16.5; EIMS [ $m/z$ (%)] 772 ( $\text{M}^+$ , 100), 634 (55), 503 (46), 383 (49), 317 (29); HRMS (EI) calcd for  $\text{C}_{42}\text{H}_{49}\text{Fe}_2\text{N}_2\text{OPS}$ : 772.2001; found 772.1990.



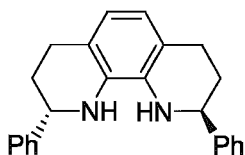
**meso-57f.** Orange solid; mp 235-236 °C ( $\text{Et}_2\text{O}$ );  $[\alpha]_{\text{D}}^{20} -0.5$  ( $c$  1.0,  $\text{CHCl}_3$ ); IR (KBr)  $\nu_{\text{max}}$  3082, 3039, 2922, 2866, 1593, 1464  $\text{cm}^{-1}$ ;  $^{31}\text{P}$  NMR (121.5 MHz,  $\text{CDCl}_3$ )  $\delta$  74.5;  $^1\text{H}$  NMR (600 MHz,  $\text{CDCl}_3$ )  $\delta$  6.53 (s, 2H), 4.85 (m, 1H), 4.77-4.75 (m, 3H), 4.21 (m,

1H), 4.18 (s, 5H), 4.17 (s, 5H), 4.16 (m, 1H), 4.12 (m, 2H), 4.10 (m, 1H), 4.08 (m, 1H), 3.00-2.87 (m, 3H), 2.81-2.78 (m, 2H), 2.53-2.52 (m, 2H), 2.35 (m, 1H), 2.27 (m, 1H), 1.68 (m, 1H), 1.34-1.27 (m, 3H), 0.83 (m, 1H), 0.65 (d, 3H,  $J = 7.2$  Hz), 0.63 (m, 1H), 0.54 (d, 3H,  $J = 6.0$  Hz), 0.53-0.40 (m, 3H), 0.44 (d, 3H,  $J = 7.2$  Hz);  $^{13}\text{C}$  NMR (150.9 MHz,  $\text{CDCl}_3$ )  $\delta$  129.48 (d,  $J^{13}\text{C}-^{31}\text{P} = 13.6$  Hz), 129.28 (d,  $J^{13}\text{C}-^{31}\text{P} = 12.1$  Hz), 117.88 (d,  $J^{13}\text{C}-^{31}\text{P} = 7.5$  Hz), 117.50 (d,  $J^{13}\text{C}-^{31}\text{P} = 7.5$  Hz), 117.48 (d,  $J^{13}\text{C}-^{31}\text{P} = 7.5$  Hz), 90.5, 89.6, 81.70 (d,  $J^{13}\text{C}-^{31}\text{P} = 13.6$  Hz), 72.9, 72.3, 68.82, 68.77, 68.1, 67.8, 67.4, 67.3, 66.83, 66.81, 49.92 (d,  $J^{13}\text{C}-^{31}\text{P} = 1.5$  Hz), 49.68 (d,  $J^{13}\text{C}-^{31}\text{P} = 1.5$  Hz), 47.68 (d,  $J^{13}\text{C}-^{31}\text{P} = 7.5$  Hz), 40.28



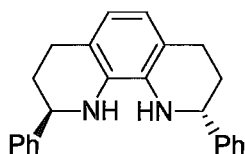
(d,  $J^{13}_{\text{C}-^{31}\text{P}} = 3.0$  Hz), 33.8, 31.3, 29.32 (d,  $J^{13}_{\text{C}-^{31}\text{P}} = 7.5$  Hz), 28.5 (d,  $J^{13}_{\text{C}-^{31}\text{P}} = 7.5$  Hz), 25.0, 24.1, 23.7, 22.8, 22.0, 21.2, 16.4.; EIMS [ $m/z(\%)$ ] 772 ( $\text{M}^+$ , 1), 548 (100), 483 (81); HRMS (EI) calcd for  $\text{C}_{42}\text{H}_{49}\text{Fe}_2\text{N}_2\text{OPS}$ : 772.2001; found 772.2130; Anal. Calcd for  $\text{C}_{42}\text{H}_{49}\text{Fe}_2\text{N}_2\text{OPS}$ : C, 65.29, H, 6.39; found C, 64.99, H, 6.38.

**(2*S*,9*S*)-Diphenyl-1,2,3,4,7,8,9,10-octahydro-1,10-phenanthroline [(*S*, *S*)-56a]**



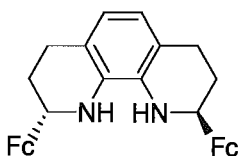
An oven-dried flask containing (*S,S*)-57a (160 mg, 0.29 mmol) and  $\text{LiAlH}_4$  (120 mg, 3.16 mmol) in THF (4 mL) under argon was heated to reflux for 2 h. After cooling to 0 °C, the reaction mixture was treated with sat. aq.  $\text{Na}_2\text{SO}_4$  solution (2 mL) resulting in the formation of a gray precipitate. When gas evolution subsided, the mixture was filtered through Celite on a sintered funnel, washing with  $\text{Et}_2\text{O}$ . The filtrate was dried over anhyd.  $\text{Na}_2\text{SO}_4$ , filtered and concentrated on a rotary evaporator. Column chromatography (silica gel, 96.5:3:0.5 hexane/ $\text{EtOAc}/\text{Et}_3\text{N}$ ,  $R_f$  0.28) gave (*S,S*)-56a (84 mg, 87%) as a yellow solid; mp 151-152 °C (acetone);  $[\alpha]_{\text{D}}^{20} -287$  ( $c$  1.23, acetone);  $^1\text{H}$  NMR (300 MHz, acetone- $\text{d}_6$ )  $\delta$  7.41 (d, 4H,  $J=7.2\text{Hz}$ ), 7.29 (m, 4H), 7.21 (d, 2H,  $J=8.4\text{Hz}$ ), 6.35 (s, 2H), 4.46-4.42 (m, 2H), 4.24 (b, 2H), 2.94-2.75 (m, 4H), 2.64 (m, 2H), 1.97-1.88 (m, 2H);  $^{13}\text{C}$  NMR (75.5 MHz, acetone- $\text{d}_6$ )  $\delta$  146.4, 1332, 129.0, 127.7, 127.5, 119.7, 119.0, 57.2, 32.1, 27.3;

**(2*R*,9*R*)-Diphenyl-1,2,3,4,7,8,9,10-octahydro-1,10-phenanthroline [(*R*, *R*)-56a]**

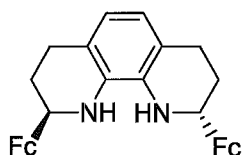


According to the same procedure with **(S,S)-56a**, **(R,R)-57a** (390 mg, 0.70 mmol) reacted with LiAlH<sub>4</sub> (294 mg, 7.7 mmol) in 15 mL THF to give **(R,R)-56a** (204 mg, 86%) as a yellow solid. Mp 146-148 °C (acetone);  $[\alpha]_D^{20} +256$  (*c* 0.95, acetone); <sup>1</sup>H NMR and <sup>13</sup>C NMR data matched that of **(S,S)-56a**.

**(+)-(2*S*,9*S*)-2,9-Diferrocenyl-1,2,3,4,7,8,9,10-octahydrophenanthroline [(*S,S*)-56f].**



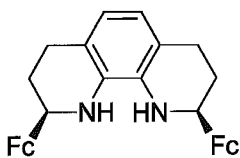
An oven-dried flask containing **(S,S)-57f** (129 mg, 0.167 mmol), LiAlH<sub>4</sub> (317 mg, 8.36 mmol) in THF (8 mL) under argon was heated to reflux for 16 h. After cooling to 0 °C, the reaction mixture was treated with sat. aq. Na<sub>2</sub>SO<sub>4</sub> solution (2 mL) resulting in the formation of a gray precipitate. When gas evolution subsided, the mixture was filtered through Celite on a sintered funnel, washing with Et<sub>2</sub>O. The filtrate was dried over anhyd. Na<sub>2</sub>SO<sub>4</sub>, filtered and concentrated on a rotary evaporator. Column chromatography (silica gel, 91.5:8:0.5 hexane/Et<sub>2</sub>O/Et<sub>3</sub>N, *R<sub>f</sub>* 0.26) gave **(S,S)-56f** (79 mg, 84%) as an orange solid; mp 155-156 °C (acetone);  $[\alpha]_D^{20} +291$  (*c* 1.25, acetone); IR (KBr)  $\nu_{max}$  3317, 3089, 2919, 2838, 1468, 1104 cm<sup>-1</sup>; <sup>1</sup>H NMR (300 MHz, acetone-d<sub>6</sub>)  $\delta$  6.37 (s, 2H), 4.39-4.37 (m, 2H), 4.34-4.32 (m, 2H), 4.30 (s, 10H), 4.20-4.11 (m, 6H), 3.94 (b, 2H), 2.91-2.78 (m, 2H), 2.69-2.60 (m, 2H), 2.14-2.08 (m, 2H), 1.77-1.64 (m, 2H); <sup>13</sup>C NMR (75.5 MHz, acetone-d<sub>6</sub>)  $\delta$  133.6, 120.4, 119.3, 94.0, 69.3, 68.6, 67.9, 67.2, 66.8, 52.5, 31.9, 27.6; FABMS [*m/z*(%)] 556 (M<sup>+</sup>, 50), 55 (100); HRMS (FAB) calcd for C<sub>32</sub>H<sub>32</sub><sup>56</sup>Fe<sub>2</sub>N<sub>2</sub>: 556.1264; found 556.1260; Anal. Calcd for C<sub>32</sub>H<sub>32</sub>Fe<sub>2</sub>N<sub>2</sub>: C, 69.09, H, 5.80; found : C, 68.51, H, 5.61.



**(-)-(2*R*,9*R*)-2,9-Ferrocenyl-1,2,3,4,7,8,9,10-octahydrophenanthroline [(*R,R*)-56f].**

An oven dried flask containing (*R,R*)-57f (86 mg, 0.11 mmol) and LiAlH<sub>4</sub> (211 mg, 5.57 mmol) in THF (5 mL) was heated to reflux for 16 h. After cooling to 0 °C, the reaction mixture was treated with sat. aq. Na<sub>2</sub>SO<sub>4</sub> solution (2 mL) resulting in the formation of a gray precipitate. When gas evolution subsided, the mixture was filtered through Celite on a sintered funnel, washing with Et<sub>2</sub>O. The filtrate was dried over anhyd. Na<sub>2</sub>SO<sub>4</sub>, filtered and concentrated on a rotary evaporator. Column chromatography (silica gel, 91.5:8:0.5 hexane/Et<sub>2</sub>O/Et<sub>3</sub>N, R<sub>f</sub> 0.26) gave (*R,R*)-56f (46 mg, 75%) as an orange solid; mp 154-155 °C (acetone); [α]<sub>D</sub><sup>20</sup> -300 (*c* 1.13, acetone); <sup>13</sup>C NMR (75.5 MHz, acetone-*d*<sub>6</sub>) δ 133.6, 120.4, 119.3, 94.0, 69.2, 68.6, 67.9, 67.2, 66.8, 52.5, 31.9, 27.6; EIMS [*m/z*(%)] 556 (M<sup>+</sup>, 47), 548 (100), 483 (89) ; HRMS (EI) calcd for C<sub>32</sub>H<sub>32</sub><sup>56</sup>Fe<sub>2</sub>N<sub>2</sub>: 556.1264; found 556.1258.

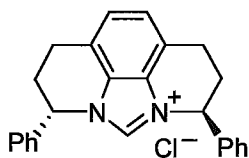
***meso*-2,9-Diferrocenyl-1,2,3,4,7,8,9,10-octahydrophenanthroline (*meso*-56f).**



An oven dried flask containing *meso*-57f (126 mg, 0.163 mmol) and LiAlH<sub>4</sub> (310 mg, 8.16 mmol) in THF (10 mL) was heated to reflux for 16h. After cooling to 0 °C, the reaction mixture was treated with sat. aq. Na<sub>2</sub>SO<sub>4</sub> solution (2 mL) resulting in the formation of a gray precipitate. When gas evolution subsided, the mixture was filtered through Celite on a sintered funnel, washing with Et<sub>2</sub>O. The filtrate was dried over anhyd. Na<sub>2</sub>SO<sub>4</sub>, filtered

and concentrated on a rotary evaporator. Column chromatography (silica gel, 91.5:8:0.5 hexane/Et<sub>2</sub>O/Et<sub>3</sub>N, R<sub>f</sub> 0.26) gave *meso*-**56f** (79 mg, 87%) as an orange solid; mp 190-192 °C (acetone); <sup>1</sup>H NMR (300 MHz, acetone-d<sub>6</sub>) δ 6.39 (s, 2H), 4.35 (m, 2H), 4.30 (m, 2H), 4.29 (s, 10H), 4.20-4.19 (m, 2H), 4.16-4.15 (m, 2H), 4.13-4.08 (m, 2H), 3.90 (b, 2H), 2.88-2.82 (m, 2H), 2.72-2.63 (m, 2H), 2.16-2.09 (m, 2H), 1.80-1.70 (m, 2H); <sup>13</sup>C NMR (75.5 MHz, acetone-d<sub>6</sub>) δ 133.6, 120.6, 119.5, 94.5, 69.2, 68.5, 68.1, 67.3, 67.0, 52.0, 31.0, 27.3; Anal. Calcd for C<sub>32</sub>H<sub>32</sub>Fe<sub>2</sub>N<sub>2</sub>: C, 69.09, H, 5.80; found : C, 68.97, H, 5.69.

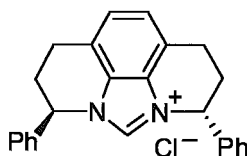
**(-)-(3*S*,5*S*)-Diphenyl-1,2,3,5,6,7-hexahydro-3a,4a-diaza-cyclopenta[def]phenanthrene nium chloride ((*S*, *S*)-**58a**)**



A stirred solution of diamine (*S,S*)-**56a** (85 mg, 0.25 mmol) in HC(OEt)<sub>3</sub> (8 mL) was treated with concentrated HCl solution (21 μL, 0.25 mmol) under argon, and heated to 80 °C. After 1 h. the septum was removed and the mixture heated at 80 °C for an additional 2 h, then cooled to ambient temperature. Et<sub>2</sub>O (12 mL) was added to induce precipitation of the product, which was collected on a Hirsch funnel, washed with cold ether and dried under high vacuum to give (*S,S*)-**58a** (82 mg, 86%) as a beige powder; mp 245-247 °C (Et<sub>2</sub>O); [α]<sub>D</sub><sup>18</sup> = -211 (*c* 1.0, CHCl<sub>3</sub>); IR (KBr) *v*<sub>max</sub> 3155, 3035, 2926, 2854, 1629, 1499, 1454, 1175 cm<sup>-1</sup>; <sup>1</sup>H NMR (600 MHz, CDCl<sub>3</sub>) δ 9.46 (s, 1H), 7.48-7.23 (m, 12H), 6.28 (b, 2H), 3.20-3.18 (m, 2H), 3.08-3.05 (m, 2H), 2.66 (b, 2H), 2.52 (b, 2H); <sup>13</sup>C NMR (150.9 MHz, CDCl<sub>3</sub>) δ 138.7, 136.8, 129.5,

129.3, 128.3, 127.0, 124.6, 123.0, 60.0, 31.9, 21.7; FABMS [ $m/z(\%)$ ] 351(M-Cl<sup>-</sup>, 100), HRMS (FAB) calcd for C<sub>25</sub>H<sub>23</sub>N<sub>2</sub>: 351.1861; found 351.1807.

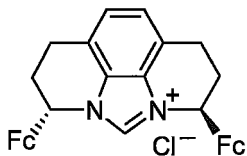
**(+)-(3*R*,5*R*)-Diphenyl-1,2,3,5,6,7-hexahydro-3a,4a-diaza-cyclopenta[def]phenanthrenium chloride [(*R,R*)-58a].**



Prepared from (*R,R*)-56a according to the procedure used for (*S,S*)-56a above. Mp 247-249 °C; [ $\alpha$ ]<sub>D</sub><sup>20</sup> +203 (*c* 1.00, CHCl<sub>3</sub>);

All spectroscopic data matched that of (*S,S*)-58a.

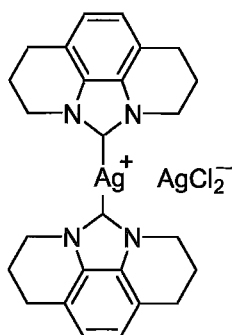
**(+)-(3*S*,5*S*)-Diferrocenyl-1,2,3,5,6,7-hexahydro-3a,4a-diaza-cyclopenta[def]phenanthrenium chloride [(*S,S*)-58f].**



A solution of (*S,S*)-56f (71 mg, 0.13 mmol) in (EtO)<sub>3</sub>CH (3 mL) was cooled to 0 °C and treated with conc. HCl solution (11  $\mu$ L, 0.13 mmol). The mixture was allowed to warm slowly to room temperature and stirred for 16 h. Diethyl ether (3 mL) was added to induce precipitation of the product, which was collected by filtration and washed with cold Et<sub>2</sub>O. Column chromatography (neutral alumina, 95:5 CH<sub>2</sub>Cl<sub>2</sub>/MeOH, R<sub>f</sub> 0.32) gave (*S,S*)-58f (45 mg, 59%) as an unstable beige solid that was of sufficient purity for complexation to iridium; mp 147-149 °C (CH<sub>2</sub>Cl<sub>2</sub>/MeOH); [ $\alpha$ ]<sub>D</sub><sup>20</sup> +34.3 (*c* 1.30, CH<sub>2</sub>Cl<sub>2</sub>); <sup>1</sup>H NMR (600 MHz, acetone-d<sub>6</sub>)  $\delta$  10.35 (b, 1H), 7.38 (s, 2H), 6.13 (s, 2H), 4.72 (b, 2H), 4.56 (s, 2H), 4.29 (s, 10H), 4.27 (s, 3H), 3.19 (m, 4H), 2.75 (b, 2H), 2.61 (b, 2H); <sup>13</sup>C NMR (75.5 MHz,

acetone- $d_6$ )  $\delta$  138.1, 127.6, 123.8, 122.9, 85.4, 69.2, 68.8, 68.6, 68.5, 66.0, 55.7, 30.2, 21.9; FABMS [ $m/z$ (%)] 567 (M-Cl, 5), 102 (100); HRMS (FAB) calcd for  $C_{33}H_{31}Fe_2N_2$ : 567.1182; found 567.1207.

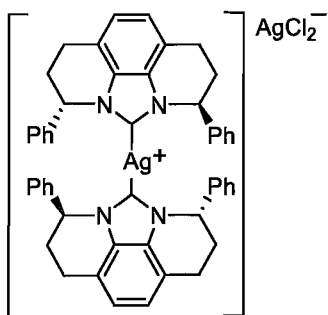
**Bis(1,2,3,5,6,7-hexahydro-3a,4a-diazacyclopenta[def]phenanthren-4-ylidene)silver(I)**



**AgCl<sub>2</sub> (90).**

A mixture of benzimidazolium chloride **66** (180 mg, 0.76 mmol) and silver oxide (100 mg, 0.43 mmol) in  $CH_2Cl_2$  (15 mL) was stirred at room temperature for 5 h under argon with exclusion of light. The resulting mixture was filtered through a small pad of Celite and the filtrate was concentrated to 1 mL. Hexane (3 mL) was added to induce precipitation of the product which was collected by filtration and dried under vacuum to give **90** (196 mg, 75%) as an off-white solid. Mp >250 °C; IR (KBr)  $\nu_{max}$  3025, 2930, 2873, 1480, 1386, 1332, 1243, 992  $cm^{-1}$ ;  $^1H$  NMR (300 MHz,  $CDCl_3$ )  $\delta$  7.04 (s, 4H), 4.32 (t, 8H,  $J = 5.7$  Hz), 2.98 (t, 8H,  $J = 6.0$  Hz), 2.30 (quin, 8H,  $J = 5.7$  Hz);  $^{13}C$  NMR (150.9 MHz,  $CDCl_3$ )  $\delta$  130.1, 121.4, 121.1, 46.0, 23.6, 23.4; FABMS [ $m/z$ (%)] 503 (M-AgCl<sub>2</sub>, 17), 199 (100); HRMS (FAB) calcd for  $C_{26}H_{28}N_4^{107}Ag$ : 503.1365; found 503.1383; Anal. Calcd for  $C_{26}H_{28}N_4Ag_2Cl_2$ : C, 45.71; H, 4.13; found C, 45.48; H, 4.02.

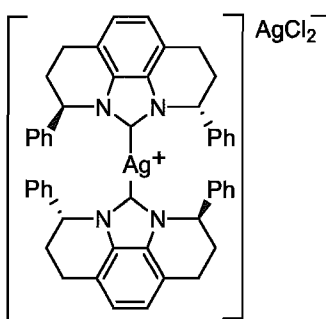
**Silver complex (–)-(S,S)-82a.**



To a mixture of benzimidazolium chloride (**S,S**)-**58a** (42 mg, 0.11 mmol) and  $Ag_2O$  (50 mg, 0.22 mmol) under argon

was added CH<sub>2</sub>Cl<sub>2</sub> (3 mL). The mixture was stirred at room temperature for 5 h in the absence of light. The resulting solution was filtered through a small pad of Celite and the filtrate was concentrated to 1 mL under reduced pressure. Addition of hexane (3 mL) induced formation of a precipitate, which was collected and dried under high vacuum to give (**S,S**)-**82a** (53 mg, 98%) as a light beige solid; mp >250 °C; [ $\alpha$ ]<sub>D</sub><sup>20</sup> -188 (*c* 0.50, CH<sub>2</sub>Cl<sub>2</sub>); IR (KBr)  $\nu_{max}$  2963, 2920, 2889, 1493, 1456, 1376, 1302, 1241 cm<sup>-1</sup>; <sup>1</sup>H NMR (300 MHz, CDCl<sub>3</sub>)  $\delta$  7.33-7.31 (m, 12H), 7.14 (s, 4H), 6.96-6.93 (m, 8H), 5.65 (t, 4H, *J* = 4.8 Hz), 3.00 (dt, 4H, *J* = 16.8, 5.1 Hz), 2.91-2.81 (m, 4H), 2.60-2.47 (m, 8H); <sup>13</sup>C NMR (75.5 MHz, CDCl<sub>3</sub>)  $\delta$  139.4, 130.4, 129.2, 128.6, 126.3, 121.6, 121.2, 59.8, 31.8, 21.0; FABMS [*m/z*(%)] 809 (M-AgCl<sub>2</sub>, 100), 457 (93), 351 (60), 245 (45); HRMS (FAB) calcd for C<sub>50</sub>H<sub>44</sub>N<sub>4</sub><sup>107</sup>Ag: 807.2617; found 807.2370; Anal. Calcd for C<sub>50</sub>H<sub>46</sub>N<sub>4</sub>Ag<sub>2</sub>Cl<sub>2</sub>: C, 60.81; H, 4.49; found C, 61.68; H, 4.49.

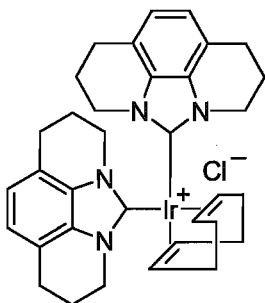
#### Silver complex (+)-(**R,R**)-**82a**.



To a mixture of benzimidazolium chloride (**R,R**)-**58a** (40 mg, 0.10 mmol) and Ag<sub>2</sub>O (24 mg, 0.10 mmol) under argon was added CH<sub>2</sub>Cl<sub>2</sub> (3 mL). The mixture was stirred at room temperature for 5 h in the absence of light. The resulting solution was filtered through a small pad of Celite and the filtrate was concentrated to 1 mL under reduced pressure. Addition of hexane (3 mL) induced formation of a precipitate, which was collected and dried under high vacuum to give (**R,R**)-**82a** (50 mg, 99%) as a light beige solid; mp: >250 °C; [ $\alpha$ ]<sub>D</sub><sup>20</sup> +186

(*c* 1.00, CH<sub>2</sub>Cl<sub>2</sub>); <sup>13</sup>C NMR (75.5 MHz, CDCl<sub>3</sub>)  $\delta$  139.4, 130.4, 129.2, 128.6, 126.3, 121.6, 121.2, 59.8, 31.8, 21.0.

**[Bis(1,2,3,5,6,7-hexahydro-3a,4a-diazacyclopenta[def]phenanthren-4-ylidene)iridium(III)(COD)] chloride (89).**

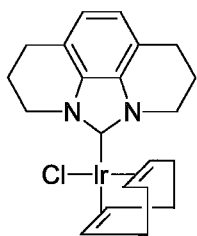


To a mixture of benzimidazolium chloride **66** (49 mg, 0.21 mmol), sodium hydride (10 mg, 60% dispersion in mineral oil, 0.25 mmol) and [Ir(COD)Cl]<sub>2</sub> (67 mg, 0.10 mmol) under inert atmosphere was added THF (3 mL). The mixture was stirred at

room temperature for 16 h, during which time the color changed from orange to red. After removing the solvent on a rotary evaporator, the crude product was purified by column chromatography (TSI silica gel, 97.5:2.5 CH<sub>2</sub>Cl<sub>2</sub>/MeOH, R<sub>f</sub> 0.21) to give **89** (56 mg, 38%) as an orange powder. Mp >250 °C; IR (KBr)  $\nu_{max}$  3007, 2926, 2877, 1626, 1483, 1387, 1328, 1243 cm<sup>-1</sup>; <sup>1</sup>H NMR (600 MHz, CDCl<sub>3</sub>)  $\delta$  6.88 (s, 4H), 4.59-4.56 (m, 4H), 4.36-4.32 (m, 4H), 3.97 (s, 4H), 3.00-2.93 (m, 8H), 2.46-2.40 (m, 8H), 2.32-2.29 (m, 4H), 2.11 (q, 4H, *J* = 8.4 Hz); <sup>13</sup>C NMR (150.9 MHz, CDCl<sub>3</sub>)  $\delta$  184.6, 130.9, 120.7, 120.0, 78.9, 46.0, 31.5, 23.8, 23.4; FABMS [*m/z*(%)] 697 (M-Cl, 100), 199 (88); HRMS (FAB) calcd for C<sub>34</sub>H<sub>40</sub>N<sub>4</sub><sup>193</sup>Ir: 697.2882; found 697.2921.

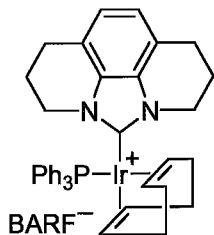
**(1,2,3,5,6,7-Hexahydro-3a,4a-diazacyclopenta[def]phenanthren-4-ylidene)iridium(III)(COD) chloride (91).**





To a flask containing silver complex **90** (41 mg, 0.06 mmol) and  $[\text{Ir}(\text{COD})\text{Cl}]_2$  (38 mg, 0.057 mmol) under an argon atmosphere was added  $\text{CH}_2\text{Cl}_2$  (2.5 mL). The orange mixture was stirred in the absence of light for 5.5 h, during which time the color changed to yellow. The mixture was filtered through a pad of Celite in a sintered funnel and the filtrate was concentrated on a rotary evaporator. Column chromatography (silica gel, 7:3 hexanes/EtOAc,  $R_f$  0.26) gave **91** (46 mg, 76%) as a yellow powder. Mp  $>250^\circ\text{C}$ ; IR (KBr)  $\nu_{\text{max}}$  2926, 2876, 2829, 1626, 1486, 1390, 1327  $\text{cm}^{-1}$ ;  $^1\text{H}$  NMR (600 MHz,  $\text{CDCl}_3$ )  $\delta$  6.86 (s, 2H), 4.69 (s, 2H), 4.62–4.58 (m, 2H), 4.40–4.36 (m, 2H), 3.05 (s, 2H), 2.90 (t, 4H,  $J = \text{Hz}$ ), 2.26 (b, 8H), 1.86–1.81 (m, 2H), 1.70–1.66 (m, 2H);  $^{13}\text{C}$  NMR (150.9 MHz,  $\text{CDCl}_3$ )  $\delta$  187.0, 131.1, 119.8, 119.6, 86.8, 51.6, 44.9, 33.8, 29.5, 23.62, 23.56; FABMS [ $m/z(\%)$ ] 534 ( $\text{M}^+$ , 28), 199 (100); HRMS (FAB) calcd for  $\text{C}_{21}\text{H}_{26}\text{N}_2^{193}\text{Ir}^{35}\text{Cl}$ : 534.1414; found 534.1498; Anal. Calcd for  $\text{C}_{21}\text{H}_{26}\text{N}_2\text{IrCl}$ : C, 47.22; H, 4.91; found C, 47.03; H, 5.24.

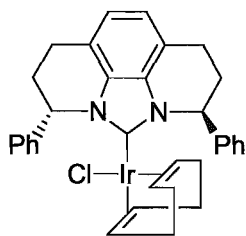
**(1,2,3,5,6,7-Hexahydro-3a,4a-diazacyclopenta[def]phenanthren-4-ylidene)triphenylphosphinoiridium(I)(COD) tetrakis(3,5-trifluoromethylphenyl)borate (**92**).**



A mixture of complex **91** (16 mg, 0.030 mmol), triphenylphosphine (7.9 mg, 0.030 mmol) and sodium tetrakis(3,5-trifluoromethyl)-phenylborate (NaBARF) (40 mg, 0.045 mmol) in dichloromethane (2 mL) was stirred at room temperature under argon for 4 h.

The red mixture was filtered through a small pad of TSI silica gel (230-400 mesh, pH 6.5 – 7) and the filtrate was evaporated, washed with cold pentane and dried under vacuum to give **92** (44 mg, 90%) as a red-orange solid; mp 175-176 °C (CH<sub>2</sub>Cl<sub>2</sub>/hexane); IR (KBr)  $\nu_{\max}$  3074, 2958, 2924, 1610, 1483, 1437, 1390, 1356, 1279, 1124 cm<sup>-1</sup>; <sup>31</sup>P NMR (121.5 MHz, CDCl<sub>3</sub>)  $\delta$  18.1; <sup>19</sup>F NMR (282.4 MHz, CDCl<sub>3</sub>)  $\delta$  -62.4; <sup>1</sup>H NMR (300 MHz, CDCl<sub>3</sub>)  $\delta$  7.74-7.72 (m, 8H), 7.52 (s, 4H), 7.41-7.20 (m, 15H), 6.88 (s, 2H), 4.39 (bs, 2H), 4.18-4.10 (m, 2H), 3.96 (bs, 2H), 3.65-3.52 (m, 2H), 2.86-2.60 (m, 4H), 2.40-2.22 (m, 4H), 2.20-1.95 (m, 6H), 1.78-1.65 (m, 2H); <sup>13</sup>C NMR (150.9 MHz, CDCl<sub>3</sub>)  $\delta$  181.7 (d,  $J^{31\text{P}-^{13}\text{C}}$  = 7.5 Hz), 161.7 (q,  $J^{11\text{B}-^{13}\text{C}}$  = 49.5 Hz), 134.8, 133.5 (d,  $J^{31\text{P}-^{13}\text{C}}$  = 8.5 Hz), 131.4, 131.0, 130.1 (d,  $J^{31\text{P}-^{13}\text{C}}$  = 51.0 Hz), 128.9, 128.83, 128.80 (q,  $J^{11\text{B}-^{13}\text{C}}$  = 31.5 Hz), 124.6 (q,  $J^{19\text{F}-^{13}\text{C}}$  = 271.5 Hz), 121.0, 119.7, 117.4, 85.64, 85.56, 83.0, 45.1, 31.3, 30.60, 30.58, 22.94, 22.90; FABMS [ $m/z$ (%)] 761 (M-BARF, 100), 199 (100); HRMS (FAB) calcd for C<sub>39</sub>H<sub>41</sub>N<sub>2</sub>P<sup>193</sup>Ir: 761.2637; found 761.2742; Anal. Calcd for C<sub>71</sub>H<sub>53</sub>BF<sub>24</sub>IrN<sub>2</sub>P: C, 52.50; H, 3.29; found C, 52.35; H, 3.21.

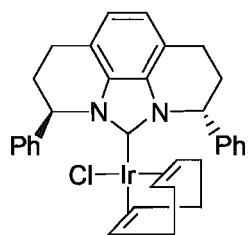
**(-)-[(3*S*,5*S*)-Diphenyl-1,2,3,5,6,7-hexahydro-3*a*,4*a*-diazacyclopenta[def]phenanthren-4-ylidene]iridium(I)(COD) chloride [(*S,S*)-**93a**].**



A flame-dried round-bottomed flask under argon was charged with silver complex (*S,S*)-**82a** (80 mg, 0.081 mmol) and [Ir(COD)Cl]<sub>2</sub> (54 mg, 0.081 mmol). Dry CH<sub>2</sub>Cl<sub>2</sub> was added (9 mL)

and the mixture was stirred in the dark at room temperature for 5 h. The resulting yellow solution was filtered through a pad of Celite, and the filtrate was concentrated on a rotary evaporator. Column chromatography (TSI silica gel, CH<sub>2</sub>Cl<sub>2</sub>, R<sub>f</sub> 0.29) gave **(S,S)-93a** (105 mg, 95%) as a yellow powder; mp >250 °C (PhMe/hexane); [ $\alpha$ ]<sub>D</sub><sup>20</sup> -115 (c 1.00, CHCl<sub>3</sub>); IR (KBr)  $\nu_{max}$  3058, 3027, 2925, 2871, 1469, 1453 cm<sup>-1</sup>; <sup>1</sup>H NMR (600 MHz, CDCl<sub>3</sub>)  $\delta$  7.35 (t, 2H, *J* = 6.6 Hz), 7.32-7.30 (m, 4H), 7.17 (d, 2H, *J* = 7.8 Hz), 7.08-7.06 (m, 2H), 7.00 (Abq, 2H, *J* = 7.2 Hz), 6.56 (d, 1H, *J* = 3 Hz), 5.78 (t, 1H, *J* = 4.8 Hz), 4.46-4.43 (m, 1H), 4.28-4.24 (m, 1H), 2.97 (dt, 1H, *J* = 16.8, 4.8 Hz), 2.88-2.83 (m, 3H), 2.76-2.73 (m, 1H), 2.60-2.51 (m, 2H), 2.49-2.44 (m, 1H), 2.31-2.28 (m, 1H), 2.17-2.14 (m, 1H), 2.04-1.98 (m, 1H), 1.88-1.81 (m, 2H), 1.56-1.50 (m, 1H), 1.41-1.35 (m, 2H), 1.08-1.00 (m, 2H); <sup>13</sup>C NMR (150.9 MHz, CDCl<sub>3</sub>)  $\delta$  190.5, 142.9, 140.4, 131.4, 128.6, 128.5, 127.7, 127.6, 127.1, 126.4, 120.3, 119.83, 119.75, 119.6, 86.5, 85.3, 59.4, 58.2, 52.8, 49.8, 33.4, 33.0, 32.8, 31.0, 29.1, 28.4, 21.4, 19.4; FABMS [*m/z*(%)] 686 (M<sup>+</sup>, 13), 647 (17), 541 (26), 149 (51), 57 (100), 41 (64); HRMS (FAB) calcd for C<sub>33</sub>H<sub>34</sub>N<sub>2</sub><sup>35</sup>Cl<sup>193</sup>Ir: 686.2040; found 686.2064.

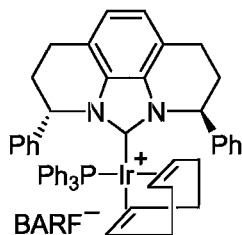
**(+)-[(3*R*,5*R*)-Diphenyl-1,2,3,5,6,7-hexahydro-3a,4a-diazacyclopenta[def]phenanthrene n-4-ylidene]iridium(I)(COD) chloride [(*R,R*)-93a].**



A flame-dried round-bottomed flask under argon was charged with silver complex **(*R,R*)-82a** (50 mg, 0.051 mmol) and

[Ir(COD)Cl]<sub>2</sub> (34 mg, 0.051 mmol). Dry CH<sub>2</sub>Cl<sub>2</sub> was added (4.5 mL) and the mixture was stirred in the dark at room temperature for 5.5 h. The resulting yellow solution was filtered through a pad of Celite, and the filtrate was concentrated on a rotary evaporator. Column chromatography (TSI silica gel, CH<sub>2</sub>Cl<sub>2</sub>, R<sub>f</sub> 0.29) gave (*R,R*)-**93a** (64 mg, 92%) as a yellow powder; mp >250 °C (PhMe/pentane); [ $\alpha$ ]<sub>D</sub><sup>20</sup> +109 (*c* 1.00, CHCl<sub>3</sub>); X-Ray analysis was performed on a yellow prism (0.22 × 0.12 × 0.08 mm) which was obtained by crystallization from toluene by vapor diffusion with pentane. Anal. Calcd for C<sub>33</sub>H<sub>34</sub>N<sub>2</sub>ClIr: C, 57.75; H, 4.99; found C, 57.58; H, 5.00. Spectroscopic data matched that of (*S,S*)-**93a**.

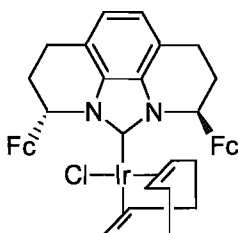
(-)-[(3*S*,5*S*)-Diphenyl-1,2,3,5,6,7-hexahydro-3a,4a-diazacyclopenta[def]phenanthren-4-ylidene]triphenylphosphinoiridium(I)(COD) tetrakis(3,5-trifluoromethylphenyl)-borate [(*S,S*)-**94a**].



A mixture of compound (*S,S*)-**93a** (46 mg, 0.067 mmol), triphenylphosphine (17.6 mg, 0.067 mmol) and sodium tetrakis(3,5-trifluoromethyl)phenyl borate (NaBARF) (89 mg, 0.101 mmol) in dichloromethane (4 mL) was stirred at room temperature under argon for 4 h. The red mixture was filtered through a small pad of TSI silica gel (230-400 mesh, pH 6.5 – 7) and the filtrate was evaporated, washed with cold pentane and dried under vacuum to give (*S,S*)-**94a** (108 mg, 91%) as a red-orange solid; mp 164-165 °C (CH<sub>2</sub>Cl<sub>2</sub>/hexane); [ $\alpha$ ]<sub>D</sub><sup>20</sup> -9.6 (*c* 1.00, CHCl<sub>3</sub>); IR (KBr)  $\nu_{max}$  3073, 2964, 2924, 1610,

1437, 1356, 1279, 1124  $\text{cm}^{-1}$ ;  $^{31}\text{P}$  NMR (121.5 MHz,  $\text{CDCl}_3$ )  $\delta$  16.6;  $^{19}\text{F}$  NMR (282.4 MHz,  $\text{CDCl}_3$ )  $\delta$  -62.4;  $^1\text{H}$  NMR (600 MHz,  $\text{CDCl}_3$ )  $\delta$  7.73 (s, 8H), 7.52 (s, 4H), 7.40 (t, 3H,  $J = 7.2$  Hz), 7.38 (b, 3H), 7.25 (b, 6H), 7.21 (m, 1H), 7.14 (d, 1H,  $J = 7.2$  Hz), 7.10-7.06 (m, 3H), 6.95 (b, 6H), 6.88 (d, 2H,  $J = 7.2$  Hz), 6.82 (b, 2H), 5.97 (d, 1H,  $J = 2.4$  Hz), 5.22 (d, 1H,  $J = 2.4$  Hz), 3.95 (t, 1H,  $J = 7.2$  Hz), 3.88 (m, 1H), 3.55-3.50 (m, 2H), 3.04 (m, 1H), 2.96-2.93 (m, 1H), 2.71-2.66 (m, 2H), 2.56-2.48 (m, 1H), 2.39-2.33 (m, 2H), 2.25 (m, 1H), 2.10 (m, 1H), 1.87-1.79 (m, 3H), 1.52 (m, 1H), 1.43 (m, 2H), 1.31 (m, 1H);  $^{13}\text{C}$  NMR (150.9 MHz,  $\text{CDCl}_3$ )  $\delta$  185.8 (d,  $J^{31}\text{P}-^{13}\text{C} = 9.0$  Hz), 161.7 (q,  $J^{11}\text{B}-^{13}\text{C} = 49.5$  Hz), 140.5, 139.7, 134.8, 133.6 (d,  $J^{31}\text{P}-^{13}\text{C} = 12.1$  Hz), 131.4, 131.3, 131.0, 130.6, 130.3, 129.3, 129.2, 128.9 (q,  $J^{11}\text{B}-^{13}\text{C} = 31.3$  Hz), 128.8, 128.7, 128.4, 126.1, 125.5, 124.6 (q,  $J^{19}\text{F}-^{13}\text{C} = 271.6$  Hz), 121.9, 121.6, 120.3, 119.8, 117.4, 88.45, 88.40, 87.5, 80.1, 80.0, 79.4, 60.1, 59.2, 33.9, 33.5, 31.2, 30.3, 28.6, 27.3, 19.3, 18.6; FABMS [ $m/z(\%)$ ] 913 (M-BarF, 100); HRMS (FAB) calcd for  $\text{C}_{51}\text{H}_{49}^{193}\text{IrN}_2\text{P}$ : 913.3263; found 913.3347; Anal. Calcd for  $\text{C}_{83}\text{H}_{61}\text{BF}_{24}\text{IrN}_2\text{P}$ : C, 56.12; H, 3.46; found C, 56.99; H, 3.74.

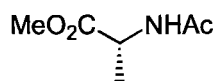
**(-)-[(3*S*,5*S*)-Diferrocenyl-1,2,3,5,6,7-hexahydro-3a,4a-diazacyclopenta[def]phenanthren-4-ylidene]iridium(I)(COD) chloride [(*S,S*)-93f].**



A flame-dried round-bottomed flask under argon was charged with benzimidazolium chloride (**(*S,S*)-58f**) (42 mg, 0.07 mmol),  $[\text{Ir}(\text{COD})\text{Cl}]_2$  (24 mg, 0.36 mmol) and  $\text{KO}^t\text{Bu}$  (22 mg, 0.18 mmol)

and THF (3 mL). The yellow solution was stirred at room temperature for 8.5 h. The solvent was removed on a rotary evaporator and column chromatography (neutral alumina, 59:40:1 hexane/CH<sub>2</sub>Cl<sub>2</sub>/Et<sub>3</sub>N, R<sub>f</sub> 0.28) gave (*S,S*)-**93f** (32 mg, 50%) as a yellow solid; mp 191-193 °C (CH<sub>2</sub>Cl<sub>2</sub>/hexane); [ $\alpha$ ]<sub>D</sub><sup>20</sup> -103 (*c* 1.00, CHCl<sub>3</sub>); X-Ray analysis was performed on a orange prism (0.45 × 0.35 × 0.33 mm) which was obtained by crystallization from dichloromethane by diffusion with hexane; IR (KBr)  $\nu_{max}$  2922, 2861, 2827, 1465, 1364, 1301, 1232 cm<sup>-1</sup>; <sup>1</sup>H NMR (600 MHz, CDCl<sub>3</sub>)  $\delta$  6.94 (d, 1H, *J* = 7.2 Hz), 6.84 (d, 1H, *J* = 7.2 Hz), 5.99 (m, 2H), 4.98 (s, 1H), 4.80-4.77 (m, 2H), 4.74 (d, 1H, *J* = 1.2 Hz), 4.34 (d, 1H, *J* = 1.8 Hz), 4.24 (s, 5H), 4.22 (s, 1H), 4.21 (s, 5H), 4.04-4.02 (m, 3H), 3.71 (s, 1H), 3.52 (m, 1H), 3.09 (m, 1H), 2.98-3.02 (m, 1H), 2.92-2.90 (m, 1H), 2.84-2.81 (m, 1H), 2.74-2.72 (m, 2H), 2.54 (m, 1H), 2.46-2.42 (m, 2H), 2.29 (m, 1H), 2.15 (m, 1H), 2.01-1.93 (m, 3H), 1.85-1.83 (m, 1H), 1.49-1.46 (m, 1H), 1.06-1.03 (m, 1H); <sup>13</sup>C NMR (150.9 MHz, CDCl<sub>3</sub>)  $\delta$  187.7, 130.34, 130.27, 120.2, 119.6, 119.2, 119.0, 91.8, 88.0, 87.7, 84.3, 71.8, 71.1, 69.1, 69.0, 68.2, 67.7, 67.64, 67.56, 65.99, 65.96, 65.85, 54.1, 53.1, 52.9, 52.5, 35.5, 32.3, 31.4, 30.5, 28.2, 27.7, 20.93, 20.87; Anal. Calcd for C<sub>41</sub>H<sub>42</sub>Fe<sub>2</sub>N<sub>2</sub>IrCl: C, 54.59, H, 4.69; found C, 54.86, H, 4.74.

**(-)-(R)-Methyl-2-acetamidopropanoate [(R)-37a].**



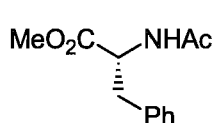
*Representative procedure:* A solution of

methyl-2-acetamidoacrylate **36a** (66 mg, 0.46 mmol) and iridium

catalyst (*S,S*)-**93a** (9 mg, 0.013 mmol, 3 mol %) in CH<sub>2</sub>Cl<sub>2</sub> (10 mL) in a vial under argon

was sealed in an autoclave. The autoclave was purged and backfilled three times with hydrogen gas, pressurized to 69 bar (1000 psi) and the apparatus was placed on a magnetic stirrer. The reaction mixture was stirred in the autoclave at room temperature for 72 h before the pressure was released. After evaporation of the solvent under reduced pressure, the remaining oil was purified by column chromatography (TSI silica gel, *t*-butyl methyl ether) to give (*R*)-**37a** (64 mg, 96%) as a colorless oil;  $[\alpha]_{\text{D}}^{20} -8.9$  (*c* 1.00, CHCl<sub>3</sub>) [lit.<sup>1</sup>  $[\alpha]_{\text{D}}^{25} -9.2$  (*c* 1.00, CHCl<sub>3</sub>) for the pure *R* enantiomer]; Chiral GC analysis (Chirasil DEX-CB; program: 30 °C for 5 min, then 5 °C/min to 150 °C) determined 90.5:9.5 er, 81% ee [ $t_{\text{R}}(\text{minor}) = 25.86$  min,  $t_{\text{R}}(\text{major}) = 26.02$  min]; <sup>1</sup>H NMR (300 MHz, CDCl<sub>3</sub>)  $\delta$  6.12 (b, 1H), 4.59 (quin, 1H, *J* = 7.2 Hz), 3.74 (s, 3H), 2.01 (s, 3H), 1.39 (d, 3H, *J* = 7.2 Hz).

**(–)-(R)-Methyl-2-acetamido-3-phenylpropanoate [(R)-37b].**



*Representative procedure:* A solution of *trans*-methyl-  $\alpha$ -acetamidocinnamate **36b** (35 mg, 0.16 mmol) and iridium catalyst **S,S-93a** (3.3 mg, 0.005 mmol, 3 mol %) in CH<sub>2</sub>Cl<sub>2</sub> (4 mL) in a vial under argon was sealed in an autoclave. The autoclave was purged and backfilled three times with hydrogen gas, pressurized to 69 bar (1000 psi) and the apparatus was placed on a magnetic stirrer. The reaction mixture was stirred in the autoclave at room temperature for 72 h before the pressure was released. After evaporation of the solvent under reduced pressure, the crude product was purified by column chromatography (TSI silica gel,

*t*-butyl methyl ether) to give (***R***)-**37b** (35 mg, 98%) as a colorless oil that solidified on standing;  $[\alpha]_{\text{D}}^{18} -48$  (*c* 0.90, CHCl<sub>3</sub>). [lit.<sup>ii</sup>  $[\alpha]_{\text{D}}^{25} -101.3$  (*c* 1.00, CHCl<sub>3</sub>) for the pure *R* enantiomer]; Chiral HPLC analysis (Chiralcel OD-H; eluent: 90:10 hexanes/*i*-PrOH, 0.5 mL/min) determined 70.5:29.5 er, 41% ee [ $t_{\text{R}}(\text{major}) = 20.76$  min,  $t_{\text{R}}(\text{minor}) = 26.65$  min].; <sup>1</sup>H NMR (300 MHz, CDCl<sub>3</sub>)  $\delta$  7.31-7.21 (m, 3H), 7.10-7.07 (m, 2H), 5.98 (b, 1H), 4.88 (dd, 1H, *J*=13.5, 5.7 Hz), 3.72 (s, 3H), 3.18-3.04 (m, 2H), 1.97 (s, 3H).



## 5. References

1. Arduengo III, A. J.; Dias, J. V.; Harlow, R. L.; Kline, M. *J. Am. Chem. Soc.* **1992**, *114*, 5530.
2. Bildstein, B. *J. Organomet. Chem.* **2001**, *617-618*, 28.
3. Reviews: a) Hahn, F. E.; Jahnke, M. C. *Angew. Chem. Int. Ed.* **2008**, *47*, 3122; b) Hahn, F. E. *Angew. Chem. Int. Ed.* **2006**, *45*, 1348; c) Herrmann, W. A. *Angew. Chem. Int. Ed.* **2002**, *41*, 1290; d) Herrmann, W. A.; Kocher, C. *Angew. Chem. Int. Ed.* **1997**, *36*, 2162.
4. Despagnet-Ayoub, E.; Grubbs, R. H. *J. Am. Chem. Soc.* **2004**, *126*, 10198.
5. Poyatos, M.; Mata J. A.; Falomir, E.; Crabtree, R. H.; Peris, E. *Organometallics* **2003**, *22*, 1110.
6. Viciano, M.; Mas-Marza, E.; Poyatos, M.; Sanau, M.; Crabtree, R. H.; Peris, E. *Angew. Chem. Int. Ed.* **2005**, *44*, 444.
7. Semeril, D.; Bruneau, C.; Dxneuf, P. H. *Adv. Synth. Catal.* **2002**, *344*, 585.
8. Metallinos, C.; Barrett, F. B.; Wang, Y.; Xu, S.; Taylor, N. J. *Tetrahedron* **2006**, *62*, 11145.
9. Perry, M. C.; Burgess, K. *Tetrahedron: Asymmetry* **2003**, *14*, 951.
10. Bourissou, D.; Guerret, O.; Gabba, F.P.; Bertrand, G. *Chem. Rev.* **2000**, *100*, 3991.
11. Clavier, H.; Nolan, S. P. *Annu. Rep. Prog. Chem., Sect B*, **2007**, *103*, 193.
12. Scholl, M.; Trnka, T.M.; Morgan, J. P.; Grubbs, R. H. *Tetrahedron Lett.* **1999**, *40*,

2247.

13. Denk, K.; Sirsch, P.; Herrmann, W. A. *J. Organomet. Chem.* **2002**, 649, 219.
14. Alder, R. W.; Allen, P. R.; Williams, S. *J. Chem. Soc., Chem. Commun.* **1995**, 1267.
15. Kim, Y. J.; Streitwieser, A. *J. Am. Chem. Soc.* **2002**, 124, 5757.
16. Magill, A. M.; Cavell, K. J.; Yates, B. F. *J. Am. Chem. Soc.* **2004**, 126, 8717.
17. Leuthauser, S.; Schwarz, D.; Plenio, H. *Chem. Eur. J.* **2007**, 13, 7195.
18. Herrmann, W. A.; Schutz, J.; Frey, G. D.; Herdtweck, E. *Organometallics* **2006**, 25, 2437.
19. Dorta, R.; Stevens, E. D.; Scott, N. M.; Costabile, C.; Cavallo, L.; Hoff, C. D.; Nolan, S. P. *J. Am. Chem. Soc.* **2005**, 127, 2485.
20. Chianese, A. R.; Li, X.; Janzen, M. C.; Faller, J. W.; Crabtree, R. H. *Organometallics* **2003**, 22, 1663.
21. Chinanese, A. R.; Kovacevic, A.; Zeglis, B. M.; faller, J. W.; Crabtree, R. H. *Organometallics* **2003**, 23, 2461.
22. O'Brien, C. J.; Assen, E.; Kantchev, B.; Chass, G.A.; Hadei, N.; Hopkinson, A. C.; Organ, M. G.; Setiadi, D. H.; Tang, T-H.; Fang, D-C. *Tetrahedron* **2005**, 61, 9723.
23. Tolman, C. A. *Chem. Rev.* **1977**, 77, 313.
24. Huang, J.; Schanz, H. J.; Stevens, E. D.; Nolan, S. P. *Organometallics* **1999**, 18, 2370.
25. Hillier, A. C.; Sommer, W. J.; Yong, B. S.; Petersen, J. L.; Cavallo, L. Nolan, S. P. *Organometallics* **2003**, 22, 4322.
26. Wurtz, S.; Glorius, F. *Acc. Chem. Res.* **2008**, Published on Web 08/23/2008.

27. Wanzlick, H. W. *Angew. Chem. Int. Ed.* **1962**, *1*, 75.
28. Öfele, K. *J. Organomet. Chem.* **1968**, *12*, 42.
29. Wanzlick, H. W.; Schonherr, H. J. *Angew. Chem.* **1968**, *7*, 141.
30. Arduengo III, A. J.; Harlow, R. L.; Kline, M. *J. Am. Chem. Soc.* **1991**, *113*, 361.
31. Arduengo III, A. J.; Goerlich, J. R.; Marshall, W. J. *J. Am. Chem. Soc.* **1995**, *117*, 11027.
32. Arduengo III, A. J.; Davidson, F.; Dias, H. V. R.; Goerlich, J. R.; Khasnis, D.; Marshall, W. J.; Prakasha, T. K. *J. Am. Chem. Soc.* **1997**, *119*, 12742.
33. Herrmann, W. A.; Elison, M.; Fischer, J.; Kocher, C.; Arthus, G. R. *Angew. Chem. Int. Ed.* **1995**, *34*, 2371.
34. Schwab, P.; Grubbs, R. H.; Ziller, J. W. *J. Am. Chem. Soc.* **1996**, *118*, 100.
35. Scholl, M.; Ding, S.; Lee, C. W.; Grubbs, R. H. *Org. Lett.* **1999**, *1*, 953.
36. Herrmann, W.A.; Goosen, L. J.; Kocher, C.; Artus, G. H. *Angew. Chem. Int. Ed.* **1996**, *35*, 2805.
37. Arduengo III, A. J. *US Patent 5,182,405*, **1993**.
38. Seiders, T. J.; Ward, D. W.; Grubbs, R. H. *Org. Lett.* **2001**, *3*, 3225.
39. Seo, H.; Kim, B. Y.; Lee, J. H.; Park, H.; Son, S. U.; Chung, Y. K. *Organometallics* **2003**, *22*, 4783.
40. Glorius, F. (ed) *N-heterocyclic Carbenes in Transition Metal Catalysis*, **2006**, Springer.
41. Douthwaite, R. E.; Houghton, J.; Kariuki, B. M. *Chem. Commun.* **2004**, 698.

42. Baker, M. V.; Brayshaw, S. K.; Skelton, B. W.; White, A. H.; Williams, C. J. *Organomet. Chem.* **2005**, *690*, 2312.
43. Kocber, C.; Herrmann, W. A. *J. Organomet. Chem.* **1997**, *532*, 261.
44. Danopoulos, A. A.; Winston, S.; Motherwell, W. B. *Chem. Commun.* **2002**, 1376.
45. Fehlammer, W P.; Bliss, T.; Kern.; Brudgam, I. *J. Organomet. Chem.* **1995**, *490*, 149.
46. Enders, D.; Gielen, H. *J. Organomet. Chem.* **2001**, *617*, 70.
47. Lee, H. M.; Chiu, P. L.; Zeng, J. Y. *Inorg. Chim. Acta.* **2004**, *357*, 4313.
48. Martin, H. G.; James, N. H.; Aitken, J.; Gaunt, J. A., Adams, H.; Haynes, A. *Organometallics* **2003**, *22*, 4451.
49. Clyne, D. S.; Jin, J.; Genest, E.; Gallucci, J. C.; Rajanbabu, T. V. *Org. Lett.* **2000**, *2*, 1125.
50. Wang, H. J.; Lin, I. B. *Organometallics* **1998**, *17*, 972.
51. Garrison, J. G.; Youngs, W. J. *Chem. Rev.* **2005**, *105*, 3978.
52. Catalano, V. J.; Malwitz, M. A.; Etogo, A. O. *Inorg. Chem.* **2004**, *43*, 5714.
53. Mata, J. A.; Chianese, A. R.; Miecznikowske, J. R.; Pouatos, M.; Peris, E.; Faller, J. W.; Cratree, R. H. *Organometallics* **2004**, *23*, 1253.
54. Wang, X.; Liu, S.; Jin, G. *Organometallics* **2004**, *23*, 6002.
55. Arnold, P. L.; Scarosnrocl. A. C.; Blake, A. J.; Wilson, C. *Chem. Commun.* **2002**, 2340.
56. Perry, M. C.; Cui, X.; Burgess, K. *Tetrahedron: Asymmetry* **2002**, *13*, 1969.
57. Douthwaite, R. E.; Green, M. H.; Silcock, P. J.; Gomes, P. T. *J. Chem. Soc., Dalton.*

- Trans.*, **2002**, 1386.
58. Herrmann, W. A.; Goossen, L. J.; Artus, G. R. J.; Kocher, C. *Organometallics* **1997**, *16*, 2472.
59. Bolm, C.; Kesselgruber, M.; Raabe, G. *Organometallics* **2002**, *21*, 707.
60. Huang, J.; Jafarpour, L.; Hillier, A. C.; Stevens, E. D.; Nolan, S. P. *Organometallics*, **2001**, *20*, 2878.
61. Huang, J.; Stevens, E. D.; Nolan, S.P.; Petersen, J. L. *J. Am. Chem. Soc.* **1999**, *121*, 2674.
62. Grubbs, R. H. (ed) *Handbook of metathesis*, **2003**, Wiley, Weinheim.
63. Seiders, T. J.; Ward, D. W.; Grubbs, R. H. *Org. Lett.* **2001**, *3*, 3225.
64. Van Veldhuizen, J. J.; Garber, S. B.; Kingsbury, J. S.; Hoveyda, A. H. *J. Am. Chem. Soc.* **2002**, *124*, 4954.
65. Bappert, E.; Helmchen, G. *Synlett*, **2004**, 1789.
66. a) Hou, D. R.; Burgess, K. *Org. Lett.* **1999**, *1*, 1745. b) Hou, D. R.; Reibenspies, J.; Colact, T. J.; Brgess, K. *Chem. Eur. J.* **2001**, *7*, 5391.
67. Hou, D. R.; Reibenspig, J. H.; Burgess, K. *J. Org. Chem.* **2001**, *66*, 206.
68. a) Ma, Y.; Song, C.; Ma, C.; Sun, Z.; Chai, Q.; Andrus, M. B. *Angew. Chem. Int. Ed.* **2003**, *42*, 5871. b) Song, C.; Ma, C.; Ma, Y.; Feng, W.; Chai, W.; Andrus, M. B. *Tetrahedron Lett.* **2005**, *46*, 3241.
69. Pytkowicz, J.; Roland, S.; Mangeney, P.; *Tetrahedron: Asymmetry* **2001**, *12*, 2087.
70. Clavier, H.; Coutable, L.; Toupet, L.; guillemin, J. C.; Mauduit, M. *J. Organomet.*

*Chem.* **2005**, 690, 5237.

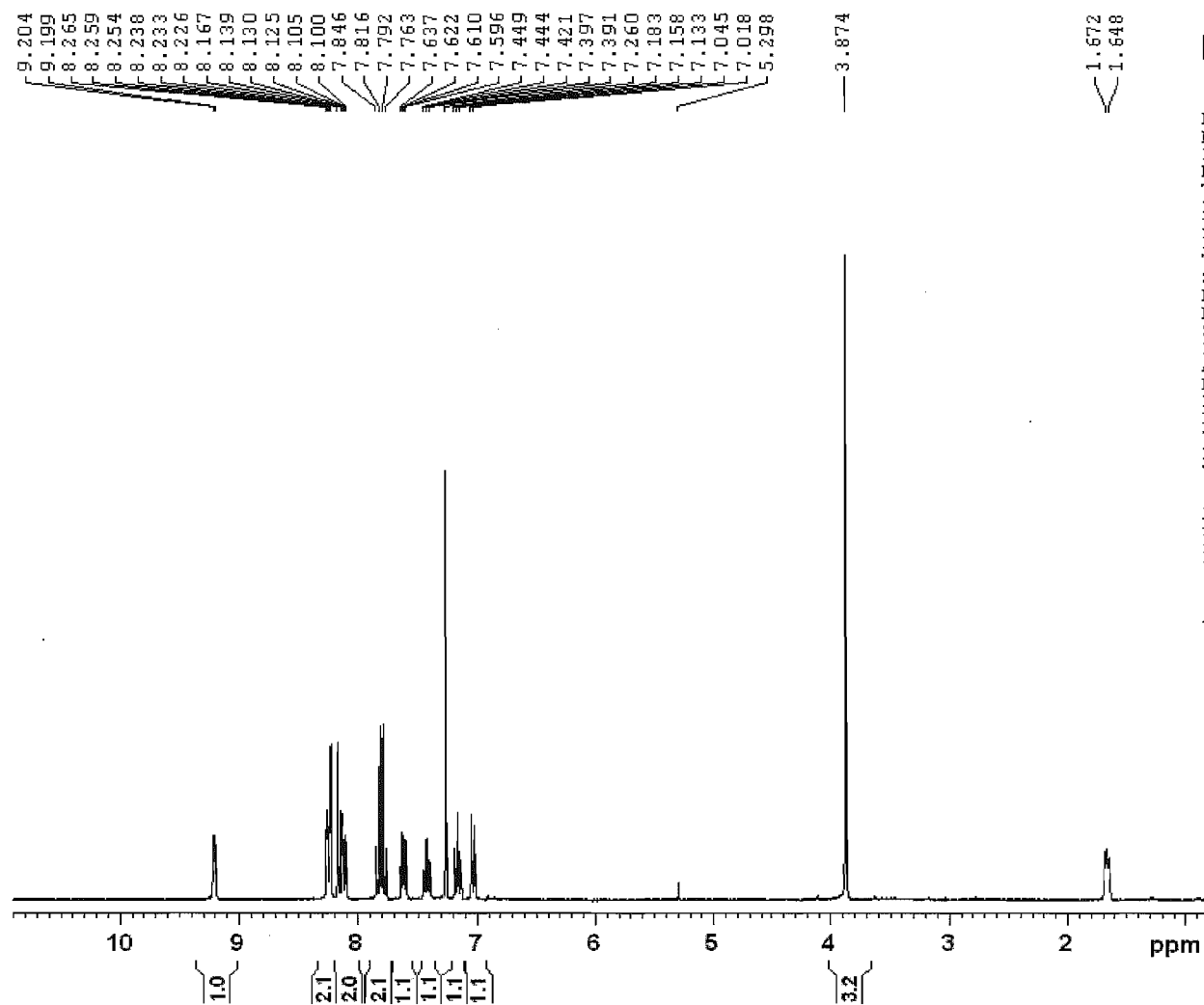
71. Huang, W.; Guo, J-P.; Xiao, Y.; Zhu, M-F.; Zou, G.; Tang, J. *Tetrahedron* **2005**, 61, 9783.
72. Liu, Y-F.; Lindner, P-E. Lemal, D. M. *J. Am. Chem. Soc.* **1999**, 121, 10626.
73. a) Rivas, F. M.; Riaz, U.; Giesset, A.; Smulik, J. A.; Diver, S. T. *Org. Lett* **2001**, 3, 2673; b) Smulick, J. A.; Diver, S. T. *Tetrahedron Let.* **2001**, 42, 171.
74. Duan, W-L.; Shi, M.; Rong, G-B. *Chem. Commun.* **2003**, 2916.
75. Zhang, T.; Shi, M. *Chem. Eur. J.* **2008**, 14, 3759.
76. Baskakov, D.; Herrmann, W. A.; Herdtweck, E.; Hoffmann, S. D. *Organometallics*, **2007**, 26, 626.
77. a) Schoffers, E. *Eur. J. Org. Chem.* **2003**, 1145; b) Chelucci, G.; Thummel, R. P. *Chem. Rev.* **2002**, 102, 3129.
78. Herrmann, W. A.; Baskakov, D.; Herdtweck, E.; Hoffmann, S. D.; Bunlaksananusorn, T.; Rampf, F.; Rodefeld, L. *Organometallics*, **2006**, 25, 2449.
79. Metallinos, C.; Dudding, T.; Zaifman, J.; Chaytor, J. L.; Taylor, N. J. *J. Org. Chem.* **2007**, 72, 957.
80. Metallinos, C.; Barrett, F. B.; Xu, S-F. *Synlett* **2008**, 5, 720.
81. Metallinos, C.; Barrett, F. B.; Chaytor, J. L.; Heska, M. E. A. *Org. Lett.* **2004**, 6, 3641.
82. Wang, Y. *MSc thesis*, **2007**.
83. Lee, S.; Hartwig, J. F. *J. Org. Chem.* **2001**, 66, 3402.

84. Sauvage, J. P. *Tetrahedron Lett.* **1982**, 23, 5291.
85. Moore, R. M.; Streitwieser, A.; Wang, H. K. *Organometallics* **1986**, 5, 1418.
86. Harder, s.; Boersma, J.; Brandsma, L.; Kanter, J. A.; Vanlenthe, J. H. *Organometallics* **1990**, 9, 511.
87. Bildstein, B.; Malaun, M.; Kopacka, H.; Wurst, K.; Mitterböck, M.; Ongania, K. H.; Opromolla, G.; Zanello, P. *Organometallics* **1999**, 18, 4325.
88. Eckhard, I. F.; Fielden, R.; Summers, L. *Aust. J. Chem.*, **1975**, 28, 1149.
89. Rueping, M.; Sugiono, E.; Schoepke, F. T. *Synlett* **2007**, 1441.
90. For similar reductions of quinolines, see: Partali, V.; Jolidon, S.; Hansen, H.-J. *Helv. Chim. Acta* **1985**, 68, 1952, and references therein.
91. Fisher, G. B.; Fuller, J. C.; Harrison, J.; Goralski, C. T.; Singaram, B. *Tetrahedron lett.* **1993**, 34, 1091.
92. Fournier, P-A.; Collins, S. K. *Organometallics*, **2007**, 26, 2946.
93. Smulik, J. A. *Ph.D dissertation*.
94. Lee, H. M.; Jiang, T.; Stevens, E. D.; Nolan, S. P. *Organometallics* **2001**, 20, 1255.
95. Vazquez-Serrano, L. D.; Owens, B. T.; Buriak, J. M. *Chem. Commun.* **2002**, 2518.
96. Vazquez-Serrano, L. F.; Owens, B. T.; Buriak, J. M.; *Inorg. Chim. Acta* **2006**, 359, 2786.
97. Crabtree, T. H.; Felkin, H.; Morris, G. E. *J. Organomet. Chem.* **1977**, 141, 205.
98. Lightfoot, A.; Schnider, P.; Pfaltz, A.; *Angew. Chem. Int. Ed.* **1998**, 37, 2897.
99. Hou, D-R.; Reibenspies, J.; Colacot, T. J.; Burgess, K. *Chem. Eur. J.* **2001**, 7, 5391.

100. Shi, M.; Duan, W-L. *Appl. Organometal. Chem.* **2005**, *19*, 40.
101. Romero P. E.; Piers, W. E.; McDonald, R. *Angew Chem Int Ed.* **2004**, *43*, 6161.
102. Muniz, K. *Angew Chem Int Ed.* **2004**, *44*, 6622.
103. Peris, E.; Crabtree, R. H. *Coordination Chemistry Reviews* **2004**, *248*, 2239.
104. Kallstrom, K.; Munslow, I.; Andersson, P. G. *Chem. Eur. J.* **2006**, *12*, 3194.
105. Cui, X.; Burgess, K. *J. Am. Chem. Soc.* **2003**, *125*, 14212.
106. Brandt, P.; Hedberg, C.; Andersson, P. G. *Chem. Eur. J.* **2003**, *9*, 339.
107. Dietiker, R.; Chen, P. *Angew. Chem. Int. Ed.* **2004**, *43*, 5513.
108. Church, T, L.; Andersson, P. G. *Coordination Chemistry Reviews* **2008**, *252*, 513.
109. Gnanamgari, D.; Moores, A.; rajaseelan, E.; Crabtree, R. H. *Organometallics* **2007**, *26*, 1226.



1D proton



```

NAME          xd-01-174
EXPNO         1
PROCNO        1
Date_         20070621
Time          10.46
INSTRUM       spect
PROBHD        5 mm PABBO BB-
PULPROG       zg30
TD            32768
SOLVENT       CDCl3
NS            8
DS            0
SWH           6172.839 Hz
FIDRES        0.188380 Hz
AQ            2.6542580 sec
RG            724.1
DW            81.000 usec
DE            6.00 usec
TE            295.6 K
D1            1.00000000 sec
TD0           1
  
```

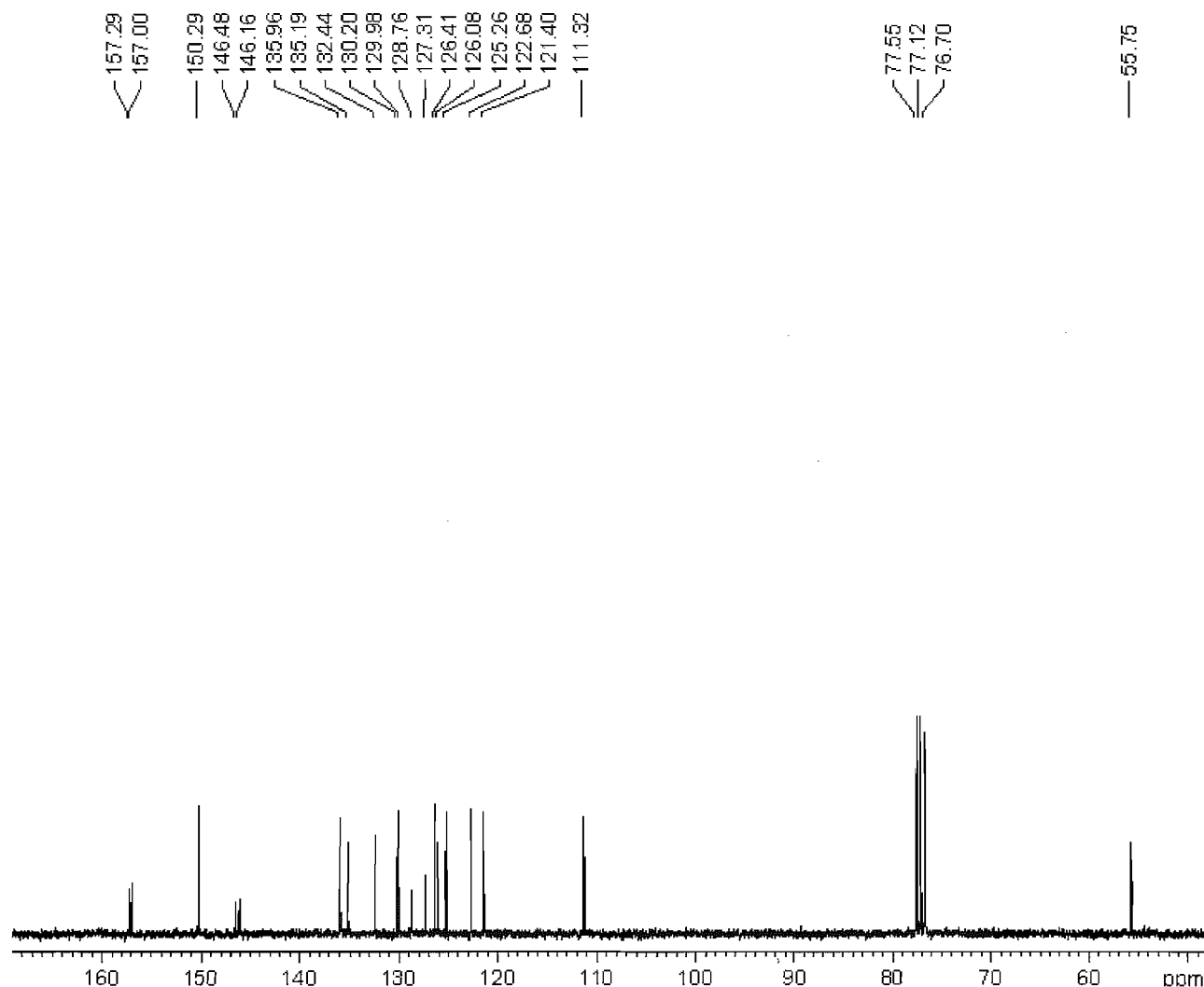
```

===== CHANNEL f1 =====
NUC1          1H
P1            11.20 usec
PL1           0.00 dB
SF01          300.1318534 MHz
SI            16384
SF            300.1300061 MHz
WDW           EM
SSB           0
LB            0.30 Hz
GB            0
PC            1.00
  
```

## 6. Appendix

Figure 12.  $^1\text{H}$  NMR spectrum of 74d.

1D carbon with proton decoupling



```

NAME          xd-01-167
EXPNO          5
PROCNO         1
Date_          20070614
Time            20.21
INSTRUM        spect
PROBHD         5 mm PABBO BB-
PULPROG        zgpg30
TD             32768
SOLVENT        CDC13
NS             139
DS             0
SWH            17985.611 Hz
FIDRES         0.548877 Hz
AQ             0.9110004 sec
RG            10321.3
DW             27.800 usec
DE             6.00 usec
TE            297.2 K
D1            2.00000000 sec
d11            0.03000000 sec
DELTA          1.89999998 sec
TD0            1
  
```

```

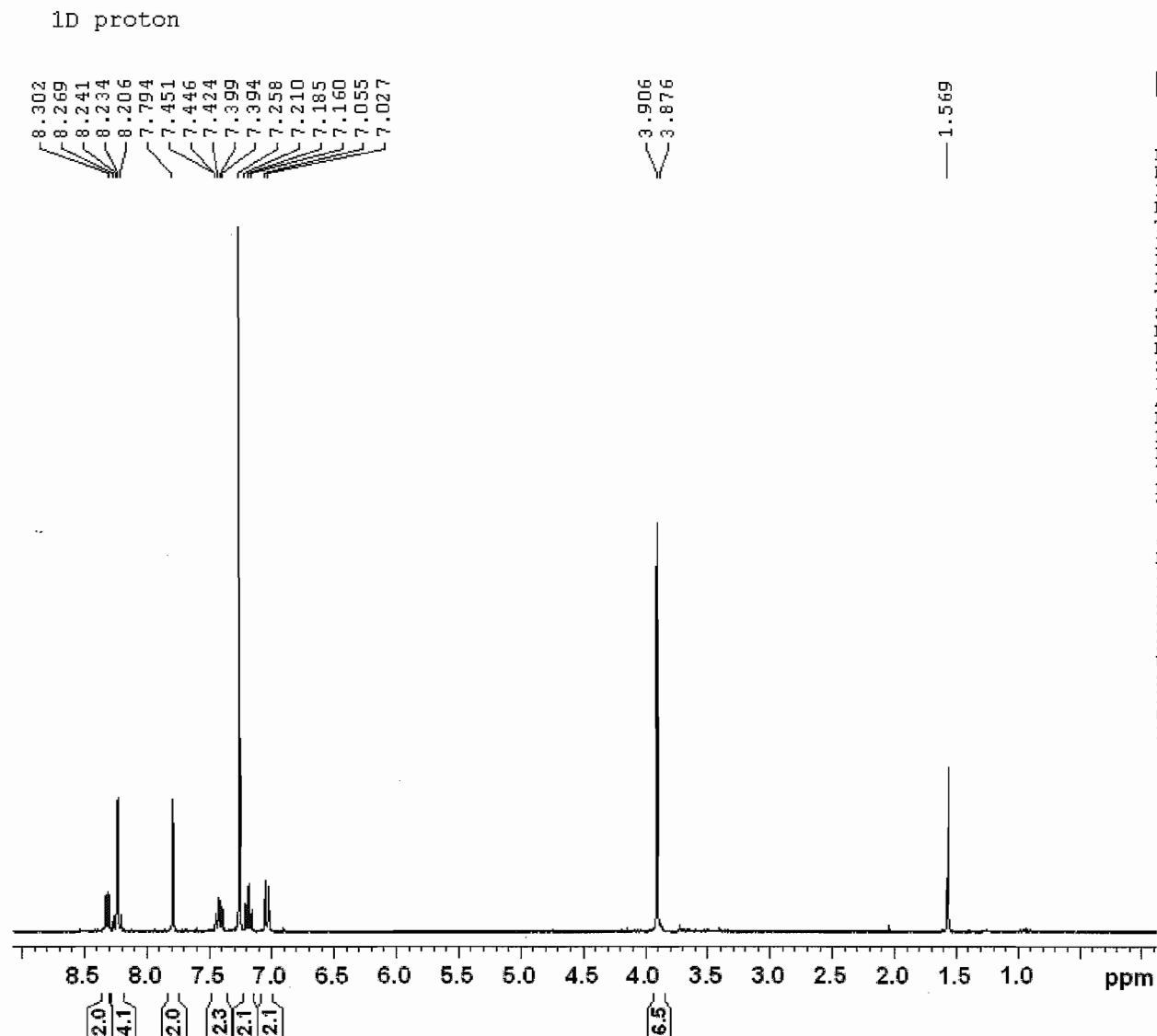
===== CHANNEL f1 =====
NUC1           13C
P1            10.00 usec
PL1           -1.00 dB
SF01          75.4752950 MHz
  
```

```

===== CHANNEL f2 =====
CPDPRG2        waltz16
NUC2           1H
PCPD2          80.00 usec
PL2            0.00 dB
PL12          17.60 dB
PL13          17.60 dB
SF02          300.1312000 MHz
SI            16384
SF            75.4677490 MHz
WDW            EM
SSB            0
LB            1.00 Hz
GB            0
PC            1.40
  
```

Figure 13.  $^{13}\text{C}$  NMR spectrum of 74d.

Figure 14.  $^1\text{H}$  NMR spectrum of 54d.



```

NAME      xd-01-169
EXPNO     2
PROCNO    1
Date_     20070621
Time      13.33
INSTRUM   spect
PROBHD    5 mm PABBO BB-
PULPROG   zg30
TD        32768
SOLVENT   CDC13
NS         8
DS         0
SWH        6172.839 Hz
FIDRES     0.188380 Hz
AQ         2.6542580 se
RG         1625.5
DW         81.000 us
DE         6.00 us
TE         295.6 K
D1         1.00000000 se
TD0        1
  
```

```

===== CHANNEL f1 =====
NUC1      1H
P1        11.20 us
PL1       0.00 dB
SFO1      300.1318534 MH
SI        16384
SF        300.1300069 MH
WDW       EM
SSB       0
LB        0.30 Hz
GB        0
PC        1.00
  
```

1D carbon with proton decoupling

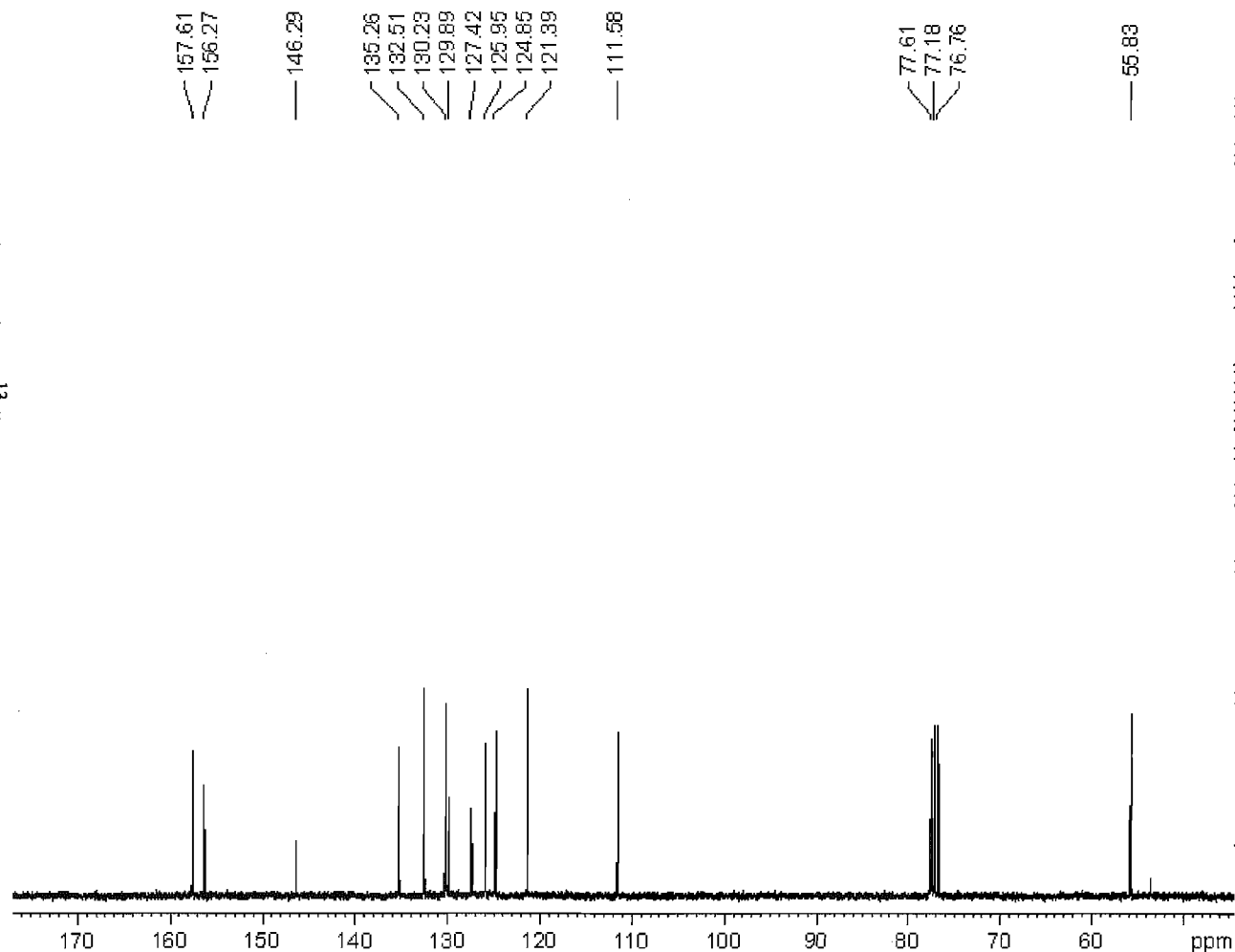


Figure 15.  $^{13}\text{C}$  NMR spectrum of 54d.



```

NAME      xd-01-169
EXPNO     4
PROCNO    1
Date_     20070619
Time      19.33
INSTRUM   spect
PROBHD    5 mm PAEB0 BB-
PULPROG   zgpg30
TD        32768
SOLVENT   CDCl3
NS        104
DS        0
SWH       17985.611 Hz
FIDRES    0.548877 Hz
AQ        0.9110004 sec
RG        11585.2
DW        27.800 usec
DE        6.00 usec
TE        297.0 K
D1        2.00000000 sec
d11       0.03000000 sec
DELTA     1.89999998 sec
TD0       1
  
```

```

===== CHANNEL f1 =====
NUC1      13C
P1        10.00 usec
PL1       -1.00 dB
SF01      75.4752950 MHz
  
```

```

===== CHANNEL f2 =====
CPDPRG2   waltz16
NUC2      1H
PCPD2     80.00 usec
PL2       0.00 dB
PL12      17.60 dB
PL13      17.60 dB
SF02      300.1312000 MHz
SI        16384
SF        75.4677490 MHz
WDW       EM
SSB       0
LB        1.00 Hz
GB        0
PC        1.40
  
```

1D proton

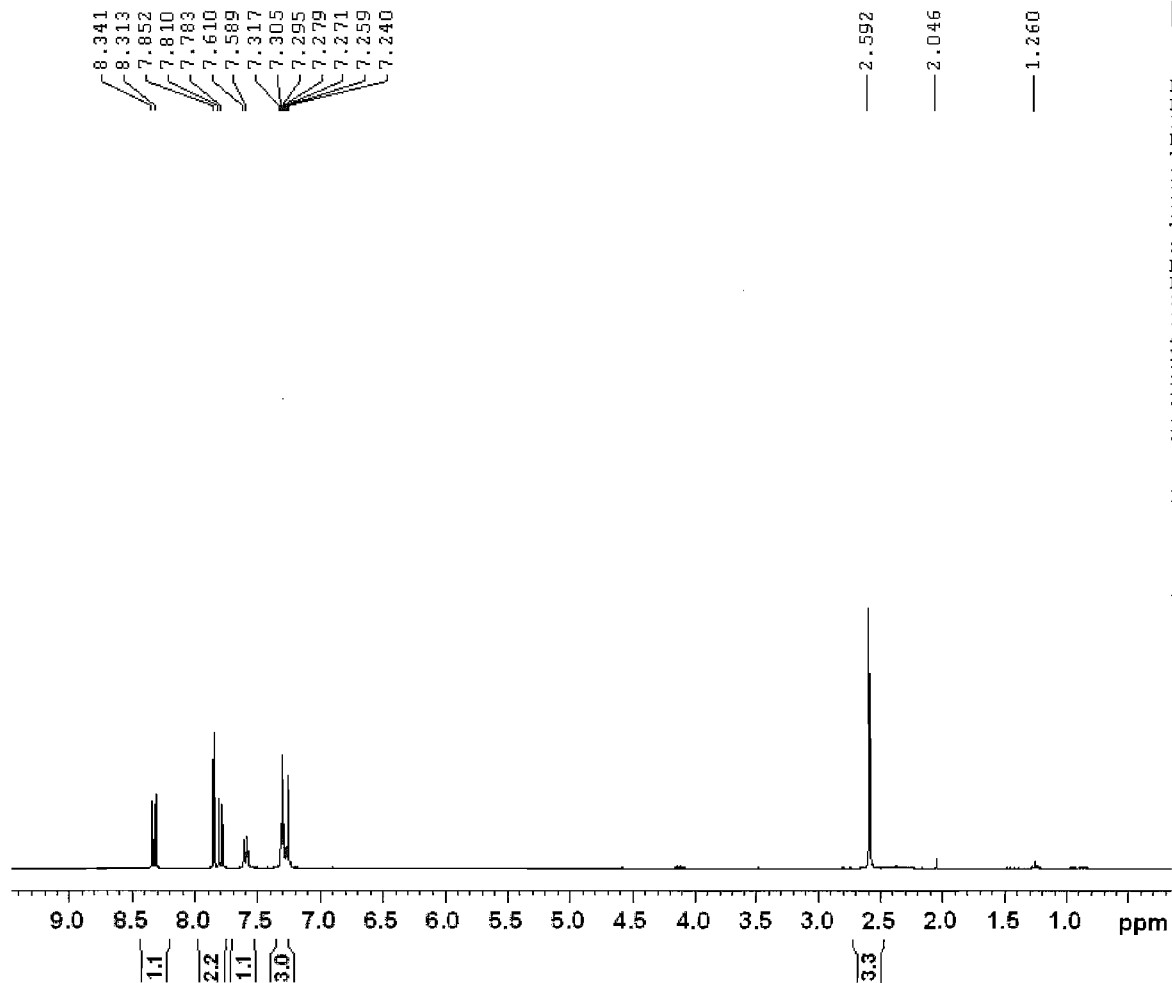


Figure 16.  $^1\text{H}$  NMR spectrum of 54e.



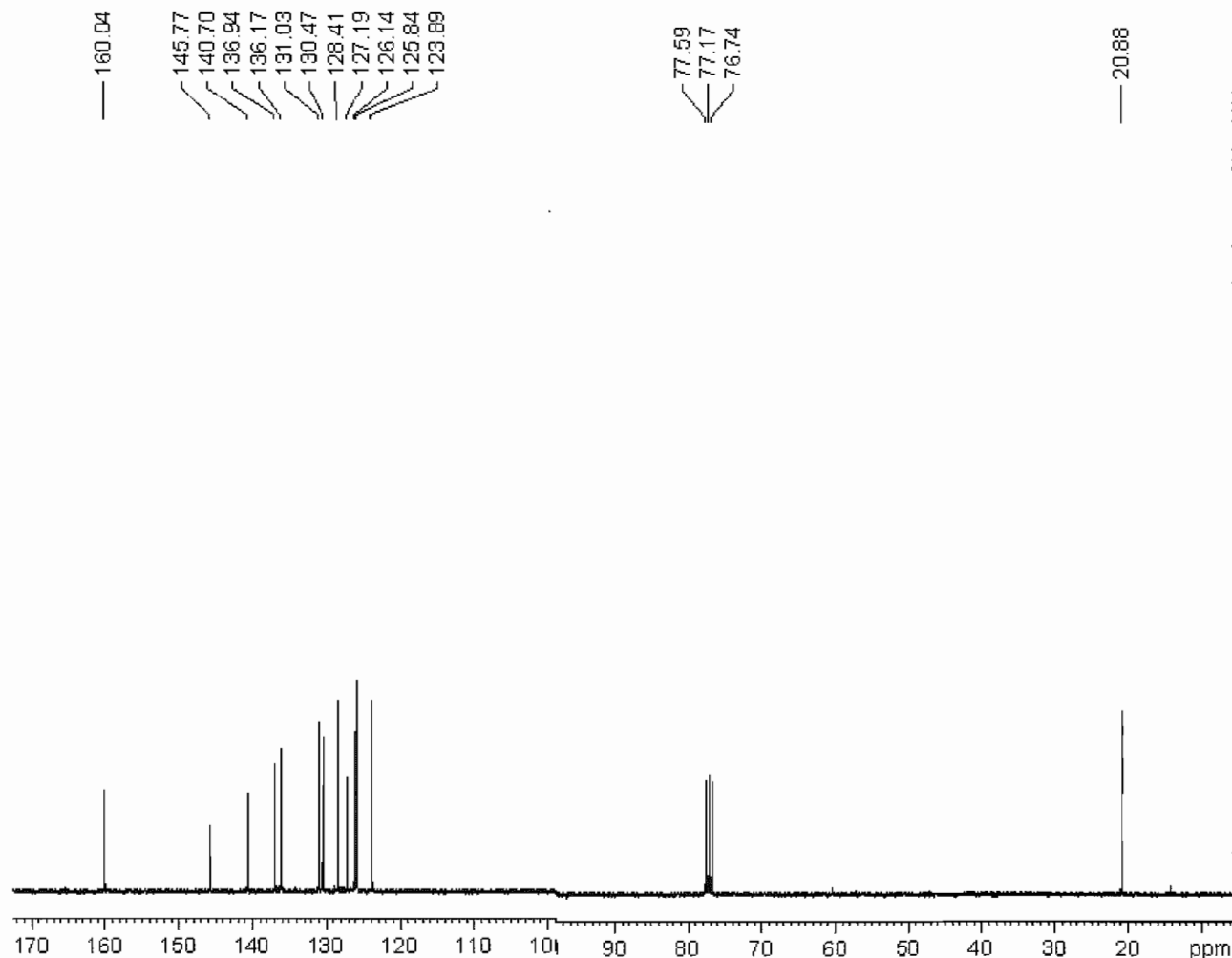
```

NAME      xd-02-087
EXPNO     1
PROCNO    1
Date_     20071029
Time      11.16
INSTRUM   spect
PROBHD    5 mm PABBO BB-
PULPROG   zg30
TD        32768
SOLVENT   CDCl3
NS         8
DS         0
SWH        6172.839 Hz
FIDRES     0.188380 Hz
AQ         2.6542580 sec
RG         456.1
DW         81.000 usec
DE         6.00 usec
TE         296.7 K
D1         1.00000000 sec
TD0        1
  
```

```

===== CHANNEL f1 =====
NUC1      1H
P1        10.20 usec
PL1       0.00 dB
SF01      300.1318534 MHz
SI        16384
SF        300.1300069 MHz
WDW       EM
SSB       0
LB        0.30 Hz
GB        0
PC        1.00
  
```

1D carbon with proton decoupling



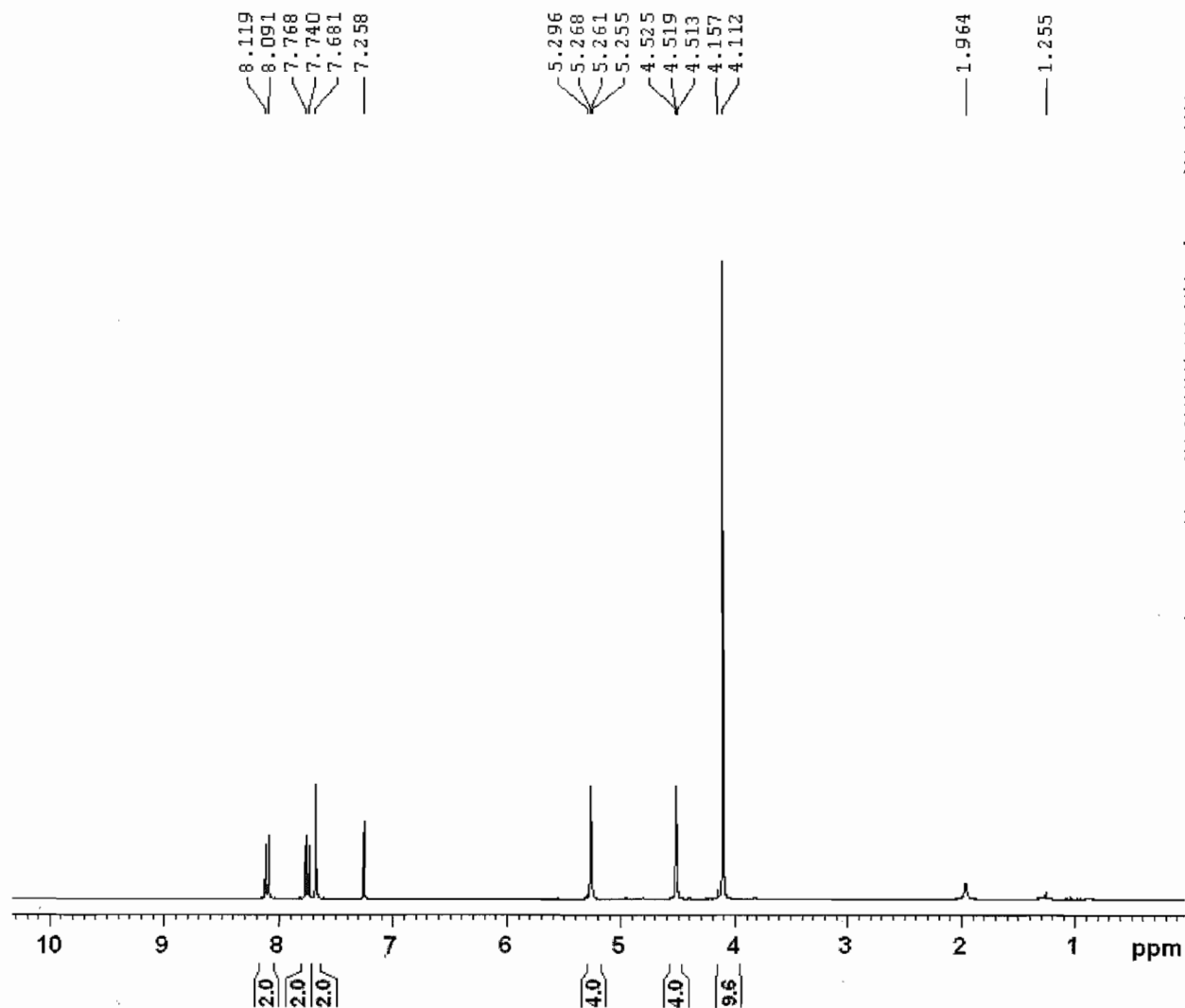
NAME xd-02-075  
EXPNO 3  
PROCNO 1  
Date\_ 20071025  
Time 20.02  
INSTRUM spect  
PROBHD 5 mm PABBO BB-  
PULPROG zgpg30  
TD 32768  
SOLVENT CDCl3  
NS 172  
DS 0  
SWH 17985.611 Hz  
FIDRES 0.548877 Hz  
AQ 0.9110004 sec  
RG 7298.2  
DW 27.800 usec  
DE 6.00 usec  
TE 298.0 K  
D1 2.00000000 sec  
d11 0.03000000 sec  
DELTA 1.89999998 sec  
TDO 1

===== CHANNEL f1 =====  
NUC1 13C  
P1 11.00 usec  
PL1 -2.00 dB  
SF01 75.4752950 MHz

===== CHANNEL f2 =====  
CPDPRG2 waltz16  
NUC2 1H  
PCPD2 80.00 usec  
PL2 0.00 dB  
PL12 17.89 dB  
PL13 17.60 dB  
SF02 300.1312000 MHz  
SI 16384  
SF 75.4677490 MHz  
WDW EM  
SSB 0  
LB 1.00 Hz  
GB 0  
PC 1.40

Figure 17.  $^{13}\text{C}$  NMR spectrum of 54c.

Fraction A 1D proton

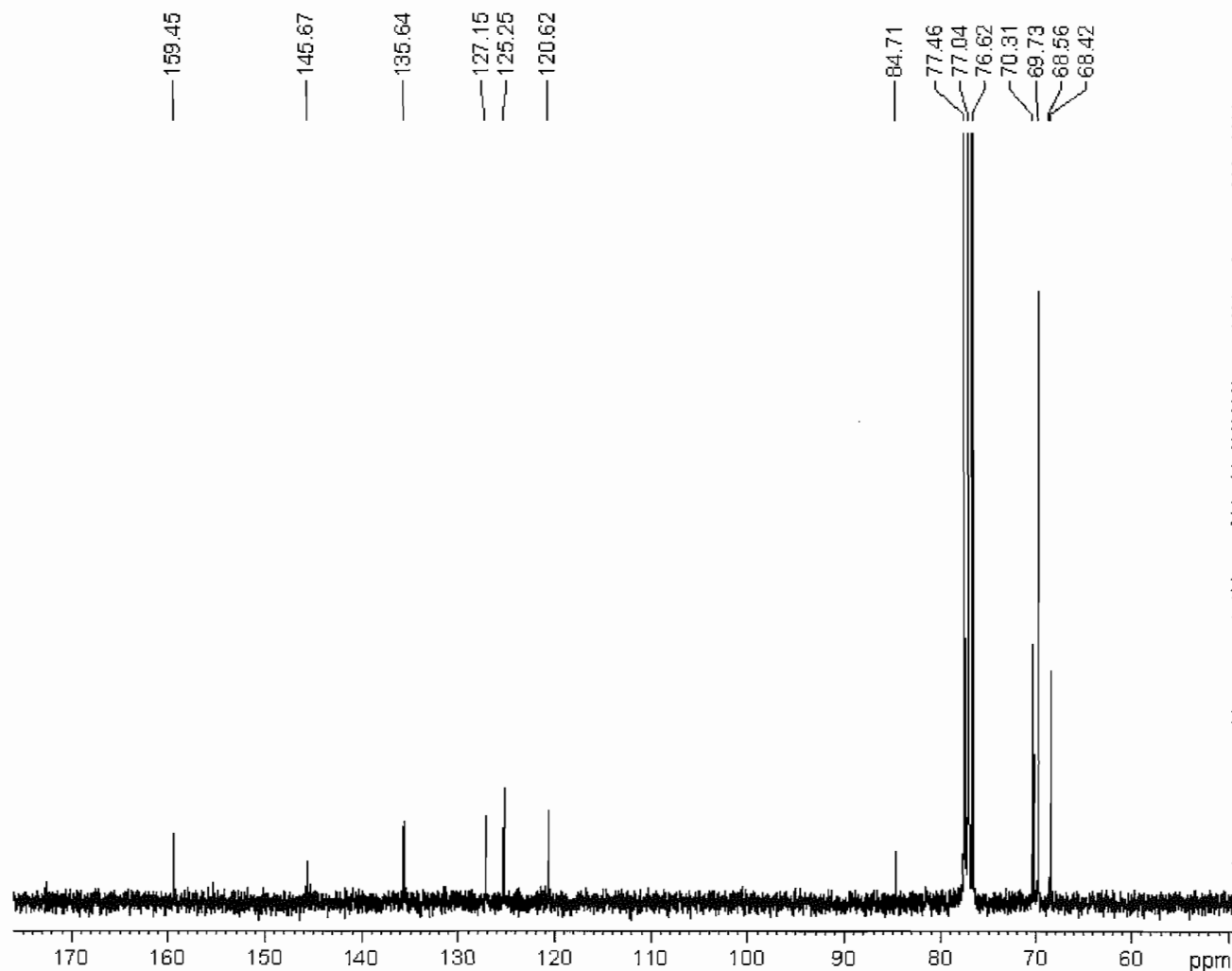


NAME xd-02-179  
 EXPNO 6  
 PROCNO 1  
 Date\_ 20080202  
 Time 15.03  
 INSTRUM spect  
 PROBHD 5 mm PABBO BB-  
 PULPROG zg30  
 TD 32768  
 SOLVENT CDCl3  
 NS 8  
 DS 0  
 SWH 6172.839 Hz  
 FIDRES 0.188380 Hz  
 AQ 2.6542580 sec  
 RG 406.4  
 DW 81.000 usec  
 DE 6.00 usec  
 TE 297.1 K  
 D1 1.00000000 sec  
 TDO 1

===== CHANNEL f1 =====  
 NUC1 1H  
 P1 10.20 usec  
 PL1 0.00 dB  
 SF01 300.1318534 MHz  
 SI 16384  
 SF 300.1300070 MHz  
 WDW EM  
 SSB 0  
 LB 0.30 Hz  
 GB 0  
 PC 1.00

Figure 18.  $^1\text{H}$  NMR spectrum of 54f.

1D carbon with proton decoupling



NAME xd-02-155  
 EXPNO 3  
 PROCNO 1  
 Date\_ 20080114  
 Time 17.33  
 INSTRUM spect  
 PROBHD 5 mm PABBO BB-  
 PULPROG zgpg30  
 TD 32768  
 SOLVENT CDCl3  
 NS 512  
 DS 0  
 SWH 17985.611 Hz  
 FIDRES 0.548877 Hz  
 AQ 0.9110004 sec  
 RG 2896.3  
 DW 27.800 usec  
 DE 6.00 usec  
 TE 298.2 K  
 D1 2.00000000 sec  
 d11 0.03000000 sec  
 DELTA 1.89999999 sec  
 TDO 1

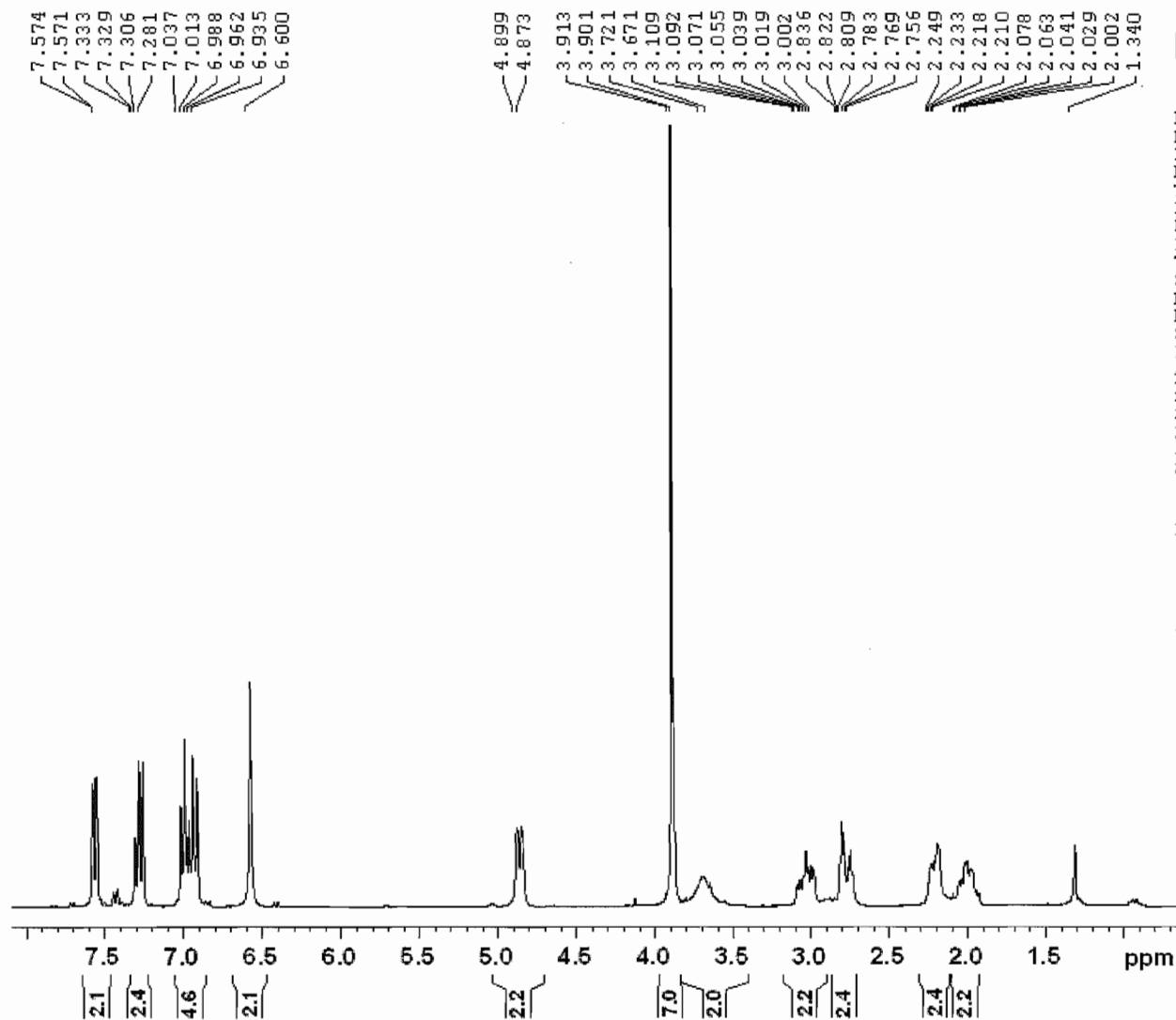
===== CHANNEL f1 =====  
 NUC1  $^{13}\text{C}$   
 P1 11.00 usec  
 PL1 -2.00 dB  
 SF01 75.4752950 MHz

===== CHANNEL f2 =====  
 CPDPRG2 waltz16  
 NUC2  $^1\text{H}$   
 PCPD2 80.00 usec  
 PL2 0.00 dB  
 PL12 17.89 dB  
 PL13 17.60 dB  
 SF02 300.1312000 MHz  
 SI 16384  
 SF 75.4677490 MHz  
 WDW EM  
 SSB 0  
 LB 1.00 Hz  
 GB 0  
 PC 1.40

Figure 19.  $^{13}\text{C}$  NMR spectrum of 54f.



1D proton



```

NAME          xd-02-002
EXPNO          5
PROCNO         1
Date_          20070702
Time           12.35
INSTRUM        spect
PROBHD         5 mm PABBO BB-
PULPROG        zg30
TD             32768
SOLVENT        CDCl3
NS              8
DS              0
SWH            6172.839 Hz
FIDRES         0.188380 Hz
AQ             2.6542580 sec
RG              90.5
DW             81.000 usec
DE              6.00 usec
TE             294.8 K
D1             1.00000000 sec
TDO            1
  
```

```

===== CHANNEL f1 =====
NUC1            1H
P1             11.20 usec
PL1             0.00 dB
SF01           300.1318534 MHz
SI             16384
SF             300.1300061 MHz
WDW             EM
SSB              0
LB              0.30 Hz
GB              0
PC              1.00
  
```

Figure 20.  $^1\text{H}$  NMR spectrum of 56d.

1D carbon with proton decoupling



```

NAME          xd-02-002
EXPNO         6
PROCNO        1
Date_         20070702
Time          12.44
INSTRUM       spect
PROBHD        5 mm PABBO BB-
PULPROG       zgpg30
TD            32768
SOLVENT       CDC13
NS            114
DS            0
SWH           17985.611 Hz
FIDRES        0.548877 Hz
AQ            0.9110004 sec
RG            10321.3
DW            27.800 usec
DE            6.00 usec
TE            295.7 K
D1            2.00000000 sec
d11           0.03000000 sec
DELTA         1.89999998 sec
TD0           1
  
```

```

===== CHANNEL f1 =====
NUC1          13C
P1            10.00 usec
PL1           -1.00 dB
SF01          75.4752950 MHz
  
```

```

===== CHANNEL f2 =====
CPDPRG2       waltz16
NUC2          1H
PCPD2         80.00 usec
PL2           0.00 dB
PL12          17.60 dB
PL13          17.60 dB
SF02          300.1312000 MHz
SI            16384
SF            75.4677490 MHz
WDW           EM
SSB           0
LB            1.00 Hz
GB            0
PC            1.40
  
```

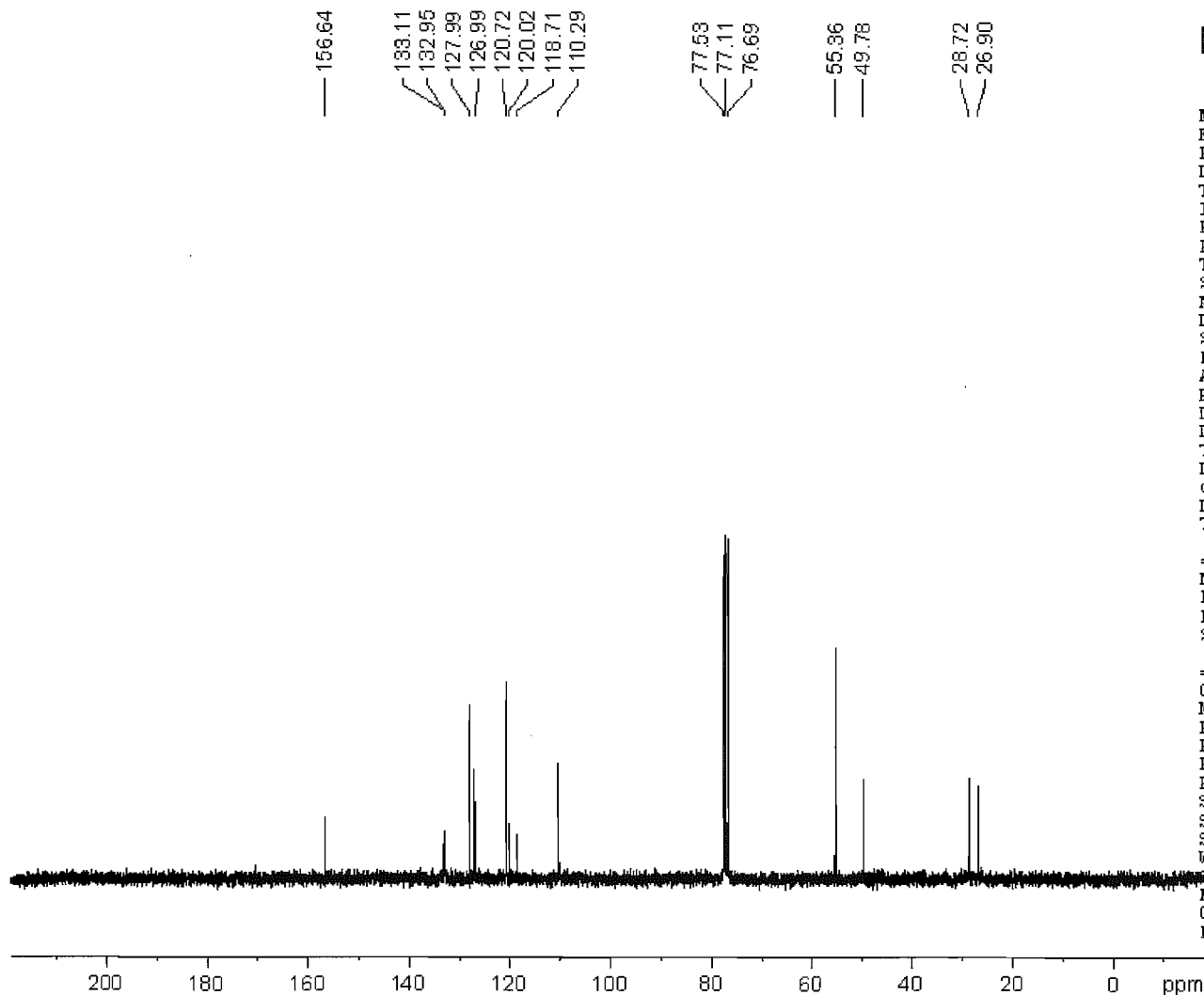
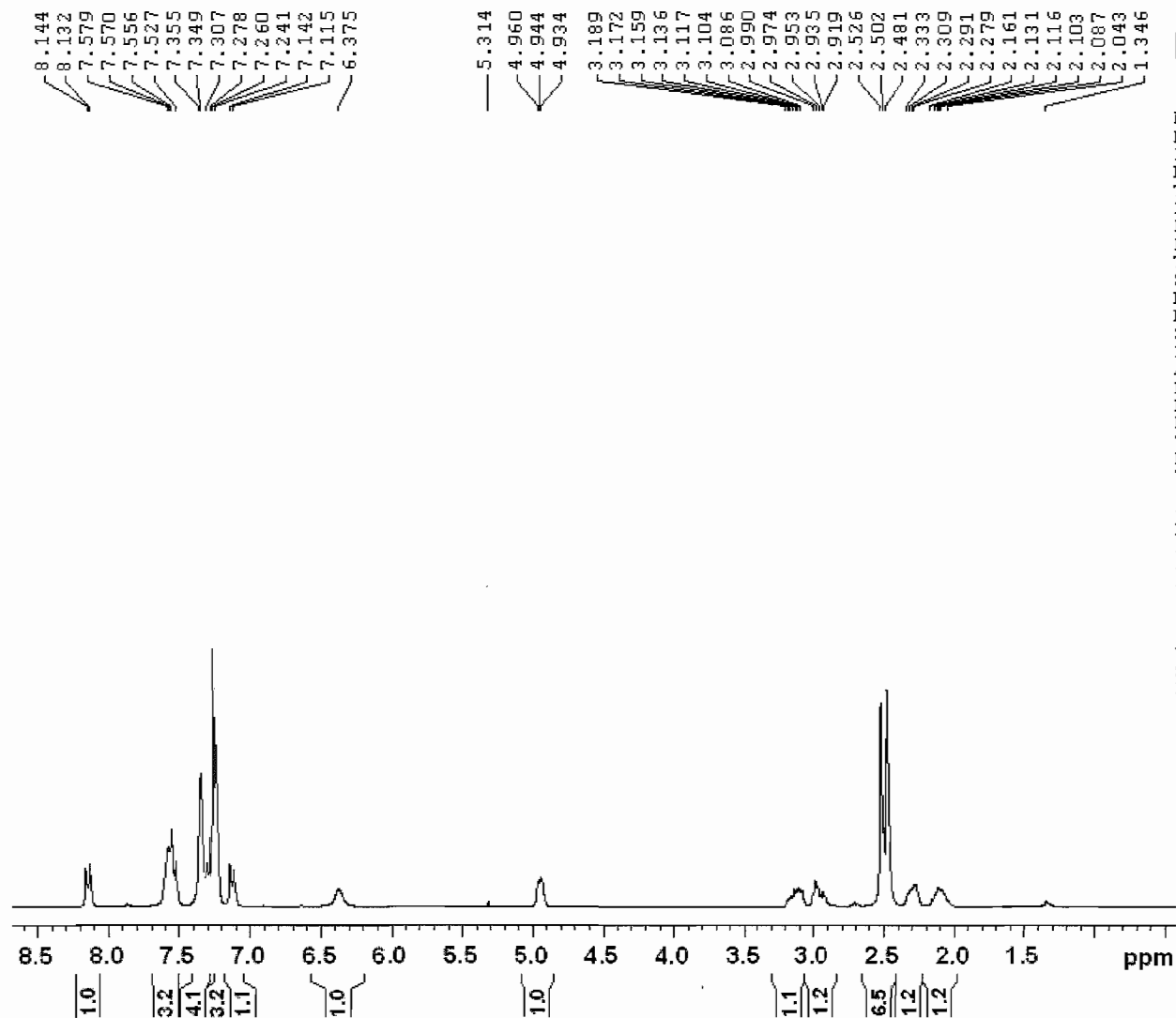


Figure 21.  $^{13}\text{C}$  NMR spectrum of 56d.

1D proton



```

NAME          xd2-89
EXPNO          1
PROCNO         1
Date_          20081117
Time_          12.12
INSTRUM        spect
PROBHD         5 mm PABBO BB-
PULPROG        zg30
TD             32768
SOLVENT        CDCl3
NS              8
DS              0
SWH            6172.839 Hz
FIDRES         0.188380 Hz
AQ             2.6542580 sec
RG              71.8
DW             81.000 usec
DE              6.00 usec
TE             295.8 K
D1             1.00000000 sec
TD0            1
  
```

```

===== CHANNEL f1 =====
NUC1            1H
P1              10.20 usec
PL1             0.00 dB
PL1W           30.14263725 W
SF01           300.1318534 MHz
SI             16384
SF             300.1300062 MHz
WDW             EM
SSB              0
LB              0.30 Hz
GB              0
PC              1.00
  
```

Figure 22.  $^1\text{H}$  NMR spectrum of 75e.

1D carbon with proton decoupling



NAME xd2-89  
EXPNO 3  
PROCNO 1  
Date\_ 20081117  
Time 12.33  
INSTRUM spect  
PROBHD 5 mm PABBO BB-  
PULPROG zgpg30  
TD 32768  
SOLVENT CDCl3  
NS 331  
DS 0  
SWH 17985.611 Hz  
FIDRES 0.548877 Hz  
AQ 0.9110004 sec  
RG 1625.5  
DW 27.800 usec  
DE 6.00 usec  
TE 296.8 K  
D1 2.00000000 sec  
D11 0.03000000 sec  
TD0 1

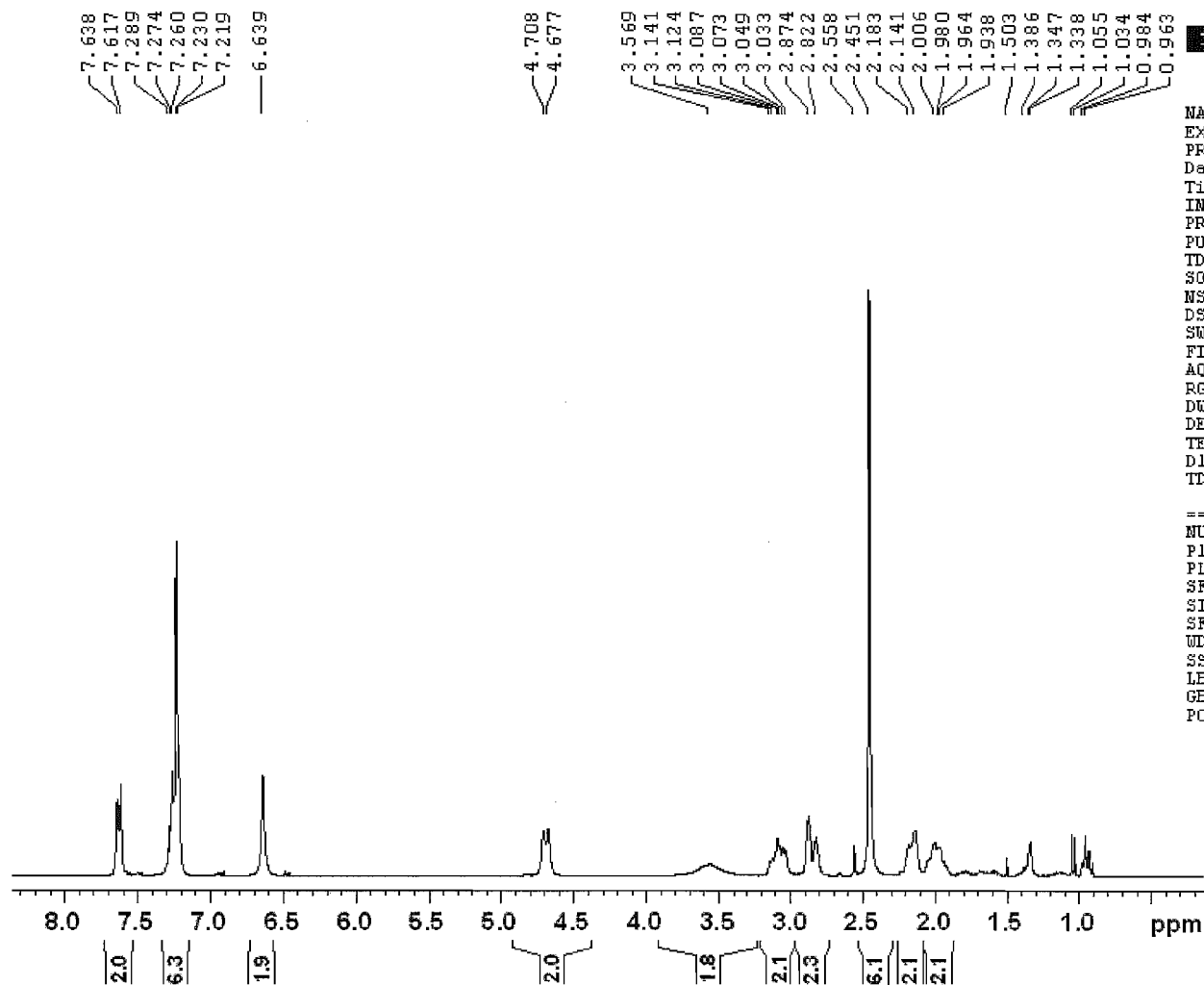
===== CHANNEL f1 =====  
NUC1 13C  
P1 11.00 usec  
PL1 -2.00 dB  
PL1W 62.50282669 W  
SF01 75.4752950 MHz

===== CHANNEL f2 =====  
CPDPRG2 waltz16  
NUC2 1H  
PCPD2 80.00 usec  
PL2 0.00 dB  
PL12 17.89 dB  
PL13 17.60 dB  
PL2W 30.14263725 W  
PL12W 0.48998332 W  
PL13W 0.52381897 W  
SF02 300.1312000 MHz  
SI 16384  
SF 75.4677576 MHz  
WDW EM  
SSB 0  
LB 1.00 Hz  
GB 0  
PC 1.40

Figure 23.  $^{13}\text{C}$  NMR spectrum of 75e.

Figure 24.  $^1\text{H}$  NMR spectrum of 56c.

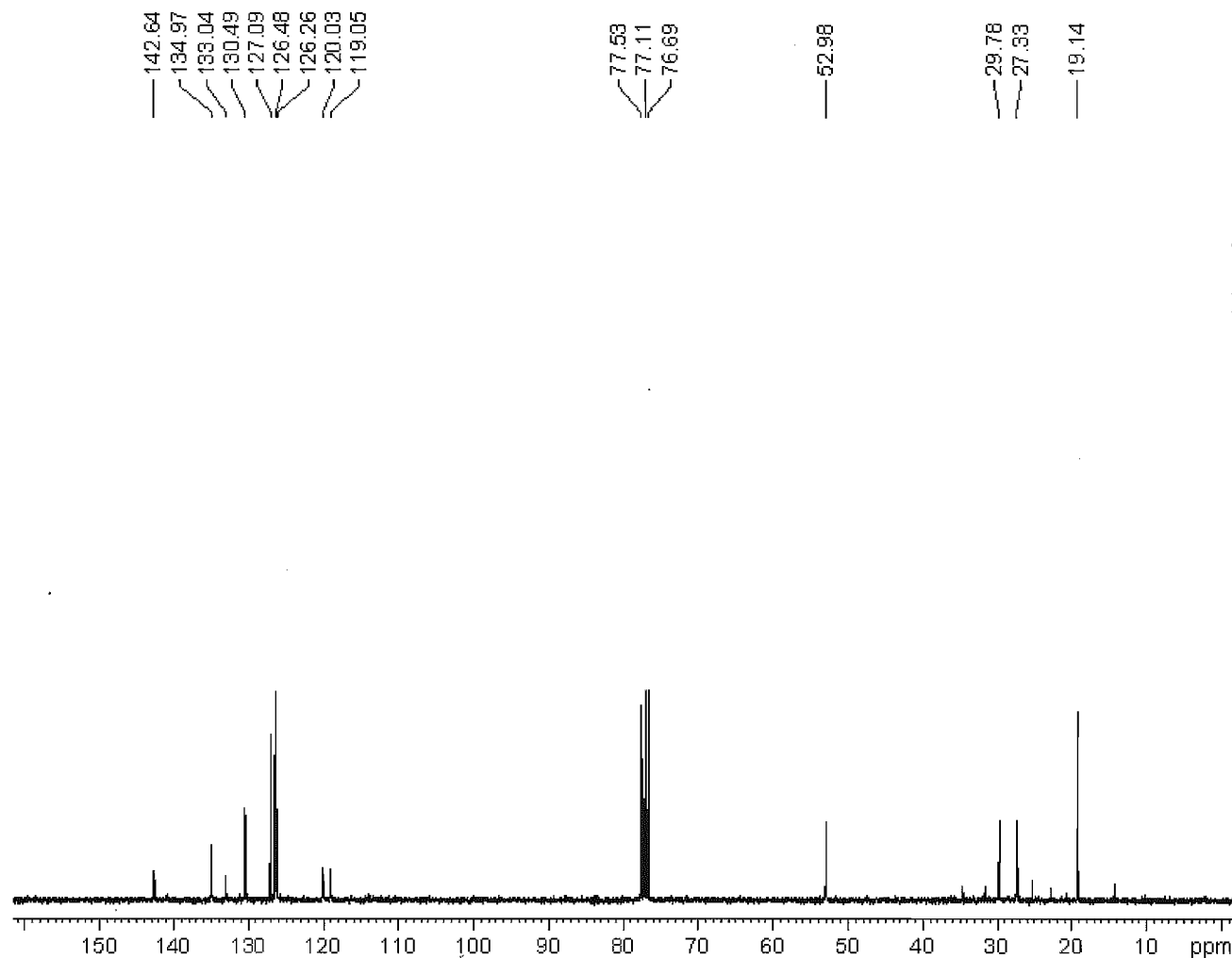
fraction D



NAME xd-02-097  
 EXPNO 3  
 PROCNO 1  
 Date\_ 20071109  
 Time 10.55  
 INSTRUM spect  
 PROBHD 5 mm PABBO BB-  
 PULPROG zg30  
 TD 32768  
 SOLVENT CDC13  
 NS 8  
 DS 0  
 SWH 6172.839 Hz  
 FIDRES 0.188380 Hz  
 AQ 2.6542580 sec  
 RG 64  
 DW 81.000 usec  
 DE 6.00 usec  
 TE 296.8 K  
 D1 1.00000000 sec  
 TDO 1

----- CHANNEL f1 -----  
 NUC1  $^1\text{H}$   
 P1 10.20 usec  
 PL1 0.00 dB  
 SF01 300.1318534 MHz  
 SI 16384  
 SF 300.1300055 MHz  
 UDW EM  
 SSB 0  
 LB 0.30 Hz  
 GB 0  
 PC 1.00

1D carbon with proton decoupling



```

NAME          xd-02-097
EXPNO         4
PROCNO        1
Date_         20071109
Time          11.13
INSTRUM       spect
PROBHD        5 mm PABBO BB-
PULPROG       zgpg30
TD            32768
SOLVENT       CDCl3
NS            256
DS            0
SWH           17985.611 Hz
FIDRES        0.548877 Hz
AQ            0.9110004 sec
RG            5792.6
DW            27.800 usec
DE            6.00 usec
TE            297.6 K
D1            2.00000000 sec
d11           0.03000000 sec
DELTA         1.89999998 sec
TDO           1
  
```

```

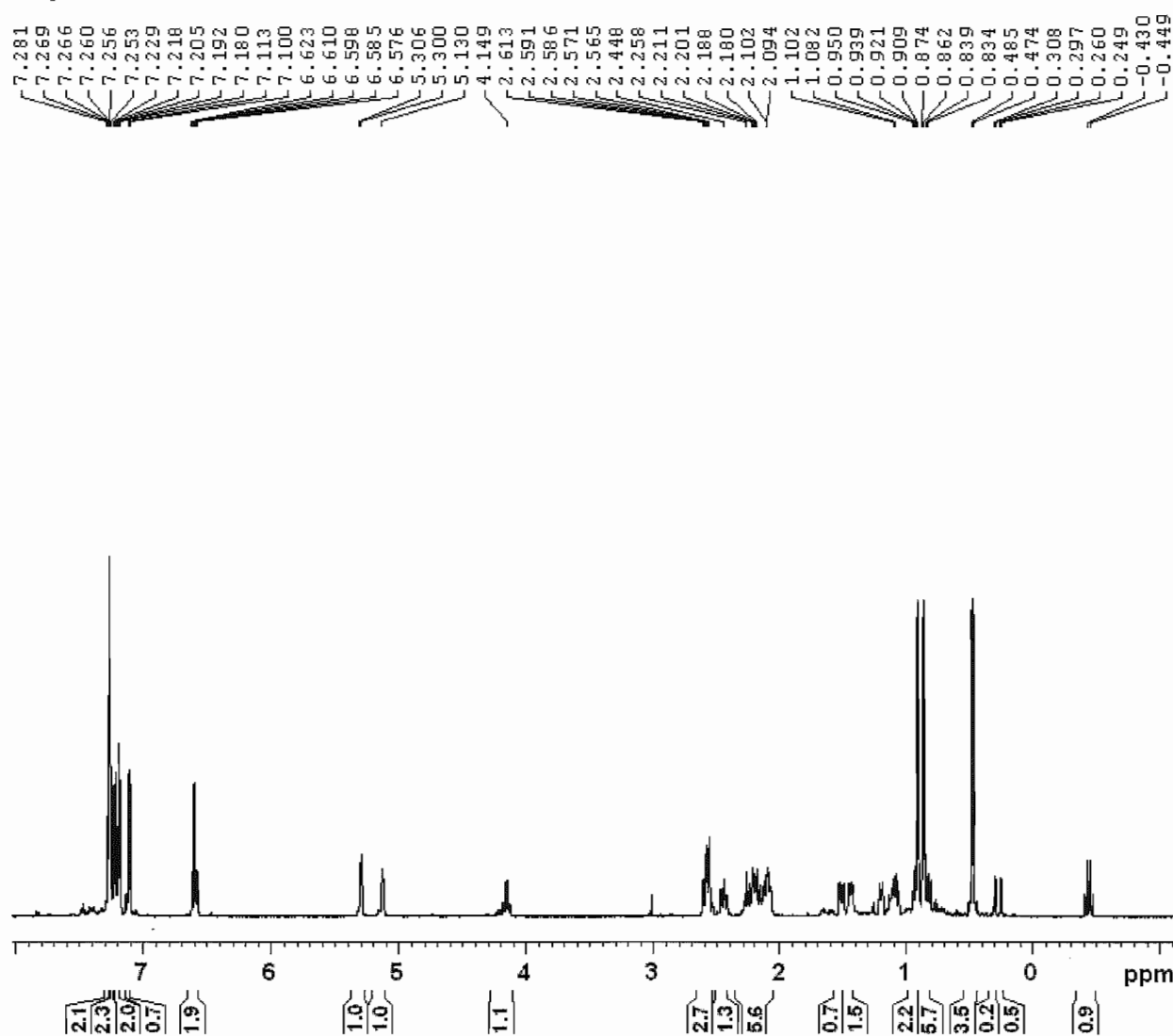
===== CHANNEL f1 =====
NUC1          13C
P1            11.00 usec
PL1           -2.00 dB
SF01          75.4752950 MHz
  
```

```

===== CHANNEL f2 =====
CPDPRG2       waltz16
NUC2          1H
PCPD2         80.00 usec
PL2           0.00 dB
PL12          17.89 dB
PL13          17.60 dB
SF02          300.1312000 MHz
SI            16384
SF            75.4677490 MHz
WDW           EM
SSB           0
LB            1.00 Hz
GB            0
PC            1.40
  
```

Figure 25.  $^{13}\text{C}$  NMR spectrum of 56c.

1d proton



```

NAME          xd-01-109
EXPNO         1
PROCNO        1
Date_         20070424
Time          11.54
INSTRUM       spect
PROBHD        5 mm PABBO BB-
PULPROG       zg30
TD            32768
SOLVENT       CDCl3
NS            4
DS            0
SWH           12376.237 Hz
FIDRES        0.377693 Hz
AQ            1.3239176 sec
RG            143.7
DW            40.400 usec
DE            6.00 usec
TE            296.7 K
D1            1.00000000 sec
TDO           1
  
```

```

===== CHANNEL f1 =====
NUC1          1H
P1            11.00 usec
PL1           -4.00 dB
SF01          600.2037065 MHz
SI            32768
SF            600.2000139 MHz
WDW           EM
SSB           0
LB            0.30 Hz
GB            0
PC            1.00
  
```

Figure 26.  $^1\text{H}$  NMR spectrum of (R,R)-57a.



```

NAME                xd-01-109
EXPNO                2
PROCNO              1
Date_                20070424
Time                12.00
INSTRUM              spect
PROBHD              5 mm PABBO BB-
PULPROG              zgpg30
TD                  32768
SOLVENT              CDC13
NS                   1024
DS                   0
SWH                  35971.223 Hz
FIDRES              1.037755 Hz
AQ                   0.4555391 sec
RG                   1824.6
DW                   13.900 usec
DE                   6.00 usec
TE                   298.2 K
D1                   2.00000000 sec
d11                  0.03000000 sec
DELTA                1.89999998 sec
TD0                  1

```

```
===== CHANNEL f1 =====  
NUC1                13C  
P1                  8.00 usec  
PL1                 -1.00 dB  
SF01               150.9355021 MHz
```

```

===== CHANNEL f2 =====
CPDPRG2          waltz16
NUC2              1H
PCPD2             70.00 usec
PL2              -4.00 dB
PL12             12.07 dB
PL13             15.00 dB
SFO2             600.2024008 MHz
SI               32768
SF              150.9204100 MHz
WDW              EM
SSB              0
LB               1.00 Hz
GB               0
PC               1.40

```

**Figure 27.**  $^{13}\text{C}$  NMR spectrum of (*R,R*)-57a.



7.260  
6.538  
6.525  
6.483  
6.470  
5.117  
5.037  
5.030  
4.834  
4.594  
4.206  
4.196  
4.177  
4.151  
4.093  
4.070  
3.751  
2.934  
2.763  
2.757  
2.737  
2.654  
2.073  
2.062  
2.042  
1.987  
1.856  
1.518  
1.498  
1.465  
1.443  
1.391  
1.369  
1.308  
1.296  
1.263  
1.061  
0.980  
0.903  
0.892  
0.880  
0.865  
0.846  
0.834  
0.799  
0.794  
0.777  
0.727  
0.715  
0.616  
0.606  
0.379  
0.359

7.5  
7.0  
6.5  
6.0  
5.5  
5.0  
4.5  
4.0  
3.5  
3.0  
2.5  
2.0  
1.5  
1.0  
0.5 ppm

1.0  
1.0  
1.0  
1.0  
6.0  
5.9  
1.1  
1.1  
2.0  
2.2  
1.0  
1.0  
1.1  
2.1  
1.1  
1.0  
2.0  
1.2  
2.3  
1.3  
1.2  
1.2  
1.7  
1.4  
1.3  
2.3  
3.6  
1.2  
3.2  
4.2



```
NAME                      xd3-017e  
EXPNO                     1  
PROCNO                   1  
Date_                    20080228  
Time                     9.16  
INSTRUM                  spect  
PROBHD      5 mm PABBO BB-  
PULPROG                 zg30  
TD                       32768  
SOLVENT                  CDC13  
NS                        4  
DS                        0  
SWH          12376.237 Hz  
FIDRES             0.377693 Hz  
AQ           1.3239176 sec  
RG                71.8  
DW            40.400 msec  
DE              6.00 msec  
TE               298.0 K  
D1           1.00000000 sec  
TD0              1
```

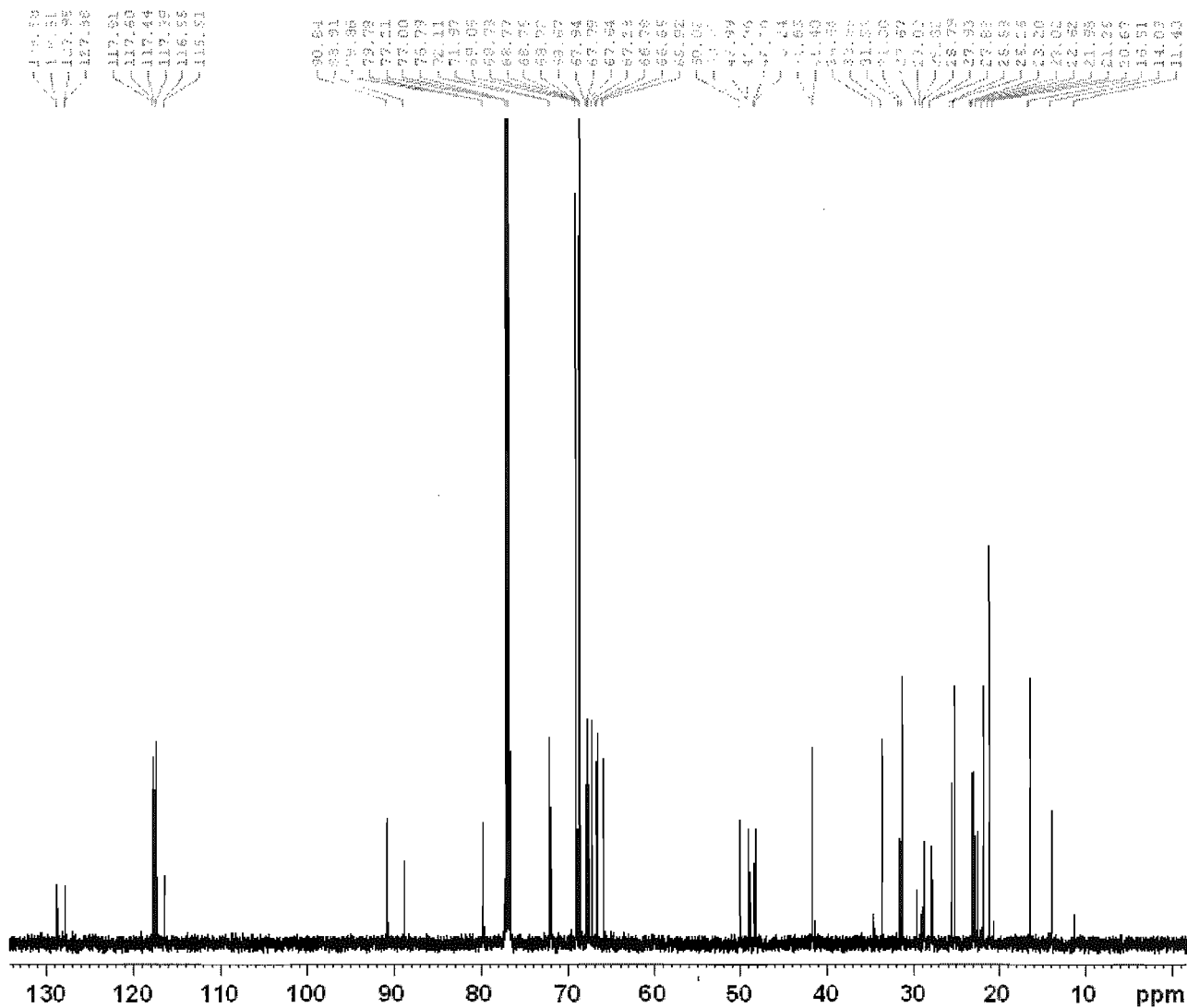
```

===== CHANNEL f1 =====
NUC1          1H
P1              11.00 usec
P11            -4.00 dB
SF01          600.2037065 MHz
SI              32768
SF            600.2000142 MHz
WDW             EM
SSB              0
LB              0.30 Hz
GB              0
PC              1.00

```

**Figure 28.**  $^1\text{H}$  NMR spectrum of (S,S)-57f.

1d carbon with proton decoupling



NAME xd3-017e  
EXPNO 2  
PROCNO 1  
Date\_ 20080228  
Time\_ 9.25  
INSTRUM spect  
PROBHD 5 mm PABBO BB-  
PULPROG zgpg30  
TD 32768  
SOLVENT CDCl3  
NS 256  
DS 0  
SWH 35971.223 Hz  
FIDRES 1.097755 Hz  
AQ 0.4555391 sec  
RG 3251  
DW 13.900 usec  
DE 6.00 usec  
TE 298.3 K  
D1 2.00000000 sec  
d11 0.03000000 sec  
DELTA 1.89999998 sec  
TD0 1

===== CHANNEL f1 =====  
NUC1  $^{13}\text{C}$   
P1 8.00 usec  
PL1 -1.00 dB  
SFO1 150.9355021 MHz

===== CHANNEL f2 =====  
CPDPRG2 waltz16  
NUC2  $^1\text{H}$   
PCPD2 70.00 usec  
PL2 -4.00 dB  
PL12 12.07 dB  
PL13 15.00 dB  
SFO2 600.2024008 MHz  
SI 32768  
SF 150.9204181 MHz  
WDW RM  
SSB 0  
LB 1.00 Hz  
GB 0  
PC 1.40

Figure 29.  $^{13}\text{C}$  NMR spectrum of (S,S)-57f.

<sup>1</sup>H NMR spectrum of compound 10 in CDCl<sub>3</sub>. The x-axis represents the chemical shift in ppm, ranging from 0 to 8. The spectrum shows several multiplets and singlets. Integration values are provided below the baseline, and chemical shift values are listed above the peaks.

Chemical shift values (ppm): 7.281, 7.269, 7.266, 7.260, 7.256, 7.253, 7.229, 7.218, 7.205, 7.192, 7.180, 7.113, 7.100, 6.623, 6.610, 6.598, 6.585, 6.576, 5.306, 5.300, 5.130, 4.149, 2.613, 2.591, 2.586, 2.571, 2.565, 2.448, 2.258, 2.211, 2.201, 2.188, 2.180, 2.102, 2.094, 1.102, 1.082, 0.950, 0.939, 0.921, 0.909, 0.874, 0.862, 0.839, 0.834, 0.485, 0.474, 0.308, 0.297, 0.260, 0.249, -0.430, -0.449.

Integration values: 2.1, 2.3, 2.0, 0.7, 1.9, 1.0, 1.0, 1.1, 2.7, 1.3, 5.6, 0.7, 1.5, 2.2, 5.7, 3.5, 0.2, 0.5, 0.9.



```
NAME          xd-01-109
EXPNO         1
PROCNO        1
Date_         20070424
Time          11.54
INSTRUM       spect
PROBHD        5 mm PABBO BB-
PULPROG       zg30
TD            32768
SOLVENT       CDCl3
NS            4
DS            0
SWH           12376.237 Hz
FIDRES        0.377693 Hz
AQ            1.3239176 sec
RG            143.7
DU            40.400 usec
DE            6.00 usec
TE            296.7 K
D1            1.00000000 sec
TD0           1
```

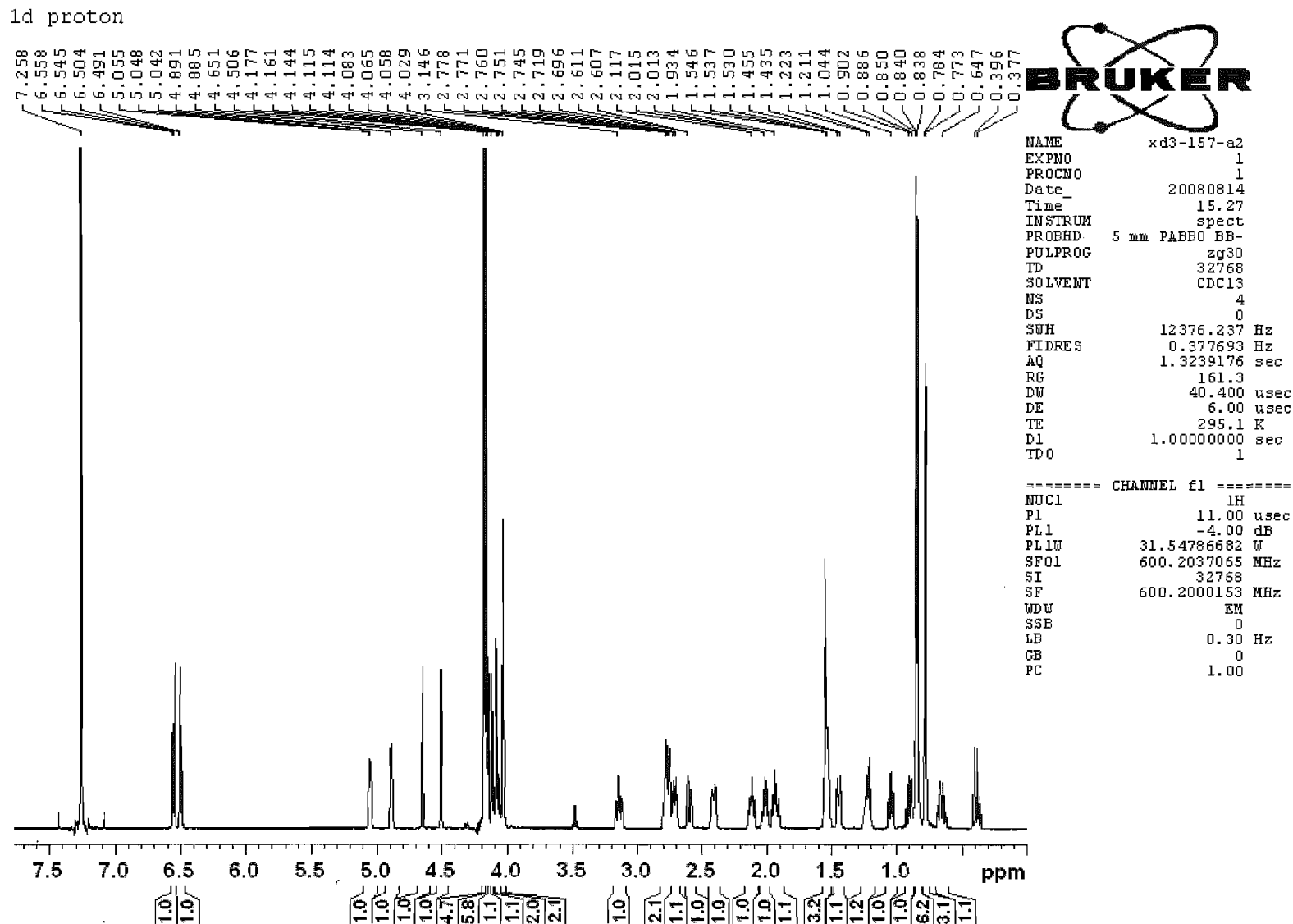
```

===== CHANNEL f1 =====
NUC1              1H
P1                11.00 usec
PL1              -4.00 dB
SF01             600.2037065 MHz
SI               32768
SF              600.2000139 MHz
WDU              EM
SSB              0
LB              0.30 Hz
GB              0
PC              1.00

```

**Figure 30.**  $^1\text{H}$  NMR spectrum of (*R,R*)-57a.







```
NAME          xd3-157-a2
EXPNO         2
PROCNO        1
Date_         20080814
Time          16.11
INSTRUM       spect
PROBHD        5 mm PABBO BB-
PULPROG       zgpg30
TD            32768
SOLVENT       CDC13
NS            16384
DS            0
SWH           35971.223 Hz
FIDRES       0.1997755 Hz
AQ           0.4555391 sec
RG           23170.5
DW           13.900 usec
DE           6.00 usec
TE           295.1 K
D1           2.00000000 sec
D11          0.03000000 sec
TD0          16
```

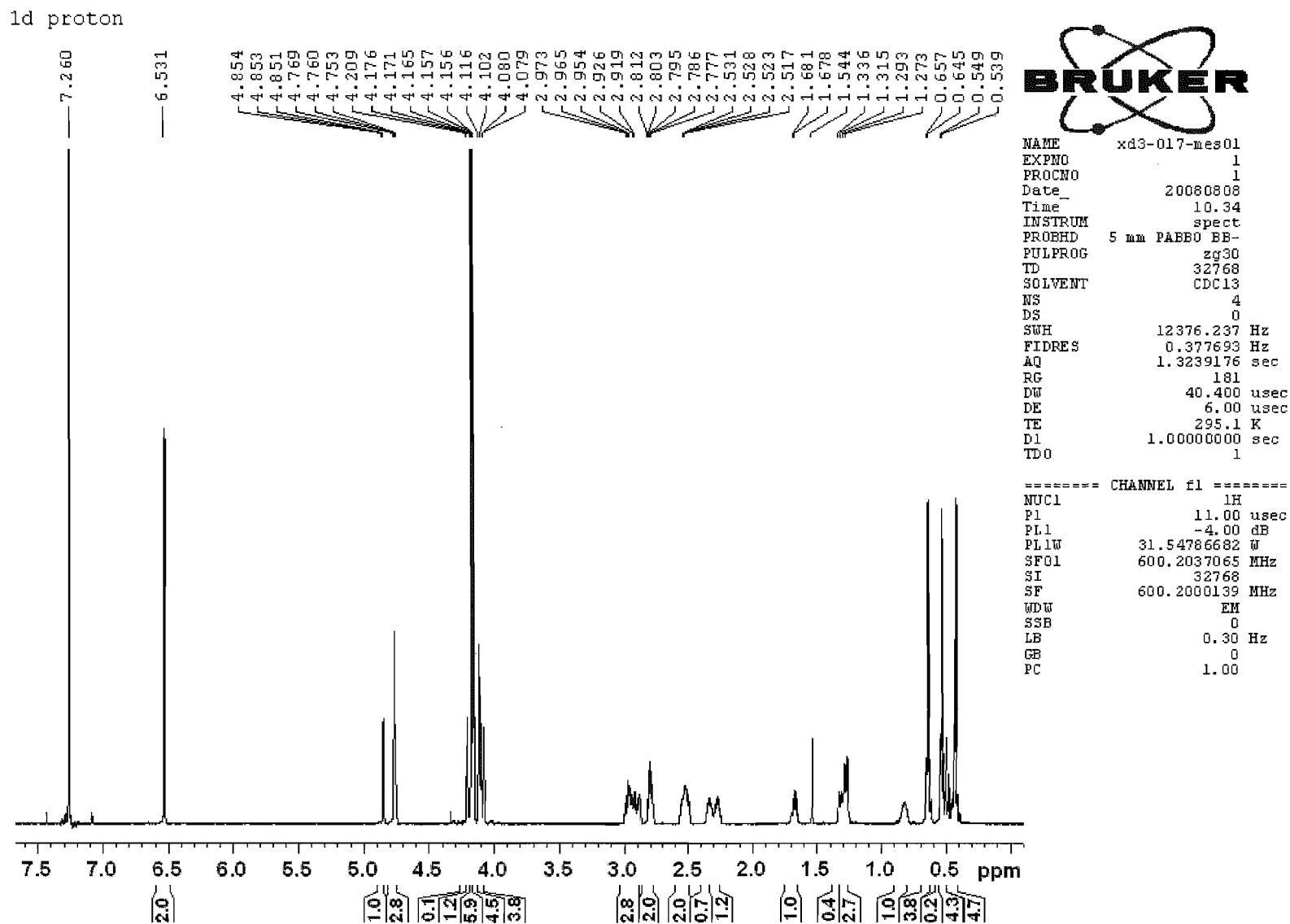
```
===== CHANNEL f1 =====
NUC1      13C
P1        8.00 usec
PL1       -1.00 dB
PL1W      92.33850861 W
SF01      150.9355021 MHz
```

```

===== CHANNEL f2 =====
CPDPRG2          waltz16
NUC2              1H
PCPD2             70.00 usec
PL2               -4.00 dB
PL12              12.07 dB
PL13              15.00 dB
PL2W              31.54786682 W
PL12W             0.77977633 W
PL13W             0.39716411 W
SF0               600.2024008 MHz
SI                32768
SF               150.9204100 MHz
WDW               EM
SSB               0
LB               1.00 Hz
GB                0
PC               1.40

```

**Figure 33.**  $^{13}\text{C}$  NMR Spectrum of (*R,R*)-57f.



[illegible]

```

NAME          xd3-017-mes01
EXPNO         2
PROCNO       1
Date_         20080808
Time          12.53
INSTRUM       spect
PROBHD        5 mm PABBO BB-
PULPROG       zgpg30
TD            32768
SOLVENT       CDC13
NS            3223
DS            0
SWH           35971.223 Hz
FIDRES       1.097755 Hz
AQ           0.4555391 sec
RG           20642.5
DW           13.900 usec
DE           6.00 usec
TE           295.1 K
D1           2.00000000 sec
D11          0.03000000 sec
TD0          4

```

```
===== CHANNEL f1 =====
NUC1      13C
P1         8.00 usec
PL1        -1.00 dB
PL1W       92.33850861 W
SF01       150.9355021 MHz
```

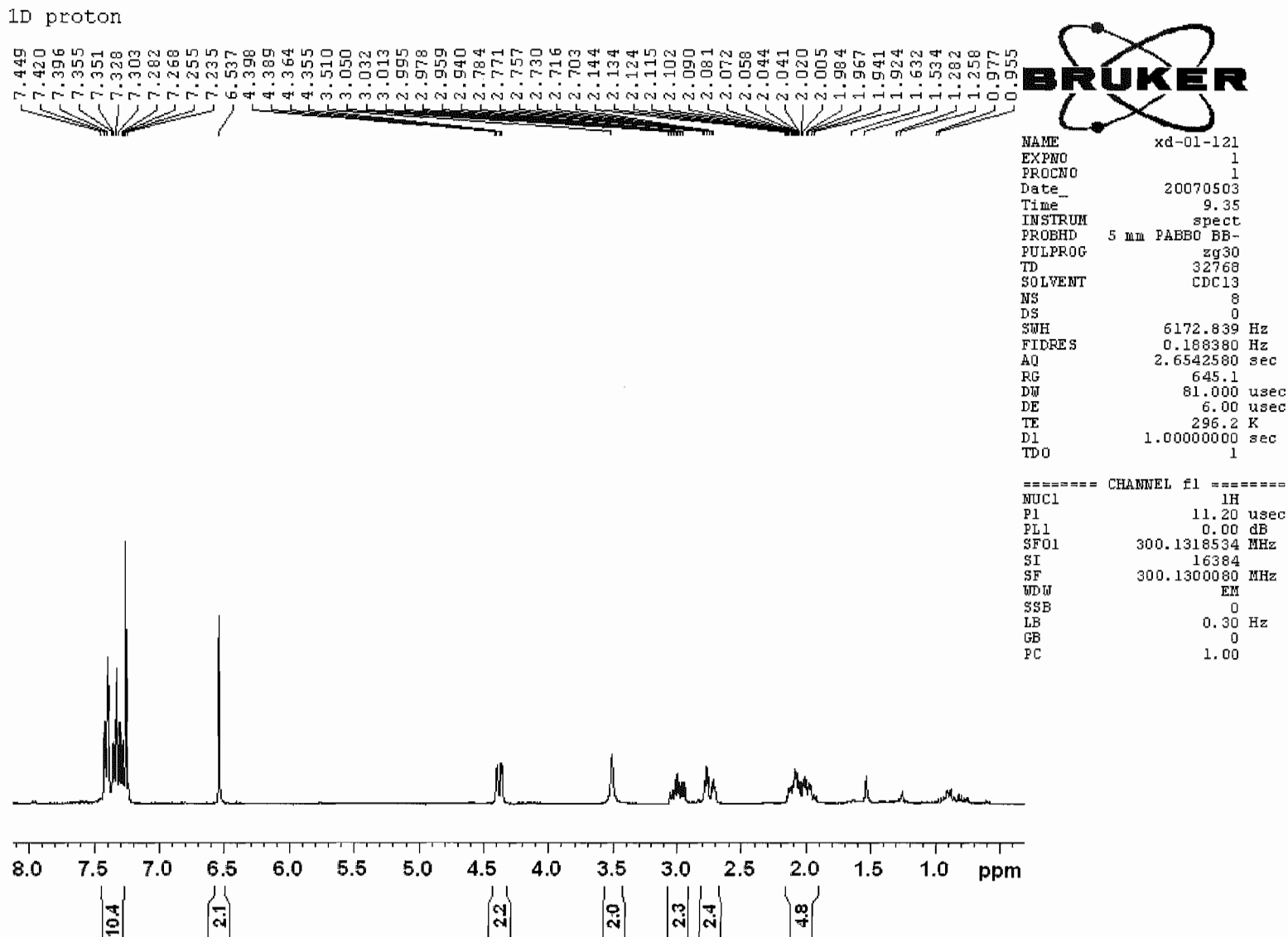
```

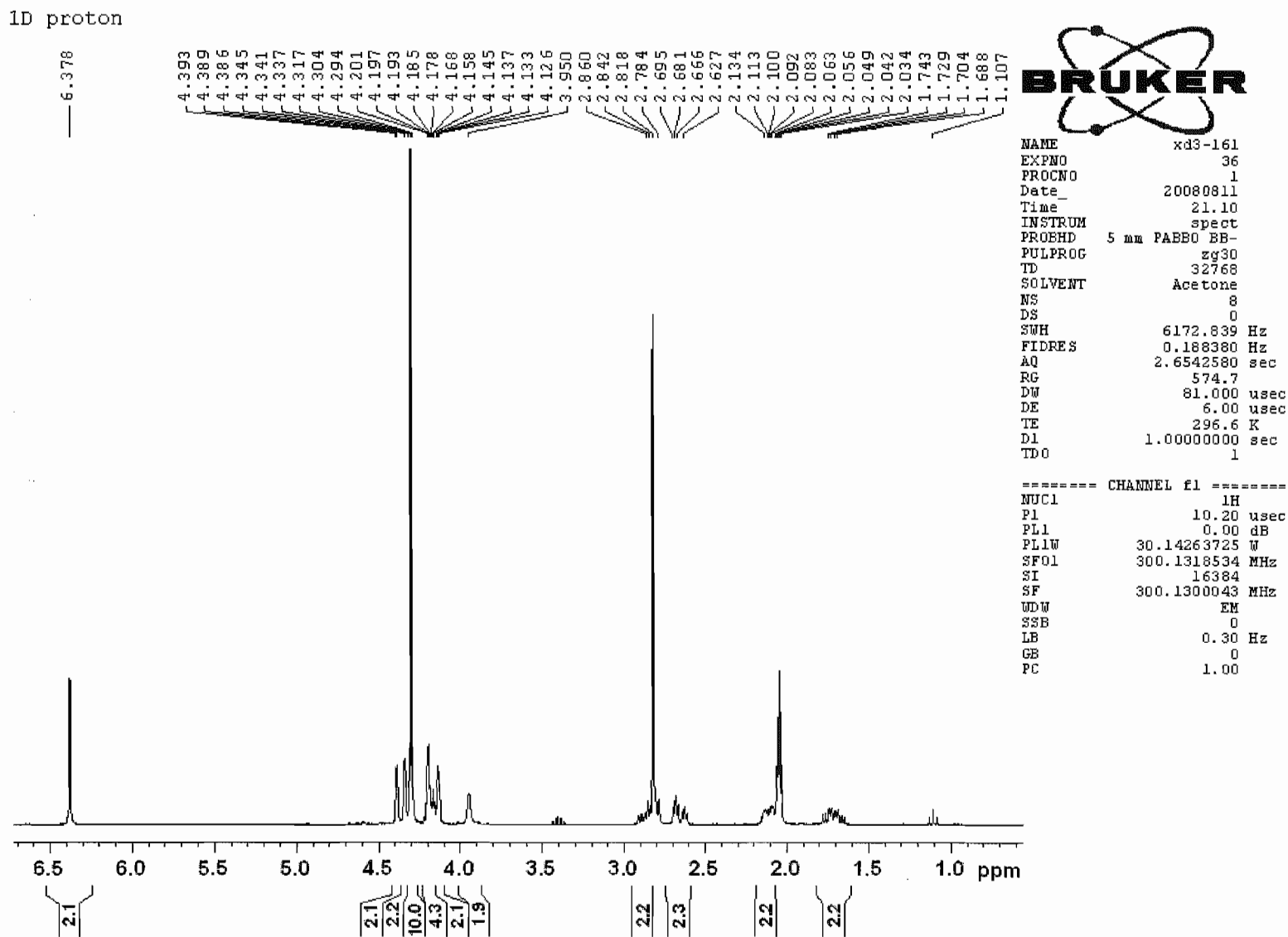
===== CHANNEL f2 =====
CPDPRG2          waltz16
NUC2              1H
PCPD2            70.00 usec
PL2              -4.00 dB
PL12             12.07 dB
PL13             15.00 dB
PL2W             31.54786682 W
PL12W            0.77977633 W
PL13W            0.39716411 W
SF02             600.2024008 MHz
SI               32768
SF               150.9204100 MHz
WDW              EM
SSB              0
LB               1.00 Hz
GB               0
PC               1.40

```

**Figure 35.**  $^{13}\text{C}$  NMR spectrum of *meso*-57f.

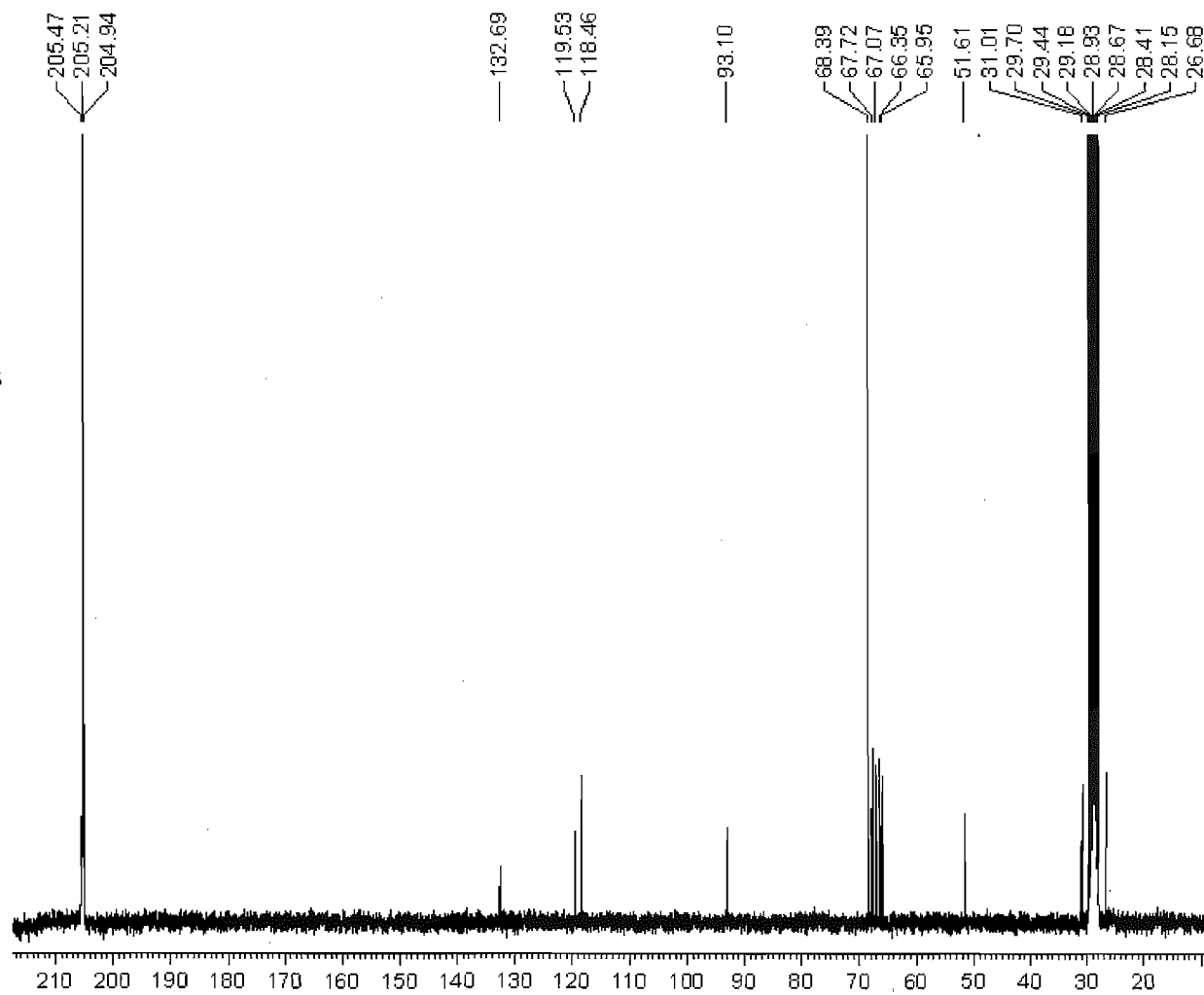






1D carbon with proton decoupling

Figure 38.  $^{13}\text{C}$  NMR spectrum of (S,S)-56f.



```

NAME      xd3-161
EXPNO     6
PROCNO    1
Date_     20080811
Time      22.35
INSTRUM   spect
PROBHD    5 mm PABBO BB-
PULPROG   zgpg30
TD        32768
SOLVENT   Acetone
NS        1871
DS        0
SWH       17985.611 Hz
FIDRES    0.548877 Hz
AQ        0.9110004 sec
RG        1290.2
DW        27.800 usec
DE        6.00 usec
TE        297.7 K
D1        2.00000000 sec
D11       0.03000000 sec
TDO       1
  
```

```

===== CHANNEL f1 =====
NUC1      13C
P1        11.00 usec
PL1       -2.00 dB
PL1W      62.50282669 W
SF01      75.4752950 MHz
  
```

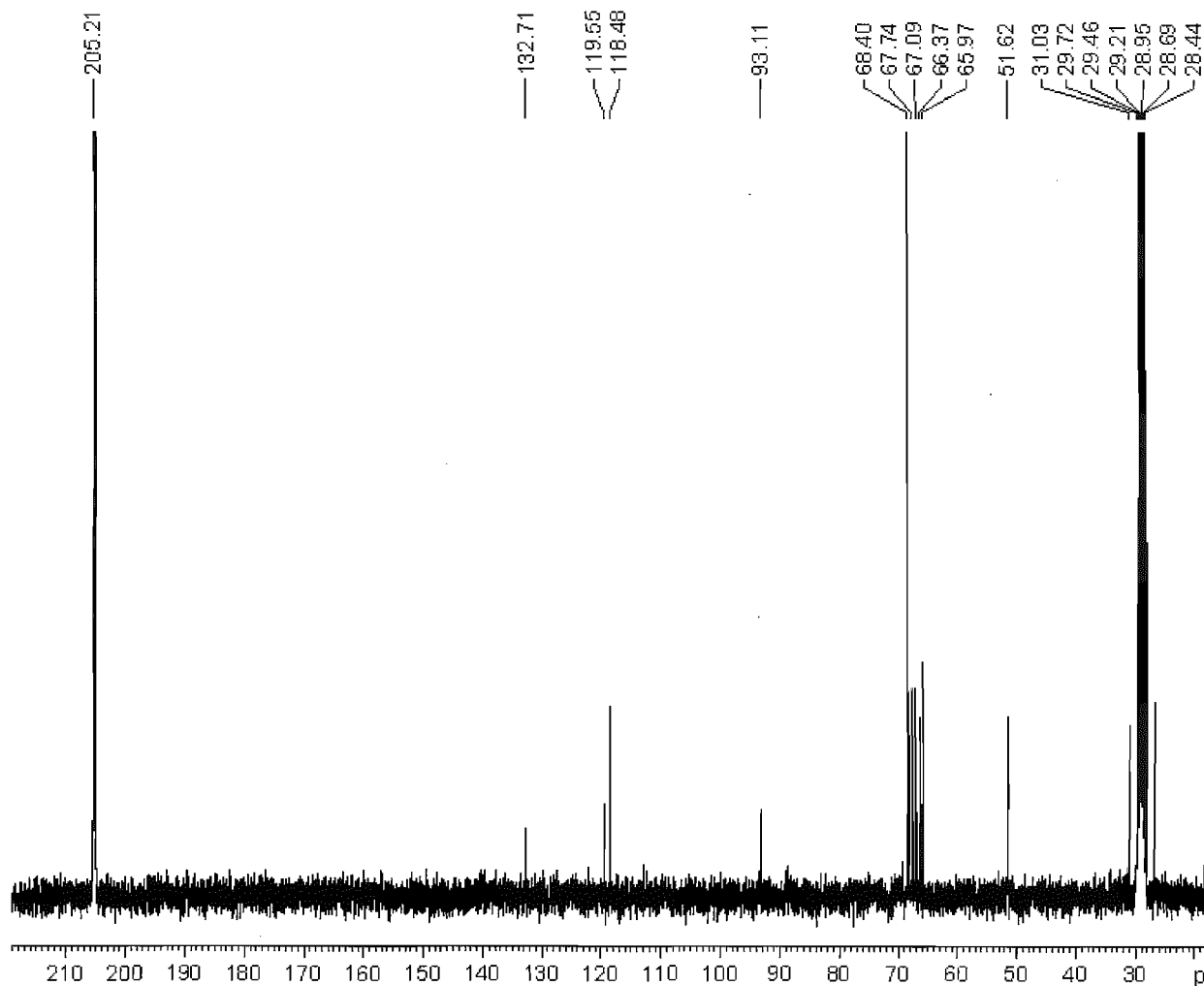
```

===== CHANNEL f2 =====
CPDPRG2   waltz16
NUC2      1H
PCPD2     80.00 usec
PL2       0.00 dB
PL12      17.89 dB
PL13      17.60 dB
PL2W      30.14263725 W
PL12W     0.48998332 W
PL13W     0.52381897 W
SF02      300.1312000 MHz
SI        16384
SF        75.4677490 MHz
WDW       EM
SSB       0
LB        1.00 Hz
GB        0
PC        1.40
  
```



chiral amine hydrolyzing from phosphous compound  
 1D carbon with proton decoupling

Figure 40.  $^{13}\text{C}$  NMR spectrum of (R,R)-56f.



NAME xd3-013  
 EXPNO 2  
 PROCNO 1  
 Date\_ 20080227  
 Time 13.39  
 INSTRUM spect  
 PROBHD 5 mm PABBO BB-  
 PULPROG zgpg30  
 TD 32768  
 SOLVENT CDC13  
 NS 256  
 DS 0  
 SWH 17985.611 Hz  
 FIDRES 0.548877 Hz  
 AQ 0.9110004 sec  
 RG 1024  
 DW 27.800 usec  
 DE 6.00 usec  
 TE 298.1 K  
 D1 2.00000000 sec  
 d11 0.03000000 sec  
 DELTA 1.89999998 sec  
 TDO 1

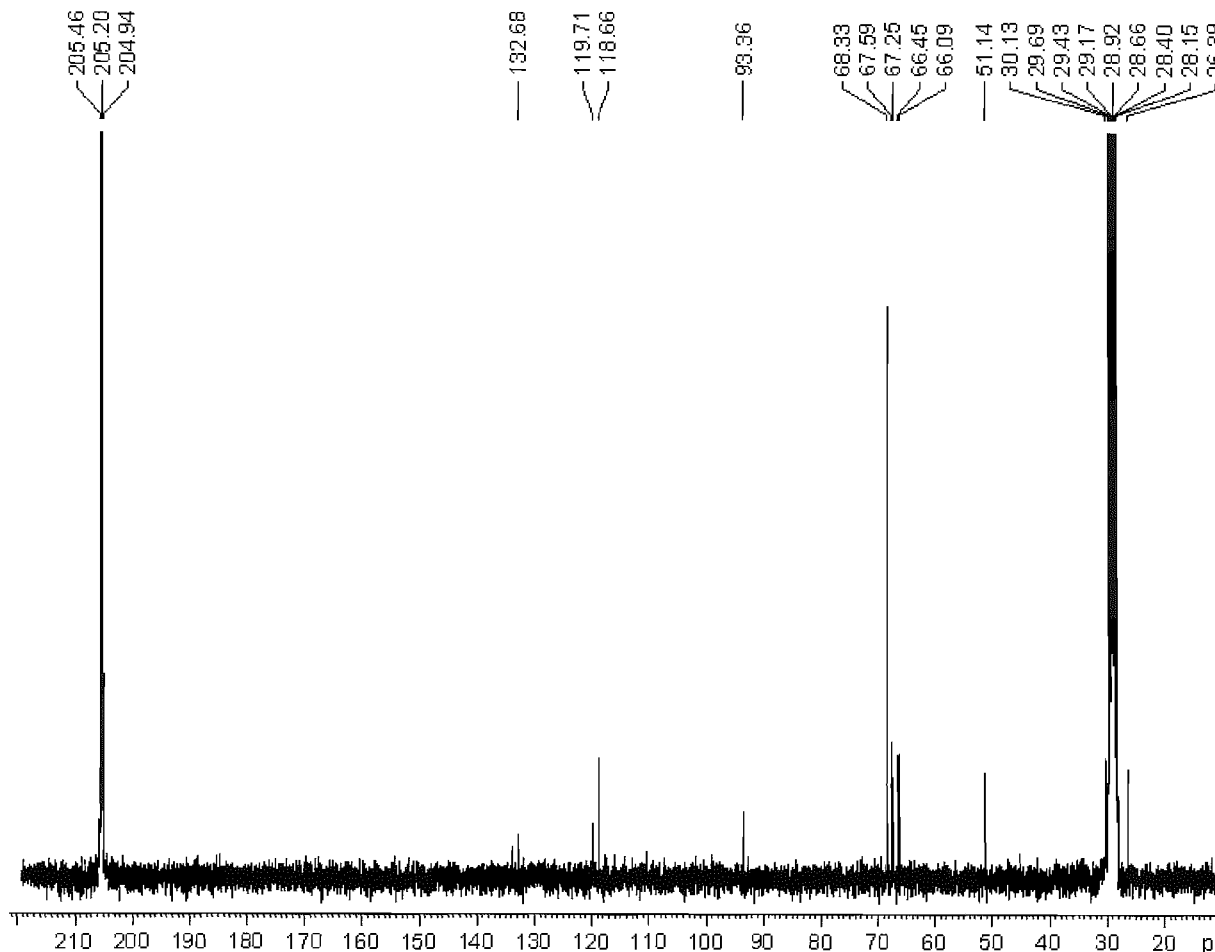
===== CHANNEL f1 =====  
 NUC1 13C  
 P1 11.00 usec  
 PL1 -2.00 dB  
 SFO1 75.4752950 MHz

===== CHANNEL f2 =====  
 CPDPRG2 waltz16  
 NUC2 1H  
 PCPD2 80.00 usec  
 PL2 0.00 dB  
 PL12 17.89 dB  
 PL13 17.60 dB  
 SFO2 300.1312000 MHz  
 SI 16384  
 SF 75.4677490 MHz  
 WDW EM  
 SSB 0  
 LB 1.00 Hz  
 GB 0  
 PC 1.40

1D carbon with proton decoupling



Figure 41.  $^{13}\text{C}$  NMR spectrum of *meso*-99c.



```

NAME          xd3-163
EXPNO         9
PROCNO        1
Date_         20080819
Time_         0.33
INSTRUM       spect
PROBHD        5 mm PABBO BB-
PULPROG       zgpg30
TD            32768
SOLVENT       Acetone
NS            4096
DS            0
SWH           17985.611 Hz
FIDRES        0.548877 Hz
AQ            0.9110004 sec
RG            1024
DW            27.800 usec
DE            6.00 usec
TE            298.2 K
D1            2.00000000 sec
D11           0.03000000 sec
TDO           1

===== CHANNEL f1 =====
NUC1          13C
P1            11.00 usec
PL1           -2.00 dB
PL1W          62.50282669 W
SF01          75.4752950 MHz

===== CHANNEL f2 =====
CPDPRG2       waltz16
NUC2          1H
PCPD2         80.00 usec
PL2           0.00 dB
PL12          17.89 dB
PL13          17.60 dB
PL2W          30.14263725 W
PL12W         0.48998332 W
PL13W         0.52381897 W
SF02          300.1312000 MHz
SI            16384
SF            75.4677490 MHz
WDW           EM
SSB           0
LB            1.00 Hz
GB            0
PC            1.40
  
```

diphenyl chloride salt (r,r)



```

NAME          xd-01-117
EXPNO         1
PROCNO        1
Date_         20070501
Time          16.18
INSTRUM       spect
PROBHD        5 mm PABBO BB-
PULPROG       zg30
TD            32768
SOLVENT       CDC13
NS            8
DS            0
SWH           6172.839 Hz
FIDRES        0.188380 Hz
AQ            2.6542580 sec
RG            456.1
DW            81.000 usec
DE            6.00 usec
TE            300.5 K
D1            1.00000000 sec
TDO           1
  
```

```

===== CHANNEL f1 =====
NUC1          1H
P1            11.20 usec
PL1           0.00 dB
SF01          300.1318534 MHz
SI            16384
SF            300.1300068 MHz
WDW           EM
SSB           0
LB            0.30 Hz
GB            0
PC            1.00
  
```

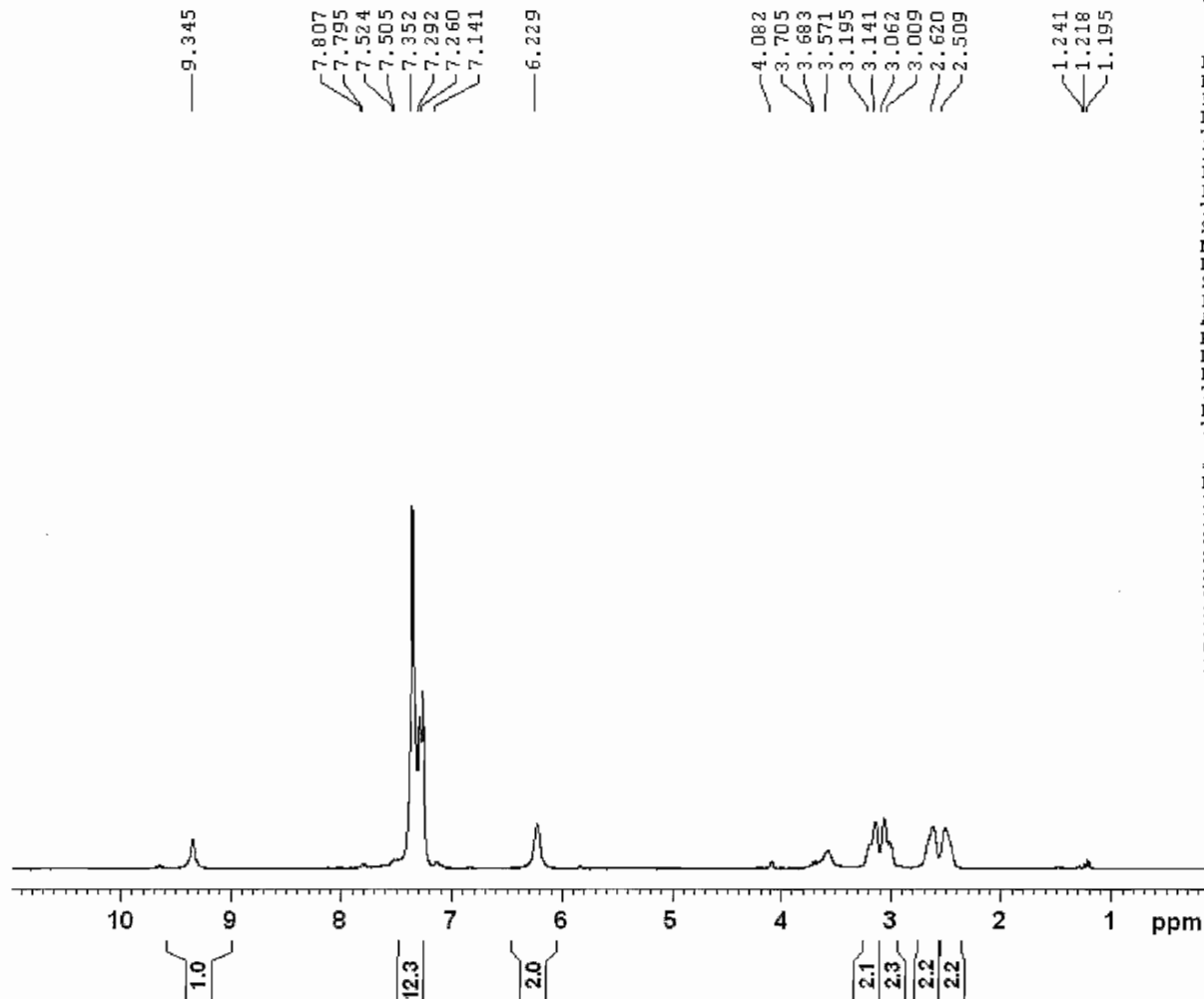
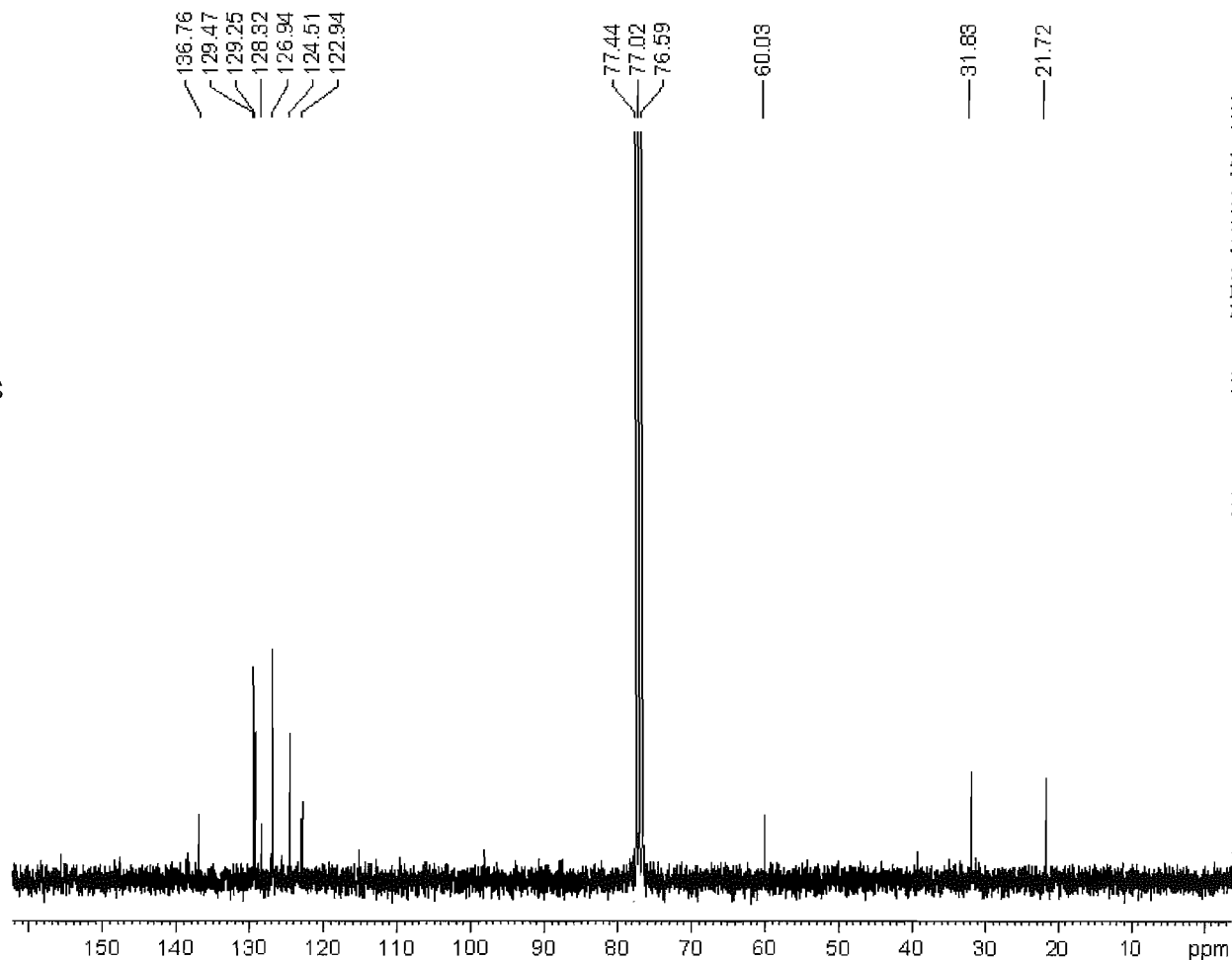


Figure 42.  $^1\text{H}$  NMR spectrum of (R,R)-58a.

1D carbon with proton decoupling



```

NAME      xd-01-117
EXPNO     2
PROCNO    1
Date_     20070501
Time      17.37
INSTRUM   spect
PROBHD    5 mm PABBO BB-
PULPROG   zgpg30
TD        32768
SOLVENT   CDC13
NS        256
DS        0
SWH       17985.611 Hz
FIDRES    0.548877 Hz
AQ        0.9110004 sec
RG        11585.2
DW        27.800 usec
DE        6.00 usec
TE        301.7 K
D1        2.00000000 sec
d11       0.03000000 sec
DELTA     1.89999998 sec
TDO       1
  
```

```

===== CHANNEL f1 =====
NUC1      13C
P1        10.00 usec
PL1       -1.00 dB
SF01      75.4752950 MHz
  
```

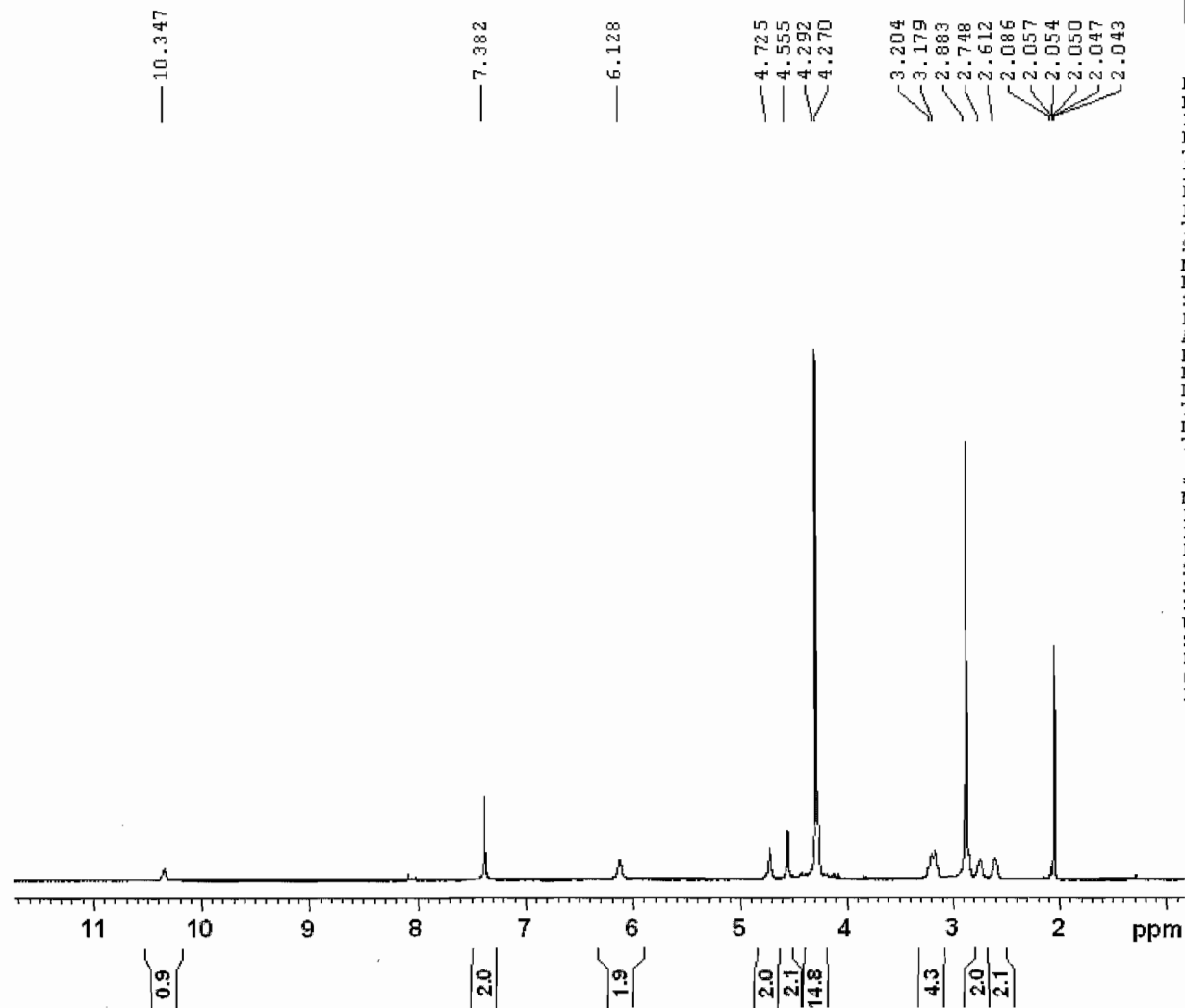
```

===== CHANNEL f2 =====
CPDPRG2   waltz16
NUC2      1H
PCPD2     80.00 usec
PL2       0.00 dB
PL12      17.60 dB
PL13      17.60 dB
SF02      300.1312000 MHz
SI        16384
SF        75.4677505 MHz
WDW       EM
SSB       0
LB        1.00 Hz
GB        0
PC        1.40
  
```

Figure 43.  $^{13}\text{C}$  NMR spectrum of (R,R)-58a.



1d proton



```

NAME      xd3-165
EXPNO     1
PROCNO    1
Date_     20080820
Time      13.55
INSTRUM    spect
PROBHD     5 mm PABBO BB-
PULPROG    zg30
TD         32768
SOLVENT    Acetone
NS         16
DS         0
SWH        12376.237 Hz
FIDRES     0.377693 Hz
AQ         1.3239176 sec
RG         228.1
DW         40.400 usec
DE         6.00 usec
TE         295.1 K
D1         2.00000000 sec
TD0        1
  
```

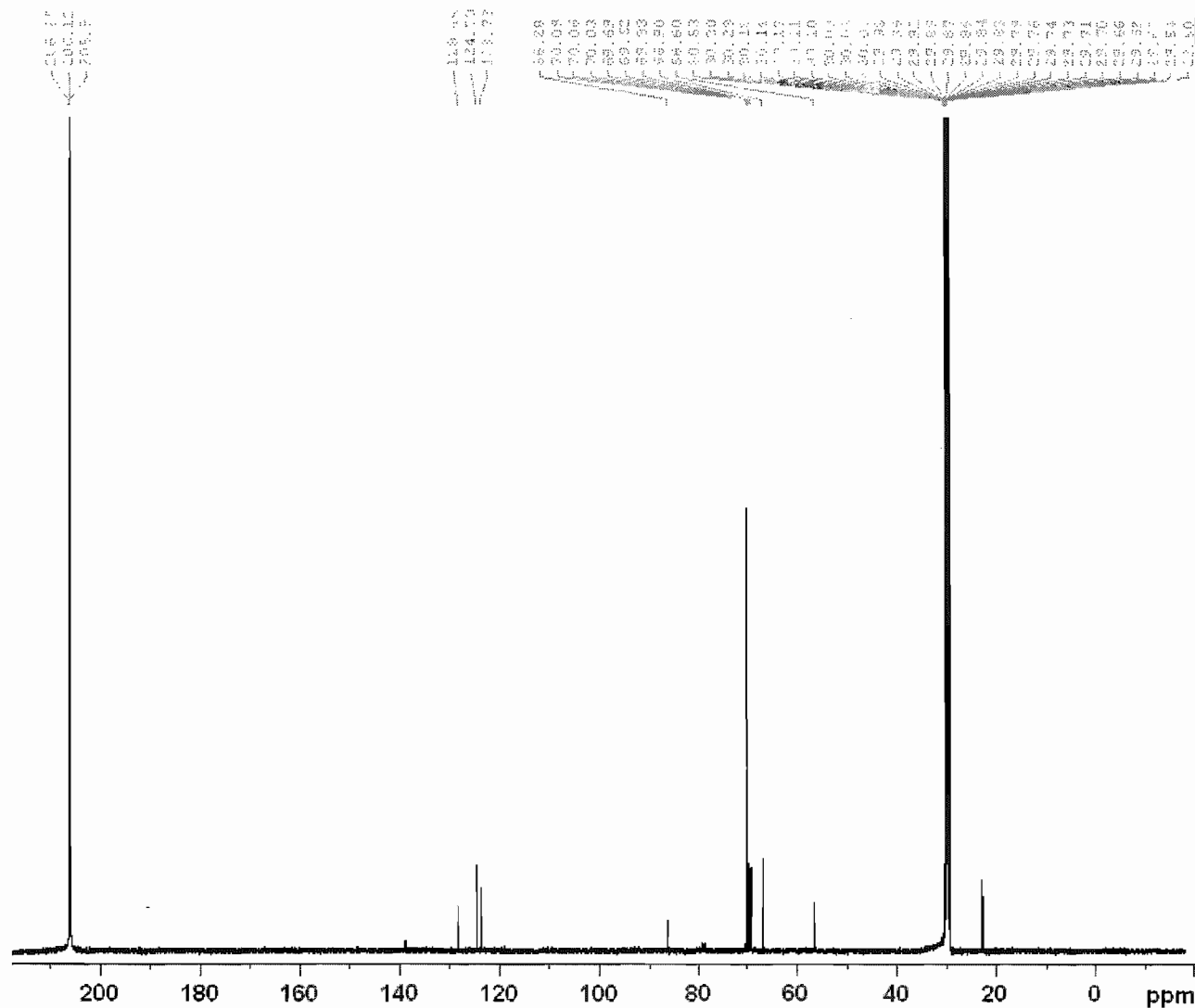
```

===== CHANNEL f1 =====
NUC1      1H
P1        11.00 usec
PL1       -4.00 dB
PL1W      31.54786682 W
SF01      600.2037065 MHz
SI        32768
SF        600.2000097 MHz
WDW       EM
SSB       0
LB        0.30 Hz
GB        0
PC        1.00
  
```

Figure 44.  $^1\text{H}$  NMR spectrum of (5*S*,5*f*)-58f.

1d carbon with proton decoupling

Figure 45.  $^{13}\text{C}$  NMR spectrum of (S,S)-58f.



silver two ligands complex attant



NAME xd-01-039  
 EXPNO 1  
 PROCNO 1  
 Date\_ 20070210  
 Time 15.10  
 INSTRUM spect  
 PROBHD 5 mm PABBO BB-  
 PULPROG zg30  
 TD 32768  
 SOLVENT CDC13  
 NS 8  
 DS 0  
 SWH 6172.839 Hz  
 FIDRES 0.188380 Hz  
 AQ 2.6542580 sec  
 RG 724.1  
 DW 81.000 usec  
 DE 6.00 usec  
 TE 297.5 K  
 D1 1.00000000 sec  
 TDO 1

===== CHANNEL f1 =====  
 NUC1 1H  
 P1 11.20 usec  
 PL1 0.00 dB  
 SF01 300.1318534 MHz  
 SI 16384  
 SF 300.1300064 MHz  
 WDW EM  
 SSB 0  
 LB 0.30 Hz  
 GB 0  
 PC 1.00

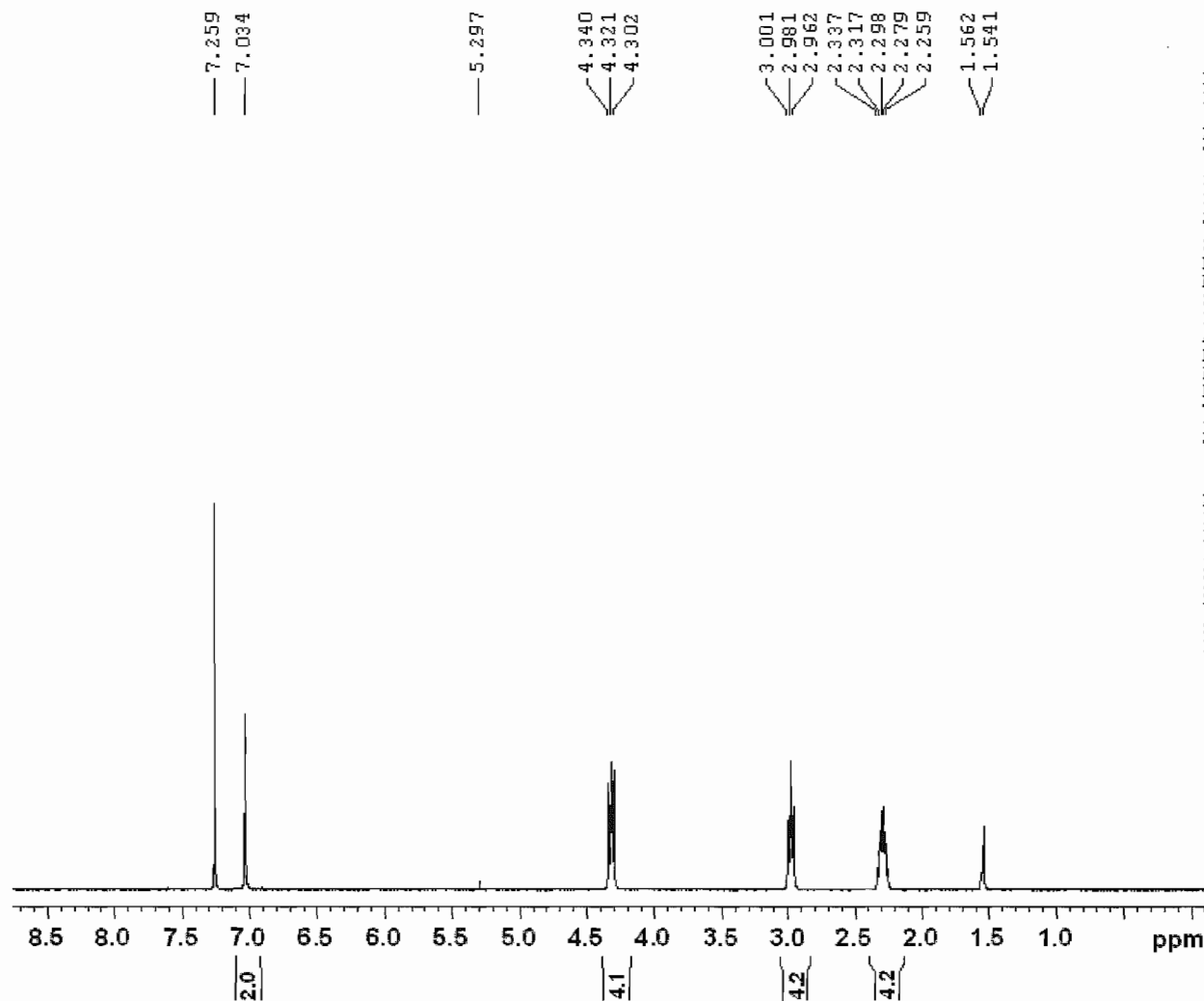


Figure 46.  $^1\text{H}$  NMR spectrum of 90.

1D carbon with proton decoupling

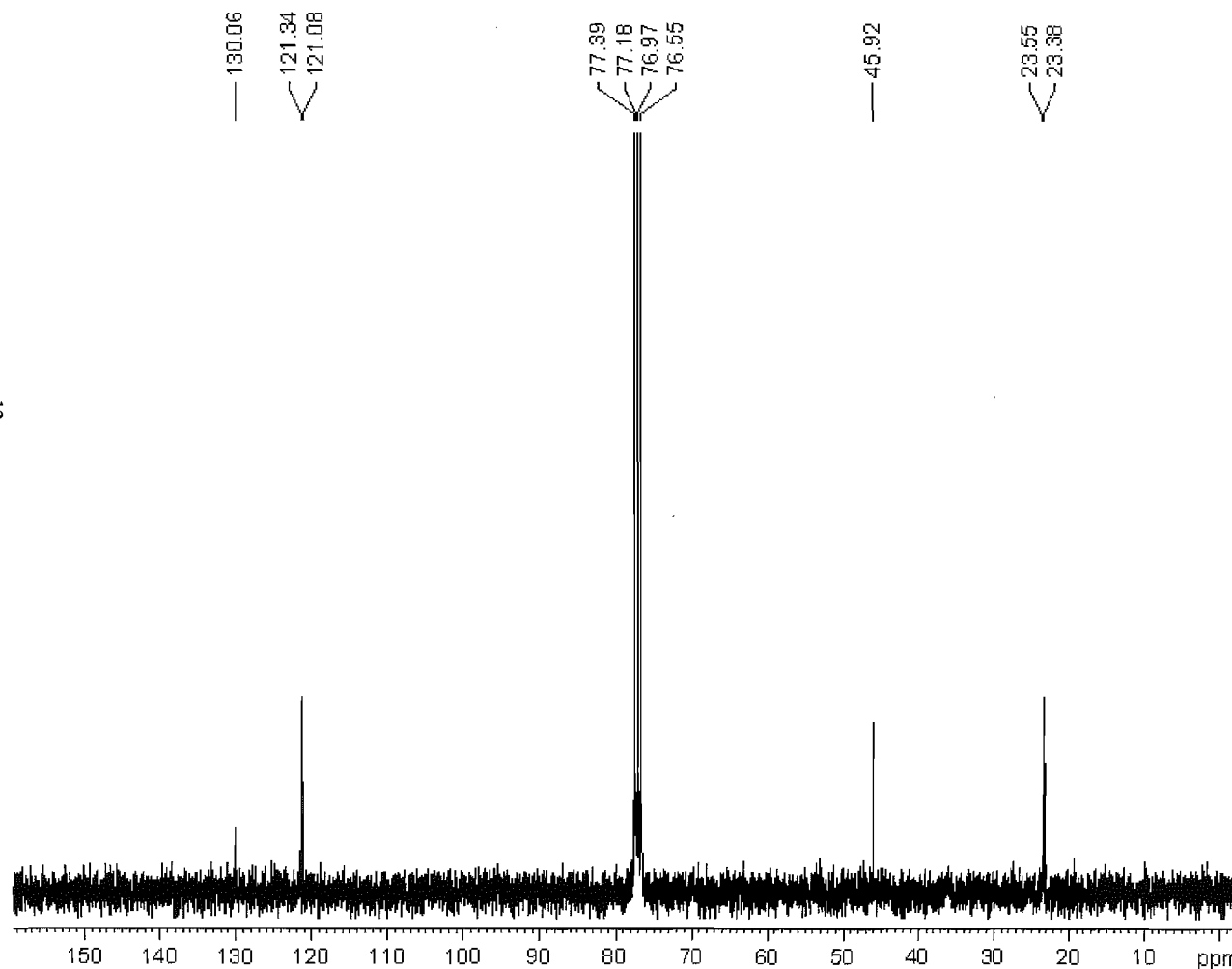


Figure 47.  $^{13}\text{C}$  NMR spectrum of 90.

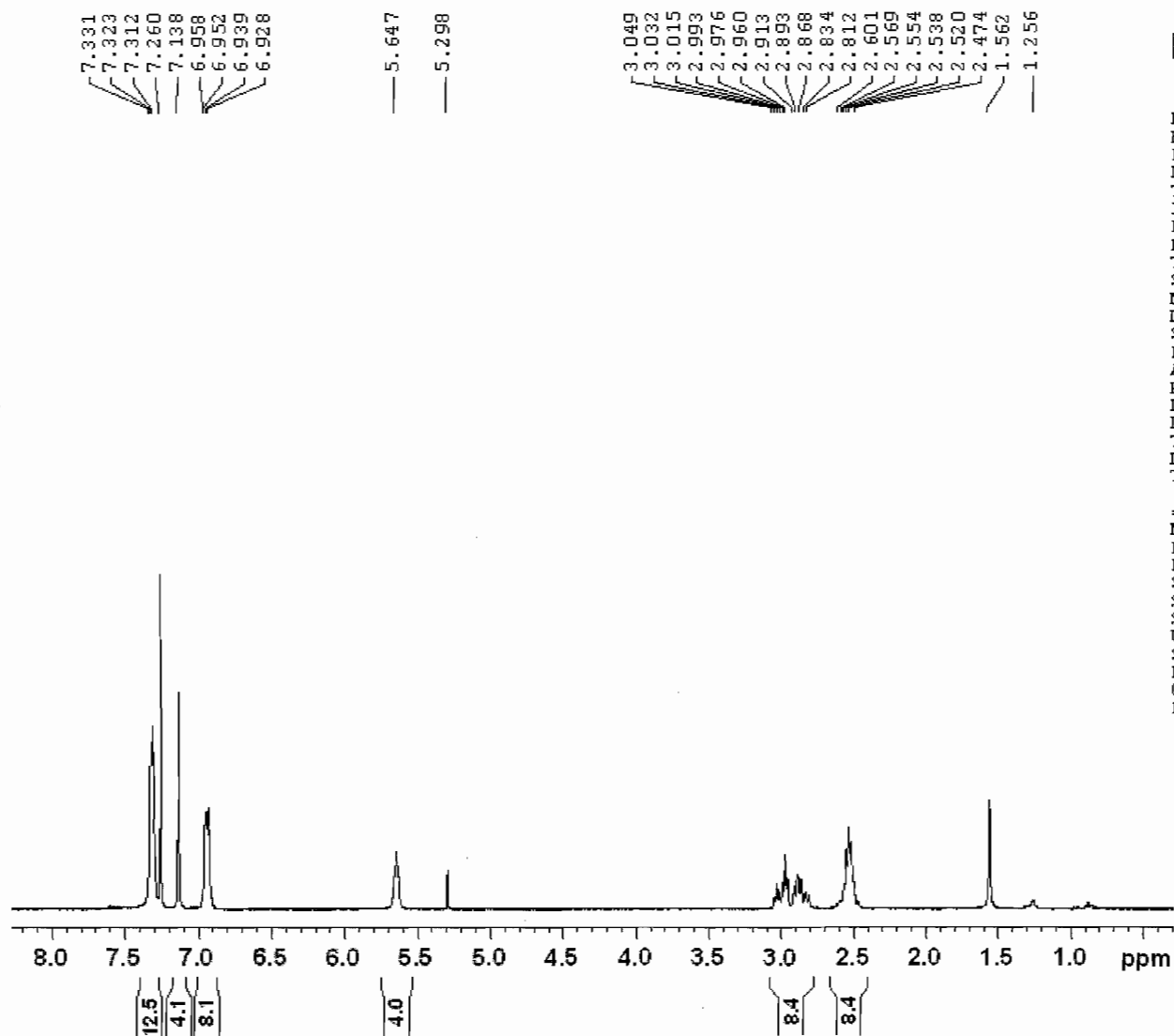


NAME xd-01-039  
EXPNO 3  
PROCNO 1  
Date\_ 20070210  
Time 17.24  
INSTRUM spect  
PROBHD 5 mm PABBO BB-  
PULPROG zgpg30  
TD 32768  
SOLVENT CDCl3  
NS 512  
DS 0  
SWH 17985.611 Hz  
FIDRES 0.548877 Hz  
AQ 0.9110004 sec  
RG 32768  
DW 27.800 usec  
DE 6.00 usec  
TE 298.4 K  
D1 2.00000000 sec  
d11 0.03000000 sec  
DELTA 1.89999998 sec  
TDO 1

===== CHANNEL f1 =====  
NUC1 13C  
P1 10.00 usec  
PL1 -1.00 dB  
SF01 75.4752950 MHz

===== CHANNEL f2 =====  
CPDPRG2 waltz16  
NUC2 1H  
PCPD2 80.00 usec  
PL2 0.00 dB  
PL12 17.60 dB  
PL13 17.60 dB  
SF02 300.1312000 MHz  
SI 16384  
SF 75.4677519 MHz  
WDW EM  
SSB 0  
LB 1.00 Hz  
GB 0  
PC 1.40

Figure 48.  $^1\text{H}$  NMR spectrum of (5*S*)-82a.



```

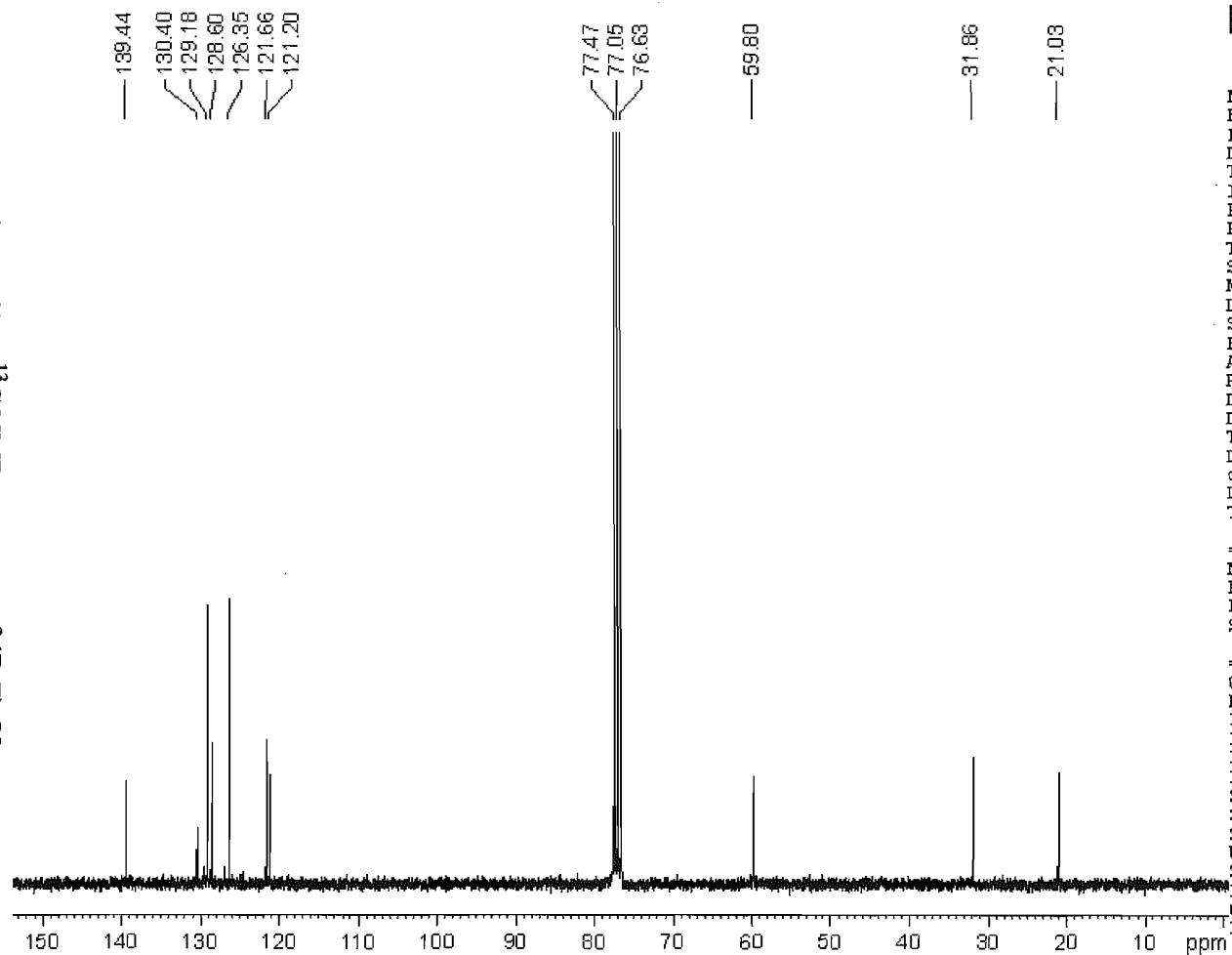
NAME      xd-01-137
EXPNO     1
PROCNO    1
Date_     20070518
Time      10.04
INSTRUM    spect
PROBHD     5 mm PABBO BB-
PULPROG    zg30
TD         32768
SOLVENT    CDCl3
NS         8
DS         0
SWH        6172.839 Hz
FIDRES     0.188380 Hz
AQ         2.6542580 sec
RG         574.7
DW         81.000 usec
DE         6.00 usec
TE         297.7 K
D1         1.000000000 sec
TD0        1
  
```

```

===== CHANNEL f1 =====
NUC1       1H
P1         11.20 usec
PL1        0.00 dB
SF01       300.1318534 MHz
SI         16384
SF         300.1300064 MHz
WDW        EM
SSB        0
LB         0.30 Hz
GB         0
PC         1.00
  
```

1D carbon with proton decoupling

Figure 49.  $^{13}\text{C}$  NMR spectrum of (R,R)-82a.



```

NAME      xd-02-023
EXPNO     3
PROCNO    1
Date_     20070808
Time      21.10
INSTRUM   spect
PROBHD    5 mm PABBO BB-
PULPROG   zgpg30
TD         32768
SOLVENT   CDCl3
NS         512
DS         0
SWH        17985.611 Hz
FIDRES     0.548877 Hz
AQ         0.9110004 sec
RG         6502
DW         27.800 usec
DE         6.00 usec
TE         297.1 K
D1         4.00000000 sec
d11        0.03000000 sec
DELTA      3.90000010 sec
TDO        1
  
```

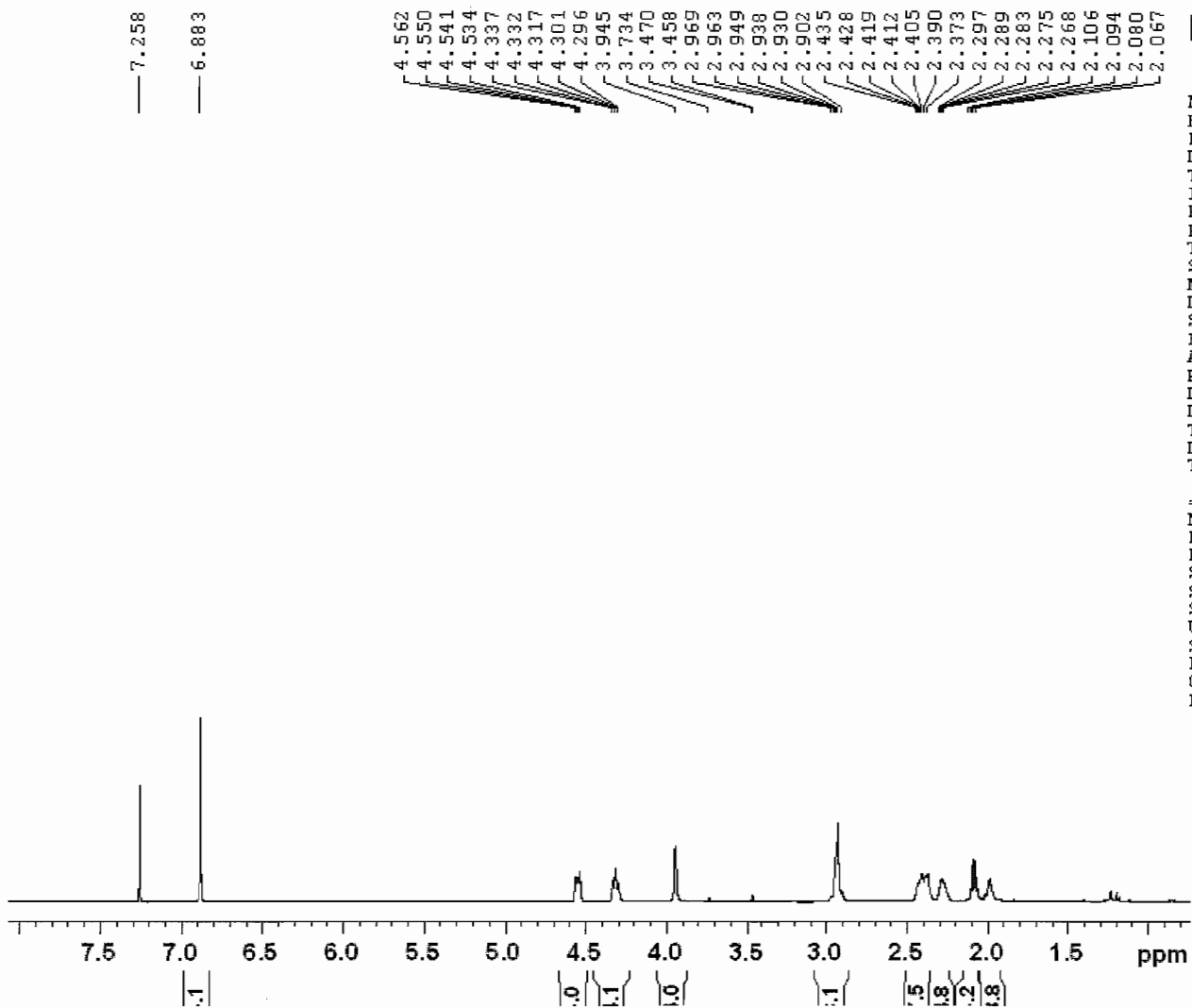
```

===== CHANNEL f1 =====
NUC1       13C
P1         11.00 usec
PL1        -2.00 dB
SF01       75.4752950 MHz
  
```

```

===== CHANNEL f2 =====
CPDPRG2    waltz16
NUC2       1H
PCPD2      80.00 usec
PL2        0.00 dB
PL12       17.89 dB
PL13       17.60 dB
SF02       300.1312000 MHz
SI         16384
SF         75.4677490 MHz
WDW        EM
SSB        0
LB         1.00 Hz
GB         0
PC         1.40
  
```

1d proton



```

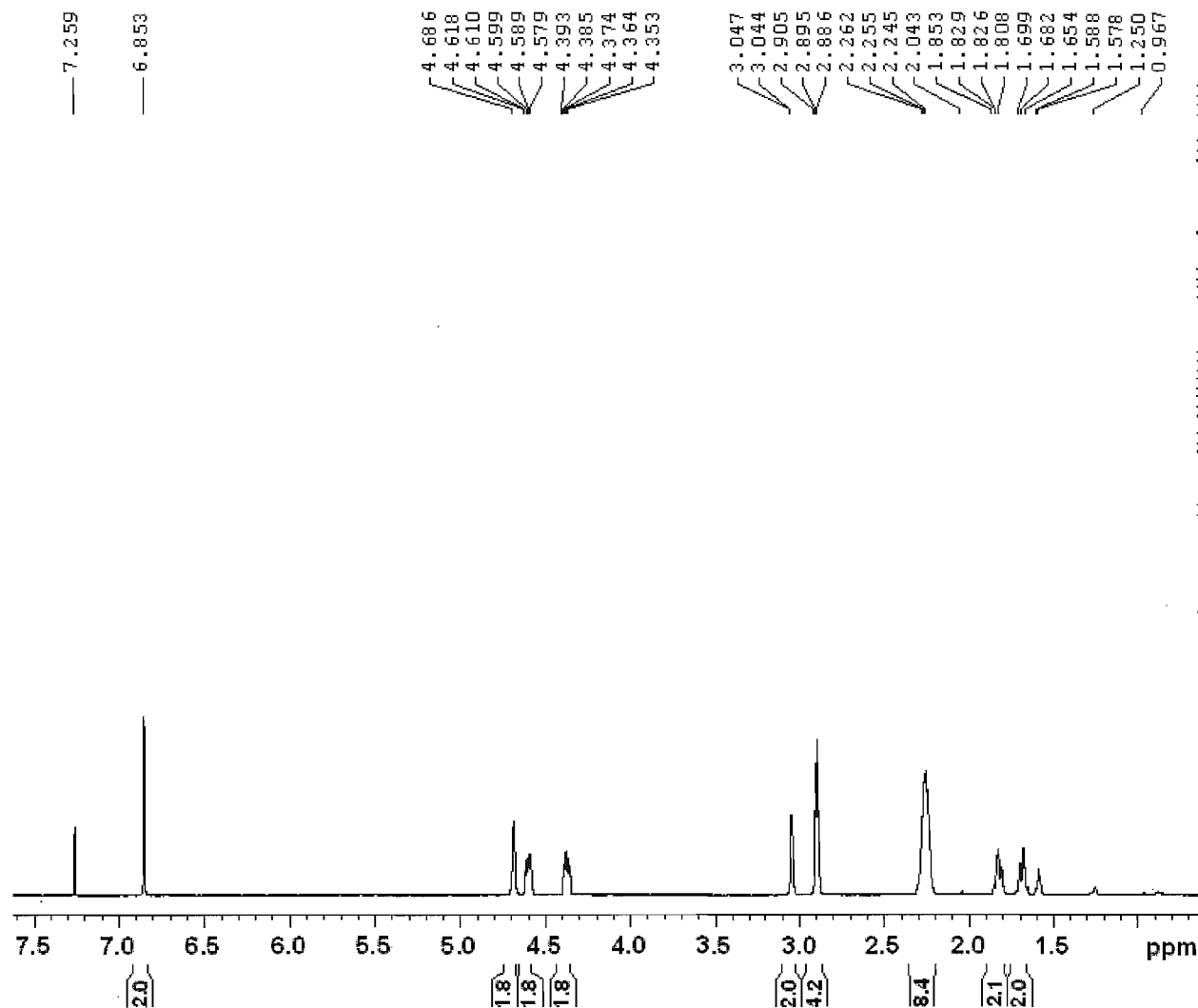
NAME      xd-01-149
EXPNO      1
PROCNO     1
Date_      20070529
Time       9.39
INSTRUM    spect
PROBHD     5 mm PABBO BB-
PULPROG    zg30
TD         32768
SOLVENT    CDCl3
NS          4
DS          0
SWH        12376.237 Hz
FIDRES     0.377693 Hz
AQ         1.3239176 sec
RG          181
DU         40.400 usec
DE          6.00 usec
TE         295.1 K
D1         1.000000000 sec
TD0         1
  
```

```

===== CHANNEL f1 =====
NUC1       1H
P1         11.00 usec
PL1        -4.00 dB
SF01       600.2037065 MHz
SI         32768
SF         600.2000160 MHz
WDW        EM
SSB        0
LB         0.30 Hz
GB         0
PC         1.00
  
```

Figure 50.  $^1\text{H}$  NMR spectrum of 89.

1d proton



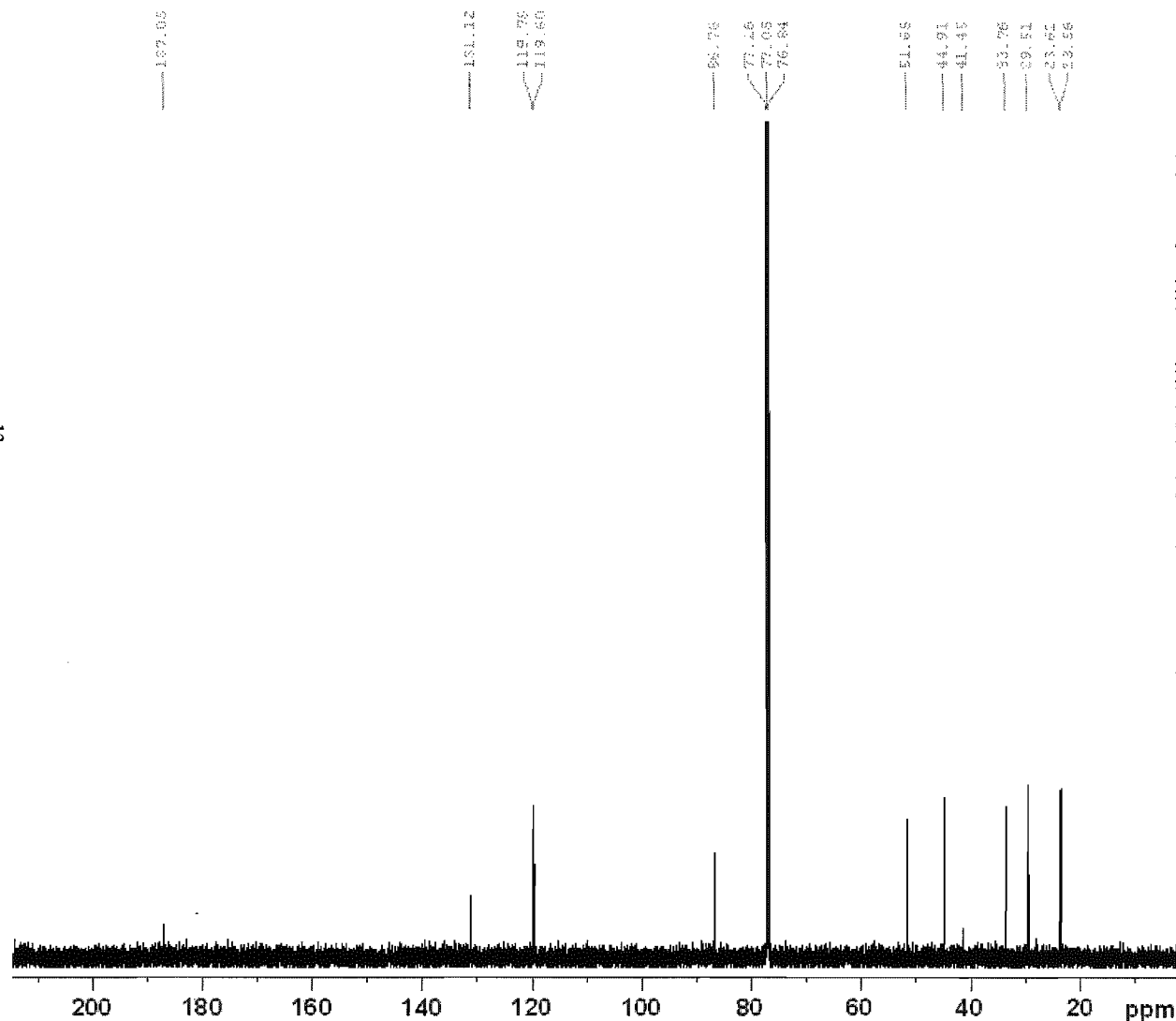
NAME xd-01-155  
 EXPNO 1  
 PROCNO 1  
 Date\_ 20070531  
 Time 11.52  
 INSTRUM spect  
 PROBHD 5 mm PABBO BB-  
 PULPROG zg30  
 TD 32768  
 SOLVENT CDC13  
 NS 4  
 DS 0  
 SWH 12376.237 Hz  
 FIDRES 0.377693 Hz  
 AQ 1.3239176 sec  
 RG 181  
 DW 40.400 usec  
 DE 6.00 usec  
 TE 295.1 K  
 D1 1.00000000 sec  
 TDO 1

===== CHANNEL f1 =====  
 NUC1 1H  
 PL 11.00 usec  
 PL1 -4.00 dB  
 SF01 600.2037065 MHz  
 SI 32768  
 SF 600.2000142 MHz  
 WDW EM  
 SSB 0  
 LB 0.30 Hz  
 GB 0  
 PC 1.00

Figure S1. <sup>1</sup>H NMR spectrum of 91.



1d carbon with proton decoupling



```

NAME      xd-01-155
EXPNO     2
PROCNO    1
Date_     20070531
Time      11.30
INSTRUM   spect
PROBHD    5 mm PABBO BB-
PULPROG   zgpg30
TD        32768
SOLVENT   CDC13
NS        64
DS        0
SWH       35971.223 Hz
FIDRES    1.097755 Hz
AQ        0.4555391 sec
RG        1149.4
DW        13.900 usec
DE        6.00 usec
TE        295.6 K
D1        2.00000000 sec
d11       0.03000000 sec
DELTA     1.89999998 sec
TD0       1
  
```

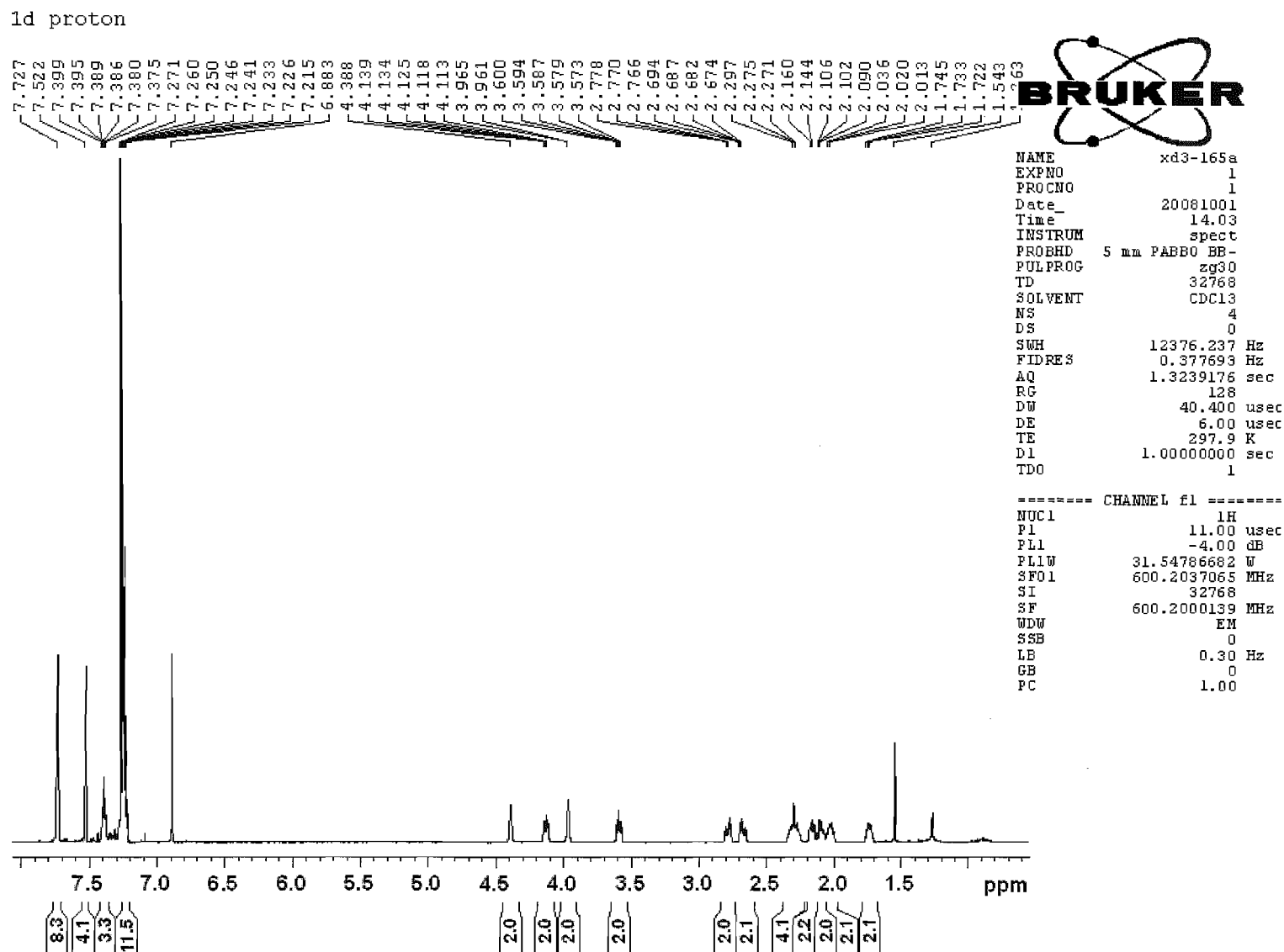
```

===== CHANNEL f1 =====
NUC1      13C
P1        8.00 usec
PL1       -1.00 dB
SF01     150.9355021 MHz
  
```

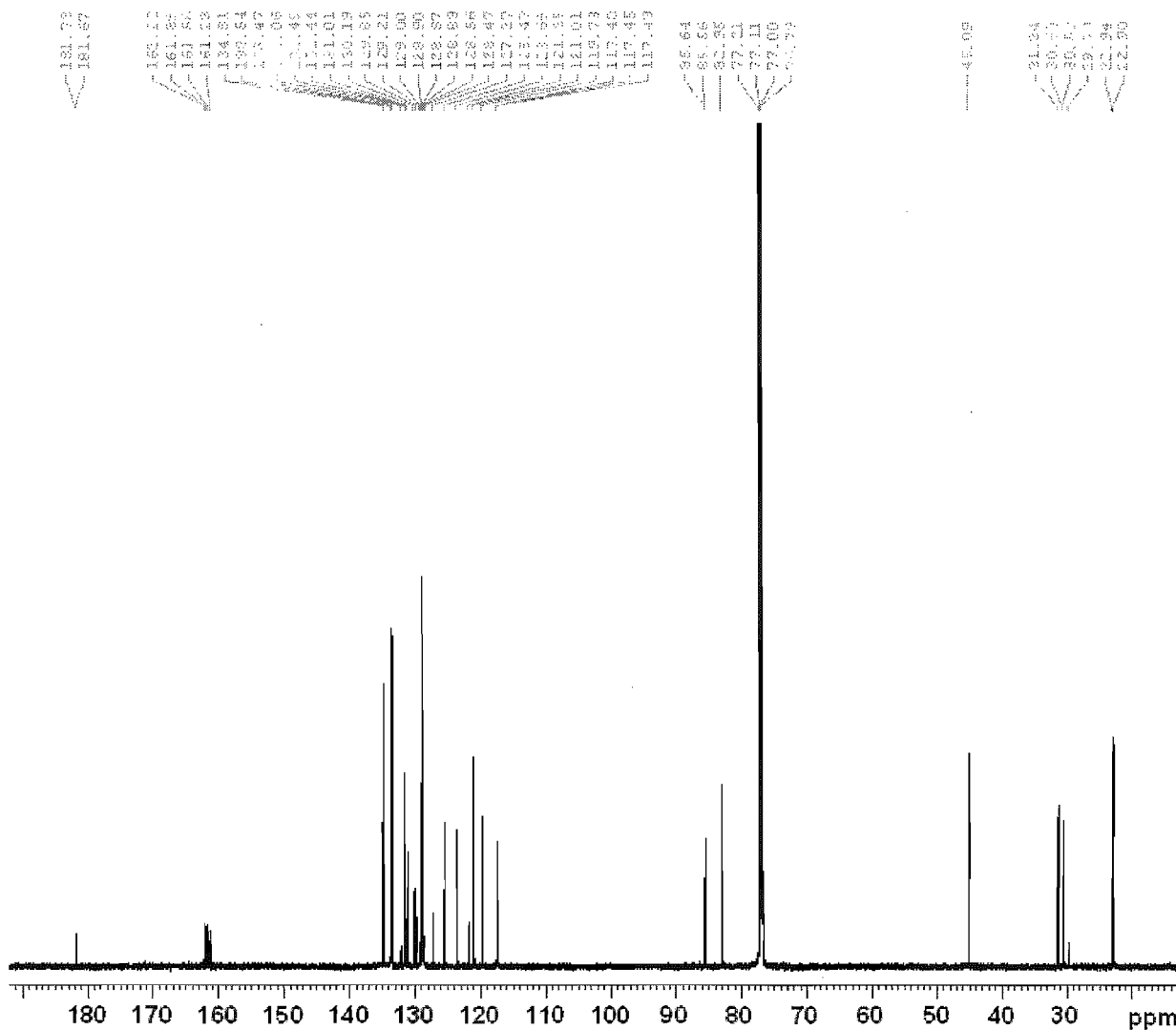
```

===== CHANNEL f2 =====
CPDPRG2   waltz16
NUC2      1H
PCPD2     70.00 usec
PL2       -4.00 dB
PL12     12.07 dB
PL13     15.00 dB
SF02     600.2024008 MHz
SI        32768
SF       150.9204100 MHz
WDW       EM
SSB       0
LB        1.00 Hz
GB        0
PC        1.40
  
```

Figure 52.  $^{13}\text{C}$  NMR spectrum of 91.



1d carbon with proton decoupling



```

NAME      xd3-165a
EXPNO     2
PROCNO    1
Date_     20081001
Time      14.52
INSTRUM   spect
PROBHD    5 mm PABBO BB-
PULPROG   zgpg30
TD         32768
SOLVENT   CDC13
NS         16384
DS         0
SWH        35971.223 Hz
FIDRES     1.097755 Hz
AQ         0.4555391 sec
RG         23170.5
DW         13.900 usec
DE         6.00 usec
TE         299.9 K
D1         2.00000000 sec
D11        0.03000000 sec
TD0        16
  
```

```

===== CHANNEL f1 =====
NUC1       13C
P1         8.00 usec
PL1        -1.00 dB
PL1W       92.33850861 W
SF01       150.9355021 MHz
  
```

```

===== CHANNEL f2 =====
CPDPRG2    waltz16
NUC2        1H
PCPD2       70.00 usec
PL2         -4.00 dB
PL12        12.07 dB
PL13        15.00 dB
PL2W        31.54786682 W
PL12W       0.77977633 W
PL13W       0.39716411 W
SF02       600.2024008 MHz
SI          32768
SF         150.9204100 MHz
WDW         EM
SSB         0
LB          1.00 Hz
GB          0
PC          1.40
  
```

Figure 54.  $^{13}\text{C}$  NMR spectrum of 92.

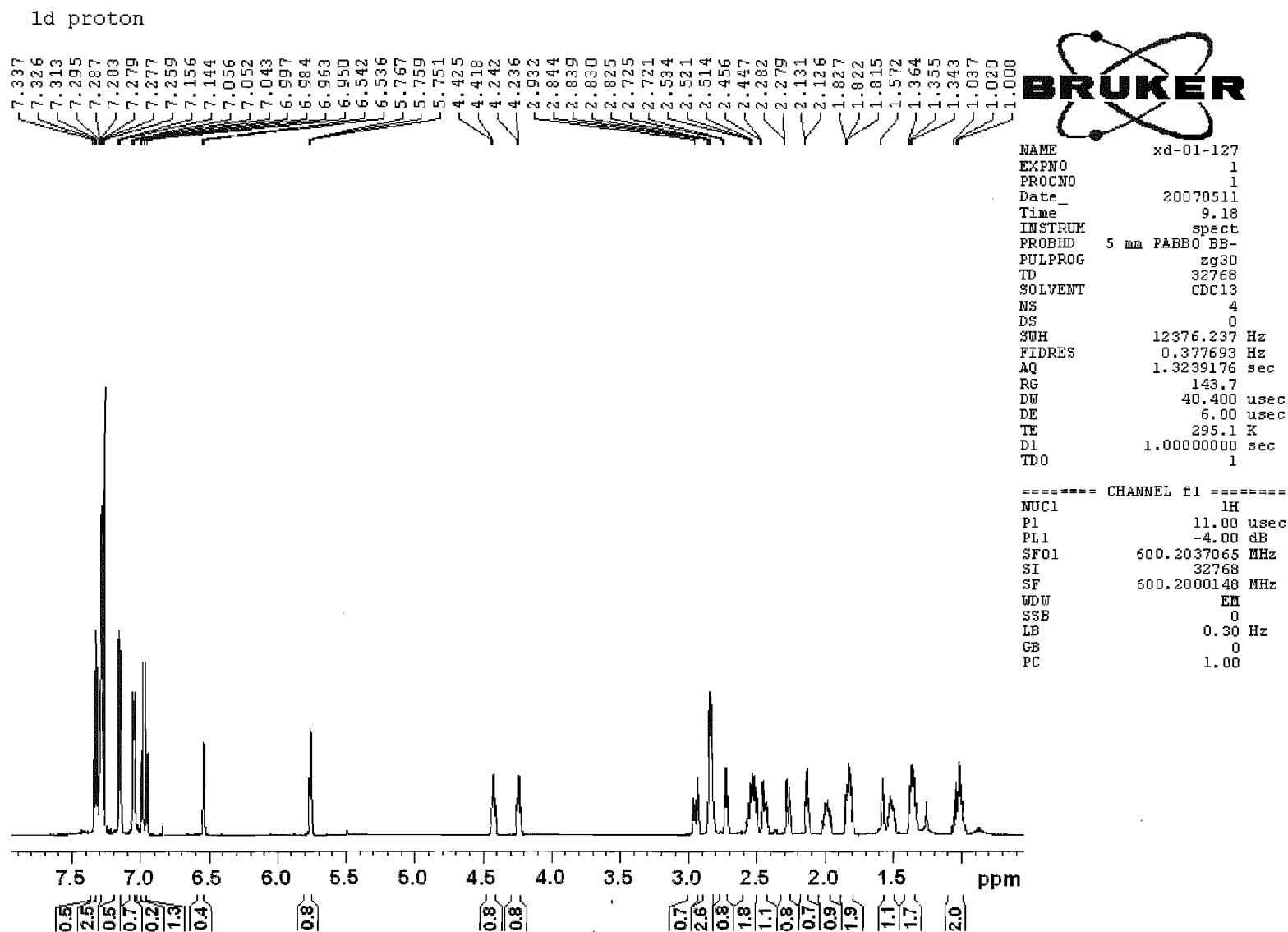




Figure 57.  $^1\text{H}$  NMR spectrum of (S,S)-94a.

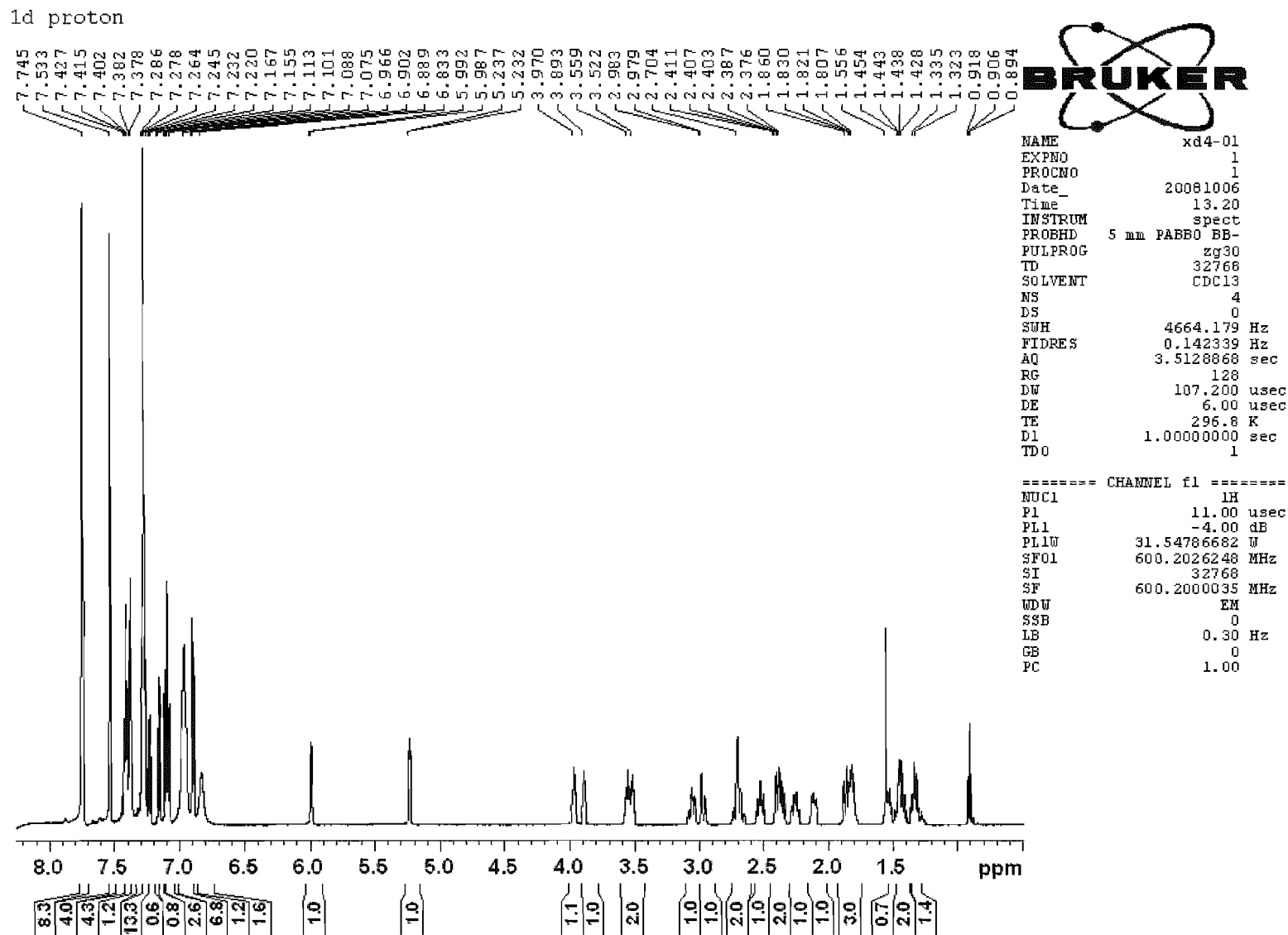
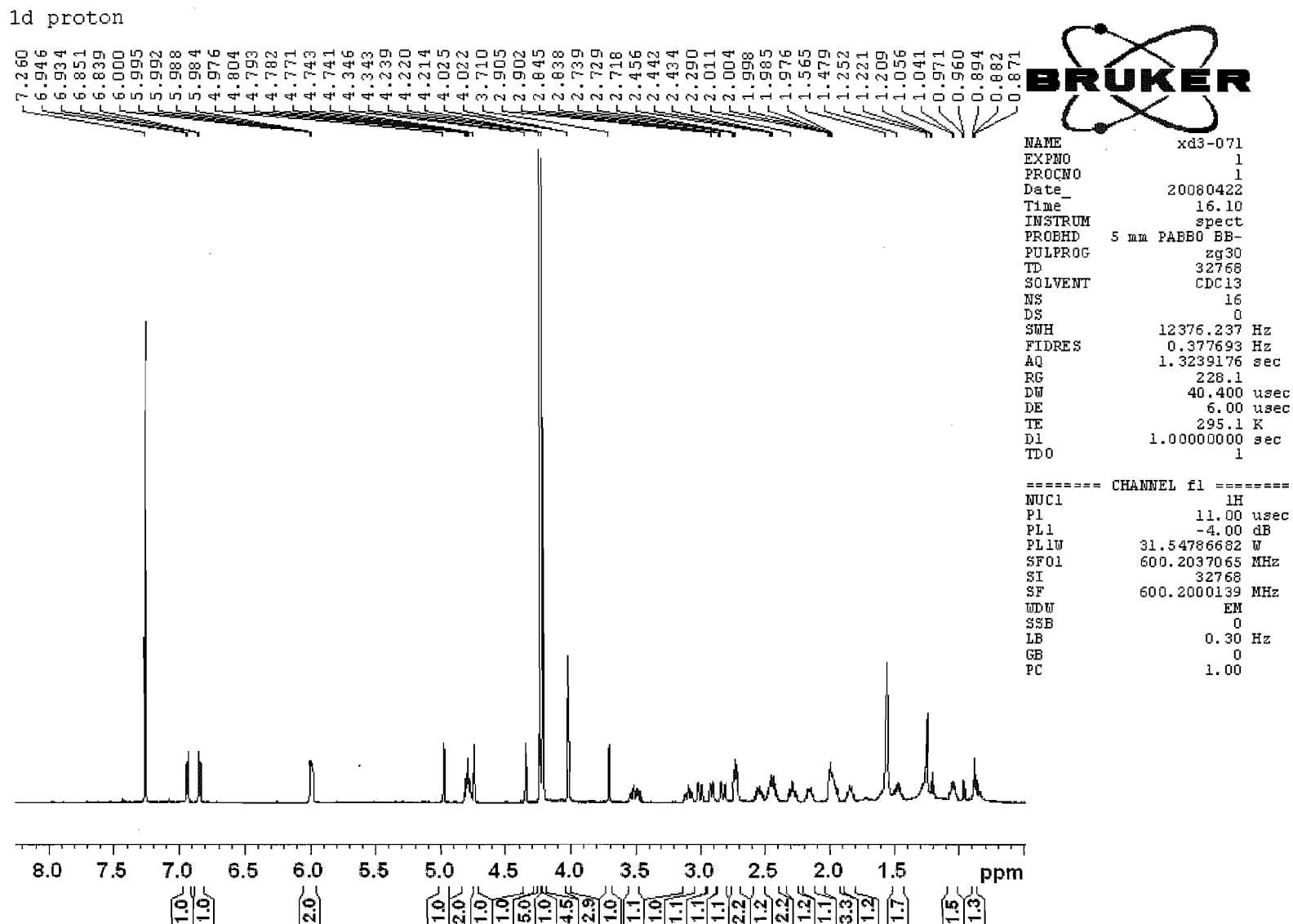


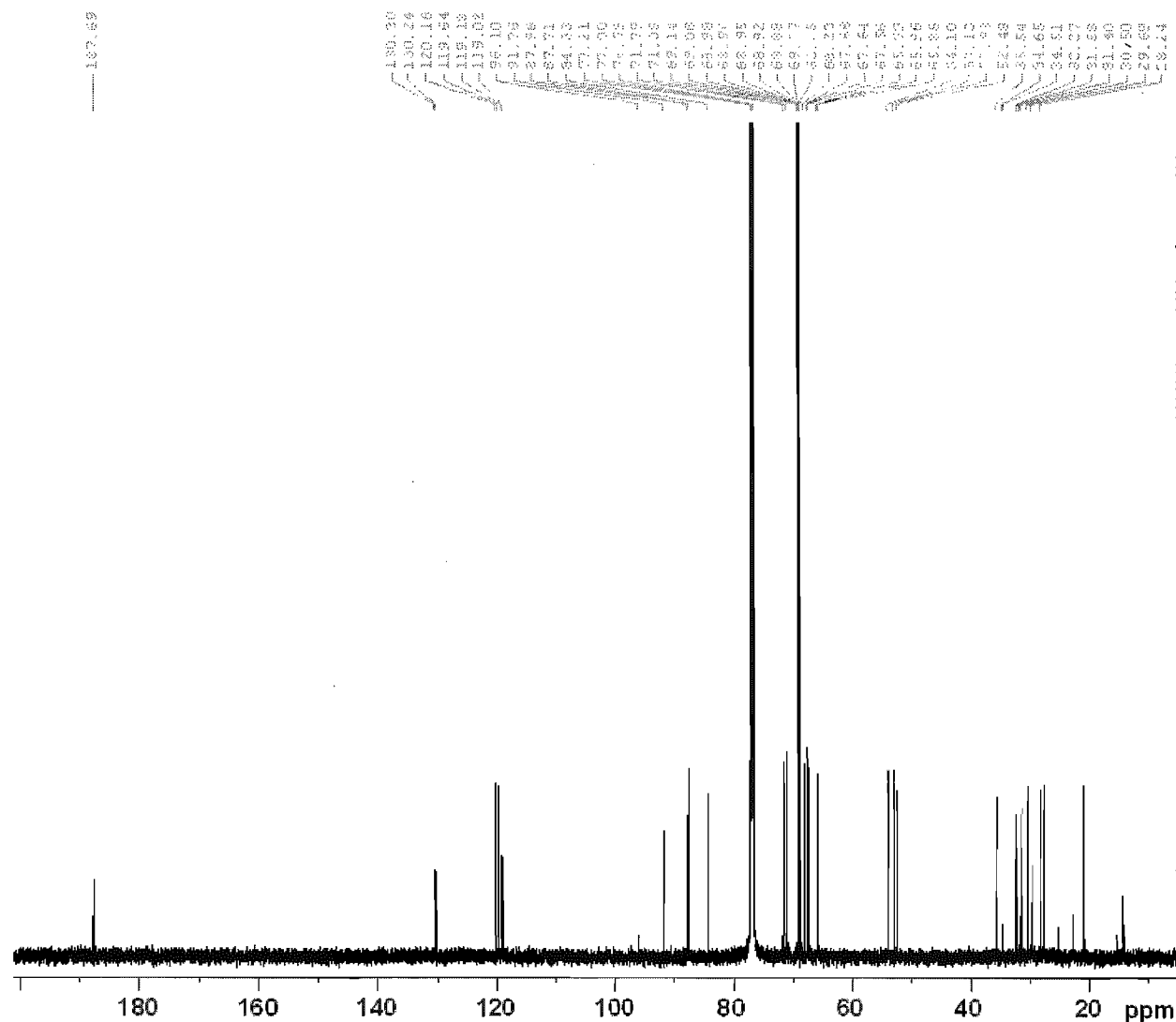


Figure 59.  $^1\text{H}$  NMR spectrum of (S,S)-93f.





1d carbon with proton decoupling



NAME xd3-071  
EXPNO 2  
PROCNO 1  
Date\_ 20080422  
Time 16.17  
INSTRUM spect  
PROBHD 5 mm PABBO BB-  
PULPROG zgpg30  
TD 32768  
SOLVENT CDCl3  
NS 10240  
DS 0  
SWH 35971.223 Hz  
FIDRES 1.097755 Hz  
AQ 0.4555391 sec  
RG 23170.5  
DW 13.900 usec  
DE 6.00 usec  
TE 295.4 K  
D1 2.00000000 sec  
D11 0.03000000 sec  
TD0 10

==== CHANNEL f1 =====  
NUC1 13C  
P1 8.00 usec  
PL1 -1.00 dB  
PL1W 92.33850861 W  
SF01 150.9355021 MHz

==== CHANNEL f2 =====  
CPDPRG2 waltz16  
NUC2 1H  
PCPD2 70.00 usec  
PL2 -4.00 dB  
PL12 12.07 dB  
PL13 15.00 dB  
PL2W 31.54786682 W  
PL12W 0.77977633 W  
PL13W 0.39716411 W  
SF02 600.2024008 MHz  
SI 32768  
SF 150.9204151 MHz  
WDW EM  
SSB 0  
LB 1.00 Hz  
GB 0  
PC 1.40

Figure 60.  $^{13}\text{C}$  NMR spectrum of (S,S)-93f.

## 7. Appendix 2 X - Ray Data for (R, R) - 93a

Table 1. Crystal data and structure refinement for costal

Identification code	costal	
Empirical formula	C33 H34 Cl Ir N2	
Formula weight	686.27	
Temperature	173(2) K	
Wavelength	0.71073 Å	
Crystal system	Orthorhombic	
Space group	P2(1)2(1)2(1)	
Unit cell dimensions	a = 11.5881(3) Å	$\alpha = 90^\circ$ .
	b = 14.3883(4) Å	$\beta = 90^\circ$ .
	c = 16.9461(4) Å	$\gamma = 90^\circ$ .
Volume	2825.48(13) Å <sup>3</sup>	
Z	4	
Density (calculated)	1.613 Mg/m <sup>3</sup>	
Absorption coefficient	4.844 mm <sup>-1</sup>	
F(000)	1360	
Crystal size	0.22 x 0.12 x 0.08 mm <sup>3</sup>	
$\theta$ range for data collection	1.86 to 31.31°.	
Index ranges	-16 ≤ h ≤ 15, -20 ≤ k ≤ 21, -20 ≤ l ≤ 24	
Reflections collected	70000	
Independent reflections	9205 [R(int) = 0.0581]	
Completeness to $\theta = 31.31^\circ$	99.7 %	
Absorption correction	Numerical	
Max. and min. transmission	1.000 and 0.884	
Refinement method	Full-matrix least-squares on F <sup>2</sup>	
Data / restraints / parameters	9205 / 240 / 334	
Goodness-of-fit on F <sup>2</sup>	1.030	
Final R indices [I > 2σ(I)]	R1 = 0.0227, wR2 = 0.0488	
R indices (all data)	R1 = 0.0262, wR2 = 0.0502	
Absolute structure parameter	0.000(5)	
Largest diff. peak and hole	0.885 and -0.653 e.Å <sup>-3</sup>	

Table 2. Atomic coordinates ( $\times 10^4$ ) and equivalent isotropic displacement parameters ( $\text{\AA}^2 \times 10^3$ ) for costal. U(eq) is defined as one third of the trace of the orthogonalized  $U_{ij}$  tensor.

	x	y	z	U(eq)
Ir(1)	8082(1)	7689(1)	7606(1)	22(1)
C(1)	3404(3)	9267(2)	8019(2)	34(1)
Cl(1)	7570(1)	6221(1)	8109(1)	35(1)
C(2)	4247(3)	9309(2)	7314(2)	33(1)
N(3A)	5794(2)	8587(2)	8081(1)	23(1)
C(3)	5184(2)	8536(2)	7313(2)	25(1)
N(4A)	6890(2)	8371(2)	9100(1)	22(1)
C(4)	6859(2)	8261(2)	8295(1)	21(1)
C(5)	7798(2)	8128(2)	9674(2)	24(1)
C(6)	7187(3)	7881(2)	10463(2)	31(1)
C(7)	6369(3)	8647(3)	10772(2)	35(1)
C(7A)	5525(3)	8920(2)	10143(2)	29(1)
C(8)	4407(3)	9265(2)	10214(2)	36(1)
C(9B)	5178(2)	8886(2)	8733(2)	25(1)
C(9C)	5872(2)	8749(2)	9377(2)	25(1)
C(9A)	4056(3)	9223(2)	8783(2)	29(1)
C(9)	3706(3)	9426(2)	9551(2)	36(1)
C(10)	4643(2)	7586(2)	7188(2)	27(1)
C(11)	4327(3)	7013(2)	7804(2)	32(1)
C(12)	3706(3)	6205(2)	7678(2)	34(1)
C(13)	3391(4)	5956(3)	6927(2)	50(1)
C(14)	3729(5)	6510(3)	6310(3)	83(2)
C(15)	4338(4)	7317(3)	6434(2)	65(1)
C(16)	8663(2)	8907(2)	9787(2)	24(1)
C(17)	8430(3)	9830(2)	9609(2)	32(1)
C(18)	9237(3)	10519(3)	9745(2)	41(1)
C(19)	10299(3)	10286(3)	10085(2)	38(1)
C(20)	10529(3)	9377(3)	10286(2)	37(1)
C(21)	9725(3)	8688(2)	10127(2)	29(1)
C(22)	9715(3)	7141(2)	7124(2)	38(1)
C(23)	8840(3)	7041(2)	6565(2)	36(1)

C(24)	8657(4)	7665(3)	5863(2)	48(1)
C(25)	8674(4)	8698(3)	6062(2)	45(1)
C(26)	8280(3)	8893(2)	6905(2)	31(1)
C(27)	9032(2)	8927(2)	7555(2)	33(1)
C(28)	10324(3)	8746(3)	7536(3)	50(1)
C(29)	10635(3)	7871(3)	7079(3)	51(1)

---

Table 3. Bond lengths [Å] and angles [°] for costal

Ir(1)-C(4)	2.012(3)	C(9B)-C(9C)	1.369(4)
Ir(1)-C(27)	2.097(3)	C(9B)-C(9A)	1.390(4)
Ir(1)-C(26)	2.113(3)	C(9A)-C(9)	1.395(4)
Ir(1)-C(23)	2.181(3)	C(9)-H(9A)	0.9500
Ir(1)-C(22)	2.207(3)	C(10)-C(11)	1.379(4)
Ir(1)-Cl(1)	2.3529(8)	C(10)-C(15)	1.381(4)
C(1)-C(9A)	1.500(4)	C(11)-C(12)	1.384(4)
C(1)-C(2)	1.545(4)	C(11)-H(11A)	0.9500
C(1)-H(1A)	0.9900	C(12)-C(13)	1.370(5)
C(1)-H(1B)	0.9900	C(12)-H(12A)	0.9500
C(2)-C(3)	1.553(4)	C(13)-C(14)	1.373(6)
C(2)-H(2A)	0.9900	C(13)-H(13A)	0.9500
C(2)-H(2B)	0.9900	C(14)-C(15)	1.375(6)
N(3A)-C(4)	1.369(4)	C(14)-H(14A)	0.9500
N(3A)-C(9B)	1.384(4)	C(15)-H(15A)	0.9500
N(3A)-C(3)	1.483(3)	C(16)-C(17)	1.389(4)
C(3)-C(10)	1.518(4)	C(16)-C(21)	1.395(4)
C(3)-H(3A)	1.0000	C(17)-C(18)	1.382(5)
N(4A)-C(4)	1.374(3)	C(17)-H(17A)	0.9500
N(4A)-C(9C)	1.381(4)	C(18)-C(19)	1.399(5)
N(4A)-C(5)	1.476(3)	C(18)-H(18A)	0.9500
C(5)-C(16)	1.516(4)	C(19)-C(20)	1.378(5)
C(5)-C(6)	1.555(4)	C(19)-H(19A)	0.9500
C(5)-H(5A)	1.0000	C(20)-C(21)	1.387(5)
C(6)-C(7)	1.545(5)	C(20)-H(20A)	0.9500
C(6)-H(6A)	0.9900	C(21)-H(21A)	0.9500
C(6)-H(6B)	0.9900	C(22)-C(23)	1.395(5)
C(7)-C(7A)	1.499(4)	C(22)-C(29)	1.498(5)
C(7)-H(7A)	0.9900	C(22)-H(22A)	1.0000
C(7)-H(7B)	0.9900	C(23)-C(24)	1.505(5)
C(7A)-C(9C)	1.381(4)	C(23)-H(23A)	1.0000
C(7A)-C(8)	1.393(5)	C(24)-C(25)	1.525(6)
C(8)-C(9)	1.406(5)	C(24)-H(24A)	0.9900
C(8)-H(8A)	0.9500	C(24)-H(24B)	0.9900

C(25)-C(26)	1.526(4)	C(3)-C(2)-H(2A)	108.6
C(25)-H(25A)	0.9900	C(1)-C(2)-H(2B)	108.6
C(25)-H(25B)	0.9900	C(3)-C(2)-H(2B)	108.6
C(26)-C(27)	1.405(4)	H(2A)-C(2)-H(2B)	107.6
C(26)-H(26A)	1.0000	C(4)-N(3A)-C(9B)	111.1(2)
C(27)-C(28)	1.520(4)	C(4)-N(3A)-C(3)	130.2(2)
C(27)-H(27A)	1.0000	C(9B)-N(3A)-C(3)	118.0(2)
C(28)-C(29)	1.521(5)	N(3A)-C(3)-C(10)	111.3(2)
C(28)-H(28A)	0.9900	N(3A)-C(3)-C(2)	107.3(2)
C(28)-H(28B)	0.9900	C(10)-C(3)-C(2)	110.9(2)
C(29)-H(29A)	0.9900	N(3A)-C(3)-H(3A)	109.1
C(29)-H(29B)	0.9900	C(10)-C(3)-H(3A)	109.1
		C(2)-C(3)-H(3A)	109.1
C(4)-Ir(1)-C(27)	92.63(11)	C(4)-N(4A)-C(9C)	111.1(2)
C(4)-Ir(1)-C(26)	93.84(11)	C(4)-N(4A)-C(5)	130.2(2)
C(27)-Ir(1)-C(26)	38.98(12)	C(9C)-N(4A)-C(5)	118.6(2)
C(4)-Ir(1)-C(23)	158.14(12)	N(3A)-C(4)-N(4A)	104.3(2)
C(27)-Ir(1)-C(23)	96.80(13)	N(3A)-C(4)-Ir(1)	128.46(18)
C(26)-Ir(1)-C(23)	81.48(12)	N(4A)-C(4)-Ir(1)	127.2(2)
C(4)-Ir(1)-C(22)	164.78(12)	N(4A)-C(5)-C(16)	112.3(2)
C(27)-Ir(1)-C(22)	80.67(12)	N(4A)-C(5)-C(6)	107.2(2)
C(26)-Ir(1)-C(22)	89.50(12)	C(16)-C(5)-C(6)	111.2(2)
C(23)-Ir(1)-C(22)	37.08(13)	N(4A)-C(5)-H(5A)	108.7
C(4)-Ir(1)-Cl(1)	88.82(7)	C(16)-C(5)-H(5A)	108.7
C(27)-Ir(1)-Cl(1)	155.53(9)	C(6)-C(5)-H(5A)	108.7
C(26)-Ir(1)-Cl(1)	165.20(9)	C(7)-C(6)-C(5)	114.1(2)
C(23)-Ir(1)-Cl(1)	90.65(9)	C(7)-C(6)-H(6A)	108.7
C(22)-Ir(1)-Cl(1)	91.73(9)	C(5)-C(6)-H(6A)	108.7
C(9A)-C(1)-C(2)	110.5(2)	C(7)-C(6)-H(6B)	108.7
C(9A)-C(1)-H(1A)	109.5	C(5)-C(6)-H(6B)	108.7
C(2)-C(1)-H(1A)	109.5	H(6A)-C(6)-H(6B)	107.6
C(9A)-C(1)-H(1B)	109.5	C(7A)-C(7)-C(6)	110.3(2)
C(2)-C(1)-H(1B)	109.5	C(7A)-C(7)-H(7A)	109.6
H(1A)-C(1)-H(1B)	108.1	C(6)-C(7)-H(7A)	109.6
C(1)-C(2)-C(3)	114.5(2)	C(7A)-C(7)-H(7B)	109.6
C(1)-C(2)-H(2A)	108.6	C(6)-C(7)-H(7B)	109.6

H(7A)-C(7)-H(7B)	108.1	C(10)-C(15)-H(15A)	119.7
C(9C)-C(7A)-C(8)	114.5(3)	C(17)-C(16)-C(21)	118.5(3)
C(9C)-C(7A)-C(7)	115.6(3)	C(17)-C(16)-C(5)	123.5(3)
C(8)-C(7A)-C(7)	129.7(3)	C(21)-C(16)-C(5)	117.9(3)
C(7A)-C(8)-C(9)	121.8(3)	C(18)-C(17)-C(16)	121.2(3)
C(7A)-C(8)-H(8A)	119.1	C(18)-C(17)-H(17A)	119.4
C(9)-C(8)-H(8A)	119.1	C(16)-C(17)-H(17A)	119.4
C(9C)-C(9B)-N(3A)	106.8(2)	C(17)-C(18)-C(19)	119.5(3)
C(9C)-C(9B)-C(9A)	123.4(3)	C(17)-C(18)-H(18A)	120.2
N(3A)-C(9B)-C(9A)	129.7(3)	C(19)-C(18)-H(18A)	120.2
C(9B)-C(9C)-N(4A)	106.7(2)	C(20)-C(19)-C(18)	119.9(3)
C(9B)-C(9C)-C(7A)	123.5(3)	C(20)-C(19)-H(19A)	120.0
N(4A)-C(9C)-C(7A)	129.6(3)	C(18)-C(19)-H(19A)	120.0
C(9B)-C(9A)-C(9)	113.7(3)	C(19)-C(20)-C(21)	120.1(3)
C(9B)-C(9A)-C(1)	115.7(3)	C(19)-C(20)-H(20A)	120.0
C(9)-C(9A)-C(1)	130.5(3)	C(21)-C(20)-H(20A)	120.0
C(9A)-C(9)-C(8)	122.9(3)	C(20)-C(21)-C(16)	120.8(3)
C(9A)-C(9)-H(9A)	118.5	C(20)-C(21)-H(21A)	119.6
C(8)-C(9)-H(9A)	118.5	C(16)-C(21)-H(21A)	119.6
C(11)-C(10)-C(15)	117.6(3)	C(23)-C(22)-C(29)	123.7(3)
C(11)-C(10)-C(3)	122.8(2)	C(23)-C(22)-Ir(1)	70.44(18)
C(15)-C(10)-C(3)	119.2(3)	C(29)-C(22)-Ir(1)	112.2(2)
C(10)-C(11)-C(12)	121.6(3)	C(23)-C(22)-H(22A)	114.2
C(10)-C(11)-H(11A)	119.2	C(29)-C(22)-H(22A)	114.2
C(12)-C(11)-H(11A)	119.2	Ir(1)-C(22)-H(22A)	114.2
C(13)-C(12)-C(11)	120.1(3)	C(22)-C(23)-C(24)	125.3(3)
C(13)-C(12)-H(12A)	120.0	C(22)-C(23)-Ir(1)	72.49(17)
C(11)-C(12)-H(12A)	120.0	C(24)-C(23)-Ir(1)	109.1(2)
C(12)-C(13)-C(14)	118.7(3)	C(22)-C(23)-H(23A)	114.1
C(12)-C(13)-H(13A)	120.7	C(24)-C(23)-H(23A)	114.1
C(14)-C(13)-H(13A)	120.7	Ir(1)-C(23)-H(23A)	114.1
C(13)-C(14)-C(15)	121.3(4)	C(23)-C(24)-C(25)	114.0(3)
C(13)-C(14)-H(14A)	119.3	C(23)-C(24)-H(24A)	108.8
C(15)-C(14)-H(14A)	119.3	C(25)-C(24)-H(24A)	108.8
C(14)-C(15)-C(10)	120.7(4)	C(23)-C(24)-H(24B)	108.8
C(14)-C(15)-H(15A)	119.7	C(25)-C(24)-H(24B)	108.8

H(24A)-C(24)-H(24B)	107.7	C(26)-C(27)-H(27A)	113.4
C(24)-C(25)-C(26)	112.4(3)	C(28)-C(27)-H(27A)	113.4
C(24)-C(25)-H(25A)	109.1	Ir(1)-C(27)-H(27A)	113.4
C(26)-C(25)-H(25A)	109.1	C(27)-C(28)-C(29)	112.7(3)
C(24)-C(25)-H(25B)	109.1	C(27)-C(28)-H(28A)	109.0
C(26)-C(25)-H(25B)	109.1	C(29)-C(28)-H(28A)	109.0
H(25A)-C(25)-H(25B)	107.9	C(27)-C(28)-H(28B)	109.0
C(27)-C(26)-C(25)	123.7(3)	C(29)-C(28)-H(28B)	109.0
C(27)-C(26)-Ir(1)	69.88(17)	H(28A)-C(28)-H(28B)	107.8
C(25)-C(26)-Ir(1)	114.1(2)	C(22)-C(29)-C(28)	112.7(3)
C(27)-C(26)-H(26A)	113.9	C(22)-C(29)-H(29A)	109.0
C(25)-C(26)-H(26A)	113.9	C(28)-C(29)-H(29A)	109.0
Ir(1)-C(26)-H(26A)	113.9	C(22)-C(29)-H(29B)	109.0
C(26)-C(27)-C(28)	126.0(3)	C(28)-C(29)-H(29B)	109.0
C(26)-C(27)-Ir(1)	71.14(17)	H(29A)-C(29)-H(29B)	107.8
C(28)-C(27)-Ir(1)	111.9(2)		

---

Symmetry transformations used to generate equivalent atoms:



Table 4. Anisotropic displacement parameters ( $\text{\AA}^2 \times 10^3$ ) for *costa1*. The anisotropic displacement factor exponent takes the form:  $-2\pi^2 [h^2 a^{*2} U^{11} + \dots + 2 h k a^* b^* U^{12}]$

	$U^{11}$	$U^{22}$	$U^{33}$	$U^{23}$	$U^{13}$	$U^{12}$
Ir(1)	23(1)	23(1)	20(1)	-2(1)	0(1)	0(1)
C(1)	23(1)	29(2)	51(2)	0(1)	-3(1)	1(1)
Cl(1)	45(1)	26(1)	33(1)	1(1)	-1(1)	-5(1)
C(2)	28(1)	30(1)	40(2)	6(1)	-8(1)	-2(1)
N(3A)	21(1)	26(1)	21(1)	-2(1)	-1(1)	-1(1)
C(3)	25(1)	31(1)	21(1)	2(1)	-6(1)	-3(1)
N(4A)	22(1)	25(1)	21(1)	-3(1)	-2(1)	0(1)
C(4)	21(1)	22(1)	21(1)	0(1)	1(1)	-4(1)
C(5)	26(1)	22(1)	24(1)	-1(1)	-5(1)	3(1)
C(6)	38(2)	33(2)	23(1)	5(1)	-3(1)	-7(1)
C(7)	43(2)	41(2)	21(1)	-1(1)	1(1)	-6(2)
C(7A)	35(2)	27(2)	24(1)	-4(1)	7(1)	-6(1)
C(8)	37(2)	35(2)	37(2)	-8(1)	14(1)	-3(1)
C(9B)	22(1)	24(1)	28(1)	-1(1)	2(1)	-2(1)
C(9C)	24(1)	24(1)	26(1)	0(1)	2(1)	-1(1)
C(9A)	24(1)	24(1)	39(2)	0(1)	2(1)	-3(1)
C(9)	24(2)	33(2)	51(2)	-5(1)	12(1)	-2(1)
C(10)	27(1)	29(2)	25(1)	0(1)	-7(1)	-2(1)
C(11)	41(2)	28(1)	26(1)	-6(1)	2(1)	-5(1)
C(12)	37(2)	28(2)	37(2)	2(1)	10(1)	-4(1)
C(13)	67(3)	32(2)	51(2)	1(2)	-25(2)	-15(2)
C(14)	157(5)	55(3)	39(2)	8(2)	-40(3)	-47(3)
C(15)	122(4)	45(2)	27(2)	8(2)	-25(2)	-36(3)
C(16)	25(1)	28(2)	19(1)	-1(1)	-2(1)	1(1)
C(17)	30(2)	29(2)	38(2)	2(1)	-11(1)	2(1)
C(18)	44(2)	28(2)	52(2)	1(2)	-6(2)	-4(2)
C(19)	37(2)	36(2)	40(2)	-5(1)	-2(1)	-8(1)
C(20)	28(2)	51(2)	32(2)	3(2)	-4(1)	-3(2)
C(21)	27(1)	31(2)	28(1)	5(1)	-4(1)	1(1)
C(22)	38(2)	35(2)	40(2)	3(1)	11(1)	14(1)
C(23)	53(2)	31(2)	25(1)	-3(1)	8(1)	10(1)

C(24)	76(2)	41(2)	26(1)	-1(2)	11(1)	10(2)
C(25)	62(2)	39(2)	33(2)	8(2)	13(2)	7(2)
C(26)	35(2)	25(1)	32(1)	3(1)	8(1)	0(1)
C(27)	30(1)	27(1)	43(2)	-5(1)	7(1)	-5(1)
C(28)	27(2)	52(2)	71(3)	-1(2)	5(2)	-8(1)
C(29)	30(2)	52(3)	71(2)	2(2)	11(2)	7(2)

---

Table 5. Hydrogen coordinates ( $\times 10^4$ ) and isotropic displacement parameters ( $\text{\AA}^2 \times 10^3$ ) for costal

	x	y	z	U(eq)
H(1A)	2903	9824	8015	41
H(1B)	2904	8712	7969	41
H(2A)	4636	9921	7316	39
H(2B)	3797	9263	6819	39
H(3A)	5746	8661	6878	30
H(5A)	8217	7565	9479	29
H(6A)	6738	7302	10388	37
H(6B)	7782	7757	10869	37
H(7A)	5946	8415	11240	42
H(7B)	6825	9196	10933	42
H(8A)	4110	9396	10725	43
H(9A)	2960	9685	9630	43
H(11A)	4540	7177	8327	38
H(12A)	3498	5822	8112	40
H(13A)	2948	5411	6837	60
H(14A)	3539	6332	5786	100
H(15A)	4551	7693	5997	78
H(17A)	7703	9992	9390	39
H(18A)	9073	11146	9610	49
H(19A)	10861	10755	10177	45
H(20A)	11240	9221	10532	44
H(21A)	9899	8060	10252	34
H(22A)	9974	6544	7368	45
H(23A)	8592	6383	6478	43
H(24A)	7905	7511	5619	57
H(24B)	9266	7536	5468	57
H(25A)	8164	9034	5690	54
H(25B)	9468	8940	5991	54
H(26A)	7618	9336	6942	37
H(27A)	8797	9392	7963	40

H(28A)	10612	8687	8083	60
H(28B)	10715	9285	7290	60
H(29A)	10767	8035	6519	61
H(29B)	11364	7614	7292	61

---

Table 6. Torsion angles [°] for costal

C(9A)-C(1)-C(2)-C(3)	51.8(3)
C(4)-N(3A)-C(3)-C(10)	79.1(3)
C(9B)-N(3A)-C(3)-C(10)	-90.5(3)
C(4)-N(3A)-C(3)-C(2)	-159.4(3)
C(9B)-N(3A)-C(3)-C(2)	30.9(3)
C(1)-C(2)-C(3)-N(3A)	-55.0(3)
C(1)-C(2)-C(3)-C(10)	66.8(3)
C(9B)-N(3A)-C(4)-N(4A)	-0.4(3)
C(3)-N(3A)-C(4)-N(4A)	-170.5(3)
C(9B)-N(3A)-C(4)-Ir(1)	176.9(2)
C(3)-N(3A)-C(4)-Ir(1)	6.7(4)
C(9C)-N(4A)-C(4)-N(3A)	0.3(3)
C(5)-N(4A)-C(4)-N(3A)	178.4(3)
C(9C)-N(4A)-C(4)-Ir(1)	-176.95(19)
C(5)-N(4A)-C(4)-Ir(1)	1.1(4)
C(27)-Ir(1)-C(4)-N(3A)	100.5(2)
C(26)-Ir(1)-C(4)-N(3A)	61.5(2)
C(23)-Ir(1)-C(4)-N(3A)	-15.2(5)
C(22)-Ir(1)-C(4)-N(3A)	163.8(4)
Cl(1)-Ir(1)-C(4)-N(3A)	-104.0(2)
C(27)-Ir(1)-C(4)-N(4A)	-82.9(2)
C(26)-Ir(1)-C(4)-N(4A)	-121.9(2)
C(23)-Ir(1)-C(4)-N(4A)	161.5(3)
C(22)-Ir(1)-C(4)-N(4A)	-19.6(6)
Cl(1)-Ir(1)-C(4)-N(4A)	72.7(2)
C(4)-N(4A)-C(5)-C(16)	88.6(3)
C(9C)-N(4A)-C(5)-C(16)	-93.4(3)
C(4)-N(4A)-C(5)-C(6)	-148.9(3)
C(9C)-N(4A)-C(5)-C(6)	29.0(3)
N(4A)-C(5)-C(6)-C(7)	-54.7(3)
C(16)-C(5)-C(6)-C(7)	68.5(3)
C(5)-C(6)-C(7)-C(7A)	53.0(3)
C(6)-C(7)-C(7A)-C(9C)	-23.9(4)
C(6)-C(7)-C(7A)-C(8)	151.4(3)

C(9C)-C(7A)-C(8)-C(9)	-0.3(5)
C(7)-C(7A)-C(8)-C(9)	-175.6(3)
C(4)-N(3A)-C(9B)-C(9C)	0.2(3)
C(3)-N(3A)-C(9B)-C(9C)	171.8(2)
C(4)-N(3A)-C(9B)-C(9A)	-176.7(3)
C(3)-N(3A)-C(9B)-C(9A)	-5.2(5)
N(3A)-C(9B)-C(9C)-N(4A)	0.0(3)
C(9A)-C(9B)-C(9C)-N(4A)	177.2(3)
N(3A)-C(9B)-C(9C)-C(7A)	-176.3(3)
C(9A)-C(9B)-C(9C)-C(7A)	0.9(5)
C(4)-N(4A)-C(9C)-C(9B)	-0.2(3)
C(5)-N(4A)-C(9C)-C(9B)	-178.5(2)
C(4)-N(4A)-C(9C)-C(7A)	175.8(3)
C(5)-N(4A)-C(9C)-C(7A)	-2.6(5)
C(8)-C(7A)-C(9C)-C(9B)	-1.3(5)
C(7)-C(7A)-C(9C)-C(9B)	174.7(3)
C(8)-C(7A)-C(9C)-N(4A)	-176.7(3)
C(7)-C(7A)-C(9C)-N(4A)	-0.7(5)
C(9C)-C(9B)-C(9A)-C(9)	1.1(4)
N(3A)-C(9B)-C(9A)-C(9)	177.7(3)
C(9C)-C(9B)-C(9A)-C(1)	-176.2(3)
N(3A)-C(9B)-C(9A)-C(1)	0.4(5)
C(2)-C(1)-C(9A)-C(9B)	-23.0(4)
C(2)-C(1)-C(9A)-C(9)	160.3(3)
C(9B)-C(9A)-C(9)-C(8)	-2.7(5)
C(1)-C(9A)-C(9)-C(8)	174.1(3)
C(7A)-C(8)-C(9)-C(9A)	2.4(5)
N(3A)-C(3)-C(10)-C(11)	25.8(4)
C(2)-C(3)-C(10)-C(11)	-93.5(3)
N(3A)-C(3)-C(10)-C(15)	-161.3(3)
C(2)-C(3)-C(10)-C(15)	79.3(4)
C(15)-C(10)-C(11)-C(12)	-1.2(5)
C(3)-C(10)-C(11)-C(12)	171.8(3)
C(10)-C(11)-C(12)-C(13)	0.0(5)
C(11)-C(12)-C(13)-C(14)	1.6(6)
C(12)-C(13)-C(14)-C(15)	-2.2(9)

C(13)-C(14)-C(15)-C(10)	1.0(9)
C(11)-C(10)-C(15)-C(14)	0.7(7)
C(3)-C(10)-C(15)-C(14)	-172.5(5)
N(4A)-C(5)-C(16)-C(17)	21.5(4)
C(6)-C(5)-C(16)-C(17)	-98.6(3)
N(4A)-C(5)-C(16)-C(21)	-162.1(2)
C(6)-C(5)-C(16)-C(21)	77.7(3)
C(21)-C(16)-C(17)-C(18)	1.7(5)
C(5)-C(16)-C(17)-C(18)	178.0(3)
C(16)-C(17)-C(18)-C(19)	-1.5(5)
C(17)-C(18)-C(19)-C(20)	-0.4(5)
C(18)-C(19)-C(20)-C(21)	2.1(5)
C(19)-C(20)-C(21)-C(16)	-1.9(5)
C(17)-C(16)-C(21)-C(20)	0.1(5)
C(5)-C(16)-C(21)-C(20)	-176.5(3)
C(4)-Ir(1)-C(22)-C(23)	-179.3(4)
C(27)-Ir(1)-C(22)-C(23)	-114.6(2)
C(26)-Ir(1)-C(22)-C(23)	-76.5(2)
Cl(1)-Ir(1)-C(22)-C(23)	88.78(19)
C(4)-Ir(1)-C(22)-C(29)	-59.9(6)
C(27)-Ir(1)-C(22)-C(29)	4.8(3)
C(26)-Ir(1)-C(22)-C(29)	43.0(3)
C(23)-Ir(1)-C(22)-C(29)	119.4(3)
Cl(1)-Ir(1)-C(22)-C(29)	-151.8(3)
C(29)-C(22)-C(23)-C(24)	-2.9(5)
Ir(1)-C(22)-C(23)-C(24)	101.4(3)
C(29)-C(22)-C(23)-Ir(1)	-104.2(3)
C(4)-Ir(1)-C(23)-C(22)	179.5(3)
C(27)-Ir(1)-C(23)-C(22)	64.6(2)
C(26)-Ir(1)-C(23)-C(22)	100.6(2)
Cl(1)-Ir(1)-C(23)-C(22)	-92.02(19)
C(4)-Ir(1)-C(23)-C(24)	57.4(5)
C(27)-Ir(1)-C(23)-C(24)	-57.5(3)
C(26)-Ir(1)-C(23)-C(24)	-21.5(3)
C(22)-Ir(1)-C(23)-C(24)	-122.1(4)
Cl(1)-Ir(1)-C(23)-C(24)	145.9(3)

C(22)-C(23)-C(24)-C(25)	-48.5(5)
Ir(1)-C(23)-C(24)-C(25)	33.2(4)
C(23)-C(24)-C(25)-C(26)	-28.5(5)
C(24)-C(25)-C(26)-C(27)	90.3(4)
C(24)-C(25)-C(26)-Ir(1)	9.2(4)
C(4)-Ir(1)-C(26)-C(27)	89.43(18)
C(23)-Ir(1)-C(26)-C(27)	-112.06(19)
C(22)-Ir(1)-C(26)-C(27)	-75.71(19)
Cl(1)-Ir(1)-C(26)-C(27)	-170.6(3)
C(4)-Ir(1)-C(26)-C(25)	-151.6(3)
C(27)-Ir(1)-C(26)-C(25)	118.9(3)
C(23)-Ir(1)-C(26)-C(25)	6.9(3)
C(22)-Ir(1)-C(26)-C(25)	43.2(3)
Cl(1)-Ir(1)-C(26)-C(25)	-51.7(5)
C(25)-C(26)-C(27)-C(28)	-2.4(5)
Ir(1)-C(26)-C(27)-C(28)	103.8(3)
C(25)-C(26)-C(27)-Ir(1)	-106.2(3)
C(4)-Ir(1)-C(27)-C(26)	-92.86(18)
C(23)-Ir(1)-C(27)-C(26)	67.38(19)
C(22)-Ir(1)-C(27)-C(26)	100.88(19)
Cl(1)-Ir(1)-C(27)-C(26)	174.21(16)
C(4)-Ir(1)-C(27)-C(28)	145.0(3)
C(26)-Ir(1)-C(27)-C(28)	-122.1(3)
C(23)-Ir(1)-C(27)-C(28)	-54.7(3)
C(22)-Ir(1)-C(27)-C(28)	-21.2(3)
Cl(1)-Ir(1)-C(27)-C(28)	52.1(4)
C(26)-C(27)-C(28)-C(29)	-47.1(5)
Ir(1)-C(27)-C(28)-C(29)	34.9(4)
C(23)-C(22)-C(29)-C(28)	93.3(4)
Ir(1)-C(22)-C(29)-C(28)	12.7(4)
C(27)-C(28)-C(29)-C(22)	-30.8(5)

---

Symmetry transformations used to generate equivalent atoms:



## 8. Appendix 3 X - Ray Date for (S, S) - 93f

Table 1. Crystal data and structure refinement for costa2\_0m.

Identification code	costa2_0m	
Empirical formula	C41 H42 Cl Fe2 Ir N2	
Formula weight	902.12	
Temperature	173(2) K	
Wavelength	0.71073 Å	
Crystal system	Monoclinic	
Space group	P2(1)	
Unit cell dimensions	a = 10.4823(10) Å	$\alpha = 90^\circ$ .
	b = 15.5160(15) Å	$\beta = 109.119(2)^\circ$ .
	c = 10.8442(10) Å	$\gamma = 90^\circ$ .
Volume	1666.4(3) Å <sup>3</sup>	
Z	2	
Density (calculated)	1.798 Mg/m <sup>3</sup>	
Absorption coefficient	4.956 mm <sup>-1</sup>	
F(000)	896	
Crystal size	0.45 x 0.35 x 0.33 mm <sup>3</sup>	
Theta range for data collection	1.99 to 45.32°.	
Index ranges	-11 < =h< =20, -30 < =k< =31, -20 < =l< =21	
Reflections collected	53155	
Independent reflections	24266 [R(int) = 0.0253]	
Completeness to theta = 45.32°	97.4 %	
Absorption correction	None	
Max. and min. transmission	0.2916 and 0.2139	
Refinement method	Full-matrix least-squares on F <sup>2</sup>	
Data / restraints / parameters	24266 / 1 / 424	
Goodness-of-fit on F <sup>2</sup>	1.056	
Final R indices [I > 2sigma(I)]	R1 = 0.0335, wR2 = 0.0775	
R indices (all data)	R1 = 0.0420, wR2 = 0.0814	
Absolute structure parameter	-0.012(3)	
Largest diff. peak and hole	3.617 and -1.229 e.Å <sup>-3</sup>	

Table 2. Atomic coordinates ( $\times 10^4$ ) and equivalent isotropic displacement parameters ( $\text{\AA}^2 \times 10^3$ ) for *costa2\_0m*.  $U(\text{eq})$  is defined as one third of the trace of the orthogonalized  $U^{ij}$  tensor.

	x	y	z	$U(\text{eq})$
Ir(1)	2005(1)	7302(1)	6277(1)	19(1)
Fe(1)	5266(1)	9794(1)	7050(1)	21(1)
Fe(2)	-1156(1)	6453(1)	1058(1)	23(1)
Cl(1)	1006(1)	8680(1)	6090(1)	38(1)
N(3A)	2253(2)	7932(1)	3715(2)	21(1)
N(4A)	4268(2)	7833(1)	5146(2)	20(1)
C(1)	1418(3)	8501(2)	975(3)	34(1)
C(2)	538(3)	8588(2)	1871(3)	30(1)
C(3)	796(2)	7903(2)	2955(2)	24(1)
C(4)	2924(2)	7693(1)	4982(2)	19(1)
C(5)	5495(2)	7749(1)	6297(2)	22(1)
C(6)	6700(2)	7571(2)	5795(3)	29(1)
C(7)	6891(3)	8210(2)	4789(3)	34(1)
C(7A)	5578(3)	8313(2)	3688(3)	27(1)
C(8)	5355(3)	8558(2)	2403(3)	34(1)
C(9A)	2879(3)	8444(2)	1804(2)	29(1)
C(9)	4042(3)	8622(2)	1481(3)	35(1)
C(9C)	4419(2)	8128(1)	3991(2)	22(1)
C(9B)	3137(2)	8186(1)	3081(2)	22(1)
C(10)	5723(2)	8500(1)	7237(2)	21(1)
C(11)	4859(3)	8725(2)	7969(2)	25(1)
C(12)	5515(3)	9364(2)	8900(2)	29(1)
C(13)	6793(3)	9544(2)	8760(3)	29(1)
C(14)	6928(2)	9009(2)	7740(2)	25(1)
C(15)	3647(3)	10112(2)	5451(4)	41(1)
C(16)	3690(3)	10642(2)	6532(4)	40(1)
C(17)	4933(3)	11094(2)	6921(3)	33(1)
C(18)	5666(3)	10840(2)	6077(3)	32(1)
C(19)	4869(4)	10236(2)	5173(3)	35(1)
C(20)	412(2)	6989(2)	2534(3)	26(1)
C(21)	913(2)	6456(2)	1728(4)	36(1)

C(22)	385(3)	5599(2)	1748(5)	51(1)
C(23)	-425(4)	5616(2)	2562(4)	45(1)
C(24)	-413(3)	6465(2)	3047(3)	37(1)
C(25)	-1862(5)	7008(5)	-737(4)	71(2)
C(26)	-2155(6)	6100(5)	-798(5)	78(2)
C(27)	-2934(4)	5932(3)	-38(7)	71(2)
C(28)	-3178(3)	6707(4)	494(5)	54(1)
C(29)	-2521(3)	7374(3)	69(4)	47(1)
C(30)	636(4)	6864(2)	7304(5)	50(1)
C(31)	1856(4)	7148(2)	8204(3)	43(1)
C(32)	3015(7)	6613(4)	9055(4)	68(2)
C(33)	3519(3)	5949(2)	8288(3)	40(1)
C(34)	3228(2)	6189(2)	6863(2)	24(1)
C(35)	1992(2)	5965(2)	5887(2)	24(1)
C(36)	869(3)	5480(2)	6176(3)	38(1)
C(37)	265(7)	5932(4)	7074(9)	101(3)

---

Table 3. Bond lengths [Å] and angles [°] for costa2\_0m.

---

Ir(1)-C(4)	2.037(2)
Ir(1)-C(35)	2.117(2)
Ir(1)-C(34)	2.121(2)
Ir(1)-C(31)	2.159(3)
Ir(1)-C(30)	2.193(3)
Ir(1)-Cl(1)	2.3588(7)
Fe(1)-C(16)	2.042(3)
Fe(1)-C(17)	2.044(3)
Fe(1)-C(12)	2.049(3)
Fe(1)-C(15)	2.050(3)
Fe(1)-C(11)	2.051(2)
Fe(1)-C(13)	2.051(3)
Fe(1)-C(18)	2.053(3)
Fe(1)-C(14)	2.055(2)
Fe(1)-C(19)	2.057(3)
Fe(1)-C(10)	2.059(2)
Fe(2)-C(26)	2.016(4)
Fe(2)-C(27)	2.022(3)
Fe(2)-C(23)	2.029(3)
Fe(2)-C(22)	2.033(3)
Fe(2)-C(25)	2.034(4)
Fe(2)-C(24)	2.039(3)
Fe(2)-C(28)	2.042(3)
Fe(2)-C(21)	2.049(2)
Fe(2)-C(20)	2.057(2)
Fe(2)-C(29)	2.058(3)
N(3A)-C(4)	1.374(3)
N(3A)-C(9B)	1.379(3)
N(3A)-C(3)	1.480(3)
N(4A)-C(4)	1.379(3)
N(4A)-C(9C)	1.390(3)
N(4A)-C(5)	1.476(3)
C(1)-C(9A)	1.503(4)
C(1)-C(2)	1.549(4)

C(1)-H(1A)	0.9900
C(1)-H(1B)	0.9900
C(2)-C(3)	1.541(3)
C(2)-H(2A)	0.9900
C(2)-H(2B)	0.9900
C(3)-C(20)	1.504(3)
C(3)-H(3A)	1.0000
C(5)-C(10)	1.514(3)
C(5)-C(6)	1.555(3)
C(5)-H(5A)	1.0000
C(6)-C(7)	1.535(4)
C(6)-H(6A)	0.9900
C(6)-H(6B)	0.9900
C(7)-C(7A)	1.506(4)
C(7)-H(7A)	0.9900
C(7)-H(7B)	0.9900
C(7A)-C(9C)	1.388(3)
C(7A)-C(8)	1.389(4)
C(8)-C(9)	1.415(5)
C(8)-H(8A)	0.9500
C(9A)-C(9B)	1.381(3)
C(9A)-C(9)	1.401(4)
C(9)-H(9A)	0.9500
C(9C)-C(9B)	1.386(3)
C(10)-C(11)	1.429(3)
C(10)-C(14)	1.438(3)
C(11)-C(12)	1.421(3)
C(11)-H(11A)	1.0000
C(12)-C(13)	1.425(4)
C(12)-H(12A)	1.0000
C(13)-C(14)	1.426(4)
C(13)-H(13A)	1.0000
C(14)-H(14A)	1.0000
C(15)-C(16)	1.419(6)
C(15)-C(19)	1.422(5)
C(15)-H(15A)	1.0000

C(16)-C(17)	1.416(5)
C(16)-H(16A)	1.0000
C(17)-C(18)	1.430(4)
C(17)-H(17A)	1.0000
C(18)-C(19)	1.414(4)
C(18)-H(18A)	1.0000
C(19)-H(19A)	1.0000
C(20)-C(21)	1.423(4)
C(20)-C(24)	1.426(4)
C(21)-C(22)	1.443(4)
C(21)-H(21A)	1.0000
C(22)-C(23)	1.410(7)
C(22)-H(22A)	1.0000
C(23)-C(24)	1.417(5)
C(23)-H(23A)	1.0000
C(24)-H(24A)	1.0000
C(25)-C(29)	1.400(7)
C(25)-C(26)	1.440(10)
C(25)-H(25A)	1.0000
C(26)-C(27)	1.362(10)
C(26)-H(26A)	1.0000
C(27)-C(28)	1.393(8)
C(27)-H(27A)	1.0000
C(28)-C(29)	1.402(6)
C(28)-H(28A)	1.0000
C(29)-H(29A)	1.0000
C(30)-C(31)	1.401(7)
C(30)-C(37)	1.498(6)
C(30)-H(30A)	1.0000
C(31)-C(32)	1.511(6)
C(31)-H(31A)	1.0000
C(32)-C(33)	1.523(7)
C(32)-H(32A)	0.9900
C(32)-H(32B)	0.9900
C(33)-C(34)	1.520(4)
C(33)-H(33A)	0.9900

C(33)-H(33B)	0.9900
C(34)-C(35)	1.421(3)
C(34)-H(34A)	1.0000
C(35)-C(36)	1.515(4)
C(35)-H(35A)	1.0000
C(36)-C(37)	1.497(7)
C(36)-H(36A)	0.9900
C(36)-H(36B)	0.9900
C(37)-H(37A)	0.9900
C(37)-H(37B)	0.9900
C(4)-Ir(1)-C(35)	97.31(9)
C(4)-Ir(1)-C(34)	94.19(9)
C(35)-Ir(1)-C(34)	39.20(9)
C(4)-Ir(1)-C(31)	154.19(13)
C(35)-Ir(1)-C(31)	94.98(12)
C(34)-Ir(1)-C(31)	81.24(12)
C(4)-Ir(1)-C(30)	167.91(16)
C(35)-Ir(1)-C(30)	80.51(12)
C(34)-Ir(1)-C(30)	91.54(13)
C(31)-Ir(1)-C(30)	37.55(18)
C(4)-Ir(1)-Cl(1)	88.17(6)
C(35)-Ir(1)-Cl(1)	153.79(7)
C(34)-Ir(1)-Cl(1)	166.25(7)
C(31)-Ir(1)-Cl(1)	90.75(9)
C(30)-Ir(1)-Cl(1)	88.79(11)
C(16)-Fe(1)-C(17)	40.56(14)
C(16)-Fe(1)-C(12)	108.15(13)
C(17)-Fe(1)-C(12)	110.65(11)
C(16)-Fe(1)-C(15)	40.60(17)
C(17)-Fe(1)-C(15)	68.20(14)
C(12)-Fe(1)-C(15)	135.33(14)
C(16)-Fe(1)-C(11)	112.13(12)
C(17)-Fe(1)-C(11)	140.64(12)
C(12)-Fe(1)-C(11)	40.55(9)
C(15)-Fe(1)-C(11)	111.08(12)

C(16)-Fe(1)-C(13)	133.80(15)
C(17)-Fe(1)-C(13)	108.29(12)
C(12)-Fe(1)-C(13)	40.67(12)
C(15)-Fe(1)-C(13)	174.20(15)
C(11)-Fe(1)-C(13)	68.42(10)
C(16)-Fe(1)-C(18)	68.39(12)
C(17)-Fe(1)-C(18)	40.84(12)
C(12)-Fe(1)-C(18)	141.18(12)
C(15)-Fe(1)-C(18)	68.08(13)
C(11)-Fe(1)-C(18)	178.17(11)
C(13)-Fe(1)-C(18)	112.59(12)
C(16)-Fe(1)-C(14)	174.30(15)
C(17)-Fe(1)-C(14)	135.64(12)
C(12)-Fe(1)-C(14)	68.25(11)
C(15)-Fe(1)-C(14)	145.00(14)
C(11)-Fe(1)-C(14)	68.30(10)
C(13)-Fe(1)-C(14)	40.64(11)
C(18)-Fe(1)-C(14)	111.36(11)
C(16)-Fe(1)-C(19)	68.25(14)
C(17)-Fe(1)-C(19)	68.18(12)
C(12)-Fe(1)-C(19)	175.83(14)
C(15)-Fe(1)-C(19)	40.53(15)
C(11)-Fe(1)-C(19)	138.08(11)
C(13)-Fe(1)-C(19)	143.39(14)
C(18)-Fe(1)-C(19)	40.25(13)
C(14)-Fe(1)-C(19)	115.51(12)
C(16)-Fe(1)-C(10)	142.82(13)
C(17)-Fe(1)-C(10)	176.56(12)
C(12)-Fe(1)-C(10)	68.58(10)
C(15)-Fe(1)-C(10)	114.82(12)
C(11)-Fe(1)-C(10)	40.71(9)
C(13)-Fe(1)-C(10)	68.84(9)
C(18)-Fe(1)-C(10)	137.90(11)
C(14)-Fe(1)-C(10)	40.93(8)
C(19)-Fe(1)-C(10)	112.84(10)
C(26)-Fe(2)-C(27)	39.4(3)



C(26)-Fe(2)-C(23)	124.3(2)
C(27)-Fe(2)-C(23)	104.43(19)
C(26)-Fe(2)-C(22)	106.3(2)
C(27)-Fe(2)-C(22)	115.09(17)
C(23)-Fe(2)-C(22)	40.6(2)
C(26)-Fe(2)-C(25)	41.6(3)
C(27)-Fe(2)-C(25)	68.3(3)
C(23)-Fe(2)-C(25)	164.6(2)
C(22)-Fe(2)-C(25)	128.7(2)
C(26)-Fe(2)-C(24)	162.1(3)
C(27)-Fe(2)-C(24)	125.8(2)
C(23)-Fe(2)-C(24)	40.76(16)
C(22)-Fe(2)-C(24)	68.53(19)
C(25)-Fe(2)-C(24)	154.4(2)
C(26)-Fe(2)-C(28)	66.8(2)
C(27)-Fe(2)-C(28)	40.1(2)
C(23)-Fe(2)-C(28)	116.49(18)
C(22)-Fe(2)-C(28)	149.02(19)
C(25)-Fe(2)-C(28)	67.4(2)
C(24)-Fe(2)-C(28)	108.33(18)
C(26)-Fe(2)-C(21)	119.8(2)
C(27)-Fe(2)-C(21)	150.9(2)
C(23)-Fe(2)-C(21)	68.83(15)
C(22)-Fe(2)-C(21)	41.39(13)
C(25)-Fe(2)-C(21)	110.46(19)
C(24)-Fe(2)-C(21)	68.39(15)
C(28)-Fe(2)-C(21)	168.42(18)
C(26)-Fe(2)-C(20)	155.2(3)
C(27)-Fe(2)-C(20)	165.2(2)
C(23)-Fe(2)-C(20)	68.77(11)
C(22)-Fe(2)-C(20)	68.94(12)
C(25)-Fe(2)-C(20)	121.4(2)
C(24)-Fe(2)-C(20)	40.74(11)
C(28)-Fe(2)-C(20)	129.89(18)
C(21)-Fe(2)-C(20)	40.55(12)
C(26)-Fe(2)-C(29)	67.9(2)

C(27)-Fe(2)-C(29)	67.77(18)
C(23)-Fe(2)-C(29)	151.49(18)
C(22)-Fe(2)-C(29)	167.8(2)
C(25)-Fe(2)-C(29)	40.0(2)
C(24)-Fe(2)-C(29)	120.31(16)
C(28)-Fe(2)-C(29)	39.98(18)
C(21)-Fe(2)-C(29)	131.14(15)
C(20)-Fe(2)-C(29)	111.53(13)
C(4)-N(3A)-C(9B)	111.64(18)
C(4)-N(3A)-C(3)	130.16(19)
C(9B)-N(3A)-C(3)	118.08(18)
C(4)-N(4A)-C(9C)	110.48(18)
C(4)-N(4A)-C(5)	131.73(18)
C(9C)-N(4A)-C(5)	117.76(17)
C(9A)-C(1)-C(2)	109.2(2)
C(9A)-C(1)-H(1A)	109.8
C(2)-C(1)-H(1A)	109.8
C(9A)-C(1)-H(1B)	109.8
C(2)-C(1)-H(1B)	109.8
H(1A)-C(1)-H(1B)	108.3
C(3)-C(2)-C(1)	115.3(2)
C(3)-C(2)-H(2A)	108.5
C(1)-C(2)-H(2A)	108.5
C(3)-C(2)-H(2B)	108.5
C(1)-C(2)-H(2B)	108.5
H(2A)-C(2)-H(2B)	107.5
N(3A)-C(3)-C(20)	108.79(18)
N(3A)-C(3)-C(2)	107.15(19)
C(20)-C(3)-C(2)	117.1(2)
N(3A)-C(3)-H(3A)	107.8
C(20)-C(3)-H(3A)	107.8
C(2)-C(3)-H(3A)	107.8
N(3A)-C(4)-N(4A)	104.59(18)
N(3A)-C(4)-Ir(1)	124.57(15)
N(4A)-C(4)-Ir(1)	130.72(15)
N(4A)-C(5)-C(10)	113.74(17)

N(4A)-C(5)-C(6)	107.62(19)
C(10)-C(5)-C(6)	113.91(18)
N(4A)-C(5)-H(5A)	107.1
C(10)-C(5)-H(5A)	107.1
C(6)-C(5)-H(5A)	107.1
C(7)-C(6)-C(5)	116.4(2)
C(7)-C(6)-H(6A)	108.2
C(5)-C(6)-H(6A)	108.2
C(7)-C(6)-H(6B)	108.2
C(5)-C(6)-H(6B)	108.2
H(6A)-C(6)-H(6B)	107.4
C(7A)-C(7)-C(6)	109.5(2)
C(7A)-C(7)-H(7A)	109.8
C(6)-C(7)-H(7A)	109.8
C(7A)-C(7)-H(7B)	109.8
C(6)-C(7)-H(7B)	109.8
H(7A)-C(7)-H(7B)	108.2
C(9C)-C(7A)-C(8)	114.9(2)
C(9C)-C(7A)-C(7)	115.7(2)
C(8)-C(7A)-C(7)	129.4(2)
C(7A)-C(8)-C(9)	122.2(2)
C(7A)-C(8)-H(8A)	118.9
C(9)-C(8)-H(8A)	118.9
C(9B)-C(9A)-C(9)	114.0(3)
C(9B)-C(9A)-C(1)	116.3(3)
C(9)-C(9A)-C(1)	129.7(3)
C(9A)-C(9)-C(8)	122.3(2)
C(9A)-C(9)-H(9A)	118.9
C(8)-C(9)-H(9A)	118.9
C(9B)-C(9C)-C(7A)	122.6(2)
C(9B)-C(9C)-N(4A)	106.99(18)
C(7A)-C(9C)-N(4A)	130.4(2)
N(3A)-C(9B)-C(9A)	129.8(2)
N(3A)-C(9B)-C(9C)	106.25(18)
C(9A)-C(9B)-C(9C)	124.0(2)
C(11)-C(10)-C(14)	107.0(2)

C(11)-C(10)-C(5)	124.98(19)
C(14)-C(10)-C(5)	127.1(2)
C(11)-C(10)-Fe(1)	69.36(13)
C(14)-C(10)-Fe(1)	69.40(13)
C(5)-C(10)-Fe(1)	134.71(16)
C(12)-C(11)-C(10)	108.6(2)
C(12)-C(11)-Fe(1)	69.64(13)
C(10)-C(11)-Fe(1)	69.94(12)
C(12)-C(11)-H(11A)	125.7
C(10)-C(11)-H(11A)	125.7
Fe(1)-C(11)-H(11A)	125.7
C(11)-C(12)-C(13)	108.3(2)
C(11)-C(12)-Fe(1)	69.81(13)
C(13)-C(12)-Fe(1)	69.77(15)
C(11)-C(12)-H(12A)	125.8
C(13)-C(12)-H(12A)	125.8
Fe(1)-C(12)-H(12A)	125.8
C(12)-C(13)-C(14)	107.7(2)
C(12)-C(13)-Fe(1)	69.56(15)
C(14)-C(13)-Fe(1)	69.81(14)
C(12)-C(13)-H(13A)	126.1
C(14)-C(13)-H(13A)	126.1
Fe(1)-C(13)-H(13A)	126.1
C(13)-C(14)-C(10)	108.4(2)
C(13)-C(14)-Fe(1)	69.55(15)
C(10)-C(14)-Fe(1)	69.68(13)
C(13)-C(14)-H(14A)	125.8
C(10)-C(14)-H(14A)	125.8
Fe(1)-C(14)-H(14A)	125.8
C(16)-C(15)-C(19)	108.0(3)
C(16)-C(15)-Fe(1)	69.39(18)
C(19)-C(15)-Fe(1)	70.01(17)
C(16)-C(15)-H(15A)	126.0
C(19)-C(15)-H(15A)	126.0
Fe(1)-C(15)-H(15A)	126.0
C(17)-C(16)-C(15)	108.1(3)

C(17)-C(16)-Fe(1)	69.82(16)
C(15)-C(16)-Fe(1)	70.01(18)
C(17)-C(16)-H(16A)	126.0
C(15)-C(16)-H(16A)	126.0
Fe(1)-C(16)-H(16A)	126.0
C(16)-C(17)-C(18)	107.9(3)
C(16)-C(17)-Fe(1)	69.61(17)
C(18)-C(17)-Fe(1)	69.88(15)
C(16)-C(17)-H(17A)	126.0
C(18)-C(17)-H(17A)	126.0
Fe(1)-C(17)-H(17A)	126.0
C(19)-C(18)-C(17)	107.9(3)
C(19)-C(18)-Fe(1)	70.05(15)
C(17)-C(18)-Fe(1)	69.27(15)
C(19)-C(18)-H(18A)	126.1
C(17)-C(18)-H(18A)	126.1
Fe(1)-C(18)-H(18A)	126.1
C(18)-C(19)-C(15)	108.1(3)
C(18)-C(19)-Fe(1)	69.70(16)
C(15)-C(19)-Fe(1)	69.47(17)
C(18)-C(19)-H(19A)	125.9
C(15)-C(19)-H(19A)	125.9
Fe(1)-C(19)-H(19A)	125.9
C(21)-C(20)-C(24)	107.5(3)
C(21)-C(20)-C(3)	128.2(2)
C(24)-C(20)-C(3)	123.8(3)
C(21)-C(20)-Fe(2)	69.40(15)
C(24)-C(20)-Fe(2)	68.94(15)
C(3)-C(20)-Fe(2)	133.09(16)
C(20)-C(21)-C(22)	107.8(3)
C(20)-C(21)-Fe(2)	70.05(13)
C(22)-C(21)-Fe(2)	68.72(15)
C(20)-C(21)-H(21A)	126.1
C(22)-C(21)-H(21A)	126.1
Fe(2)-C(21)-H(21A)	126.1
C(23)-C(22)-C(21)	107.8(3)

C(23)-C(22)-Fe(2)	69.53(18)
C(21)-C(22)-Fe(2)	69.89(16)
C(23)-C(22)-H(22A)	126.1
C(21)-C(22)-H(22A)	126.1
Fe(2)-C(22)-H(22A)	126.1
C(22)-C(23)-C(24)	108.4(3)
C(22)-C(23)-Fe(2)	69.8(2)
C(24)-C(23)-Fe(2)	70.00(17)
C(22)-C(23)-H(23A)	125.8
C(24)-C(23)-H(23A)	125.8
Fe(2)-C(23)-H(23A)	125.8
C(23)-C(24)-C(20)	108.6(3)
C(23)-C(24)-Fe(2)	69.24(19)
C(20)-C(24)-Fe(2)	70.32(16)
C(23)-C(24)-H(24A)	125.7
C(20)-C(24)-H(24A)	125.7
Fe(2)-C(24)-H(24A)	125.7
C(29)-C(25)-C(26)	106.5(5)
C(29)-C(25)-Fe(2)	70.9(2)
C(26)-C(25)-Fe(2)	68.5(3)
C(29)-C(25)-H(25A)	126.7
C(26)-C(25)-H(25A)	126.7
Fe(2)-C(25)-H(25A)	126.7
C(27)-C(26)-C(25)	108.7(5)
C(27)-C(26)-Fe(2)	70.5(3)
C(25)-C(26)-Fe(2)	69.8(2)
C(27)-C(26)-H(26A)	125.7
C(25)-C(26)-H(26A)	125.7
Fe(2)-C(26)-H(26A)	125.7
C(26)-C(27)-C(28)	108.3(5)
C(26)-C(27)-Fe(2)	70.1(2)
C(28)-C(27)-Fe(2)	70.7(2)
C(26)-C(27)-H(27A)	125.9
C(28)-C(27)-H(27A)	125.9
Fe(2)-C(27)-H(27A)	125.9
C(27)-C(28)-C(29)	109.0(4)

C(27)-C(28)-Fe(2)	69.2(2)
C(29)-C(28)-Fe(2)	70.60(19)
C(27)-C(28)-H(28A)	125.5
C(29)-C(28)-H(28A)	125.5
Fe(2)-C(28)-H(28A)	125.5
C(25)-C(29)-C(28)	107.6(5)
C(25)-C(29)-Fe(2)	69.1(2)
C(28)-C(29)-Fe(2)	69.4(2)
C(25)-C(29)-H(29A)	126.2
C(28)-C(29)-H(29A)	126.2
Fe(2)-C(29)-H(29A)	126.2
C(31)-C(30)-C(37)	123.2(5)
C(31)-C(30)-Ir(1)	69.92(17)
C(37)-C(30)-Ir(1)	113.1(3)
C(31)-C(30)-H(30A)	114.3
C(37)-C(30)-H(30A)	114.3
Ir(1)-C(30)-H(30A)	114.3
C(30)-C(31)-C(32)	128.4(4)
C(30)-C(31)-Ir(1)	72.5(2)
C(32)-C(31)-Ir(1)	110.7(2)
C(30)-C(31)-H(31A)	112.6
C(32)-C(31)-H(31A)	112.6
Ir(1)-C(31)-H(31A)	112.6
C(31)-C(32)-C(33)	113.1(4)
C(31)-C(32)-H(32A)	109.0
C(33)-C(32)-H(32A)	109.0
C(31)-C(32)-H(32B)	109.0
C(33)-C(32)-H(32B)	109.0
H(32A)-C(32)-H(32B)	107.8
C(34)-C(33)-C(32)	113.5(3)
C(34)-C(33)-H(33A)	108.9
C(32)-C(33)-H(33A)	108.9
C(34)-C(33)-H(33B)	108.9
C(32)-C(33)-H(33B)	108.9
H(33A)-C(33)-H(33B)	107.7
C(35)-C(34)-C(33)	121.8(2)

C(35)-C(34)-Ir(1)	70.24(13)
C(33)-C(34)-Ir(1)	113.87(19)
C(35)-C(34)-H(34A)	114.5
C(33)-C(34)-H(34A)	114.5
Ir(1)-C(34)-H(34A)	114.5
C(34)-C(35)-C(36)	123.2(2)
C(34)-C(35)-Ir(1)	70.57(13)
C(36)-C(35)-Ir(1)	113.6(2)
C(34)-C(35)-H(35A)	114.0
C(36)-C(35)-H(35A)	114.0
Ir(1)-C(35)-H(35A)	114.0
C(37)-C(36)-C(35)	115.1(3)
C(37)-C(36)-H(36A)	108.5
C(35)-C(36)-H(36A)	108.5
C(37)-C(36)-H(36B)	108.5
C(35)-C(36)-H(36B)	108.5
H(36A)-C(36)-H(36B)	107.5
C(36)-C(37)-C(30)	114.8(3)
C(36)-C(37)-H(37A)	108.6
C(30)-C(37)-H(37A)	108.6
C(36)-C(37)-H(37B)	108.6
C(30)-C(37)-H(37B)	108.6
H(37A)-C(37)-H(37B)	107.6

---

Symmetry transformations used to generate equivalent atoms:



Table 4. Anisotropic displacement parameters ( $\text{\AA}^2 \times 10^3$ ) for costa2\_0m. The anisotropic displacement factor exponent takes the form:  $-2\pi^2 [h^2 a^{*2} U^{11} + \dots + 2 h k a^* b^* U^{12}]$

	U <sup>11</sup>	U <sup>22</sup>	U <sup>33</sup>	U <sup>23</sup>	U <sup>13</sup>	U <sup>12</sup>
Ir(1)	18(1)	19(1)	20(1)	0(1)	7(1)	-1(1)
Fe(1)	23(1)	18(1)	23(1)	1(1)	9(1)	-3(1)
Fe(2)	17(1)	26(1)	22(1)	2(1)	3(1)	0(1)
Cl(1)	41(1)	27(1)	47(1)	-1(1)	16(1)	11(1)
N(3A)	20(1)	22(1)	19(1)	2(1)	5(1)	-2(1)
N(4A)	19(1)	21(1)	19(1)	-1(1)	6(1)	-3(1)
C(1)	43(1)	33(1)	21(1)	6(1)	4(1)	-5(1)
C(2)	32(1)	26(1)	28(1)	5(1)	2(1)	1(1)
C(3)	22(1)	23(1)	24(1)	2(1)	3(1)	1(1)
C(4)	20(1)	16(1)	20(1)	0(1)	5(1)	-1(1)
C(5)	19(1)	20(1)	23(1)	-2(1)	4(1)	-2(1)
C(6)	21(1)	30(1)	36(1)	-6(1)	8(1)	1(1)
C(7)	25(1)	42(1)	39(1)	-6(1)	15(1)	-6(1)
C(7A)	27(1)	27(1)	32(1)	-4(1)	16(1)	-7(1)
C(8)	40(1)	35(1)	35(1)	-2(1)	23(1)	-8(1)
C(9A)	39(1)	25(1)	22(1)	2(1)	10(1)	-5(1)
C(9)	49(2)	34(1)	27(1)	3(1)	19(1)	-7(1)
C(9C)	24(1)	20(1)	23(1)	-1(1)	10(1)	-4(1)
C(9B)	26(1)	22(1)	20(1)	0(1)	7(1)	-4(1)
C(10)	22(1)	19(1)	22(1)	0(1)	5(1)	-4(1)
C(11)	32(1)	22(1)	22(1)	0(1)	11(1)	-7(1)
C(12)	40(1)	24(1)	22(1)	-2(1)	10(1)	-7(1)
C(13)	33(1)	23(1)	27(1)	-3(1)	4(1)	-7(1)
C(14)	22(1)	22(1)	27(1)	-1(1)	2(1)	-4(1)
C(15)	36(1)	36(1)	39(1)	12(1)	-3(1)	-5(1)
C(16)	32(1)	42(2)	52(2)	17(1)	21(1)	12(1)
C(17)	48(2)	22(1)	33(1)	2(1)	16(1)	4(1)
C(18)	39(1)	23(1)	38(1)	7(1)	18(1)	-1(1)
C(19)	55(2)	26(1)	26(1)	5(1)	15(1)	4(1)
C(20)	20(1)	23(1)	29(1)	6(1)	-1(1)	-3(1)
C(21)	19(1)	27(1)	62(2)	-7(1)	11(1)	0(1)

C(22)	27(1)	23(1)	84(3)	-5(1)	-7(1)	4(1)
C(23)	42(2)	32(1)	47(2)	16(1)	-4(1)	-12(1)
C(24)	39(1)	40(1)	27(1)	10(1)	1(1)	-14(1)
C(25)	54(2)	124(5)	29(1)	32(2)	6(2)	13(2)
C(26)	73(3)	94(4)	43(2)	-30(3)	-15(2)	28(3)
C(27)	33(2)	47(2)	101(4)	1(2)	-23(2)	-11(1)
C(28)	22(1)	78(3)	59(2)	15(2)	8(1)	8(1)
C(29)	37(1)	38(2)	47(2)	5(2)	-11(1)	8(1)
C(30)	51(2)	40(2)	79(3)	-4(2)	52(2)	-6(1)
C(31)	60(2)	46(2)	37(1)	8(1)	34(1)	10(1)
C(32)	101(4)	76(3)	30(2)	15(2)	27(2)	22(3)
C(33)	39(1)	46(2)	26(1)	4(1)	0(1)	6(1)
C(34)	24(1)	21(1)	28(1)	2(1)	7(1)	0(1)
C(35)	29(1)	22(1)	22(1)	1(1)	7(1)	-5(1)
C(36)	40(1)	33(1)	38(1)	4(1)	11(1)	-16(1)
C(37)	103(4)	57(3)	197(8)	-33(4)	124(6)	-40(3)

---

Table 5. Hydrogen coordinates ( $\times 10^4$ ) and isotropic displacement parameters ( $\text{\AA}^2 \times 10^3$ )  
for *costa2\_0m*.

	x	y	z	U(eq)
H(1A)	1154	7977	429	41
H(1B)	1277	9007	389	41
H(2A)	696	9165	2284	36
H(2B)	-424	8558	1322	36
H(3A)	286	8079	3549	29
H(5A)	5377	7223	6781	26
H(6A)	7540	7564	6556	35
H(6B)	6584	6988	5404	35
H(7A)	7187	8775	5210	41
H(7B)	7597	7995	4444	41
H(8A)	6110	8687	2134	41
H(9A)	3945	8791	613	42
H(11A)	3943	8479	7841	29
H(12A)	5140	9642	9540	34
H(13A)	7474	9968	9284	35
H(14A)	7720	8998	7419	30
H(15A)	2891	9719	4972	49
H(16A)	2968	10689	6944	48
H(17A)	5242	11516	7655	40
H(18A)	6581	11051	6120	38
H(19A)	5126	9942	4467	42
H(21A)	1513	6643	1226	43
H(22A)	563	5085	1272	61
H(23A)	-924	5114	2761	54
H(24A)	-910	6664	3640	45
H(25A)	-1318	7320	-1202	85
H(26A)	-1839	5664	-1313	94
H(27A)	-3287	5354	100	85
H(28A)	-3720	6775	1094	65
H(29A)	-2514	7997	309	56

H(30A)	-147	7256	7210	59
H(31A)	1761	7711	8616	52
H(32A)	2722	6312	9721	81
H(32B)	3770	7001	9516	81
H(33A)	4506	5878	8705	47
H(33B)	3089	5387	8334	47
H(34A)	4035	6174	6564	29
H(35A)	2086	5823	5021	29
H(36A)	143	5365	5341	45
H(36B)	1225	4916	6566	45
H(37A)	554	5629	7925	121
H(37B)	-730	5886	6706	121

---

Table 6. Torsion angles [°] for *costa2\_0m*.

C(9A)-C(1)-C(2)-C(3)	-51.9(3)
C(4)-N(3A)-C(3)-C(20)	-77.2(3)
C(9B)-N(3A)-C(3)-C(20)	98.5(2)
C(4)-N(3A)-C(3)-C(2)	155.3(2)
C(9B)-N(3A)-C(3)-C(2)	-29.0(3)
C(1)-C(2)-C(3)-N(3A)	55.3(3)
C(1)-C(2)-C(3)-C(20)	-67.2(3)
C(9B)-N(3A)-C(4)-N(4A)	2.0(2)
C(3)-N(3A)-C(4)-N(4A)	177.9(2)
C(9B)-N(3A)-C(4)-Ir(1)	178.42(15)
C(3)-N(3A)-C(4)-Ir(1)	-5.7(3)
C(9C)-N(4A)-C(4)-N(3A)	-1.7(2)
C(5)-N(4A)-C(4)-N(3A)	176.3(2)
C(9C)-N(4A)-C(4)-Ir(1)	-177.83(15)
C(5)-N(4A)-C(4)-Ir(1)	0.2(3)
C(35)-Ir(1)-C(4)-N(3A)	91.76(18)
C(34)-Ir(1)-C(4)-N(3A)	131.05(18)
C(31)-Ir(1)-C(4)-N(3A)	-150.4(2)
C(30)-Ir(1)-C(4)-N(3A)	13.0(6)
Cl(1)-Ir(1)-C(4)-N(3A)	-62.52(17)
C(35)-Ir(1)-C(4)-N(4A)	-92.83(19)
C(34)-Ir(1)-C(4)-N(4A)	-53.5(2)
C(31)-Ir(1)-C(4)-N(4A)	25.0(3)
C(30)-Ir(1)-C(4)-N(4A)	-171.6(5)
Cl(1)-Ir(1)-C(4)-N(4A)	112.89(18)
C(4)-N(4A)-C(5)-C(10)	-79.0(3)
C(9C)-N(4A)-C(5)-C(10)	99.0(2)
C(4)-N(4A)-C(5)-C(6)	153.9(2)
C(9C)-N(4A)-C(5)-C(6)	-28.2(3)
N(4A)-C(5)-C(6)-C(7)	53.2(3)
C(10)-C(5)-C(6)-C(7)	-73.9(3)
C(5)-C(6)-C(7)-C(7A)	-51.5(3)
C(6)-C(7)-C(7A)-C(9C)	24.3(3)
C(6)-C(7)-C(7A)-C(8)	-155.0(3)

C(9C)-C(7A)-C(8)-C(9)	0.6(4)
C(7)-C(7A)-C(8)-C(9)	179.9(3)
C(2)-C(1)-C(9A)-C(9B)	21.2(3)
C(2)-C(1)-C(9A)-C(9)	-158.2(3)
C(9B)-C(9A)-C(9)-C(8)	-1.3(4)
C(1)-C(9A)-C(9)-C(8)	178.0(3)
C(7A)-C(8)-C(9)-C(9A)	0.2(5)
C(8)-C(7A)-C(9C)-C(9B)	-0.2(4)
C(7)-C(7A)-C(9C)-C(9B)	-179.6(2)
C(8)-C(7A)-C(9C)-N(4A)	177.0(2)
C(7)-C(7A)-C(9C)-N(4A)	-2.4(4)
C(4)-N(4A)-C(9C)-C(9B)	0.9(2)
C(5)-N(4A)-C(9C)-C(9B)	-177.52(18)
C(4)-N(4A)-C(9C)-C(7A)	-176.7(2)
C(5)-N(4A)-C(9C)-C(7A)	5.0(4)
C(4)-N(3A)-C(9B)-C(9A)	177.7(2)
C(3)-N(3A)-C(9B)-C(9A)	1.2(4)
C(4)-N(3A)-C(9B)-C(9C)	-1.5(3)
C(3)-N(3A)-C(9B)-C(9C)	-177.99(19)
C(9)-C(9A)-C(9B)-N(3A)	-177.3(3)
C(1)-C(9A)-C(9B)-N(3A)	3.3(4)
C(9)-C(9A)-C(9B)-C(9C)	1.8(4)
C(1)-C(9A)-C(9B)-C(9C)	-177.7(2)
C(7A)-C(9C)-C(9B)-N(3A)	178.2(2)
N(4A)-C(9C)-C(9B)-N(3A)	0.4(2)
C(7A)-C(9C)-C(9B)-C(9A)	-1.1(4)
N(4A)-C(9C)-C(9B)-C(9A)	-178.9(2)
N(4A)-C(5)-C(10)-C(11)	65.0(3)
C(6)-C(5)-C(10)-C(11)	-171.2(2)
N(4A)-C(5)-C(10)-C(14)	-127.4(2)
C(6)-C(5)-C(10)-C(14)	-3.6(3)
N(4A)-C(5)-C(10)-Fe(1)	-30.0(3)
C(6)-C(5)-C(10)-Fe(1)	93.8(2)
C(16)-Fe(1)-C(10)-C(11)	-54.8(3)
C(17)-Fe(1)-C(10)-C(11)	115.0(18)
C(12)-Fe(1)-C(10)-C(11)	37.30(14)

C(15)-Fe(1)-C(10)-C(11)	-94.02(18)
C(13)-Fe(1)-C(10)-C(11)	81.10(16)
C(18)-Fe(1)-C(10)-C(11)	-178.19(17)
C(14)-Fe(1)-C(10)-C(11)	118.4(2)
C(19)-Fe(1)-C(10)-C(11)	-138.46(16)
C(16)-Fe(1)-C(10)-C(14)	-173.2(2)
C(17)-Fe(1)-C(10)-C(14)	-3.4(19)
C(12)-Fe(1)-C(10)-C(14)	-81.08(16)
C(15)-Fe(1)-C(10)-C(14)	147.61(18)
C(11)-Fe(1)-C(10)-C(14)	-118.4(2)
C(13)-Fe(1)-C(10)-C(14)	-37.28(15)
C(18)-Fe(1)-C(10)-C(14)	63.4(2)
C(19)-Fe(1)-C(10)-C(14)	103.16(18)
C(16)-Fe(1)-C(10)-C(5)	64.5(3)
C(17)-Fe(1)-C(10)-C(5)	-125.8(18)
C(12)-Fe(1)-C(10)-C(5)	156.6(2)
C(15)-Fe(1)-C(10)-C(5)	25.3(3)
C(11)-Fe(1)-C(10)-C(5)	119.3(3)
C(13)-Fe(1)-C(10)-C(5)	-159.6(2)
C(18)-Fe(1)-C(10)-C(5)	-58.9(3)
C(14)-Fe(1)-C(10)-C(5)	-122.3(3)
C(19)-Fe(1)-C(10)-C(5)	-19.2(3)
C(14)-C(10)-C(11)-C(12)	0.3(3)
C(5)-C(10)-C(11)-C(12)	170.0(2)
Fe(1)-C(10)-C(11)-C(12)	-59.11(17)
C(14)-C(10)-C(11)-Fe(1)	59.45(16)
C(5)-C(10)-C(11)-Fe(1)	-130.8(2)
C(16)-Fe(1)-C(11)-C(12)	-92.4(2)
C(17)-Fe(1)-C(11)-C(12)	-55.3(3)
C(15)-Fe(1)-C(11)-C(12)	-136.2(2)
C(13)-Fe(1)-C(11)-C(12)	37.59(17)
C(18)-Fe(1)-C(11)-C(12)	161(4)
C(14)-Fe(1)-C(11)-C(12)	81.46(17)
C(19)-Fe(1)-C(11)-C(12)	-174.0(2)
C(10)-Fe(1)-C(11)-C(12)	119.8(2)
C(16)-Fe(1)-C(11)-C(10)	147.79(17)

C(17)-Fe(1)-C(11)-C(10)	-175.09(18)
C(12)-Fe(1)-C(11)-C(10)	-119.8(2)
C(15)-Fe(1)-C(11)-C(10)	103.99(18)
C(13)-Fe(1)-C(11)-C(10)	-82.21(15)
C(18)-Fe(1)-C(11)-C(10)	41(4)
C(14)-Fe(1)-C(11)-C(10)	-38.34(13)
C(19)-Fe(1)-C(11)-C(10)	66.2(2)
C(10)-C(11)-C(12)-C(13)	-0.1(3)
Fe(1)-C(11)-C(12)-C(13)	-59.35(18)
C(10)-C(11)-C(12)-Fe(1)	59.30(17)
C(16)-Fe(1)-C(12)-C(11)	103.10(19)
C(17)-Fe(1)-C(12)-C(11)	146.15(17)
C(15)-Fe(1)-C(12)-C(11)	66.7(2)
C(13)-Fe(1)-C(12)-C(11)	-119.5(2)
C(18)-Fe(1)-C(12)-C(11)	-179.06(18)
C(14)-Fe(1)-C(12)-C(11)	-81.61(16)
C(19)-Fe(1)-C(12)-C(11)	73.2(15)
C(10)-Fe(1)-C(12)-C(11)	-37.44(15)
C(16)-Fe(1)-C(12)-C(13)	-137.41(18)
C(17)-Fe(1)-C(12)-C(13)	-94.36(18)
C(15)-Fe(1)-C(12)-C(13)	-173.80(19)
C(11)-Fe(1)-C(12)-C(13)	119.5(2)
C(18)-Fe(1)-C(12)-C(13)	-59.6(2)
C(14)-Fe(1)-C(12)-C(13)	37.88(14)
C(19)-Fe(1)-C(12)-C(13)	-167.3(15)
C(10)-Fe(1)-C(12)-C(13)	82.05(16)
C(11)-C(12)-C(13)-C(14)	-0.3(3)
Fe(1)-C(12)-C(13)-C(14)	-59.63(18)
C(11)-C(12)-C(13)-Fe(1)	59.37(18)
C(16)-Fe(1)-C(13)-C(12)	63.0(2)
C(17)-Fe(1)-C(13)-C(12)	100.67(17)
C(15)-Fe(1)-C(13)-C(12)	48.7(12)
C(11)-Fe(1)-C(13)-C(12)	-37.48(15)
C(18)-Fe(1)-C(13)-C(12)	144.17(16)
C(14)-Fe(1)-C(13)-C(12)	-118.9(2)
C(19)-Fe(1)-C(13)-C(12)	178.47(18)



C(10)-Fe(1)-C(13)-C(12)	-81.34(15)
C(16)-Fe(1)-C(13)-C(14)	-178.12(17)
C(17)-Fe(1)-C(13)-C(14)	-140.45(16)
C(12)-Fe(1)-C(13)-C(14)	118.9(2)
C(15)-Fe(1)-C(13)-C(14)	167.6(11)
C(11)-Fe(1)-C(13)-C(14)	81.39(15)
C(18)-Fe(1)-C(13)-C(14)	-96.96(16)
C(19)-Fe(1)-C(13)-C(14)	-62.7(2)
C(10)-Fe(1)-C(13)-C(14)	37.53(14)
C(12)-C(13)-C(14)-C(10)	0.5(3)
Fe(1)-C(13)-C(14)-C(10)	-59.01(16)
C(12)-C(13)-C(14)-Fe(1)	59.47(18)
C(11)-C(10)-C(14)-C(13)	-0.5(3)
C(5)-C(10)-C(14)-C(13)	-169.9(2)
Fe(1)-C(10)-C(14)-C(13)	58.93(17)
C(11)-C(10)-C(14)-Fe(1)	-59.42(16)
C(5)-C(10)-C(14)-Fe(1)	131.2(2)
C(16)-Fe(1)-C(14)-C(13)	13.8(12)
C(17)-Fe(1)-C(14)-C(13)	59.9(2)
C(12)-Fe(1)-C(14)-C(13)	-37.91(15)
C(15)-Fe(1)-C(14)-C(13)	-177.8(2)
C(11)-Fe(1)-C(14)-C(13)	-81.72(16)
C(18)-Fe(1)-C(14)-C(13)	100.22(17)
C(19)-Fe(1)-C(14)-C(13)	144.06(16)
C(10)-Fe(1)-C(14)-C(13)	-119.9(2)
C(16)-Fe(1)-C(14)-C(10)	133.6(12)
C(17)-Fe(1)-C(14)-C(10)	179.71(16)
C(12)-Fe(1)-C(14)-C(10)	81.94(15)
C(15)-Fe(1)-C(14)-C(10)	-58.0(3)
C(11)-Fe(1)-C(14)-C(10)	38.14(14)
C(13)-Fe(1)-C(14)-C(10)	119.9(2)
C(18)-Fe(1)-C(14)-C(10)	-139.92(15)
C(19)-Fe(1)-C(14)-C(10)	-96.09(17)
C(17)-Fe(1)-C(15)-C(16)	-37.76(19)
C(12)-Fe(1)-C(15)-C(16)	60.0(2)
C(11)-Fe(1)-C(15)-C(16)	99.8(2)

C(13)-Fe(1)-C(15)-C(16)	15.9(13)
C(18)-Fe(1)-C(15)-C(16)	-81.9(2)
C(14)-Fe(1)-C(15)-C(16)	-178.24(19)
C(19)-Fe(1)-C(15)-C(16)	-119.2(3)
C(10)-Fe(1)-C(15)-C(16)	144.03(18)
C(16)-Fe(1)-C(15)-C(19)	119.2(3)
C(17)-Fe(1)-C(15)-C(19)	81.5(2)
C(12)-Fe(1)-C(15)-C(19)	179.28(17)
C(11)-Fe(1)-C(15)-C(19)	-140.93(17)
C(13)-Fe(1)-C(15)-C(19)	135.1(11)
C(18)-Fe(1)-C(15)-C(19)	37.31(18)
C(14)-Fe(1)-C(15)-C(19)	-59.0(3)
C(10)-Fe(1)-C(15)-C(19)	-96.73(19)
C(19)-C(15)-C(16)-C(17)	0.1(4)
Fe(1)-C(15)-C(16)-C(17)	59.7(2)
C(19)-C(15)-C(16)-Fe(1)	-59.6(2)
C(12)-Fe(1)-C(16)-C(17)	100.82(19)
C(15)-Fe(1)-C(16)-C(17)	-119.0(3)
C(11)-Fe(1)-C(16)-C(17)	143.94(17)
C(13)-Fe(1)-C(16)-C(17)	63.2(2)
C(18)-Fe(1)-C(16)-C(17)	-37.95(18)
C(14)-Fe(1)-C(16)-C(17)	50.7(12)
C(19)-Fe(1)-C(16)-C(17)	-81.4(2)
C(10)-Fe(1)-C(16)-C(17)	179.06(18)
C(17)-Fe(1)-C(16)-C(15)	119.0(3)
C(12)-Fe(1)-C(16)-C(15)	-140.14(19)
C(11)-Fe(1)-C(16)-C(15)	-97.0(2)
C(13)-Fe(1)-C(16)-C(15)	-177.81(18)
C(18)-Fe(1)-C(16)-C(15)	81.1(2)
C(14)-Fe(1)-C(16)-C(15)	169.8(11)
C(19)-Fe(1)-C(16)-C(15)	37.62(19)
C(10)-Fe(1)-C(16)-C(15)	-61.9(3)
C(15)-C(16)-C(17)-C(18)	-0.2(3)
Fe(1)-C(16)-C(17)-C(18)	59.6(2)
C(15)-C(16)-C(17)-Fe(1)	-59.8(2)
C(12)-Fe(1)-C(17)-C(16)	-94.1(2)

C(15)-Fe(1)-C(17)-C(16)	37.8(2)
C(11)-Fe(1)-C(17)-C(16)	-59.3(3)
C(13)-Fe(1)-C(17)-C(16)	-137.3(2)
C(18)-Fe(1)-C(17)-C(16)	119.0(3)
C(14)-Fe(1)-C(17)-C(16)	-173.7(2)
C(19)-Fe(1)-C(17)-C(16)	81.6(2)
C(10)-Fe(1)-C(17)-C(16)	-170.5(18)
C(16)-Fe(1)-C(17)-C(18)	-119.0(3)
C(12)-Fe(1)-C(17)-C(18)	146.85(18)
C(15)-Fe(1)-C(17)-C(18)	-81.3(2)
C(11)-Fe(1)-C(17)-C(18)	-178.33(18)
C(13)-Fe(1)-C(17)-C(18)	103.66(19)
C(14)-Fe(1)-C(17)-C(18)	67.3(2)
C(19)-Fe(1)-C(17)-C(18)	-37.45(19)
C(10)-Fe(1)-C(17)-C(18)	70.5(19)
C(16)-C(17)-C(18)-C(19)	0.2(3)
Fe(1)-C(17)-C(18)-C(19)	59.64(19)
C(16)-C(17)-C(18)-Fe(1)	-59.5(2)
C(16)-Fe(1)-C(18)-C(19)	-81.4(2)
C(17)-Fe(1)-C(18)-C(19)	-119.1(3)
C(12)-Fe(1)-C(18)-C(19)	-173.8(2)
C(15)-Fe(1)-C(18)-C(19)	-37.6(2)
C(11)-Fe(1)-C(18)-C(19)	26(4)
C(13)-Fe(1)-C(18)-C(19)	148.66(19)
C(14)-Fe(1)-C(18)-C(19)	104.70(19)
C(10)-Fe(1)-C(18)-C(19)	65.7(2)
C(16)-Fe(1)-C(18)-C(17)	37.7(2)
C(12)-Fe(1)-C(18)-C(17)	-54.7(3)
C(15)-Fe(1)-C(18)-C(17)	81.6(2)
C(11)-Fe(1)-C(18)-C(17)	145(4)
C(13)-Fe(1)-C(18)-C(17)	-92.2(2)
C(14)-Fe(1)-C(18)-C(17)	-136.18(18)
C(19)-Fe(1)-C(18)-C(17)	119.1(3)
C(10)-Fe(1)-C(18)-C(17)	-175.17(18)
C(17)-C(18)-C(19)-C(15)	-0.1(3)
Fe(1)-C(18)-C(19)-C(15)	59.0(2)

C(17)-C(18)-C(19)-Fe(1)	-59.2(2)
C(16)-C(15)-C(19)-C(18)	0.0(3)
Fe(1)-C(15)-C(19)-C(18)	-59.2(2)
C(16)-C(15)-C(19)-Fe(1)	59.2(2)
C(16)-Fe(1)-C(19)-C(18)	81.8(2)
C(17)-Fe(1)-C(19)-C(18)	37.98(18)
C(12)-Fe(1)-C(19)-C(18)	112.5(15)
C(15)-Fe(1)-C(19)-C(18)	119.5(3)
C(11)-Fe(1)-C(19)-C(18)	-178.81(17)
C(13)-Fe(1)-C(19)-C(18)	-53.6(3)
C(14)-Fe(1)-C(19)-C(18)	-93.50(18)
C(10)-Fe(1)-C(19)-C(18)	-138.47(17)
C(16)-Fe(1)-C(19)-C(15)	-37.7(2)
C(17)-Fe(1)-C(19)-C(15)	-81.5(2)
C(12)-Fe(1)-C(19)-C(15)	-7.0(16)
C(11)-Fe(1)-C(19)-C(15)	61.7(3)
C(13)-Fe(1)-C(19)-C(15)	-173.1(2)
C(18)-Fe(1)-C(19)-C(15)	-119.5(3)
C(14)-Fe(1)-C(19)-C(15)	147.00(19)
C(10)-Fe(1)-C(19)-C(15)	102.0(2)
N(3A)-C(3)-C(20)-C(21)	-61.0(3)
C(2)-C(3)-C(20)-C(21)	60.6(3)
N(3A)-C(3)-C(20)-C(24)	110.0(3)
C(2)-C(3)-C(20)-C(24)	-128.4(3)
N(3A)-C(3)-C(20)-Fe(2)	-158.1(2)
C(2)-C(3)-C(20)-Fe(2)	-36.5(4)
C(26)-Fe(2)-C(20)-C(21)	-45.1(5)
C(27)-Fe(2)-C(20)-C(21)	146.9(6)
C(23)-Fe(2)-C(20)-C(21)	81.8(2)
C(22)-Fe(2)-C(20)-C(21)	38.1(2)
C(25)-Fe(2)-C(20)-C(21)	-85.2(3)
C(24)-Fe(2)-C(20)-C(21)	119.3(3)
C(28)-Fe(2)-C(20)-C(21)	-170.8(2)
C(29)-Fe(2)-C(20)-C(21)	-128.8(2)
C(26)-Fe(2)-C(20)-C(24)	-164.4(5)
C(27)-Fe(2)-C(20)-C(24)	27.6(7)

C(23)-Fe(2)-C(20)-C(24)	-37.4(2)
C(22)-Fe(2)-C(20)-C(24)	-81.1(2)
C(25)-Fe(2)-C(20)-C(24)	155.6(3)
C(28)-Fe(2)-C(20)-C(24)	70.0(3)
C(21)-Fe(2)-C(20)-C(24)	-119.3(3)
C(29)-Fe(2)-C(20)-C(24)	111.9(2)
C(26)-Fe(2)-C(20)-C(3)	78.5(5)
C(27)-Fe(2)-C(20)-C(3)	-89.5(6)
C(23)-Fe(2)-C(20)-C(3)	-154.5(3)
C(22)-Fe(2)-C(20)-C(3)	161.8(3)
C(25)-Fe(2)-C(20)-C(3)	38.5(4)
C(24)-Fe(2)-C(20)-C(3)	-117.1(4)
C(28)-Fe(2)-C(20)-C(3)	-47.1(3)
C(21)-Fe(2)-C(20)-C(3)	123.6(3)
C(29)-Fe(2)-C(20)-C(3)	-5.2(3)
C(24)-C(20)-C(21)-C(22)	0.1(3)
C(3)-C(20)-C(21)-C(22)	172.2(2)
Fe(2)-C(20)-C(21)-C(22)	-58.5(2)
C(24)-C(20)-C(21)-Fe(2)	58.60(19)
C(3)-C(20)-C(21)-Fe(2)	-129.3(2)
C(26)-Fe(2)-C(21)-C(20)	160.0(3)
C(27)-Fe(2)-C(21)-C(20)	-163.3(4)
C(23)-Fe(2)-C(21)-C(20)	-81.7(2)
C(22)-Fe(2)-C(21)-C(20)	-119.4(3)
C(25)-Fe(2)-C(21)-C(20)	114.8(3)
C(24)-Fe(2)-C(21)-C(20)	-37.76(17)
C(28)-Fe(2)-C(21)-C(20)	37.8(9)
C(29)-Fe(2)-C(21)-C(20)	74.2(3)
C(26)-Fe(2)-C(21)-C(22)	-80.7(4)
C(27)-Fe(2)-C(21)-C(22)	-43.9(5)
C(23)-Fe(2)-C(21)-C(22)	37.7(3)
C(25)-Fe(2)-C(21)-C(22)	-125.8(3)
C(24)-Fe(2)-C(21)-C(22)	81.6(3)
C(28)-Fe(2)-C(21)-C(22)	157.2(8)
C(20)-Fe(2)-C(21)-C(22)	119.4(3)
C(29)-Fe(2)-C(21)-C(22)	-166.4(3)

C(20)-C(21)-C(22)-C(23)	-0.1(4)
Fe(2)-C(21)-C(22)-C(23)	-59.4(2)
C(20)-C(21)-C(22)-Fe(2)	59.4(2)
C(26)-Fe(2)-C(22)-C(23)	-124.2(3)
C(27)-Fe(2)-C(22)-C(23)	-82.9(3)
C(25)-Fe(2)-C(22)-C(23)	-164.4(3)
C(24)-Fe(2)-C(22)-C(23)	37.7(2)
C(28)-Fe(2)-C(22)-C(23)	-52.4(5)
C(21)-Fe(2)-C(22)-C(23)	118.9(3)
C(20)-Fe(2)-C(22)-C(23)	81.5(2)
C(29)-Fe(2)-C(22)-C(23)	176.1(7)
C(26)-Fe(2)-C(22)-C(21)	116.9(3)
C(27)-Fe(2)-C(22)-C(21)	158.2(3)
C(23)-Fe(2)-C(22)-C(21)	-118.9(3)
C(25)-Fe(2)-C(22)-C(21)	76.7(4)
C(24)-Fe(2)-C(22)-C(21)	-81.2(2)
C(28)-Fe(2)-C(22)-C(21)	-171.3(3)
C(20)-Fe(2)-C(22)-C(21)	-37.4(2)
C(29)-Fe(2)-C(22)-C(21)	57.2(8)
C(21)-C(22)-C(23)-C(24)	0.1(4)
Fe(2)-C(22)-C(23)-C(24)	-59.6(2)
C(21)-C(22)-C(23)-Fe(2)	59.7(2)
C(26)-Fe(2)-C(23)-C(22)	74.1(3)
C(27)-Fe(2)-C(23)-C(22)	111.9(3)
C(25)-Fe(2)-C(23)-C(22)	52.0(7)
C(24)-Fe(2)-C(23)-C(22)	-119.4(3)
C(28)-Fe(2)-C(23)-C(22)	152.9(2)
C(21)-Fe(2)-C(23)-C(22)	-38.36(19)
C(20)-Fe(2)-C(23)-C(22)	-82.0(2)
C(29)-Fe(2)-C(23)-C(22)	-178.3(3)
C(26)-Fe(2)-C(23)-C(24)	-166.5(3)
C(27)-Fe(2)-C(23)-C(24)	-128.7(3)
C(22)-Fe(2)-C(23)-C(24)	119.4(3)
C(25)-Fe(2)-C(23)-C(24)	171.4(6)
C(28)-Fe(2)-C(23)-C(24)	-87.7(3)
C(21)-Fe(2)-C(23)-C(24)	81.0(2)

C(20)-Fe(2)-C(23)-C(24)	37.41(19)
C(29)-Fe(2)-C(23)-C(24)	-58.9(4)
C(22)-C(23)-C(24)-C(20)	0.0(4)
Fe(2)-C(23)-C(24)-C(20)	-59.52(19)
C(22)-C(23)-C(24)-Fe(2)	59.5(2)
C(21)-C(20)-C(24)-C(23)	0.0(3)
C(3)-C(20)-C(24)-C(23)	-172.6(2)
Fe(2)-C(20)-C(24)-C(23)	58.9(2)
C(21)-C(20)-C(24)-Fe(2)	-58.9(2)
C(3)-C(20)-C(24)-Fe(2)	128.6(2)
C(26)-Fe(2)-C(24)-C(23)	38.7(7)
C(27)-Fe(2)-C(24)-C(23)	68.6(3)
C(22)-Fe(2)-C(24)-C(23)	-37.6(2)
C(25)-Fe(2)-C(24)-C(23)	-174.7(4)
C(28)-Fe(2)-C(24)-C(23)	109.6(3)
C(21)-Fe(2)-C(24)-C(23)	-82.2(2)
C(20)-Fe(2)-C(24)-C(23)	-119.8(3)
C(29)-Fe(2)-C(24)-C(23)	151.8(2)
C(26)-Fe(2)-C(24)-C(20)	158.5(6)
C(27)-Fe(2)-C(24)-C(20)	-171.6(2)
C(23)-Fe(2)-C(24)-C(20)	119.8(3)
C(22)-Fe(2)-C(24)-C(20)	82.2(2)
C(25)-Fe(2)-C(24)-C(20)	-54.9(5)
C(28)-Fe(2)-C(24)-C(20)	-130.6(2)
C(21)-Fe(2)-C(24)-C(20)	37.59(17)
C(29)-Fe(2)-C(24)-C(20)	-88.4(2)
C(26)-Fe(2)-C(25)-C(29)	117.3(5)
C(27)-Fe(2)-C(25)-C(29)	80.8(3)
C(23)-Fe(2)-C(25)-C(29)	145.2(6)
C(22)-Fe(2)-C(25)-C(29)	-173.7(2)
C(24)-Fe(2)-C(25)-C(29)	-47.9(6)
C(28)-Fe(2)-C(25)-C(29)	37.4(3)
C(21)-Fe(2)-C(25)-C(29)	-130.4(3)
C(20)-Fe(2)-C(25)-C(29)	-86.6(3)
C(27)-Fe(2)-C(25)-C(26)	-36.5(3)
C(23)-Fe(2)-C(25)-C(26)	27.9(8)

C(22)-Fe(2)-C(25)-C(26)	68.9(4)
C(24)-Fe(2)-C(25)-C(26)	-165.2(4)
C(28)-Fe(2)-C(25)-C(26)	-79.9(4)
C(21)-Fe(2)-C(25)-C(26)	112.3(3)
C(20)-Fe(2)-C(25)-C(26)	156.0(3)
C(29)-Fe(2)-C(25)-C(26)	-117.3(5)
C(29)-C(25)-C(26)-C(27)	-1.1(5)
Fe(2)-C(25)-C(26)-C(27)	60.0(3)
C(29)-C(25)-C(26)-Fe(2)	-61.1(3)
C(23)-Fe(2)-C(26)-C(27)	69.2(4)
C(22)-Fe(2)-C(26)-C(27)	109.9(3)
C(25)-Fe(2)-C(26)-C(27)	-119.5(5)
C(24)-Fe(2)-C(26)-C(27)	39.6(8)
C(28)-Fe(2)-C(26)-C(27)	-37.9(3)
C(21)-Fe(2)-C(26)-C(27)	152.7(3)
C(20)-Fe(2)-C(26)-C(27)	-175.2(3)
C(29)-Fe(2)-C(26)-C(27)	-81.4(3)
C(27)-Fe(2)-C(26)-C(25)	119.5(5)
C(23)-Fe(2)-C(26)-C(25)	-171.3(3)
C(22)-Fe(2)-C(26)-C(25)	-130.6(3)
C(24)-Fe(2)-C(26)-C(25)	159.1(5)
C(28)-Fe(2)-C(26)-C(25)	81.5(3)
C(21)-Fe(2)-C(26)-C(25)	-87.8(3)
C(20)-Fe(2)-C(26)-C(25)	-55.7(6)
C(29)-Fe(2)-C(26)-C(25)	38.1(3)
C(25)-C(26)-C(27)-C(28)	1.1(5)
Fe(2)-C(26)-C(27)-C(28)	60.7(3)
C(25)-C(26)-C(27)-Fe(2)	-59.6(3)
C(23)-Fe(2)-C(27)-C(26)	-127.1(4)
C(22)-Fe(2)-C(27)-C(26)	-85.3(4)
C(25)-Fe(2)-C(27)-C(26)	38.5(4)
C(24)-Fe(2)-C(27)-C(26)	-166.0(3)
C(28)-Fe(2)-C(27)-C(26)	118.7(5)
C(21)-Fe(2)-C(27)-C(26)	-54.9(6)
C(20)-Fe(2)-C(27)-C(26)	172.1(5)
C(29)-Fe(2)-C(27)-C(26)	81.8(4)



C(26)-Fe(2)-C(27)-C(28)	-118.7(5)
C(23)-Fe(2)-C(27)-C(28)	114.2(3)
C(22)-Fe(2)-C(27)-C(28)	156.0(3)
C(25)-Fe(2)-C(27)-C(28)	-80.2(3)
C(24)-Fe(2)-C(27)-C(28)	75.3(3)
C(21)-Fe(2)-C(27)-C(28)	-173.6(3)
C(20)-Fe(2)-C(27)-C(28)	53.4(7)
C(29)-Fe(2)-C(27)-C(28)	-36.9(3)
C(26)-C(27)-C(28)-C(29)	-0.7(5)
Fe(2)-C(27)-C(28)-C(29)	59.6(3)
C(26)-C(27)-C(28)-Fe(2)	-60.3(3)
C(26)-Fe(2)-C(28)-C(27)	37.3(4)
C(23)-Fe(2)-C(28)-C(27)	-80.8(4)
C(22)-Fe(2)-C(28)-C(27)	-45.6(6)
C(25)-Fe(2)-C(28)-C(27)	82.7(4)
C(24)-Fe(2)-C(28)-C(27)	-124.2(4)
C(21)-Fe(2)-C(28)-C(27)	164.2(8)
C(20)-Fe(2)-C(28)-C(27)	-164.4(3)
C(29)-Fe(2)-C(28)-C(27)	120.2(5)
C(26)-Fe(2)-C(28)-C(29)	-82.8(4)
C(27)-Fe(2)-C(28)-C(29)	-120.2(5)
C(23)-Fe(2)-C(28)-C(29)	159.0(3)
C(22)-Fe(2)-C(28)-C(29)	-165.8(4)
C(25)-Fe(2)-C(28)-C(29)	-37.4(3)
C(24)-Fe(2)-C(28)-C(29)	115.6(3)
C(21)-Fe(2)-C(28)-C(29)	44.1(10)
C(20)-Fe(2)-C(28)-C(29)	75.4(3)
C(26)-C(25)-C(29)-C(28)	0.6(4)
Fe(2)-C(25)-C(29)-C(28)	-58.9(3)
C(26)-C(25)-C(29)-Fe(2)	59.6(3)
C(27)-C(28)-C(29)-C(25)	0.0(4)
Fe(2)-C(28)-C(29)-C(25)	58.7(3)
C(27)-C(28)-C(29)-Fe(2)	-58.7(3)
C(26)-Fe(2)-C(29)-C(25)	-39.6(4)
C(27)-Fe(2)-C(29)-C(25)	-82.3(4)
C(23)-Fe(2)-C(29)-C(25)	-161.4(4)

C(22)-Fe(2)-C(29)-C(25)	23.8(9)
C(24)-Fe(2)-C(29)-C(25)	158.2(3)
C(28)-Fe(2)-C(29)-C(25)	-119.3(4)
C(21)-Fe(2)-C(29)-C(25)	71.4(4)
C(20)-Fe(2)-C(29)-C(25)	113.7(3)
C(26)-Fe(2)-C(29)-C(28)	79.7(4)
C(27)-Fe(2)-C(29)-C(28)	37.0(4)
C(23)-Fe(2)-C(29)-C(28)	-42.2(4)
C(22)-Fe(2)-C(29)-C(28)	143.1(7)
C(25)-Fe(2)-C(29)-C(28)	119.3(4)
C(24)-Fe(2)-C(29)-C(28)	-82.5(3)
C(21)-Fe(2)-C(29)-C(28)	-169.3(3)
C(20)-Fe(2)-C(29)-C(28)	-127.0(3)
C(4)-Ir(1)-C(30)-C(31)	-168.2(4)
C(35)-Ir(1)-C(30)-C(31)	111.2(2)
C(34)-Ir(1)-C(30)-C(31)	73.4(2)
Cl(1)-Ir(1)-C(30)-C(31)	-92.8(2)
C(4)-Ir(1)-C(30)-C(37)	73.2(8)
C(35)-Ir(1)-C(30)-C(37)	-7.4(5)
C(34)-Ir(1)-C(30)-C(37)	-45.1(5)
C(31)-Ir(1)-C(30)-C(37)	-118.6(6)
Cl(1)-Ir(1)-C(30)-C(37)	148.6(5)
C(37)-C(30)-C(31)-C(32)	2.2(6)
Ir(1)-C(30)-C(31)-C(32)	-102.9(4)
C(37)-C(30)-C(31)-Ir(1)	105.1(4)
C(4)-Ir(1)-C(31)-C(30)	174.4(2)
C(35)-Ir(1)-C(31)-C(30)	-67.4(2)
C(34)-Ir(1)-C(31)-C(30)	-104.2(2)
Cl(1)-Ir(1)-C(31)-C(30)	87.0(2)
C(4)-Ir(1)-C(31)-C(32)	-60.4(5)
C(35)-Ir(1)-C(31)-C(32)	57.9(4)
C(34)-Ir(1)-C(31)-C(32)	21.0(4)
C(30)-Ir(1)-C(31)-C(32)	125.2(5)
Cl(1)-Ir(1)-C(31)-C(32)	-147.7(4)
C(30)-C(31)-C(32)-C(33)	52.9(6)
Ir(1)-C(31)-C(32)-C(33)	-30.8(6)

C(31)-C(32)-C(33)-C(34)	24.9(6)
C(32)-C(33)-C(34)-C(35)	-87.6(4)
C(32)-C(33)-C(34)-Ir(1)	-6.8(4)
C(4)-Ir(1)-C(34)-C(35)	-96.44(14)
C(31)-Ir(1)-C(34)-C(35)	109.13(18)
C(30)-Ir(1)-C(34)-C(35)	72.90(19)
Cl(1)-Ir(1)-C(34)-C(35)	164.1(2)
C(4)-Ir(1)-C(34)-C(33)	146.6(2)
C(35)-Ir(1)-C(34)-C(33)	-117.0(3)
C(31)-Ir(1)-C(34)-C(33)	-7.9(2)
C(30)-Ir(1)-C(34)-C(33)	-44.1(2)
Cl(1)-Ir(1)-C(34)-C(33)	47.1(4)
C(33)-C(34)-C(35)-C(36)	0.4(4)
Ir(1)-C(34)-C(35)-C(36)	-106.1(3)
C(33)-C(34)-C(35)-Ir(1)	106.4(3)
C(4)-Ir(1)-C(35)-C(34)	87.65(15)
C(31)-Ir(1)-C(35)-C(34)	-69.60(17)
C(30)-Ir(1)-C(35)-C(34)	-104.4(2)
Cl(1)-Ir(1)-C(35)-C(34)	-171.52(13)
C(4)-Ir(1)-C(35)-C(36)	-153.66(19)
C(34)-Ir(1)-C(35)-C(36)	118.7(3)
C(31)-Ir(1)-C(35)-C(36)	49.1(2)
C(30)-Ir(1)-C(35)-C(36)	14.3(2)
Cl(1)-Ir(1)-C(35)-C(36)	-52.8(3)
C(34)-C(35)-C(36)-C(37)	62.1(6)
Ir(1)-C(35)-C(36)-C(37)	-19.4(5)
C(35)-C(36)-C(37)-C(30)	13.2(9)
C(31)-C(30)-C(37)-C(36)	-81.4(8)
Ir(1)-C(30)-C(37)-C(36)	-1.0(9)

---

Symmetry transformations used to generate equivalent atoms:

## VITA

Name: Xiangdong Du

Place of Birth: Hebei, China

Education: Dalian University of Technology, B. Sc. 1994  
Beijing University of chemical technology, M. Sc. 2001

Experience: Beijing Yansan Petrochemical Corporation, 1994-1999  
Tsinghua Ziguang Yingli company, 2001-2004

Publications: Metallinos, C.; Du, X. *Organometallics*, **2008**, in press.